Biomimetic Synthesis and Chemical Proteomics Reveal the Mechanism of Action and Functional Targets of Phloroglucinol Meroterpenoids

Amy K. Bracken[1], Colby E. Gekko[1], Nina O. Suss[1], Emma E. Lueders[1], Qi Cui[1], Qin Fu[2], Andy C. W. Lui[2], Elizabeth T. Anderson[2], Sheng Zhang[2], Mikail E. Abbasov[1]*

[1]*Department of Chemistry and Chemical Biology, Cornell University, Ithaca, NY 14853, USA.*
[2]*Proteomics and Metabolomics Facility, Cornell University, Ithaca, NY 14853, USA.*
**correspondence to mikail.abbasov@cornell.edu*

Supporting Information

Table of Contents

Extended Data Figures and Discussion

Combined spectroscopic and computational studies into the mechanism of the formation of cattleianal (supplemental discussion related to Extended Data Figure S1).

Based on NMR studies and molecular mechanics simulations, **1** adopts three conformational states in solution: αα (48%), βα (28%), and ββ (24%), with a rapid interconversion between αα and βα down to –100 °C.[1] These conformers are distinguished based on the relative disposition of the exocyclic methylene and olefinic methyl groups. Furthermore, under the reaction conditions, no conformational interconversion between αα/βα and ββ was observed (**Extended Data Figure S1A**). Examination of the crude reaction mixture by ^{1}H-NMR revealed the initial formation of cattleianal as a 3:1 mixture of diastereomers. Careful chromatographic purification improved the diastereomeric ratio to 9:1 (**Extended Data Figure S1B**). We ascertained that cattleianal and an unassigned minor diastereomer do not interconvert under the reaction conditions, thereby confirming the irreversible nature of cycloadduct formation (**Extended Data Figure S1C**). Consequently, the observed ratio of cattleianal and an unassigned minor diastereomer, computationally anticipated to be 4,10-*epi*-cattleianal, from the crude reaction mixture aligns well with detected αα/βα and ββ conformational distributions (**Extended Data Figure S1D**).

Geometry optimizations of all minima and transition states involved were carried out using M06-2X[2] functional and SMD[3] solvation model in nitromethane as a solvent with the basis set def2SVP[4] using Gaussian 16 program.[5] Frequency calculations at the same level were performed to validate each structure as either a minimum (zero imaginary frequencies) or a transition state (one imaginary frequency) and to evaluate its zero-point energy and thermal corrections at 298 K. High-level single-point energies were computed using ωB97xD[6] functional paired with the SMD solvation model and def2QZVPP[7] basis set. The overarching level of theory was denoted as ωB97xD/def2QZVPP/SMD($MeNO_2$)//M06-2X/def2SVP/SMD($MeNO_2$). The results derived from the frontier molecular orbital analysis further underscore the inverse-electron-demand nature of the hetero-Diels-Alder cycloaddition with the HOMO-LUMO energy gap of 9.49 eV (**Extended Data Figure S1E**).

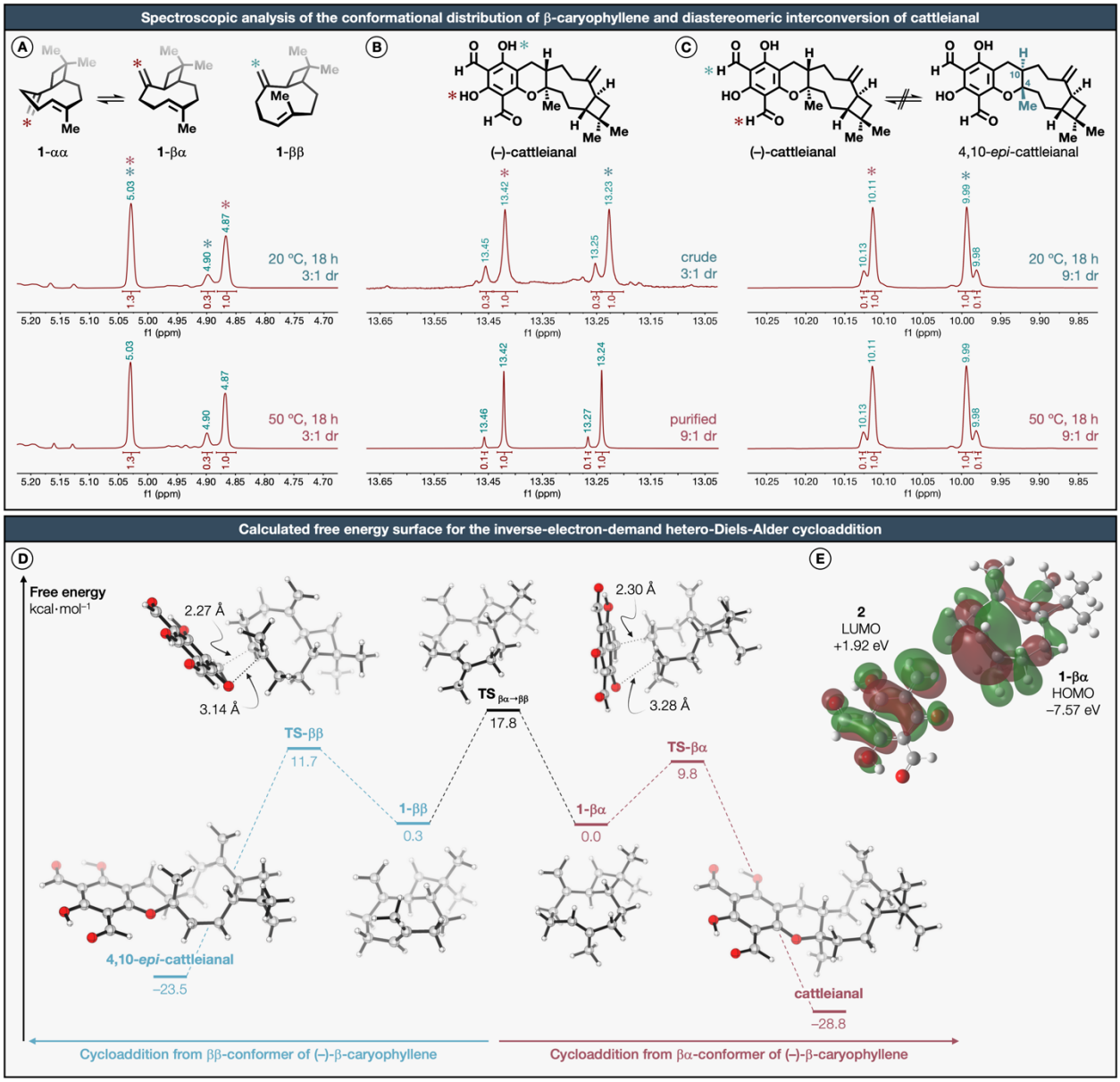

Extended Data Figure S1. Combined spectroscopic and computational studies into the mechanism of the formation of cattleianal. (A) ^{1}H-NMR spectra showing that (–)-β-caryophyllene predominantly exists as a 3:1 conformational mixture of αα/βα (75%) and ββ (25%) at 20 °C, which do not interconvert under reaction conditions (50 °C, 18 h). (B) ^{1}H-NMR spectra of the crude reaction mixture show the initial formation of cattleianal as a 3:1 mixture of diastereomers, which upon careful purification was improved to 9:1. (C)^{1}H-NMR spectra showing that (–)-cattleianal and the computationally predicted 4,10-*epi*-cattleianal do not interconvert either at 20 °C or under reaction conditions (50 °C, 18 h). (D) Calculated free energy surface for the inverse-electron-demand hetero-Diels-Alder cycloaddition with geometries of the transition states and cycloadducts (bond distances are given in Å). (E) HOMO/LUMO composition and energies of the frontier molecular orbitals of **1**-βα (HOMO) and **2** (LUMO). For a detailed description of computational methods, computed energies for stationary points, and the frontier molecular orbital analysis, see pages S59–S71.

Physicochemical and kinetic studies of representative phloroglucinol meroterpenoids with a model amine nucleophile (supplemental discussion related to Extended Data Figure S2).

It is noteworthy that pK_a is a key physicochemical parameter that significantly affects pharmacokinetic behavior of small molecules, that is, absorption, distribution, metabolism, and excretion.[8] It further modulates lipophilicity, solubility, protein binding, and permeability of a compound; for instance, compounds with pK_a < 4 and >10 display slower diffusion rate across biological membranes such as the blood-brain barrier.[9]

To our knowledge, no systematic investigations delineating the reactivity profiles of these natural products with amine nucleophiles have been reported. The time-dependent formation of the respective imine (Schiff base) adducts was subsequently quantified using butylamine as a prototypical amine nucleophile, with kinetic data collected over the course of 24 hours by ^{1}H-NMR (see **Supplementary Figures S1–S8** on pages S32–S39). A mixture comprising grandinol or jensenone with butylamine, alongside a focused set of benzaldehyde analogues, was incubated for 24 hours and upon 20-fold dilution in DMSO-d_6:PBS (3:1, pH 7.4), ^{1}H-NMR spectra were recorded at different time points (**Extended Data Figure S2C–D**; also see **Supplementary Figures S9–S14** on pages S40-S45).

Our observations aligns with prior investigations which have elucidated that salicylaldehyde-based Schiff bases are resistant to hydrolysis, primarily due to intramolecular resonance-assisted hydrogen bonding.[10-13] It is noteworthy that aryl imines bearing electron-donating hydroxyl groups in ortho and para positions with respect to the imine moiety, akin to those found in phloroglucinol meroterpenoids, exhibit stronger intramolecular resonance-assisted hydrogen bonding and greater resistance to hydrolysis.[14,15]

It is also noteworthy that in the presence of superstoichiometric quantities of butylamine, jensenone exclusively forms the bisadduct **13**. The exclusively formed bisadduct **13** exists as an inseparable 1:1 mixture of imine/enaminone tautomers (**Extended Data Figure S2D**; also see pages S95-S108), while the corresponding monoadduct, although not isolable, can be detected by ^{1}H-NMR in reactions with substoichiometric quantities of butylamine (see **Supplementary Figure S2**).

Due to the intrinsic stability of these Schiff base adducts against hydrolytic degradation under physiological conditions, our subsequent objective was to investigate their susceptibility to cleavage by a more nucleophilic amine (**Extended Data Figure S2E**). MDA-MB-231 cells were subjected to treatment with the clickable azide probe (–)-**10** at 100 μM for 8 hours, followed by cell harvest, lysis, and subsequent partitioning into soluble and insoluble fractions. Subsequent to copper-catalysed azide-alkyne cycloaddition (CuAAC)[16] conjugation with fluorophore BDP-TMR-alkyne, the cellular lysates were quenched using Laemmli buffer under denaturing and reducing conditions, followed by hydroxylamine treatment at specified concentrations. The samples were resolved by SDS-PAGE and analysed by in-gel fluorescence scanning.

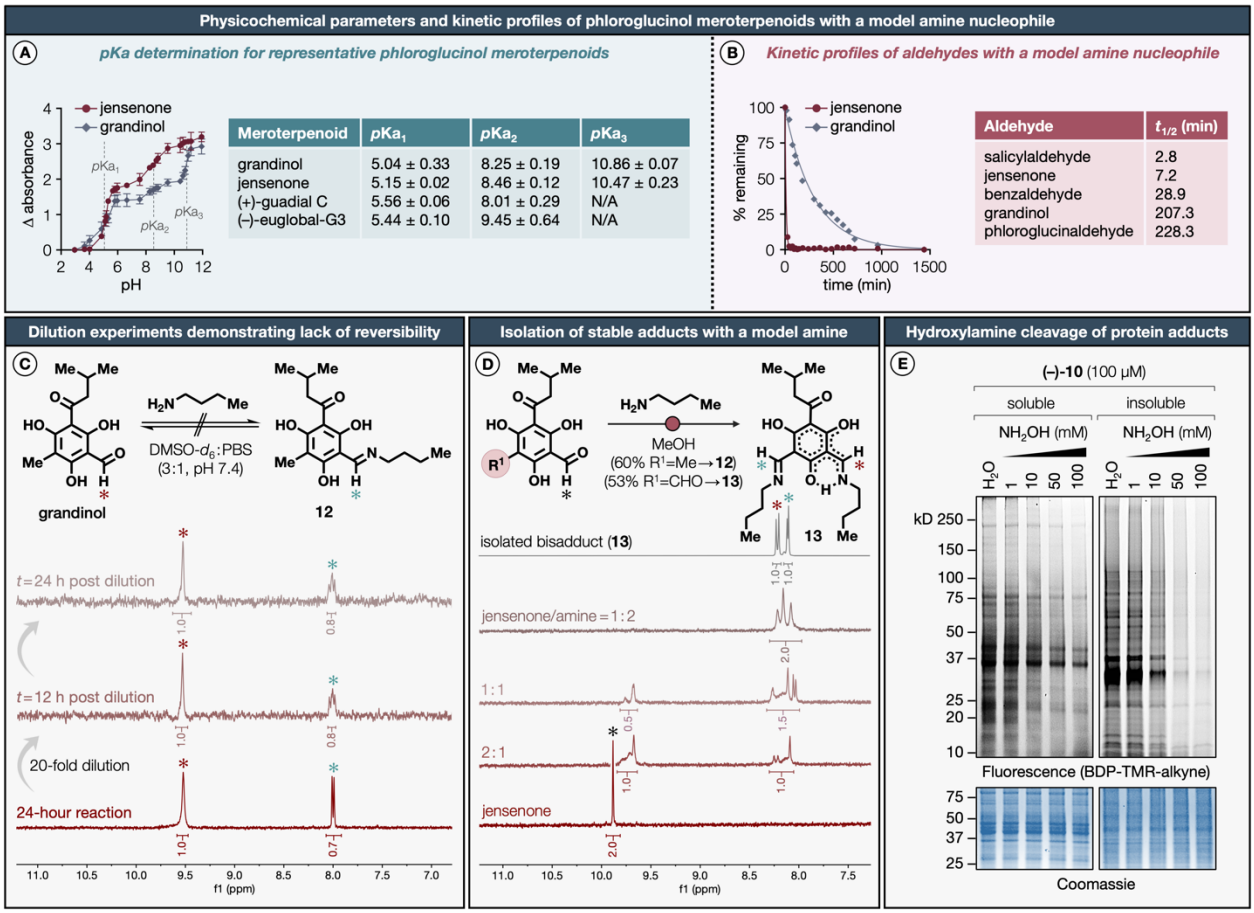

Extended Data Figure S2. Physicochemical and kinetic studies of representative meroterpenoids with a model amine nucleophile. (A) Plots of the total absorbance difference versus pH with corresponding tabulated pK_a values for representative meroterpenoids. Data shown are representative of three independent experiments (n=3). (B) Kinetic profiles of selected meroterpenoids and analogous aldehydes with corresponding tabulated half-life ($t_{1/2}$) values. As an example, grandinol (10 mM) was treated with butylamine (100 mM) in DMSO-d_6:D_2O (3:1) and monitored over the course of 24 hours by ^{1}H-NMR. (C) ^{1}H-NMR spectra demonstrating lack of reversible addition of butylamine to grandinol. For example, grandinol (10 mM) was treated with butylamine (20 mM) in DMSO-d_6:D_2O (3:1) for 24 hours (*bottom spectrum*). Upon 20-fold dilution with DMSO-d_6:PBS (3:1, pH 7.4), ^{1}H-NMR spectra were recorded at different time points. Representative acquired spectra are shown for 12 hours (*middle spectrum*) and 24 hours (*top spectrum*) following dilution. Red and blue asterisks indicate protons used to determine ratios of grandinol and butylamine adduct **12**. (D) *Top:* Isolation of grandinol-butylamine monoadduct (**12**) and jensenone-butylamine bisadduct (**13**) in a 60% and 53% yield, respectively. Bisadduct **13** was isolated as an inseparable 1:1 mixture of imine/enaminone tautomers. *Bottom:* Nonisolable jensenone-butylamine monoadduct can be detected by ^{1}H-NMR in reactions with substoichiometric amounts of butylamine. (E) Dose-dependent hydroxylamine cleavage of meroterpenoid-protein adducts. MDA-MB-231 cells were treated with (–)-**10** (100 μM, 8 h), harvested, lysed, and separated into soluble and insoluble fractions. Following CuAAC with BDP-TMR-alkyne, cellular lysates were quenched with Laemmli buffer (4×) and subjected to hydroxylamine treatment at indicated concentrations (1 h, 20 °C). Samples were resolved by SDS-PAGE and analysed by in-gel fluorescence scanning. For a detailed description of kinetic and physicochemical studies, including spectral analysis and tautomeric structural assignments by two-dimensional NMR, see pages S32–S45 and S95–S108.

In-gel fluorescence profiling of clickable phloroglucinol meroterpenoid probes in breast cancer cells (supplemental discussion related to Figure 2).

BRCA1 is a pivotal tumor suppressor gene integral to a multitude of biological processes, most notably the maintenance of genomic fidelity in the nucleus. Germline mutations in BRCA1 account for an estimated 30% of hereditary breast cancers, and confer the highest identifiable lifetime risk for the onset of breast and ovarian cancers, ranging from 56 to 80%.[17-20] TNBC constitutes approximately 15% of all breast cancer cases and represents the most aggressive and invasive subtype.[21] This subtype comprises the largest fraction of BRCA-deficient breast tumors,[22] with more than 80% of BRCA1-associated breast cancers corresponding to TNBC.[23,24]

Competitive profiling experiments were generally performed as follows: MDA-MB-231 cells were treated at different concentrations of (–)-euglobal-G4 for 8 hours, followed by in-cell labelling with (–)-**11** at 10 μM for an additional 4 hours, and analysis by SDS–PAGE and in-gel fluorescence scanning (also see pages S16-S17).

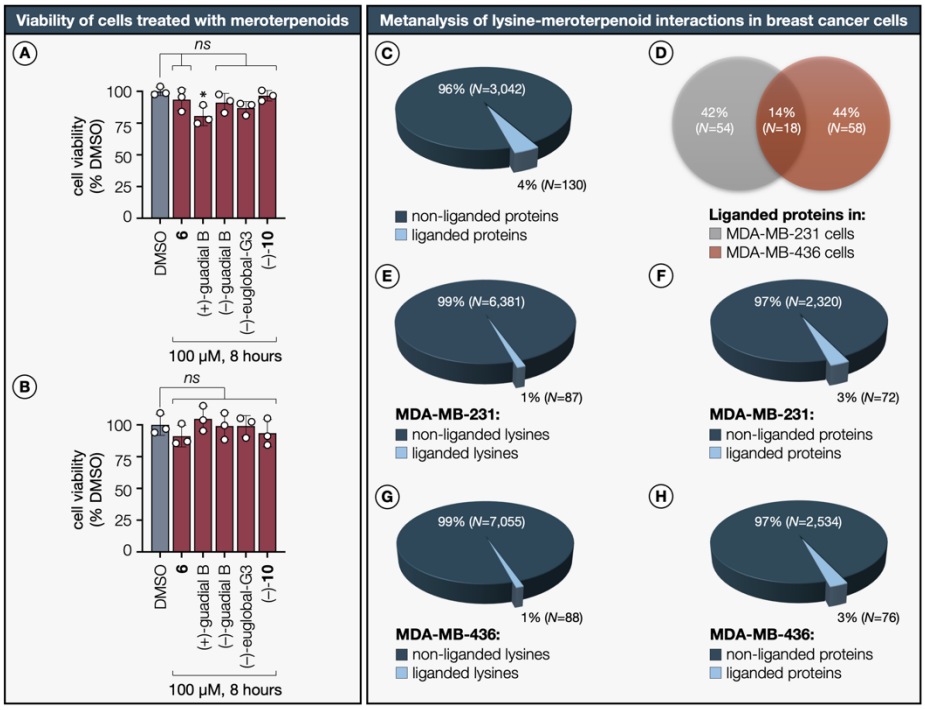

Extended Data Figure S3. (A) Viability of MDA-MB-231 breast cancer cells treated with representative meroterpenoids and clickable probes (100 μM, 8 h). (B) Viability of MDA-MB-436 breast cancer cells treated with representative meroterpenoids and clickable probes (100 μM, 8 h). (C) Fraction of total quantified proteins liganded by natural products. (D) Overlap of liganded proteins in MDA-MB-231 and MDA-MB-436 cells. (E) Fraction of total quantified lysines liganded by natural products in MDA-MB-231 cells. (F) Fraction of total quantified proteins liganded by natural products in MDA-MB-231 cells. (G) Fraction of total quantified lysines liganded by natural products in MDA-MB-436 cells. (H)Fraction of total quantified proteins liganded by natural products in MDA-MB-436 cells.

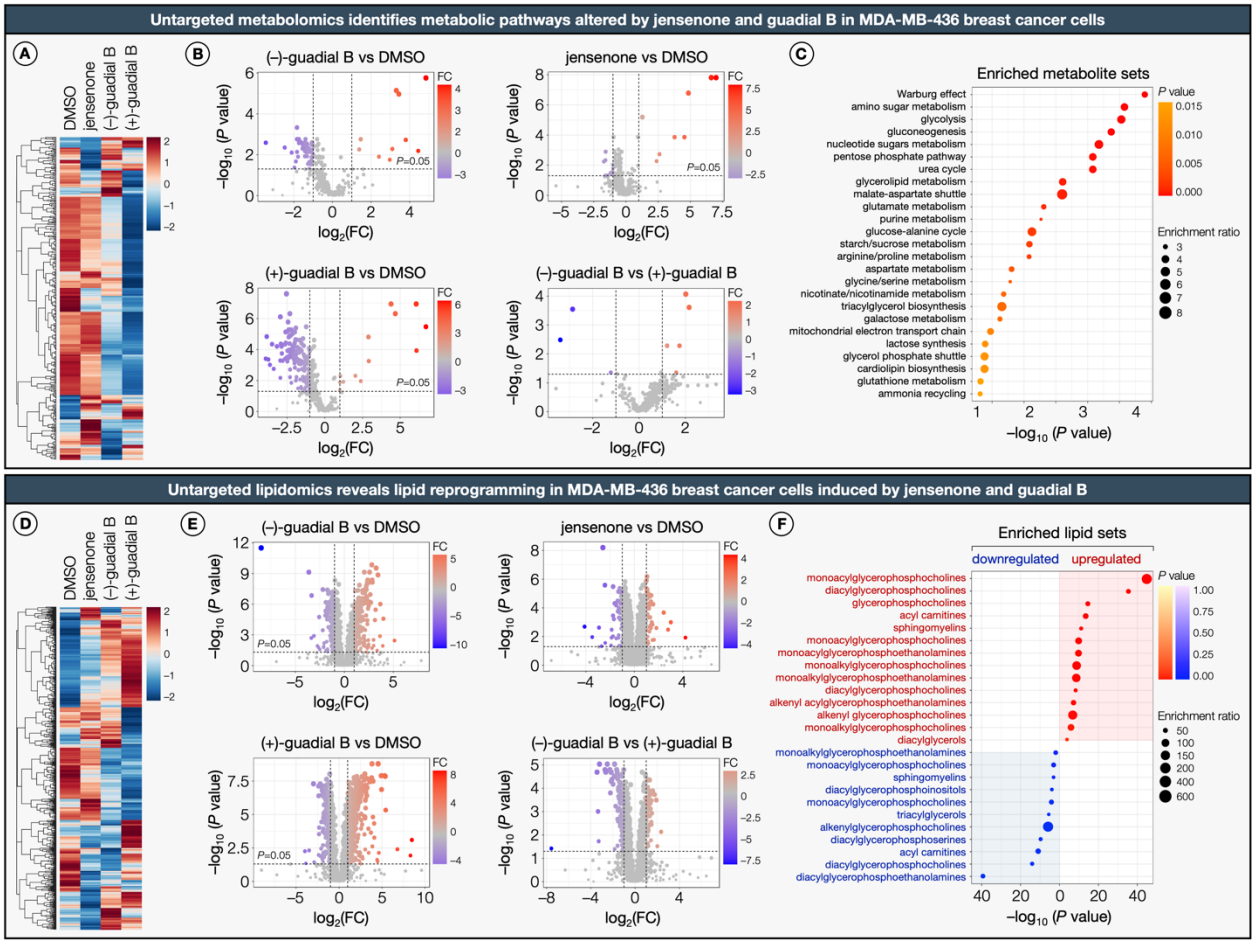

Extended Data Figure S4. (A) Hierarchical clustering heatmap (Euclidean distance, complete-linkage method) of identified metabolites in MDA-MB-436 cells treated with representative phloroglucinol meroterpenoids (also see Supplementary Dataset). Shades of red and blue represent upregulation and downregulation of a metabolite, respectively. (B) Volcano plots depicting statistically significant (false discovery rate-corrected *P* value < 0.05 and fold change > 2.0) altered metabolites in MDA-MB-436 cells treated with jensenone and guadial B. *P* values were determined by Student's t-test (two-tailed, two-sample equal variance). Blue circles represent metabolites selectively downregulated by meroterpenoids, red circles represent metabolites selectively upregulated by meroterpenoids, grey circles represent metabolites with no significant difference. Data represent average values ± SD, n=6 per group from six biologically independent experiments. FC, fold change. (C) Top-25 metabolic pathway enrichment of metabolites significantly altered by representative phloroglucinol meroterpenoids. Colors represent the statistical significance (*P* value) of the enriched pathways, and point size represents the enrichment ratio of matched metabolites and total metabolites in the corresponding pathway. (D) Hierarchical clustering heatmap (Euclidean distance, complete-linkage method) of identified lipid species in MDA-MB-436 cells treated with representative phloroglucinol meroterpenoids (also see Supplementary Dataset). Shades of red and blue represent upregulation and downregulation of a lipid, respectively. (E) Volcano plots depicting statistically significant (false discovery rate-corrected *P* value < 0.05 and fold change > 2.0) altered lipid species in MDA-MB-436 cells treated with jensenone and guadial B. *P* values were determined by Student's t-test (two-tailed, two-sample equal variance). Blue circles represent metabolites selectively downregulated by meroterpenoids, red circles represent metabolites selectively upregulated by

meroterpenoids, grey circles represent metabolites with no significant difference. Data represent average values ± SD, n=6 per group from six biologically independent experiments. FC, fold change. (F) Top-25 enriched lipid species significantly upregulated and downregulated by representative phloroglucinol meroterpenoids. Shades of red and blue represent upregulation and downregulation of a lipid, respectively. Point size represents the enrichment ratio of matched lipid species and total lipids in the corresponding pathway.

Functional impact and structure-activity relationship for phloroglucinol meroterpenoid engagement of lysine K373 in the lysophosphatidylserine lipase ABHD12 (supplemental discussion related to Figure 6 and Extended Data Figure S5).

Given that the intracellular distribution of phosphatidylserine (PS) is largely confined to the ER and mitochondrial membranes,[25] and considering that lyso-PS homeostasis is governed by the interplay between ABHD12 and ABHD16A[26] — which itself mediates ER-associated mitochondrial constriction for fission and fusion[27] — it can be hypothesized that ABHD12 may serve a crucial function in regulating mitochondrial dynamics. This supposition is further substantiated by the striking phenotypic similarities between PHARC (polyneuropathy, hearing loss, ataxia, retinitis pigmentosa, cataract) – a disease caused by mutations in ABHD12[28] – and mitochondrial disorders such as NARP (neuropathy, ataxia, retinitis pigmentosa) and Kearns-Sayre syndrome (ophthalmoplegia, retinal pigmentation, ataxia, peripheral neuropathy).[29]

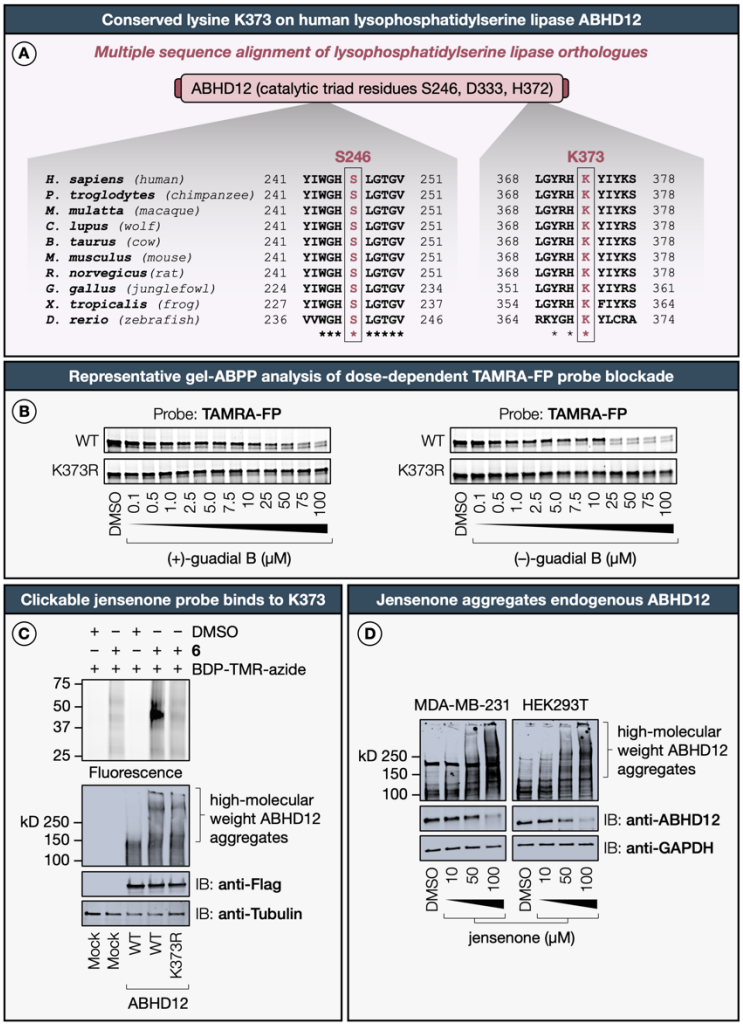

Extended Data Figure S5. (A) Multiple sequence alignment of lysophosphatidylserine lipase orthologues across multiple vertebrate species. (B) Representative in-gel fluorescence data for (+)-guadial B (*left*) and (–)-guadial B (*right*) showing dose-dependent blockade of TAMRA-FP probe labelling of recombinantly expressed Flag-tagged WT and K373R mutant forms of ABHD12 in HEK293T cell lysates. (C) Clickable probe **6** (100 μM, 8 h, 37 ºC) specifically binds to K373 in the recombinantly expressed WT-ABHD12, but not in the K373R mutant, further reinforcing the specificity of the K373-jensenone interaction. Analogous to jensenone, clickable probe **6** induced high-molecular weight ABHD12 aggregation in a K373-independent manner. (D) Jensenone (10 μM, 50 μM, 100 μM, 1 h, 37 ºC) triggers high-molecular weight ABHD12 aggregation with endogenous ABHD12 in MDA-MB-231 and HEK293T cell lines, characterized by a marked reduction in the monomeric form of ABHD12 and a concomitant increase in high molecular weight ABHD12 aggregates following dose-dependent administration of jensenone.

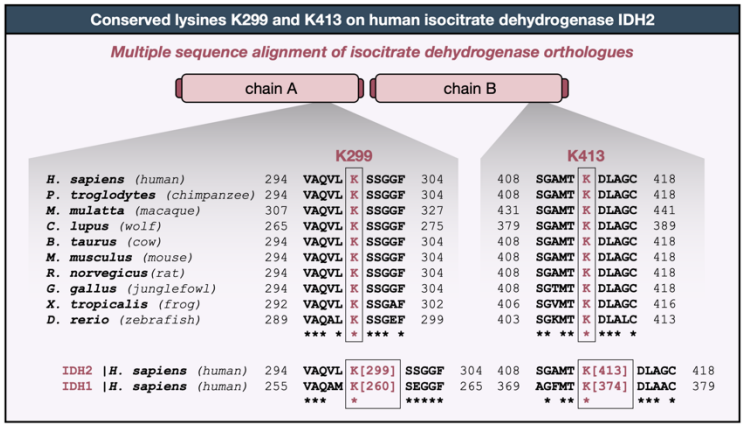

Extended Data Figure S6. Multiple sequence alignment of isocitrate dehydrogenase orthologues across multiple vertebrate species.

Supplemental discussion related to Conclusions and Perspective

During this study, we have noted a compelling concordance between proteins harbouring liganded lysines and the physicochemical and kinetic attributes of phloroglucinol meroterpenoids. First, our kinetic observations substantiate that the rate of meroterpenoid-lysine adduct formation is modulated by the balance between electron-donating phenolic and electron-withdrawing carbonyl groups present within the phloroglucinol core. This distinct reactivity pattern was detected by chemical proteomics, whereby natural products were found to engage discrete sets of liganded lysines and displayed marked differences in their overall lysine reactivity. Second, the measured pKa values for phloroglucinol meroterpenoids indicate that these natural products may predominantly adopt anionic forms under physiological pH, thereby bearing profound biological implications. This negatively charged core and lipophilic terpenoid framework may mimic lipid architectures, potentially facilitating interactions with proteins implicated in lipid metabolic pathways. This proposition finds support in our analysis of biological processes through GO-term enrichment of proteins harbouring liganded lysines, where lipid metabolism emerged as the most prominently enriched term. In the concurrent analysis, the second most prominently enriched term was translation, underpinned by the abundance of RNA-binding proteins bearing liganded lysines. This could be rationalized by considering the resemblance between the richly oxygenated anionic core of phloroglucinol meroterpenoids and the negatively charged RNA ribose-phosphate backbone. Given the pronounced predilection for positively charged lysine residues in the amino acid composition at the RNA-protein complex interface,[30] it is plausible that this electrostatic preference may serve as a guiding factor in directing meroterpenoids toward such interfaces. This may provide an unprecedented opportunity in the development of precision chemical tools with specificity for RNA-binding proteins and on-target potency gained through covalent modification. Finally, we noted the analogous structural and physicochemical features shared between phloroglucinol meroterpenoids and ubiquinol that may function as prognostic determinants for their subcellular trafficking to mitochondria and subsequent engagement with mitochondrial proteins. This assertion was substantiated by term enrichment analyses, revealing the presence of liganded lysines in proteins linked to key mitochondrial metabolic pathways and implicated in mitochondrial pathologies, and subsequently validated by cell imaging.

Our study reveals SARs that point to unique and substantial contributions arising not only from the reactivity and recognition elements but also from the absolute stereochemical configuration of phloroglucinol meroterpenoids. For instance, the evolutionarily conserved lysines in the allosteric nucleotide effector site across the PFK1 family, combined with our initial evidence of enantiodivergent SAR for phloroglucinol meroterpenoid interactions with K677, K678 and K688 in PFKL, PFKM and PFKP, respectively, indicates the potential to create covalent probes with subtype selectivity for individual PFK1s. The molecular understanding of PFK isoform selectivity, coupled with future studies of meroterpenoids, could open the door to selective inactivation of PFK isoforms, and the development of new pharmacological therapies for diabetes and cancer.

Finally, in view of our findings, it is compelling to postulate that phloroglucinol meroterpenoids may function as chemical probes to explore the potential link between BRCA1 mutational status and the regulation of mitochondrial dynamics and mitophagy.[31] Recent studies corroborate this

line of inquiry; one report has revealed that BRCA1 deficiency causes aberrant mitochondrial dynamics and impairs mitophagy,[32] another study has elucidated BRCA1 degradation in response to mitochondrial damage in breast cancer cells,[33] while a recent report presented the inhibitory effect of related meroterpenoids on mitochondrial depolarization. Efforts to further delineate the role of phloroglucinol meroterpenoids in this context are ongoing.

Biological Materials and Methods

Cell culture

HEK293T (CRL-3216), MDA-MB-231 (HTB-26), and MDA-MB-436 (HTB-130) cell lines were purchased from ATCC, tested negative for mycoplasma contamination, and were used without further authentication. All cells were grown at 37 °C with a humidified 5% CO_2 atmosphere in DMEM (Corning, 15-013-CV) supplemented with 10% (v/v) fetal bovine serum (Corning, 35-011-CV), penicillin (100 $U \cdot mL^{-1}$), streptomycin (100 $\mu g \cdot mL^{-1}$), and GlutaMAX™ (2 mM, Gibco, 35050061). All the cell lines were maintained at a low passage number (<15 passages).

Treatment of live cells with natural products

MDA-MB-231 or MDA-MB-436 cells were grown in 15-cm tissue culture dishes to 95% confluency under standard conditions. Cell media was replaced with fresh media (20 mL) containing natural products at the indicated concentrations or the DMSO vehicle, with the total DMSO content maintained <0.2%. Cells were then harvested in cold Dulbecco's phosphate-buffered saline (DPBS, Corning, 21-031-CV) by scraping, centrifuged (1,400 × g, 3 min, 4 °C), and cell pellets were washed with cold DPBS (2×). Pellets were either directly processed or kept frozen at −80 °C until further use.

CuAAC-based protocol for fluorescence microscopy imaging in fixed cells

MDA-MB-231 cells (3×10^5) were seeded into a 35-mm glass bottom dish (MatTek) the day before treatment. Cell media was replaced with fresh media (2 mL) containing a clickable probe at a final concentration of 100 µM and incubated for 8 hours at 37 °C and 5% CO_2. Cells were washed with DPBS at ambient temperature (2×), fixed with 4% formaldehyde in DPBS for 20 min with gentle rocking in the dark, and washed again with DPBS (2×). CuAAC reagents were premixed prior to their addition to the proteome samples. BDP-TMR-alkyne (Lumiprobe, B24B0) (40 µL of 1.25 mM stock in DMSO to a final concentration of 5 µM), $CuSO_4$ (200 µL of 50 mM stock in H_2O to a final concentration of 1 mM), tris(benzyltriazolylmethyl)amine ligand (600 µL of a 100 µM stock in DMSO/^{t}BuOH 1:4 to a final concentration of 100 µM), and sodium ascorbate (500 µL of freshly prepared 50 mM stock in H_2O to a final concentration of 2.5 mM) were combined in a 15-mL centrifuge tube and diluted to 10 mL with 0.1% Triton-X and 5% BSA in DPBS. CuAAC reagents (2 mL) were added to fixed cells and incubated for 30 min with gentle rocking in the dark and washed with 0.1% Triton-X, 5% BSA in DPBS (2×). NucBlue™ Fixed Cell ReadyProbes™ (2 drops, DAPI, R37606) and MitoView™ Green (2 drops, Biotium, 70054) in 0.1% Triton-X, 5% BSA in DPBS (2 mL) were added and incubated for 30 min with gentle rocking in the dark and washed with 0.1% Triton-X, 5% BSA (2×). Finally, samples were mounted with ProLong™ Glass Mountant and cured overnight at ambient temperature in the dark. Cells were imaged using the BioTek Cytation 5 plate reader following manufacturer's instructions (BioTek Instruments, Winooski, VT, BTCYT5MPW) and Gen5 Image+ Software (Version 3.10.06).

CuAAC-based protocol for in-gel fluorescence

Alkyne- or azide-tagged probe-treated cells were lysed by sonication (Qsonica Q700, 1 × Amplitude = 100, Process time = 20 sec, Pulse-ON time = 2 sec, Pulse-OFF time = 1 sec, 4 °C) and fractionated (100,000 × g, 1 h, 4 °C) to yield soluble (supernatant) and insoluble (pellet) fractions. After separation, insoluble pellets were resuspended in cold DPBS by sonication.

Soluble and insoluble fractions were then normalized to 1.0 mg·mL^{-1} using the DC Protein Assay II (BioRad, 5000112) and the absorbance was measured using a BioTek Cytation 5 plate reader following manufacturer's instructions (BioTek Instruments, Winooski, VT, BTCYT5MPW). Samples were next conjugated to the fluorophore using a CuAAC reaction. CuAAC reagents were premixed prior to their addition to the proteome samples. BDP-TMR-alkyne (Lumiprobe, B24B0) or BDP TMR azide (22430) (15 µL of 1.25 mM stock in DMSO to a final concentration of 100 µM), tris(benzyltriazolylmethyl)amine ligand (45 µL of 1.7 mM stock in DMSO/^{t}BuOH 1:4 to a final concentration of 100 µM), tris(2-carboxyethyl)phosphine hydrochloride (15 µL of freshly prepared 50 mM stock in H_2O to a final concentration of 1 mM) and $CuSO_4$ (15 µL of 50 mM stock in H_2O at a final concentration of 1 mM) were combined in an Eppendorf tube, vortexed and added to the samples (6 µL per 50 µl sample), which were incubated at ambient temperature for 1 hour. Protein lysate was heated at 95 °C for 10 min in Laemmli sample buffer (4×). Proteins were resolved by 4-20% SDS-PAGE gels (BioRad, 4561096), visualized using the ChemiDoc™ MP Imaging System (BioRad, 12003154) for in-gel fluorescence analysis, and stained with GelCode™ Blue Stain Reagent (ThermoScientific, 24590).

Hydroxylamine cleavage of meroterpenoid-protein adducts by in-gel fluorescence

Solutions of hydroxylamine at the following concentrations were prepared: 0.05, 0.50, 2.5, and 5 M. Preparation of cell lysates and subsequent CuAAC conjugation were performed as above. Protein lysates were quenched with Laemmli sample buffer (4×) and subjected to treatment with hydroxylamine at the indicated final concentrations for 1 hour at ambient temperature. Proteins were then resolved by 4-20% SDS-PAGE gels (BioRad, 4561096), visualized using the ChemiDoc™ MP Imaging System (BioRad, 12003154), and stained with GelCode™ Blue Stain Reagent (ThermoScientific, 24590).

Competitive gel-based ABPP in live cells

MDA-MB-231 cells were grown to 95% confluency under standard conditions. Media was aspirated and replaced with 20 mL of fresh media containing (–)-euglobal G4 at the indicated concentrations or DMSO vehicle for 8 hours, maintaining DMSO content <0.2%. Media was then aspirated and replaced with 20 mL of fresh media containing clickable probe (–)-**11** at a final concentration of 10 µM for 4 hours. Cells were washed and scraped with cold DPBS, cell pellets were isolated by centrifugation (1,400 × g, 3 min, 4 °C), and subsequently frozen at –80 °C until further use. Cell pellets were processed as above for in-gel fluorescence analysis.

Competitive gel-based ABPP in recombinantly expressed cellular lysates

Transiently transfected HEK293T cells were harvested 48 hours after transfection in DPBS on ice. Cell pellets were sonicated using a Qsonica Q700 sonicator (1 × Amplitude = 100, Process time = 40 sec, Pulse-ON time = 2 sec, Pulse-OFF time = 1 sec) at 4°C. Cellular lysates were then normalized for total protein concentration using the DC Protein Assay Kit II (BioRad, Hercules, CA, 5000112) to 0.25 mg·mL^{-1} for ABHD12 or 0.3 mg·mL^{-1} for PFKP. Small molecules or DMSO vehicle were added at the indicated final concentrations and incubated for 1 hour at ambient temperature. Lysates were then treated with NHS-fluorescein (carboxyfluorescein succinimidyl ester) (**P1**) at a final concentration of 1 µM (ThermoScientific, 46409) or ActivX™ TAMRA-FP serine hydrolase probe at a final concentration of 0.5 µM (ThermoScientific, 88318) for 1 hour at ambient temperature and quenched with Laemmli sample buffer (4×). Proteins were resolved by

10% or 4-20% SDS-PAGE gels (BioRad, 5671035), visualized using the ChemiDoc™ MP Imaging System (BioRad, 12003154) for in-gel fluorescence analysis. Fluorescence was normalized to loading control by western blotting and relative band intensities were quantified using ImageJ software (https://imagej.nih.gov/ij/). Percentage inhibition was calculated relative to the positive and negative control and used to calculate IC_{50} values.

Western blot analysis

Cell lysates were prepared as indicated above for each protein analysis prior to normalization of total protein concentration using the DC Protein Assay Kit II (BioRad, Hercules, CA, 5000112). Proteins were resolved using either 10% or 4-20% SDS-PAGE gels (BioRad) and transferred to 0.2 µm nitrocellulose membrane (BioRad, 1704270 and 1704271). The membrane was blocked with 5% non-fat dry milk (BioRad, 1706404XTU) in Tris-buffered saline (20 mM Tris-HCl, 150 mM NaCl, pH 7.6) with Tween20 (TBST) buffer (0.1% Tween20, 20 mM Tris-HCl, pH 7.6, 10 mM NaCl) for 1 hour at ambient temperature with gentle rocking. Primary antibodies were diluted with 5% non-fat dry milk in TBST buffer in the following ratios: anti-HA (1:5000, Cell Signaling Technology), anti-FLAG (1:5000, Cell Signaling Technology), anti-PFKP (1:5000, Bio-Rad VMA00145), anti-β-actin (1:5000, LI-COR), anti-IDH2 (1:5000, Cell Signaling Technology), anti-ABHD12 (1:1500, Abcam) and anti-α-tubulin (1:5000, Cell Signaling Technology) before incubation overnight at 4°C with gentle rocking. Membranes were washed with TBST buffer (3×, 5 min) before the appropriate secondary antibodies (1:5000, LI-COR, 926-32211, 926-32212, 926-68071, 926-68072) were diluted with 5% non-fat dry milk in TBST buffer and incubated for 1 hour at ambient temperature with gentle rocking. Membranes were washed with TBST (3×, 5 min) prior to visualization using ChemiDoc™ MP Imaging System (BioRad, 12003154). Relative band intensities were quantified using ImageJ software (https://imagej.nih.gov/ij/).

Table S1. Subcloning primers

Protein	Fwd/Rev	Sequence
IDH2	Fwd	ctgcaggtcgacgATGGCCGGCTACCTGCGGG
IDH2	Rev	gttgacgcggccgcCTACTGCCTGCCCAGGGCTCTG

Table S2. Mutagenesis primers

Protein	Mutation	Fwd/Rev	Sequence
ABHD12	K373M	Fwd	CAGACCTTGGCTACAGGCACatgTACATTTACAAGAGC
ABHD12	K373M	Rev	catGTGCCTGTAGCCAAGGTCTGAATGAAAGGGC
ABHD12	K373R	Fwd	CAGACCTTGGCTACAGGCACaggTACATTTACAAGAG
ABHD12	K373R	Rev	cctGTGCCTGTAGCCAAGGTCTGAATGAAAGGG
ABHD12	S246A	Fwd	GTACATCTGGGGCCACgccCTGGGCACTG
ABHD12	S246A	Rev	ggcGTGGCCCCAGATGTACACGGGGTTGTCAC
IDH2	R140Q	Fwd	GAAAAGTCCCAATGGAACTATCcagAACATCCTGGGGG
IDH2	R140Q	Rev	ctgGATAGTTCCATTGGGACTTTTCCACATCTTCTTCAGC
IDH2	K299M	Fwd	GACATGGTGGCTCAGGTCCTCatgTCTTCGGGTG
IDH2	K299M	Rev	catGAGGACCTGAGCCACCATGTCATCAATGAGCCG

IDH2	K299R	Fwd	GACATGGTGGCTCAGGTCCTCaggTCTTCGGGTG
IDH2	K299R	Rev	cctGAGGACCTGAGCCACCATGTCATCAATGAGCCG
IDH2	K413R	Fwd	GAGAGTGGAGCCATGACCaggGACCTGGC
IDH2	K413R	Rev	cctGGTCATGGCTCCACTCTCCACCGTCTC
PFKL	K315R	Fwd	GATCCTGAGCAGCcggATGGGCATGGAG
PFKL	K315R	Rev	ccgGCTGCTCAGGATCCGGTCGAAGG
PFKL	K677R	Fwd	GACCGGAACTATGGGACCaggCTGGGGGTG
PFKL	K677R	Rev	cctGGTCCCATAGTTCCGGTCAAAGGGGGTTGG
PFKL	K681R	Fwd	CTGGGGGTGcggGCCATGCTGTGGTTGTCG
PFKL	K681R	Rev	ccgCACCCCCAGCTTGGTCCCATAGTTCCGG
PFKM	K678R	Fwd	ATAGGAATTTTGCCACTaggATGGGCGCCAAGG
PFKM	K678R	Rev	cctAGTGGCAAAATTCCTATCAAATGGGGTTGGGCTC
PFKP	K688R	Rev	cctGGTTCCAAAGTTTCTATCAAATGGAGAGGGTGCC
PFKP	K688R	Fwd	GATAGAAACTTTGGAACCaggATCTCTGCCAGAGCTATGG

Functional characterization of IDH2

Subcloning and site-directed mutagenesis

To generate pRK5-IDH2^{WT}, IDH2^{WT} was amplified by PCR from pcDNA3.1-entry vector (Addgene, 87926). Gene products were subcloned into the pRK5 vector with a C-terminal FLAG tag using SalI (N-terminal) and NotI (C-terminal) restriction sites. DNA was amplified with custom forward and reverse primers (**Table S1**) using Phusion Polymerase (ThermoScientific, F-530L), following the manufacturers' instructions, digested with the indicated restriction enzymes, and ligated into the pRK5 vector with the appropriate affinity tag. Mutants were generated using QuikChange site-directed mutagenesis with Phusion High-Fidelity DNA Polymerase and custom primers that contained the desired mutations and their respective complements (**Table S2**). Identity of all vectors were confirmed by sequencing performed by the Biotechnology Resource Center (BRC) Genomics Facility (RRID:SCR_021727) at the Cornell Institute of Biotechnology (http://www.biotech.cornell.edu/brc/genomics-facility).

Recombinant expression of IDH2 by transient transfection

HEK293T cells were grown to 60% confluency under standard growth conditions in 10-cm tissue culture dishes. To 3-µg of DNA diluted in 300 µL of serum-free DMEM was added 15 µL of aqueous polyethyleneimine 'MAX' (1 mg·mL^{-1}, molecular mass 40,000, polyethylenimine; Polysciences, Inc.). 'Mock' transfected HEK293T cells were transfected with an empty pRK5 vector. The mixture was incubated at ambient temperature for 20 min and added dropwise to the cells. Cells were grown for 48 hours at 37 °C in a humidified 5% CO_2 atmosphere. Cells were then harvested in media, centrifuged (1,400 × g, 3 min, 4 °C), and cell pellets were washed with cold DPBS (3×). Pellets were either directly processed or kept frozen at –80 °C until further use.

IDH2 activity assay

IDH2 oxidative activity assay was conducted as previously reported with minor modifications.[34] Transfected HEK293T cell pellets were sonicated using a Qsonica Q700 sonicator (1 × Amplitude = 100, Process time = 40 sec, Pulse-ON time = 2 sec, Pulse-OFF time = 1 sec) at 4 °C. Lysates

were then normalized for total protein concentration using the DC Protein Assay Kit II (BioRad, Hercules, CA, 5000112) to 0.25 mg·mL^{-1} and promptly used. IDH2 oxidative activity (WT-IDH2) was determined by incubating meroterpenoids or DMSO vehicle at the indicated final concentrations for 1 hour at 37 °C and admixing 2.5 µg of cellular lysates with 100 µL of assay buffer (33 mM Tris-acetate buffer, pH 7.4, 1.3 mM $MgCl_2$, 0.33 mM EDTA, 100 µM NADP, and 1.3 mM *D*-(+)-*threo*-isocitrate). The increase in 340 nm absorbance over time was measured to assess NADPH production. IDH2 reductive activity was determined by incubating meroterpenoids or DMSO vehicle at the indicated final concentrations for 2 hours at 25 °C and admixing 20 µg of cellular lysates with 200 µL of assay buffer (33 mM HEPES buffer, pH 7.5, 1.3 mM $MgCl_2$, 25 µM NADPH, and 600 µM α-ketoglutarate). The decrease in 340 nm absorbance over time was measured to assess NADPH consumption. Triplicate reactions were measured every 60 seconds for 30 min or 1 hour, respectively, at 340 nm using a microplate spectrophotometer (BioTek Instruments, Winooski, VT, BioTek Cytation 5, BTCYT5MPW) and Gen5 Image+ Software (Version 3.10.06). The slope of the linear regression of the linear portion of the absorbance over time was used as the measure of activity. Apparent activity was calculated relative to the WT- and Mock-transfected cells. Percentage inhibition was calculated relative to the positive and negative control and used to calculate IC_{50} values by non-linear regression analysis from a dose–response curve generated using GraphPad Prism 9.

Functional characterization of ABHD12

Site-directed mutagenesis

ABHD12 cDNA clone (SinoBiological, HG22745-CF) was used for PCR amplification. Mutants were generated using QuikChange site-directed mutagenesis with Phusion High-Fidelity DNA Polymerase and custom primers that contained the desired mutations and their respective complements (**Table S2**). Identity of all vectors were confirmed by sequencing performed by the Biotechnology Resource Center (BRC) Genomics Facility (RRID:SCR_021727) at the Cornell Institute of Biotechnology (http://www.biotech.cornell.edu/brc/genomics-facility).

Recombinant expression of ABHD12 by transient transfection

HEK293T cells were grown to 60% confluency under standard growth conditions in 10-cm tissue culture dishes. To 3-µg of DNA diluted in 300 µL of serum-free DMEM was added 15 µL of aqueous polyethyleneimine 'MAX' (1 mg·mL^{-1}, molecular mass 40,000, polyethylenimine; Polysciences, Inc.). 'Mock' transfected HEK293T cells were transfected with an empty pcDNA3.1 vector. The mixture was incubated at ambient temperature for 20 min and added dropwise to the cells. Cells were grown for 48 hours at 37 °C in a humidified 5% CO_2 atmosphere. Cells were then harvested in cold DPBS by scraping, centrifuged (1,400 × g, 3 min, 4 °C) and cell pellets were washed with cold DPBS (2×). Pellets were either directly processed or kept frozen at –80 °C until further use.

Sample preparation for ABHD12 activity assay

The lyso-PS lipase activity of ABHD12 was determined as previously described.[35] Transfected HEK293T cell pellets were sonicated using a Qsonica Q700 sonicator (1 × Amplitude = 100, Process time = 40 sec, Pulse-ON time = 2 sec, Pulse-OFF time = 1 sec) at 4 °C. The proteome concentrations were adjusted to 0.25 mg·mL^{-1} in DPBS (80 µL per reaction). Cellular lysates were then treated with meroterpenoids at indicated final concentrations for 1 hour at 37 °C. 20 µL of

500 µM 17:1 lyso-PS (Avanti Polar Lipids, Birmingham, AL, 858141) in DPBS was added to each reaction (100 µM final concentration) and incubated at 37 °C for 20 min. The reaction was quenched with 400 µL of 2:1 $CHCl_3$/MeOH (v/v) with 1 nmol pentadecylic acid (15:0) (CAS: 1002-84-2) as an internal standard. The mixture was vortexed and centrifuged at 1,400 × g to separate the aqueous and organic phase. The organic phase was dried under a stream of nitrogen gas and resolubilized in 150 µL of 2:1 $CHCl_3$/MeOH for LC-MS/MS analysis. In the ABHD12 activity assay, a Mock-expressed control group was utilized to account for the background activity contributed by endogenously expressed ABHD12. This background activity was subtracted from the measurements obtained for cells expressing WT and mutant ABHD12 enzymes, enabling for an accurate assessment of the specific impact of the K373R mutation on enzyme activity in a biologically relevant context. This approach was chosen to assess relative changes in enzyme activity in a biologically relevant context, providing insights into the physiological implications of the K373R mutation.

LC-MS/MS analysis

Samples were analyzed on an Exion HPLC system coupled to an X500B QTOF mass spectrometer (AB Sciex LLC, Framingham, MA) with an ESI source operated in negative ion mode. A reverse-phase liquid chromatography on a Gemini 5U C18 column (50 × 4.6 mm i.d., 5 µm; Phenomenex) was used for LC separation. Solvent A was 95:5 water/MeOH + 0.1% ammonium hydroxide (NH_4OH) in water, and solvent B was 60:35:5 isopropyl alcohol /MeOH/H_2O + 0.1% NH_4OH. The linear gradient used for the LC method was: 0-1.4 min, 100% solvent A at flow rate 0.1 mL·min^{-1}; 1.5-6.5 min, from 0% to 100% solvent B at flow rate 0.5 mL·min^{-1}; 6.5-12 min, 100% solvent B at flow rate 0.5 mL·min^{-1}; 12-15 min, 100% solvent A at flow rate 0.5 mL·min^{-1} for equilibration. Samples (2-6 µL) were injected for LC-MS analysis. The parameters of X500B MS instrument and its multiple reaction monitor (MRM) were optimized by infusing 1 mM 15:0, an internal standard (IS) at 2 µL·min^{-1} that was tee-in 50% B solvent delivered at 500 µL·min^{-1} by the Exion LC. The electrospray voltage was set at –3.8 kV and the temperature of the heated capillary was set at 450 °C. It was operated under the Ion Source gas1 at 40 psi and gas2 at 30 psi, CAD gas at 7 (arbitrary unit). The declustering potential (DP) was set to –90V with accumulation time of 0.15 s for MS full scan from m/z 100 to m/z 800 in profile mode followed by MRM HR scan of three fragment ions for each of the targeted 17:1 and 15:0 IS. The optimized DP and CE by guided MRM HR for each of the three fragment ions from their precursor analyte were used for MRMR HR quantitation with accumulation time at 0.1 s for each transition pair. Collision energy values were optimized to –25–30% for these transitions. The raw data were acquired and processed using Sciex OS 2.0 software. The quantitation ratio of 17:1 / 15:0 IS in each sample was calculated by integrating the peak areas of each top MRM transition signal in the same software and used for quantitative comparison of hydrolysis product in the assay. Meanwhile, a metric plot for IS peak area across all samples under each batch was used for assessment of sample preparation variation and matrix effect. A consistent result with CV <10% was obtained, suggesting data were reliable.

Functional characterization of phosphofructokinase (PFK1) isoforms

Site-Directed Mutagenesis

The following cDNA clones were used for PCR amplification from pCMV vector: PFKP (SinoBiological, HG15003-NY), PFKM (SinoBiological, HG14133-NY), PFKL (SinoBiological,

HG14223-NY). Mutants for each isoform of PFK1 were generated using QuikChange site-directed mutagenesis with Phusion High-Fidelity DNA Polymerase and custom primers that contained the desired mutations and their respective complements (**Table S2**). Identity of all vectors were confirmed by sequencing performed by the Biotechnology Resource Center (BRC) Genomics Facility (RRID:SCR_021727) at the Cornell Institute of Biotechnology (http://www.biotech.cornell.edu/brc/genomics-facility).

Recombinant expression of PFK1 isoforms by transient transfection

HEK293T cells were grown to 60% confluency under standard growth conditions in 10-cm tissue culture dishes. To 3-µg of DNA diluted in 300 µL of serum-free DMEM was added 30 µL of aqueous polyethyleneimine 'MAX' (1 mg·mL^{-1}, molecular mass 40,000, polyethylenimine; Polysciences, Inc.). 'Mock' transfected HEK-293T cells were transfected with an empty pCMV vector. The mixture was incubated at ambient temperature for 25 min and added dropwise to the cells. Cells were grown for 48 hours at 37 °C in a humidified 5% CO2 atmosphere. Cells were then harvested in cold DPBS by scraping, centrifuged (1,400 × g, 3 min, 4 °C) and cell pellets were washed with cold DPBS (2×). Pellets were either directly processed or kept frozen at –80 °C until further use.

PFK activity assay

PFK activity assay was performed with modifications as previously described.[36,37] Briefly, HEK293T pellets with transfected PFK1 isoforms were resuspended in DPBS for PFKL and PFKM or 50 mM HEPES buffer (1 M buffer solution, pH 7.5, ThermoScientific J60712.AK) for PFKP. Cell pellets were sonicated using a Qsonica Q700 sonicator (1 × Amplitude = 100, Process time = 40 sec, Pulse-ON time = 2 sec, Pulse-OFF time = 1 sec) at 4 °C. Lysates were then normalized for total protein concentration using the DC Protein Assay Kit II (BioRad, 5000112) to 0.25 mg·mL^{-1}. Due to documented instability of PFKL in purified form or in cellular lysates,[38,39] each assay was performed using freshly lysed cellular lysates for all PFK1 isoforms. For inhibition experiments, 50 µL of soluble proteome (initial total protein concentration of 0.5 mg·m^{-1}) were incubated with meroterpenoids or DMSO vehicle at the indicated final concentrations and incubated for 1 hour at 20 °C for PFKP and PFKL or 2 hours at 37°C for PFKM. Reactions were diluted with 450 µL of 50 mM HEPES buffer for PFKP and PFKM or 50 mM MOPS (1 M buffer solution, pH 7.5, ThermoScientific, J61843.AP) for PFKL and 10 µL of this mixture was added to a clear 96-well flat-bottom plate (Fisher Scientific, 12565501). An additional 80 µL of 50 mM HEPES (for PFKP and PFKM) or 50 mM MOPS (for PFKL) was added to each well, and then 10 µL of a master mix containing 4 M KCl, 500 mM $MgCl_2$, 100 mM ATP, 20 mM NADH, 500 mM fructose-6-phosphate, aldolase (2 µL of 50U·mL^{-1}), and GDH/TPI (2 µL of a 50U:500U·mL^{-1} mixture) was added to begin the enzymatic reactions. Final concentrations of each master mix component per well were as follows: 80mM KCl, 5mM $MgCl_2$, 1mM ATP, 200uM NADH, 5mM fructose-6-phosphate, 1U aldolase, and 1U:5U GDH/TPI. The absorbance decrease corresponding to consumption of NADH was tracked at 340 nm every minute for 1 hour using a microplate spectrophotometer (BioTek Instruments, Winooski, VT, BioTek Cytation 5, BTCYT5MPW) and Gen5 Image+ Software (Version 3.10.06). The slope of the linear regression of the linear portion of the absorbance over time was used as the measure of activity. Apparent activity was calculated relative to the WT- and Mock-transfected cells. Percentage inhibition was calculated relative to the positive and negative control and used to calculate IC_{50} values by non-linear regression analysis from a dose–response curve generated using GraphPad Prism 9.

TMTpro18plex-based protocol for mapping lysine-meroterpenoid interactions

Treatment in cells and sample preparation (lysis, probe treatment, reduction, alkylation)

MDA-MB-231 and MDA-MB-436 cells were grown to 95% confluence. Media was then aspirated and replaced with 20 mL of fresh media containing the indicated meroterpenoids or DMSO for 8 hours, maintaining DMSO content <0.2%. Cells were washed with cold DPBS (2×), scraped in cold DPBS, and cell pellets were isolated by centrifugation (1,400 × g, 3 min, 4 °C) and frozen at –80 °C until further use. Cells were resuspended in cold solution of DPBS containing Pierce™ Protease and Phosphatase Inhibitor Mini Tablet (ThermoFisher, A32961) or 100 µL Halt™ Protease and Phosphatase Inhibitor Cocktail (ThermoFisher, 78446) (1 tablet or 100 µL per 10 mL), then lysed using a Branson 550 probe sonicator (3 × 10 pulses, 0.4 sec, 40% power, 4 °C) and fractionated (100,000 × g, 1 h, 4 °C) to yield soluble (supernatant) and insoluble (pellet) fractions. Insoluble pellets were separated and resuspended in cold DPBS by sonication. Soluble and insoluble fractions were then normalized to 2.0 $mg \cdot mL^{-1}$ using the DC Protein Assay (BioRad) and absorbance was measured using a BioTek Cytation 5 plate reader following manufacturer's instructions (BioTek Instruments, Winooski, VT, BTCYT5MPW). Normalized cellular lysates were then treated with desthiobiotin-tagged STP ester probe (100 µM) at ambient temperature for 1 hour by rotating end-over-end (20 rpm). Proteins were precipitated with 600 µL of cold methanol (–20 °C), 200 µL of $CHCl_3$ and 100 µL of chilled water (4 °C). Following centrifugation (15,000 rpm, 10 min, 4 °C), a protein disk formed at the interface of $CHCl_3$ and aqueous layers. Both layers were aspirated without perturbing the disk, which was resuspended in cold methanol (600 µL, –20 °C) and $CHCl_3$ (200 µL, 4 °C) by vortexing and sonicator equipped with a horn cup (1 × Qsonica Q700, Amplitude = 100, Process time = 20 sec, Pulse-ON time = 2 sec, Pulse-OFF time = 1 sec, 4 °C). The proteins were pelleted (15,000 rpm, 10 min, 4 °C), and 100 µL of the digestion buffer (8 M urea, 50 mM TEAB, pH 8.5) was added to the resulting pellets. The pellets were resuspended with sonication and agitated on a thermal mixer (65 °C, 10 min, 1,000 rpm). Then, 5 µL of 200 mM dithiothreitol in water was added to each sample, and the mixture was agitated on a thermal mixer (65 °C, 10 min, 1,000 rpm). Next, 10 µL of 100 mM iodoacetamide in water was added to each sample, and the mixture was agitated on a thermal mixer (37 °C, 30 min, 1,000 rpm).

Trypsin/Lysine-C digestion and streptavidin enrichment

40 µg of Pierce™ Trypsin/Lysine-C Protease Mix (ThermoScientific, MS-Grade A40007) was reconstituted in 60 µL of 50 mM acetic acid and 20 µL of 100 mM calcium chloride. Samples were diluted with 400 µL of 50 mM TEAB (ThermoScientific, 90114) and 4 µL of the Trypsin/Lysine-C solution. Proteins were digested with agitation overnight on a thermal mixer (37 °C, 1,000 rpm). To each sample was then added 500 µL of the enrichment buffer (50 mM TEAB, 0.2% IgepalTM CA-630, pH 8.5) containing 50 µL of Pierce™ Streptavidin agarose resin (ThermoFisher, 20353). Samples were enriched by rotating end-over-end (20 rpm) for 3 hours at ambient temperature. Samples were next transferred onto Micro Bio-Spin™ Chromatography Columns (Bio-Rad, 7326204) and washed with the wash buffer (3 × 50 mM TEAB, 150 mM NaCl, 0.1% Igepal™ CA-630), DPBS (3×), and water (3×) by carefully aspirating from the bottom of each Bio-Spin column without drying the resin. Peptides were eluted with 50% acetonitrile in water containing 0.1% formic acid and each sample evaporated to dryness using vacuum centrifugation overnight (Savant, SpeedVac SPD-2030, temperature = 40 °C, vacuum pressure = 5.1 Torr).

TMTpro-18plex labeling

Peptides were redissolved in 100 µL EPPS buffer (200 mM, pH 8.5) with 30% acetonitrile. TMT tags (10 µL per channel in acetonitrile, 20 µg·µL^{-1}) were added to the corresponding tubes and agitated on a thermal mixer (25 °C, 90 min, 1,000 rpm). Each reaction was quenched by the addition of 10 µL of 5% hydroxylamine and mixed (25 °C, 15 min, 1,000 rpm). To each sample, 10 µL of formic acid was added and mixed (25 °C, 5 min, 1,000 rpm). TMT-labeled samples were combined into a single Protein LoBind microcentrifuge tube and evaporated to dryness using vacuum centrifugation.

Peptide desalting

Sep-Pak® C18 cartridges (Waters, WAT054955) were conditioned with acetonitrile (3×) and desalting buffer (3×, 95% water, 5% acetonitrile, 0.5% formic acid). TMT-labeled peptides were redissolved in 500 µL of the desalting buffer, loaded dropwise onto the cartridge, and eluted at the rate of approximately 1 drop per second. The cartridge was then reloaded with the flow-through and subsequently desalted by slowly passing desalting buffer (3 × 1 mL). The peptides were eluted by adding 500 µL of 80% acetonitrile, 20% water, 0.5% formic acid (3×), eluates were combined into a clean Protein LoBind microcentrifuge tube, and sample was evaporated to dryness using vacuum centrifugation.

High pH reverse-phase fractionation

The spin columns for high pH fractionation (Pierce high pH reverse-phase peptide fractionation kit, ThermoScientific, 84868) were pre-equilibrated according to manufacturer's instructions prior to use. Desalted peptides were redissolved in 0.1% trifluoracetic acid aqueous solution and loaded onto the column. The columns were spun down (2,000 × g, 2 min) with eluate retained, washed with 300 µL of water with eluate retained, and subjected to fractionation with a series of 0.1% triethylamine/acetonitrile buffers (2,000 × g, 2 min) with each eluate collected into a clean Protein LoBind tube. The following buffers were used for peptide elution (% acetonitrile): 5, 7, 9, 11, 12, 13, 14, 15, 16, 17, 18, 19, 20, 21, 22, 23, 24, 25, 26, 27, 28, 29, 30, 35, 40, 45, 50, 80. Fractions were evaporated to dryness using vacuum centrifugation, resuspended in water, and peptide concentrations determined using NanoDrop One Spectrophotometer (ThermoScientific, ND-ONEC-W, version 2.2.0.16). Fractions were combined with at least 7 fractions separation to yield 10 total fractions with approximately equivalent peptide amounts, filtered through CoStar Spin-X columns (Corning, 8160) and evaporated to dryness. The resulting 10 fractions were reconstituted in 62 µL of 2% acetonitrile with 0.5% formic acid for subsequent nanoLC-MS/MS analysis.

Nano-scale reverse phase chromatography and tandem MS (nanoLC-MS/MS)

The nanoLC-MS/MS analysis was carried out using an Orbitrap Eclipse (ThermoScientific, San Jose, CA) mass spectrometer equipped with a nanospray Flex Ion Source coupled with the UltiMate 3000 RSLCnano (Dionex, Sunnyvale, CA). Each reconstituted fraction (3.5 mL = 0.7 µg for global proteomics fractions) was injected onto a PepMap C-18 RP nano trap column (5 µm, 100 µm × 20 mm, Dionex) at 20 µL·min^{-1} flow rate for rapid sample loading, and separated on a PepMap C-18 RP nano column (2 µm, 75 µm × 25 cm). The column was equilibrated with 2% acetonitrile in 0.1% aqueous formic acid (eluant A) prior to each run. The labeled peptides were eluted in a 120-min gradient of 5% to 33% eluant B containing 95% acetonitrile in 0.1% formic

acid at 300 nL·min^{-1}, followed by an 8-min ramping to 90% B, a 7-min hold and 21-min re-equilibration with 2% acetonitrile and 0.1% formic acid prior to the next run. The Orbitrap Eclipse was operated in positive ion mode with nano spray voltage set at 1.9 kV and source temperature at 300 °C. External calibration for FT, IT and quadrupole mass analyzers were performed. Raw MS data files for all the fractions were acquired using a real-time search (RTS) synchronous precursor selection (SPS) MS^3 workflow as reported previously.[4041] Specifically, the RTS MS3 workflow consisted of 2.5 second "Top Speed" data-dependent CID-MS/MS scans (for peptide identifications by RTS) that enabled to trigger SPS of 10 MS2 product ions for subsequent MS3 in FT. In RTS node, the *Homo sapiens* FASTA database containing 20,520 sequences was imported along with trypsin as the enzyme for real-time spectral database search for the samples from corresponding species. The search parameters included: TMTpro modification on N-terminal amines (Δ mass 304.2071) and carbamidomethyl modification of cysteine (Δ mass 57.0215) as static modifications; TMTpro modification (Δ mass 304.2071) on lysine, desthiobiotin-tagged STP ester probe (Δ mass 196.1212), and methionine oxidation (Δ mass 15.9949) as dynamic modifications; maximum 3 variables per peptide; and 2 maximum missed cleavage allowed. A maximum search time for 35 ms was allowed for the RTS MS3 searching. The MS3 scan was carried out using a mass range of 110-500 m/z, an MS isolation window of 1.1 m/z and MS2 isolation window of 2.0 m/z were used. A resolving power of 50,000 at MS3 with a normalized collision energy of 55% was used for peptide quantitation. Other parameters included 200% normalized AGT target and 120 ms for maximum injection time. Dynamic exclusion parameters were set at 1 count within 50s exclusion duration with ±10 ppm exclusion mass window. All data were acquired under Xcalibur 4.4 operation software in Orbitrap Eclipse (ThermoScientific, San Jose, CA).

Data processing, protein identification, and data analysis

All raw MS spectra were processed and searched using the Sequest HT search engine within the Proteome Discoverer 3.0 (PD3.0, ThermoScientific). The same database for human proteins used for RTS data acquisition as described above was used for post-MS database searches. The default search settings used for 18-plex TMT quantitative processing and protein identification in PD3.0 searching software were: two mis-cleavage for full trypsin with fixed carbamidomethyl modification of cysteine, fixed 18-plex TMT modifications on lysine and N-terminal amines along with variable modifications of methionine oxidation, and protein N-terminal acetylation. The peptide mass tolerance and fragment mass tolerance values were 10 ppm for MS survey scan, 0.6 Da for MS2 and 20 ppm for MS3, respectively. Identified peptides were further filtered for maximum 1% FDR using the Percolator algorithm in PD3.0 along with additional peptide confidence set to high and peptide mass accuracy ≤5 ppm. The TMT18-plex quantification method within Proteome Discoverer 3.0 software was used to calculate the reporter ion abundances in MS3 spectra that were corrected for the isotopic impurities. Both unique and razor peptides were used for relative protein quantitation. Signal-to-noise (S/N) values were used to represent the reporter ion abundance with a co-isolation threshold of 50% and an average reporter S/N (intensity) threshold of ≥10 used for quantitation spectra. The intensities of peptides, which were summed from the intensities of the PSMs, were summed to represent the abundance of the proteins. For relative ratio between the two groups, normalization on sum of total peptide intensities for each sample was applied. The search results including ratio, peptide abundance for each sample were output to Microsoft Excel software for further data analysis.

Untargeted Metabolomics Experiments

Treatment and sample preparation

MDA-MB-231 and MDA-MB-436 cells were grown to 95% confluence. Media was then aspirated and replaced with 20 mL of fresh media containing the indicated meroterpenoids or DMSO for 8 hours, maintaining DMSO content <0.2%. Cells were washed with cold DPBS (2×), scraped in cold DPBS, and cell pellets were isolated by centrifugation (750 × g, 5 min, 4° C) and frozen at –80 °C until further use. Cell pellets were then resuspended in 3 mL 80% MeOH/H_2O (v/v) by vortexing, incubated at –80 °C for 20 min, sonicated in an ice-water bath for 10 min, and resuspended again by vortexing. For untargeted metabolomics, 1.5 mL of the resuspended sample were pelleted by centrifugation at 18000 × g for 10 min at 4 °C. 700 µL of the supernatant were then transferred to a new 1.5-mL microcentrifuge tube, which were then evaporated to dryness by speed vacuum and stored at –20 °C until LC-MS/MS analysis. Prior to LC-MS/MS analysis, each dried sample was reconstituted in 200 µL of 20% acetonitrile/H_2O (v/v). Quality controls (QC) were prepared accordingly: one global QC consisted of a pool of 30 µL from all samples (n=48, $\sum$ 1440 µL); eight group QCs with each of them consisting of a pool of 30 µL from samples (n=6, $\sum$ 180 µL) of an individual group (2 cell lines × 4 treatments).

Liquid chromatography and tandem MS (LC-MS/MS)

Polar metabolites from the samples were then separated on a SeQuant ZIC pHILIC (5 µm, 2.1 mm I.D. x 150 mm) column (Millipore Sigma, Burlington, MA) connected to a Vanquish Horizon UPHLC system (Thermo Fisher Scientific, Waltham, MA) as described previously.[42,43] Column compartment temperature was held at 24 °C throughout the analysis. Solvent flow rate was maintained at 250 µL/min. The autosampler tray was held at 4 °C and sample injection volume was 4 µL. The following solvents and elution gradients were used. Solvent A: 10 mM $AcONH_4$ in H_2O, pH 9.8; Solvent B: Acetonitrile. Elution gradient: 0.0-1.0 min (90% B), 1.0-15 min (90-30% B), 15-18 min (30% B), 18-19 min (30-90% B), 19-29 min (90% B). Tandem MS analyses were performed with a Q-Exactive Hybrid Quadrupole-Orbitrap mass spectrometer (Thermo Fisher Scientific, Waltham, MA). The ESI voltage was –3.2 kV, the sheath gas flow rate was 20 AU, the auxiliary gas flow rate was 7 AU, and the sweep gas flow rate was 1 AU. The capillary temperature was 320 °C and the auxiliary gas heater temperature was 250 °C. The S-Lens RF level was 60% and all analyses were run in negative mode.

Data processing and analysis

Initial data analyses were conducted using commercial software (Compound Discoverer 3.3 SP1, Thermo Fisher Scientific, Waltham, MA) to perform normalization, peak alignment, compound identification and related statistical analyses. The initially identified molecules in samples were processed by CD 3.3 SP1 software through background subtraction, exclusion of false positive or repetitive features without MS2 spectra, removal of compounds absent in group QC samples, and pathway mapping to Metabolika database. Filtered data was then analyzed using MetaboAnalyst 5.0 (https://www.metaboanalyst.ca)[44] to generate volcano plots and heatmaps.

Untargeted Lipidomics Experiments

Treatment in cells and sample preparation

MDA-MB-231 and MDA-MB-436 cells were grown to 95% confluence. Media was then aspirated and replaced with 20 mL of fresh media containing the indicated meroterpenoids or DMSO for 8 hours, maintaining DMSO content <0.2%. Cells were washed with cold DPBS (2×), scraped in cold DPBS, and cell pellets were isolated by centrifugation (750 × g, 5 min, 4 °C) and frozen at

–80°C until further use. Cell pellets were then resuspended in 3 mL 80% MeOH/H_2O (v/v) by vortexing, incubated at –80 °C for 20 min, sonicated in an ice-water bath for 10 min, and resuspended again by vortexing. For untargeted lipidomics, 1.3 mL of the resuspended sample (from the 3 mL initial extract) were first transferred into high G-force 1.5 mL microcentrifuge tubes (catalog #20170-038, VWR, Radnor, PA) and evaporated to dryness by speed vacuum. Samples were then reconstituted in 130 µL H_2O by sonication in an ice water bath for 10 min. To each sample, 30 µL of a panel of 15 internal lipid standards in IPA/ACN/H_2O (65:30:5, v/v/v) were added for normalization of each lipid classes (**Table S3**). In addition, 350 µL of ice-cold $CHCl_3$:MeOH (1:2; v/v) were added simultaneously. Samples were vortexed and sonicated in an ice water bath for 10 min. Chloroform (125 µL) was then added to each sample and samples were vortexed again. Lastly, 125 µL water were added to each sample following by vortexing. Sample mixtures were allowed to equilibrate for 10 min at room temperature, followed by centrifugation (18,000 × g, 10 min, 4 °C). Gel loading tips were then used to transfer 400 µL (200 µL twice) of the lower lipid-rich phase into a clean glass culture tube. Samples were then evaporated to dryness by speed vacuum, capped and stored at –20 °C until lipid analysis by LC-MS/MS. Dried samples were reconstituted with 120 µL of ACN/IPA/H_2O (65:30:5 v/v/v) prior to LC-MS/MS analysis.

Liquid chromatography and tandem MS (LC-MS/MS)

Lipids from samples were separated on an Accucore C30 (2.6 µm, 2.1 mm I.D. × 150mm) column (Thermo Fisher Scientific, Waltham, MA) connected to the same UHPLC system and column temperature was held at 55 °C as described previously.[42,43] Solvent flow rate was maintained 260 µL/min. The autosampler tray was held at 4 °C and sample injection volume was 4 µL. The following solvents and elution gradients were used. Solvent A: 60% acetonitrile, 40% water, 10 mM ammonium formate with 0.1% formic acid. Solvent B: 90% isopropanol, 10% acetonitrile, 10 mM ammonium formate with 0.1% formic acid. Elution gradient: 0.0-1.5 min (32% B), 1.5-4.0 min (32-45% B), 4.0-5.0 min (45-52% B), 5.0-8.0 min (52-58% B), 8.0-11 min (58-66% B), 11-14 min (66-70% B), 14-18 min (70-75% B), 18-21 min (75-97% B), 21-25 min (97% B), 25-30 min (97-32% B). The experimental conditions for the tandem mass spectrometry for C30 analyses were as follows. The ESI voltage was 3.8 kV and –3.2 kV for positive and negative mode, respectively; the sheath gas flow rate was 20 AU, the auxiliary gas flow rate was 7 AU, and the sweep gas flow rate was 1 AU. The capillary temperature was 320 °C and the auxiliary gas heater temperature was 250 °C. The S-Lens RF level was 60% and all analyses were run in both positive and negative modes.

Data processing and analysis

Data analysis was conducted using commercial software (LipidSearch 5.1.8, Thermo Fisher Scientific, Waltham, MA) to perform normalization, peak alignment, compound identification and related statistical analyses. Other analyses were performed in the same way as described above for untargeted metabolomics analyses.

Table S3. Internal lipid standards

Protein	Final concentration (µg/mL)
Phosphatidylcholine (15:0_18:1-*d7*)	4.303
Phosphatidylethanolamine(15:0_18:1-*d7*)	0.151
Phosphatidylserine (15:0_18:1-*d7*)	0.111
Phosphatidylglycerol (15:0_18:1-*d7*)	0.763
Phosphatidylinositol (15:0_18:1-*d7*)	0.243
Phosphatidic acid (15:0_18:1-*d7*)	0.197

Lysohosphatidylcholine (18:1-*d*7)	0.680
Lysophosphatidylethanolamine (18:1-*d*7)	0.140
Cholesterol ester (18:1-*d*7)	9.403
Monoglyceride (18:1-*d*7)	6.718
Diglyceride (15:0_18:1-*d*7)	0.251
Triglyceride (15:0_18:1-*d*7_15:0)	1.509
Sphingomyelin (d18:1_18:1-*d*9)	0.846
Cholesterol-*d*7	2.811
Ceramide (d18:1_12:0)	3.332

Statistical analysis

Unless otherwise stated, quantitative data are expressed in bar and line graphs with mean ± SD (error bars) shown with $n=3$ per group from three biologically independent experiments. Statistical significance was calculated using a one-way ANOVA with Dunnett's post hoc test, where significant P values are indicated (*$P < 0.05$, **$P < 0.01$, ***$P < 0.001$, ****$P < 0.0001$).

Determination of Ionization Constants (pK_a)

The pK_a values for jensenone, grandinol, (+)-guadial C, and (–)-euglobal 3 were determined according to previously reported procedures.[45,46]

Preparation of buffers

The pH of each buffer was measured at 25 °C with a glass electrode (Mettler Toledo pH Sensor InLab® Solids Pro-ISM). All solutions were prepared with ultrapurified water (Thermo Scientific, Barnstead™ Smart2Pure™ Water Purification System, 50129845) and stock solutions covering a range of 2.9 to 12.0 were prepared according to the previously described protocol.[45] The buffers were stored at 4 °C and equilibrated to 25 °C prior to use.

Experimental procedure

For each compound, a 10 mM stock in DMSO was prepared prior to analysis. The experimental procedure was performed with slight modification from a previous report.[45] Briefly, 196 µL of each buffer solution was added to a clear 96-well flat-bottom plate (Fisher Scientific, 12565501) using a multichannel micropipette. Then, 4 µL of the 10 mM compound stock was added to the buffer-filled wells, and the mixture was thoroughly premixed with a multichannel micropipette. Per well, the total volume was 200 µL and the final compound concentration was 200 µM (2% DMSO, v/v). One blank solution was prepared for each buffer by adding 4 µL of DMSO to allow for the background subtraction. The 96-well plate was loaded onto an Agilent BioTek Cytation 5 plate reader (BioTek Instruments, Winooski, VT) controlled with Gen5 Image+ Software (Version 3.10.06). The temperature was set to 25 °C and the plate was shaken for 10 min. UV-Vis spectral scans were recorded from 250 nm to 500 nm with a 2 nm resolution, and all readings were performed in triplicate.

Data analysis

Data analysis was adapted from previously described protocols.[45,46] The background absorbance was removed by subtracting the corresponding blank from each respective buffer. The absorbance difference at each wavelength was then obtained by subtracting the corrected absorbances of each pH from the corrected absorbance of the most acidic pH. From the spectral difference, the wavelengths corresponding to the maximum positive absorbance difference and the maximum negative absorbance were selected (**Table S4**). The absolute sum of the maximum positive and maximum negative absorbance differences at each pH was then calculated. The values were imported to GraphPad Prism 9 and the absolute sum of the absorbance differences were plotted against pH. A sigmoidal (four parameter logistic) non-linear regression analysis was performed and fit to the curve to determine each pK_a value.

Table S4. Wavelengths used for pK_a determination of selected meroterpenoids

Compound	λ_{max} positive Δ absorbance	λ_{max} negative Δ absorbance
jensenone	304 nm	410 nm
grandinol	306 nm	428 nm
(+)-guadial C	296 nm	418 nm
(–)-euglobal G3	296 nm	436 nm

Representative data analysis for pK_a determination of jensenone

Absolute absorbance values of jensenone between pH 3–7, used to determine pK_{a1} value. A sigmoidal non-linear fit (shown on the graph in red) was used to calculate the numerical value of the pK_{a1} (mean values shown with n=3 per group from three independent experiments).

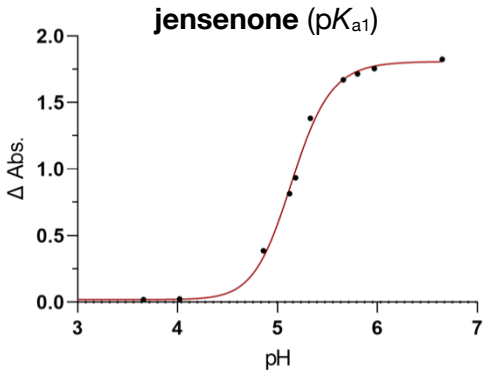

Absolute absorbance values of jensenone between pH 6–11, used to determine pK_{a2} value. A sigmoidal non-linear fit (shown on the graph in red) was used to calculate the numerical value of the pK_{a2} (mean values shown with n=3 per group from three independent experiments).

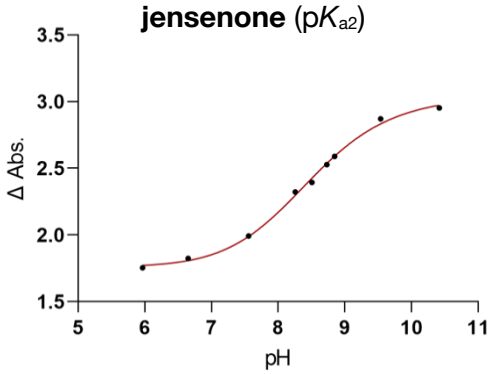

Absolute absorbance values of jensenone between pH 9.5–11.5, used to determine pK_{a3} value. A sigmoidal non-linear fit (shown on the graph in red) was used to calculate the numerical value of the pK_{a3} (mean values shown with n=3 per group from three independent experiments).

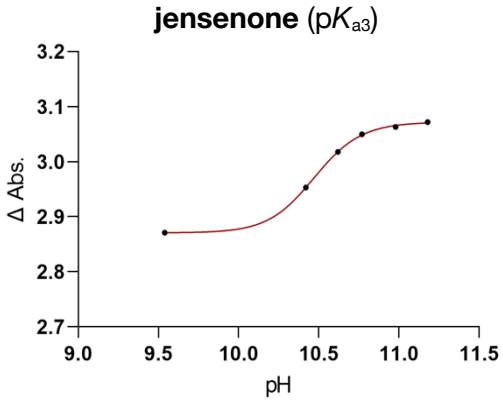

Full pK_a curves for grandinol, (+)-guadial C and (–)-euglobal G3

Plot of pH versus change in absorbance for grandinol, (+)-guadial C, and (–)-euglobal G3. The pK_a values for each were determined by the procedure described above in the methods section (mean values shown with n=3 per group from three independent experiments).

grandinol

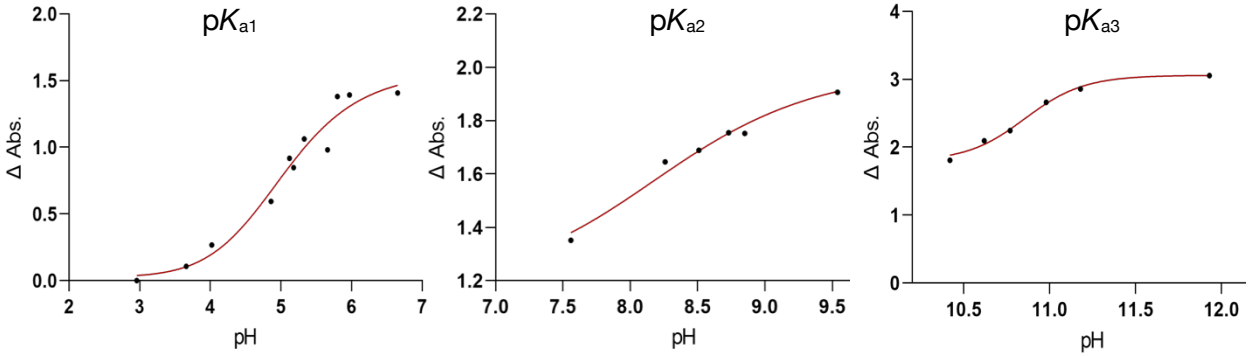

(+)-guadial C

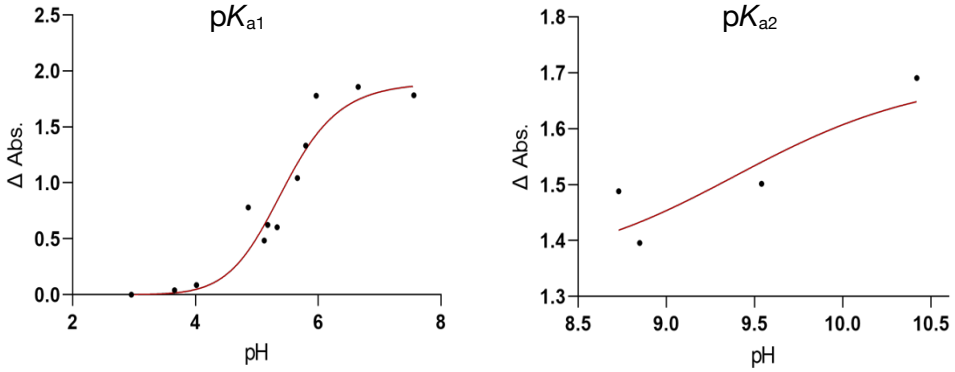

(–)-euglobal-G3

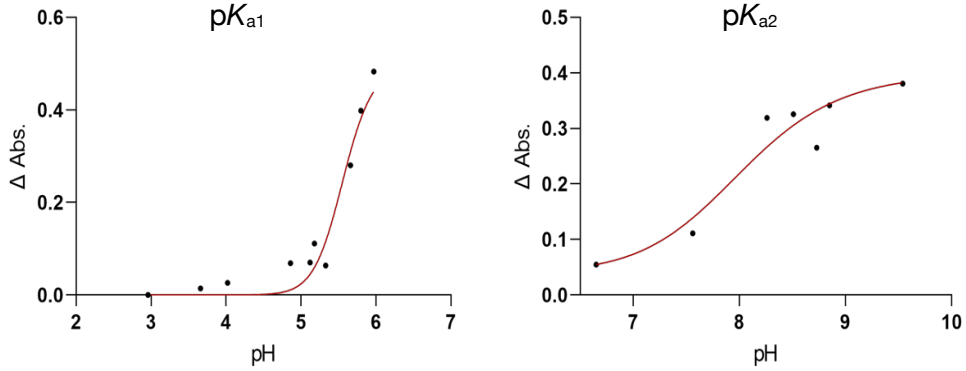

Spectroscopic analysis of meroterpenoid reactivity and reversibility

General procedure for dose-response with a model amine nucleophile

Reactions between grandinol and jensenone with butylamine were performed in a mixture of DMSO-d_6 and D_2O (3:1) with a final concentration of 5 mM for each natural product and 1-100 mM concentration range for butylamine. Each reaction was allowed to proceed for 24 hours to reach maximal product formation prior to ^{1}H-NMR spectra acquisition.

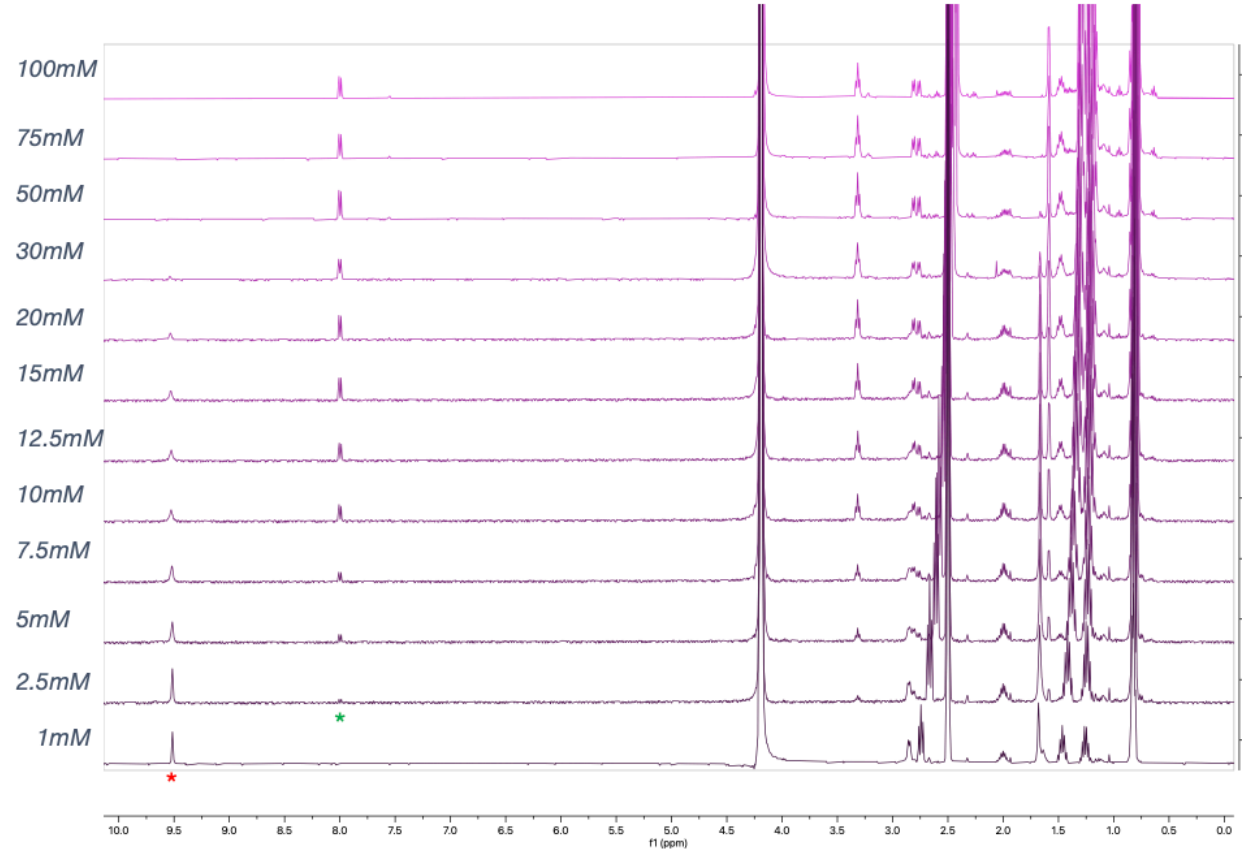

Supplementary Figure S1. ^{1}H-NMR spectra for the reactions between grandinol with butylamine at various concentrations. Reactions with grandinol (5 mM) and butylamine (1-100 mM) were performed in DMSO-d_6:D_2O (3:1) mixture for 24 hours prior to ^{1}H-NMR analysis. The peak of the aldehyde of grandinol is designated by the red asterisk, at 9.5 ppm, while the imine proton of the product is designated by the green asterisk, at 8.0 ppm. The concentrations of butylamine used for each reaction are indicated to the left of each corresponding spectral trace.

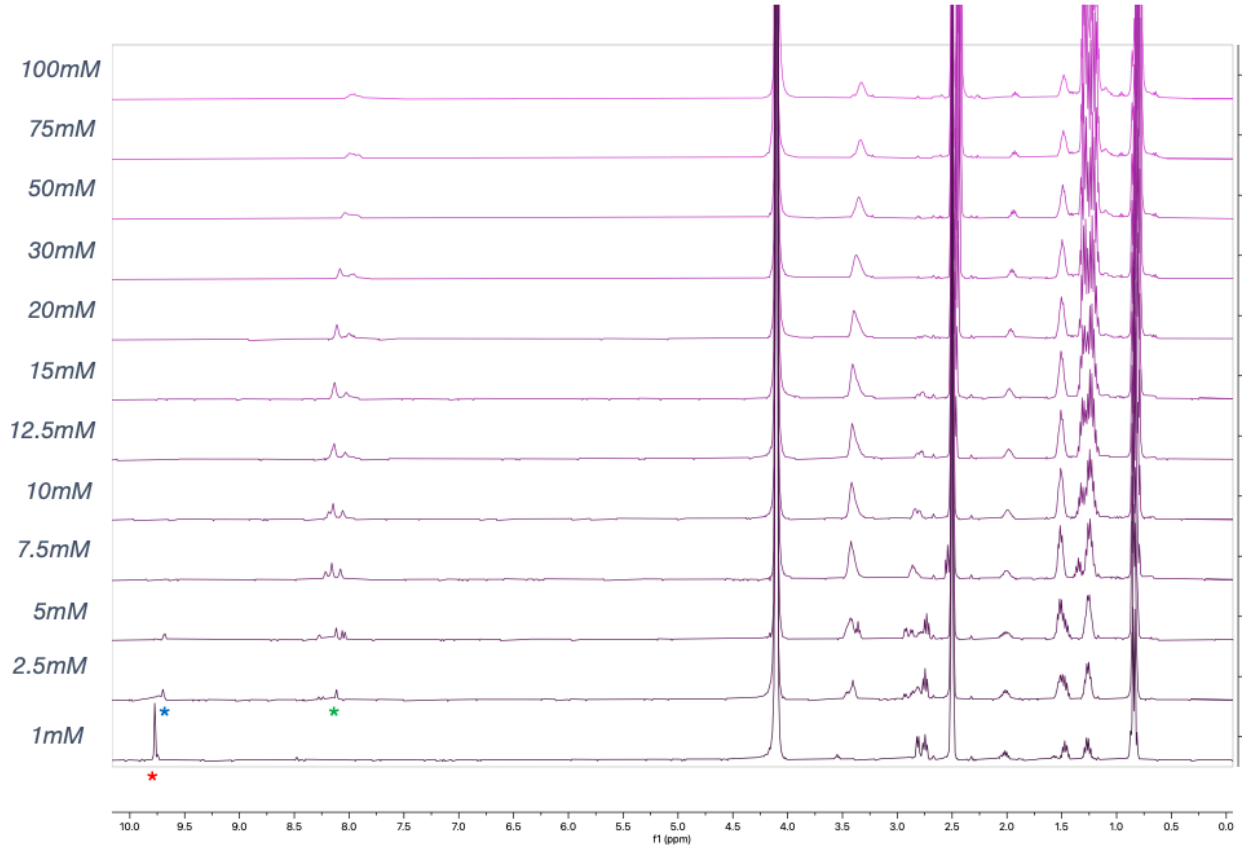

Supplementary Figure S2. ^{1}H-NMR spectra for the reactions between jensenone with butylamine at various concentrations. Reactions with jensenone (5 mM) and butylamine (1-100 mM) were performed in DMSO-d_6:D_2O (3:1) mixture for 24 hours prior to ^{1}H-NMR analysis. The peak corresponding to the unconjugated aldehydes of jensenone is designated by the red asterisk, at 9.8 ppm. In reactions with less than 1 equivalent of butylamine, monoadduct can be detected at 9.7 ppm, indicated by the blue asterisk. With increasing concentrations of butylamine, multiple imine/enamine tautomeric species form, corresponding to bisadduct formation. These species are designated broadly by the green asterisk at 8.2 ppm. The concentrations of butylamine used for each reaction are indicated to the left of each corresponding spectral trace.

General procedure for the half-life determination

Reactions between grandinol, jensenone, salicylaldehyde, benzaldehyde, phloroglucinaldehyde and butylamine were performed in DMSO-d_6:D_2O (3:1) with a final concentration of 10 mM for each natural product and 100 mM for butylamine. All reactions were monitored by ^{1}H-NMR with spectra taken every 15 min for the first 2 hours, followed by spectra taken every hour up to 12 hours, with final spectra taken at 16 and 24 hours. The concentration of remaining starting material was determined by integration of the aldehyde peak, and was plotted against time. Half-lives for each reaction were calculated by non-linear regression analysis from a one-phase decay fit generated using GraphPad Prism 9 software.

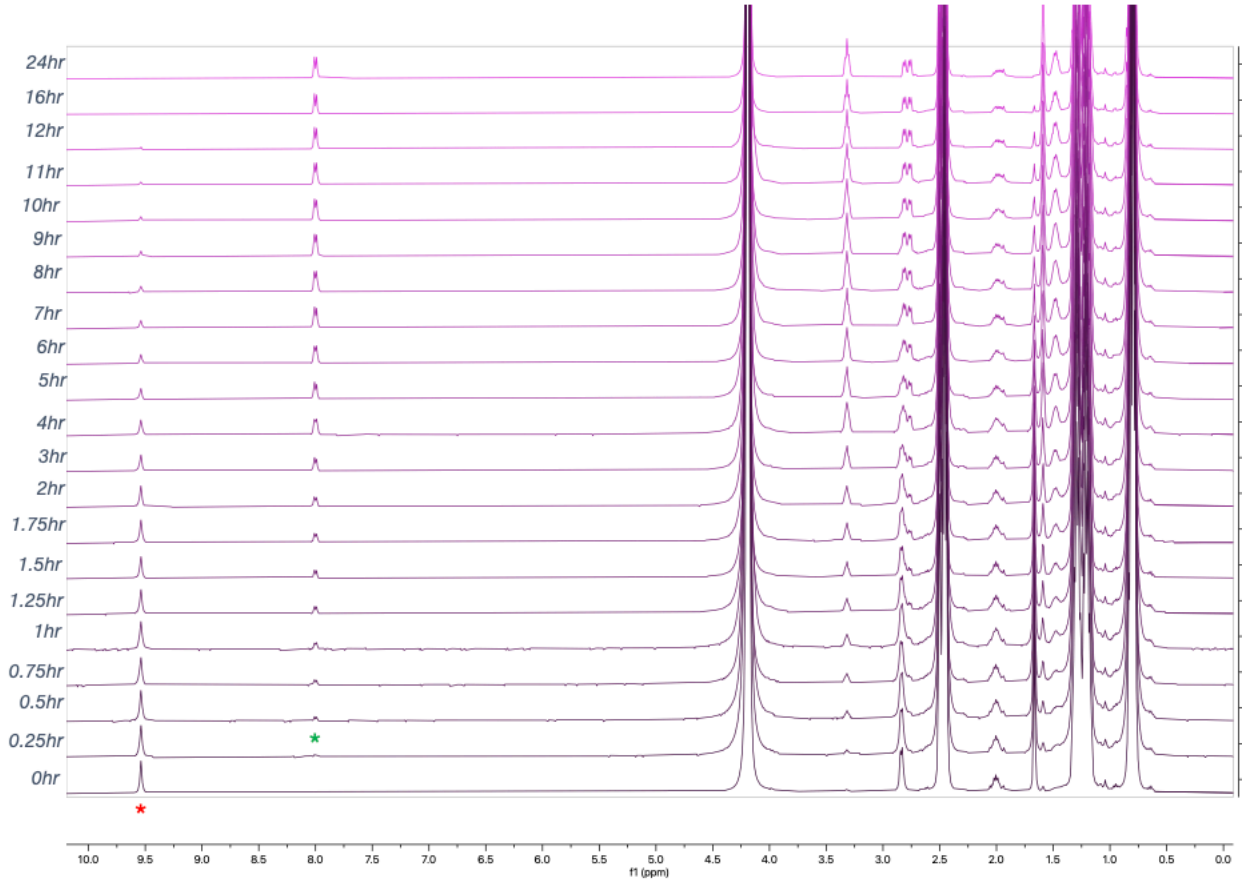

Supplementary Figure S3. ^{1}H-NMR time-course for the determination of the half-life for the reaction between grandinol and butylamine. The reaction of grandinol (10 mM) and butylamine (100 mM) was performed in DMSO-d_6:D_2O (3:1) mixture and analyzed over the course of 24 hours by ^{1}H-NMR analysis. The peak of the aldehyde of grandinol is designated by the red asterisk, at 9.5 ppm, while the imine proton of the product is designated by the green asterisk, at 8.0 ppm. Grandinol is slow to react, with trace amounts of starting material remained until 12 hours into the reaction. Time points taken during the reaction are indicated to the left of each corresponding spectral trace.

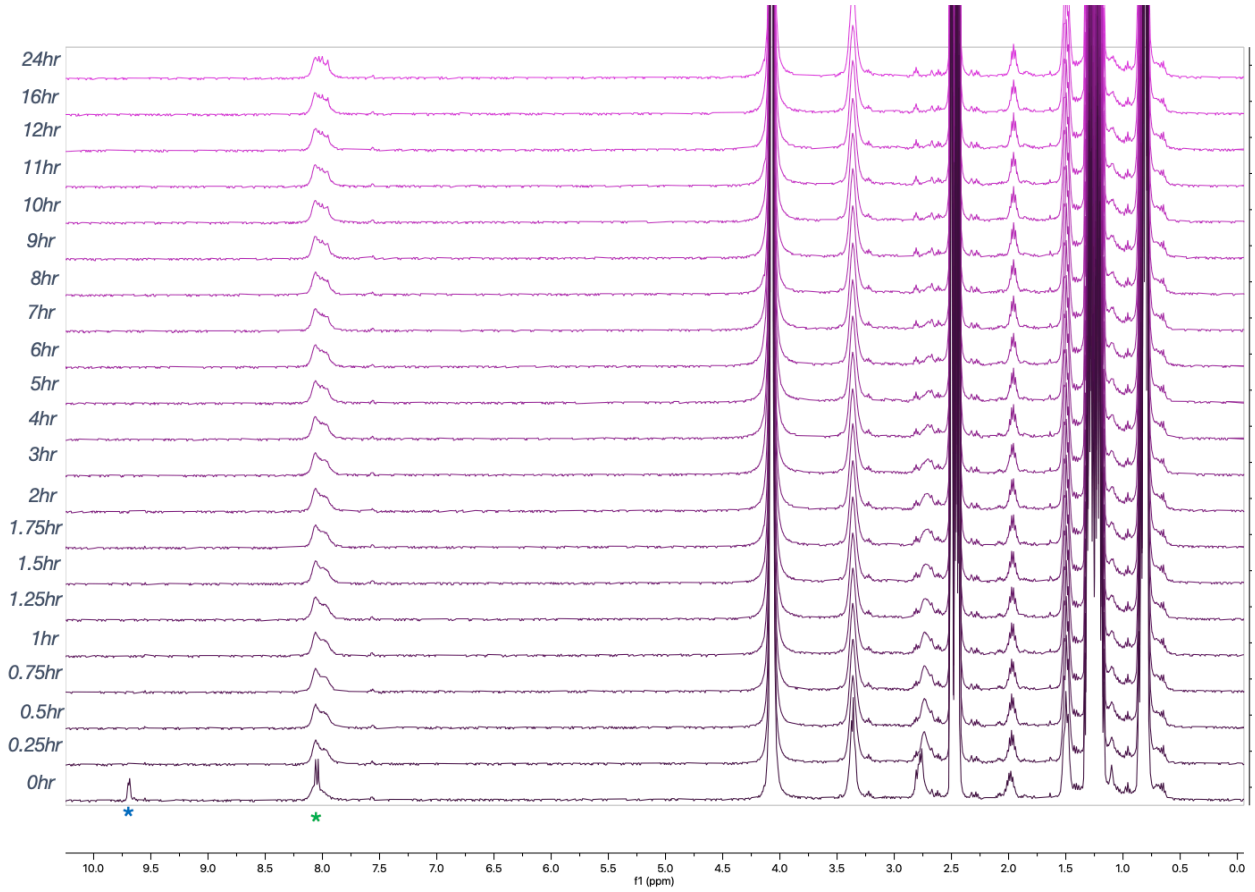

Supplementary Figure S4. ^{1}H-NMR time-course for the determination of the half-life for the reaction between jensenone and butylamine. The reaction of jensenone (10 mM) and butylamine (100 mM) was performed in DMSO-d_6:D_2O (3:1) mixture and analyzed over the course of 24 hours by ^{1}H-NMR analysis. In the delay between starting the reaction and the first spectral recording (about 5 minutes), most of the jensenone was converted to monoadduct (also see Supplementary Figure S2) with the remaining aldehyde designated by the blue asterisk at 9.7 ppm and imine adduct designated by the green asterisk at 8.1 ppm. Within the next fifteen minutes, all the monoadduct was converted to the bisadduct, indicated by the loss of the aldehyde proton in the 0.25-hour spectrum. Time-points taken during the reaction are indicated to the left of each corresponding spectral trace.

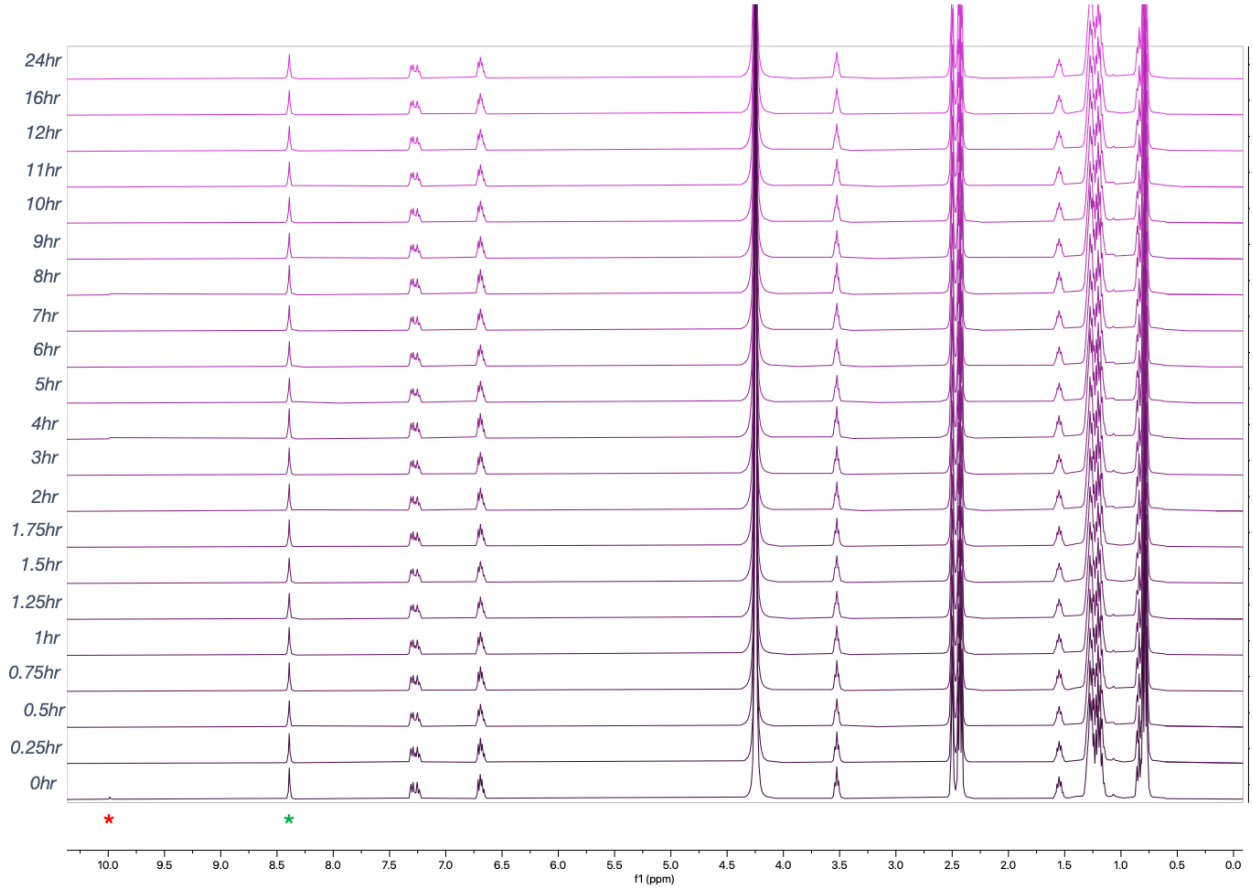

Supplementary Figure S5. ^{1}H-NMR time-course for the determination of the half-life for the reaction between salicylaldehyde and butylamine. The reaction of salicylaldehyde (10 mM) and butylamine (100 mM) was performed in DMSO-d_6:D_2O (3:1) mixture and analyzed over the course of 24 hours by ^{1}H-NMR analysis. In the delay between starting the reaction and the first spectral recording (about 5 minutes), most of the salicylaldehyde was consumed, with the remaining aldehyde peak designated by the red asterisk at 10.0 ppm and the newly formed imine proton designated by the green asterisk at 8.4 ppm. Within the next fifteen minutes, all the salicylaldehyde was consumed, indicated by the loss of the aldehyde proton in the 0.25-hour spectrum. Time points taken during the reaction are indicated to the left of each corresponding spectral trace.

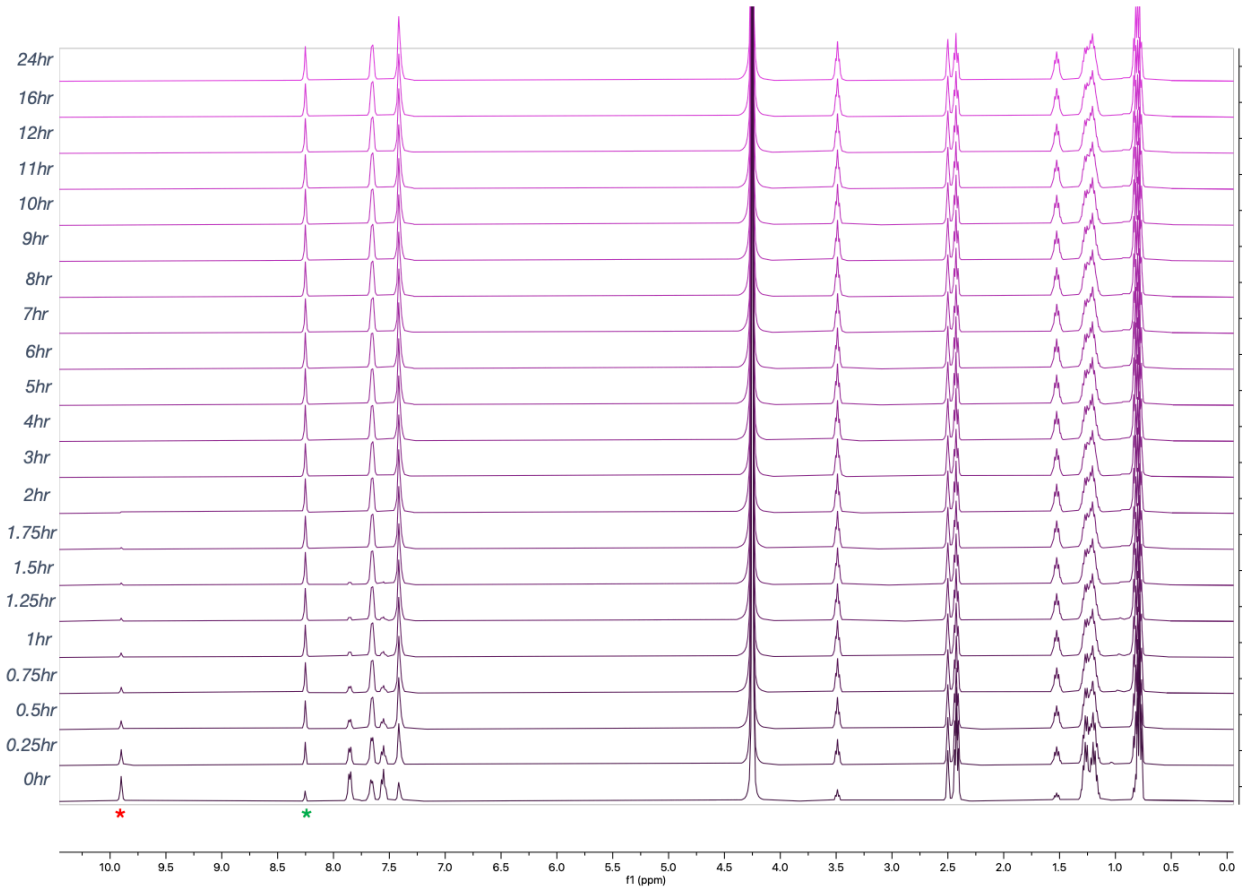

Supplementary Figure S6. ^{1}H-NMR time-course for the determination of the half-life for the reaction between benzaldehyde and butylamine. The reaction of benzaldehyde (10 mM) and butylamine (100 mM) was performed in DMSO-d_6:D_2O (3:1) mixture and analyzed over the course of 24 hours by ^{1}H-NMR analysis. The remaining aldehyde peak is designated by the red asterisk at 9.9 ppm and the newly formed imine proton designated by the green asterisk at 8.25 ppm. Benzaldehyde, while slower than jensenone and salicylaldehyde, reacts faster than grandinol as it only takes about 2 hours for full consumption of the starting material. Time points taken during the reaction are indicated to the left of each corresponding spectral trace.

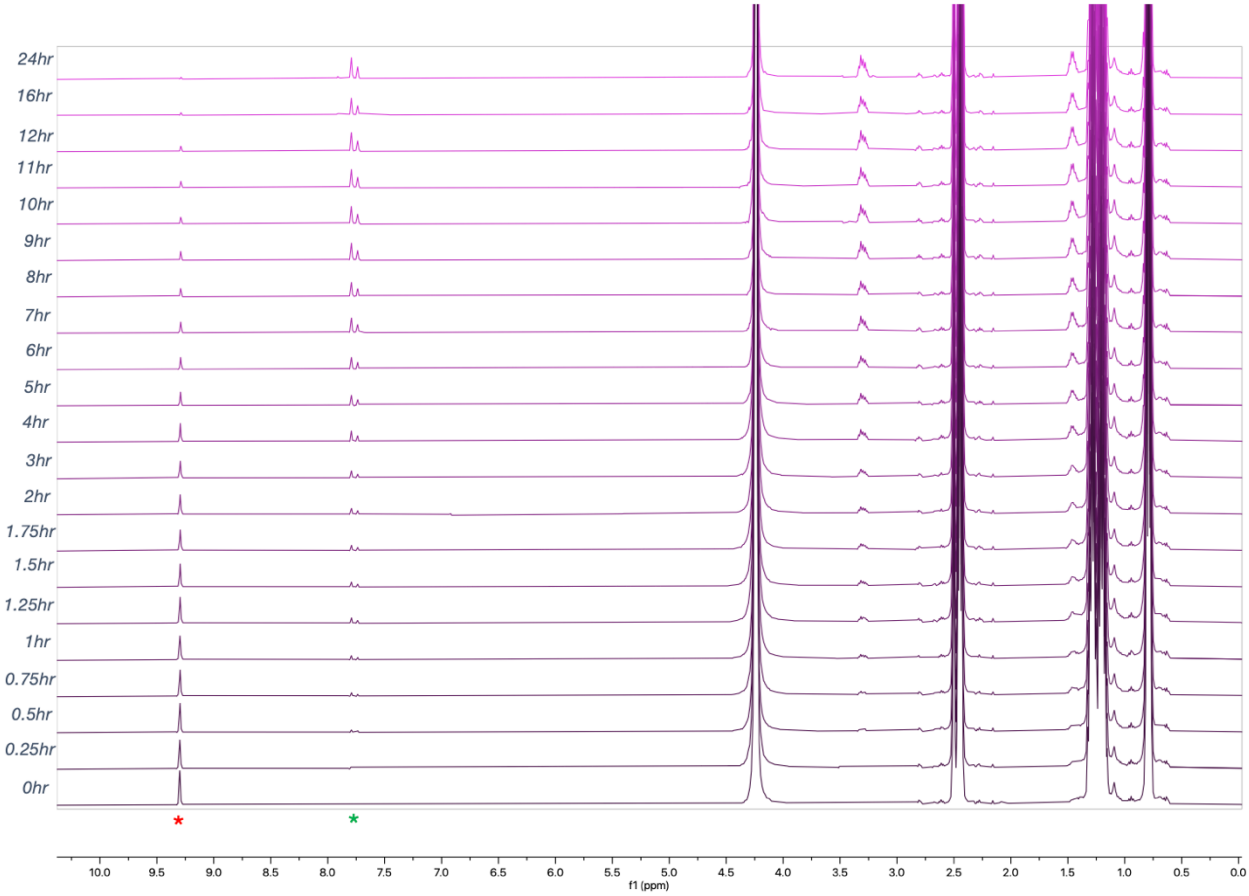

Supplementary Figure S7. ^{1}H-NMR time-course for the determination of the half-life for the reaction between phloroglucinaldehyde and butylamine. The reaction of phloroglucinaldehyde (10 mM) and butylamine (100 mM) was performed in DMSO-d_6:D_2O (3:1) mixture and analyzed over the course of 24 hours by ^{1}H-NMR analysis. The remaining aldehyde peak is designated by the red asterisk at 9.3 ppm and the newly formed imine proton designated by the green asterisk at 7.75 ppm. This is the least reactive of all aldehydes analyzed, with starting material still present after 24 hours. Time-points taken during the reaction are indicated to the left of each corresponding spectral trace.

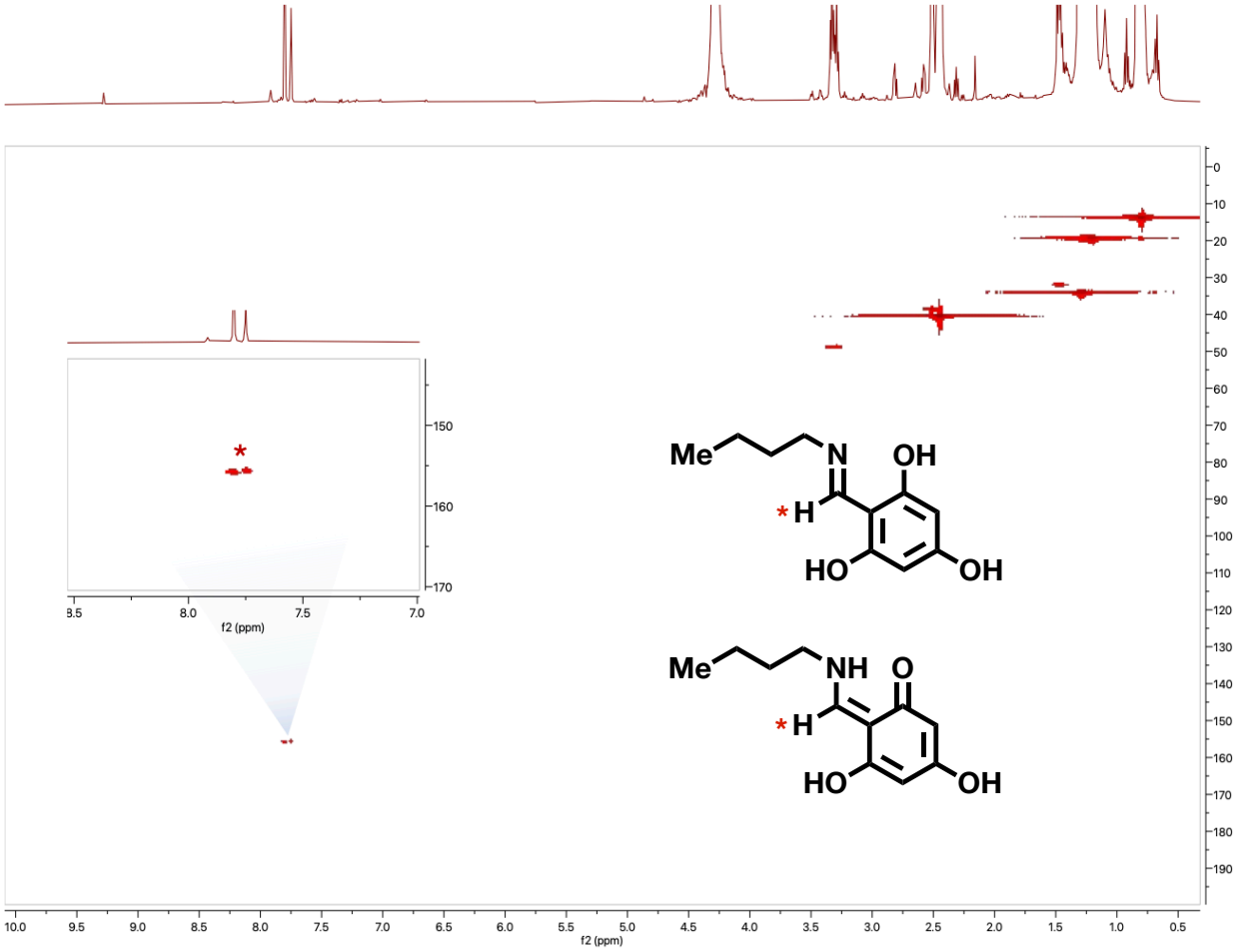

Supplementary Figure S8. HSQC of phloroglucinaldehyde and butylamine reaction from the time-course analysis in Supplementary Figure S7. After a 24-hour reaction between phloroglucinaldehyde (10 mM) and butylamine (100 mM), an HSQC spectrum was acquired to identify the proton peaks corresponding to the butylamine-adduct. Carbons in the expected imine/enamine region were detected for the new proton signals at 7.75 ppm and 7.8 ppm (signals indicated with red asterisk), which apparently correspond to the imine and enamine tautomers shown. No carbon was detected for the new peak at 7.92 ppm, indicating this is most likely the NH proton of the enamine tautomer.

Dilution experiments to interrogate reversibility

Reactions between grandinol, jensenone, salicylaldehyde, benzaldehyde, phloroglucinaldehyde and butylamine were performed in DMSO-d_6:D_2O (3:1) a final concentration of 10 mM for each natural product and 100 mM for butylamine. All reactions were allowed to proceed for 24 hours to reach maximum conversion to product. After 24 hours, each reaction was diluted 20-fold with a mixture of DMSO-d_6:PBS (3:1) and were monitored by ^{1}H-NMR with spectra taken immediately upon dilution (t=0), and then after 1, 2, 6, 12, and 24 hours.

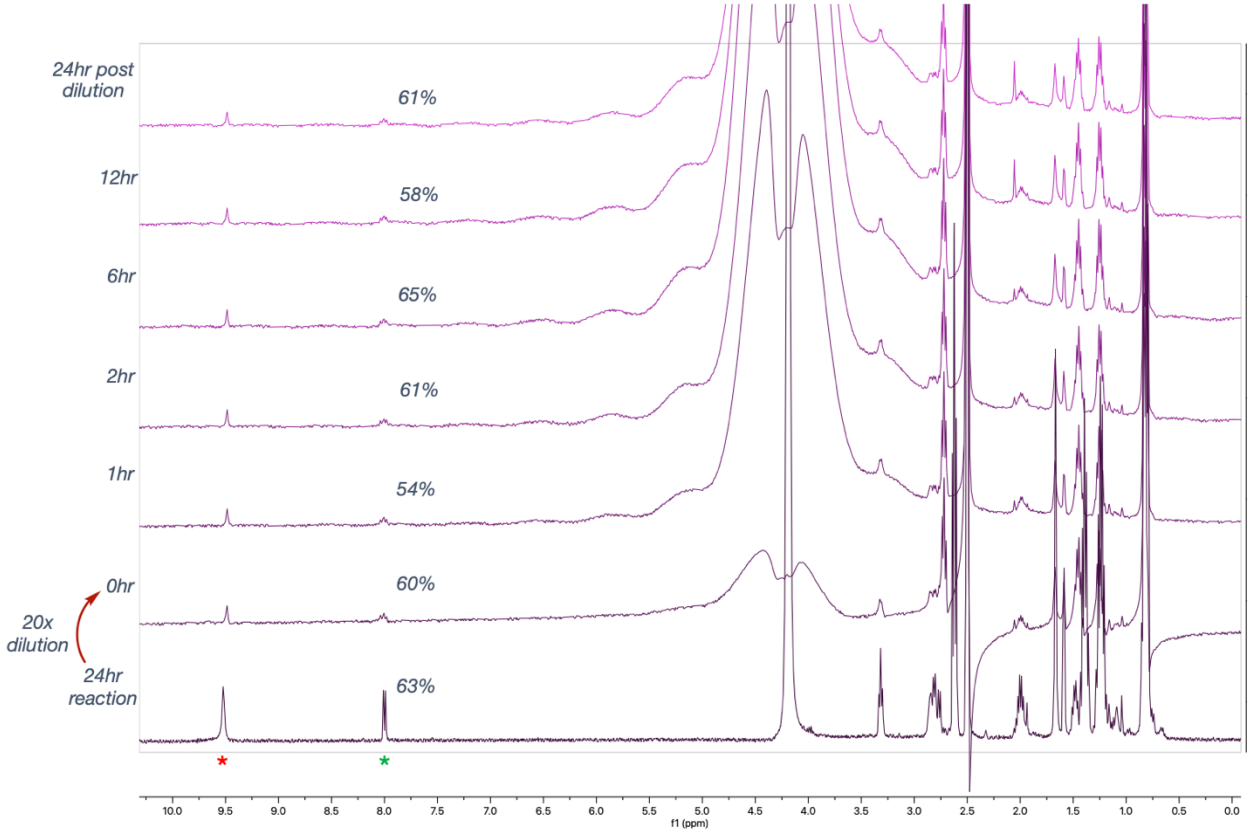

Supplementary Figure S9. ^{1}H-NMR time-course of dilution experiment for the reaction between grandinol and butylamine. The reaction of grandinol (10 mM) and butylamine (20 mM) was performed in DMSO-d_6:D_2O (3:1) mixture and allowed to react for 24 hours prior to a 20-fold dilution in a 3:1 mixture of DMSO-d_6:PBS. The aldehyde peak for grandinol is designated by the red asterisk at 9.5 ppm, while the imine proton of the product is designated by the green asterisk, at 8.0 ppm. Upon dilution, there are additional tautomers detected by additional imine/enamine protons formed around 8.0 ppm. There have been extensive investigations into the tendency of this rearrangement by similar species under minimal change to both the percentage of organic and aqueous solvent, as well as pH, and therefore we believe these minimal changes due to our dilution conditions results in isomeric populations.[47-51] Integrations of the product are indicated on each corresponding spectral trace as percentages of imine/enamine proton compared to the remaining aldehyde proton. Only the peaks corresponding to the initial imine/enamine species prior to dilution were used to determine percentage of product remaining. Time points taken during the reaction are indicated to the left of each corresponding spectral trace. Due to the high concentration of water in the mixture, ^{1}H-NMR spectra post-dilution were acquired using WET 1F (1 frequency) solvent suppression, causing the large, broad signal around 4.25 ppm.

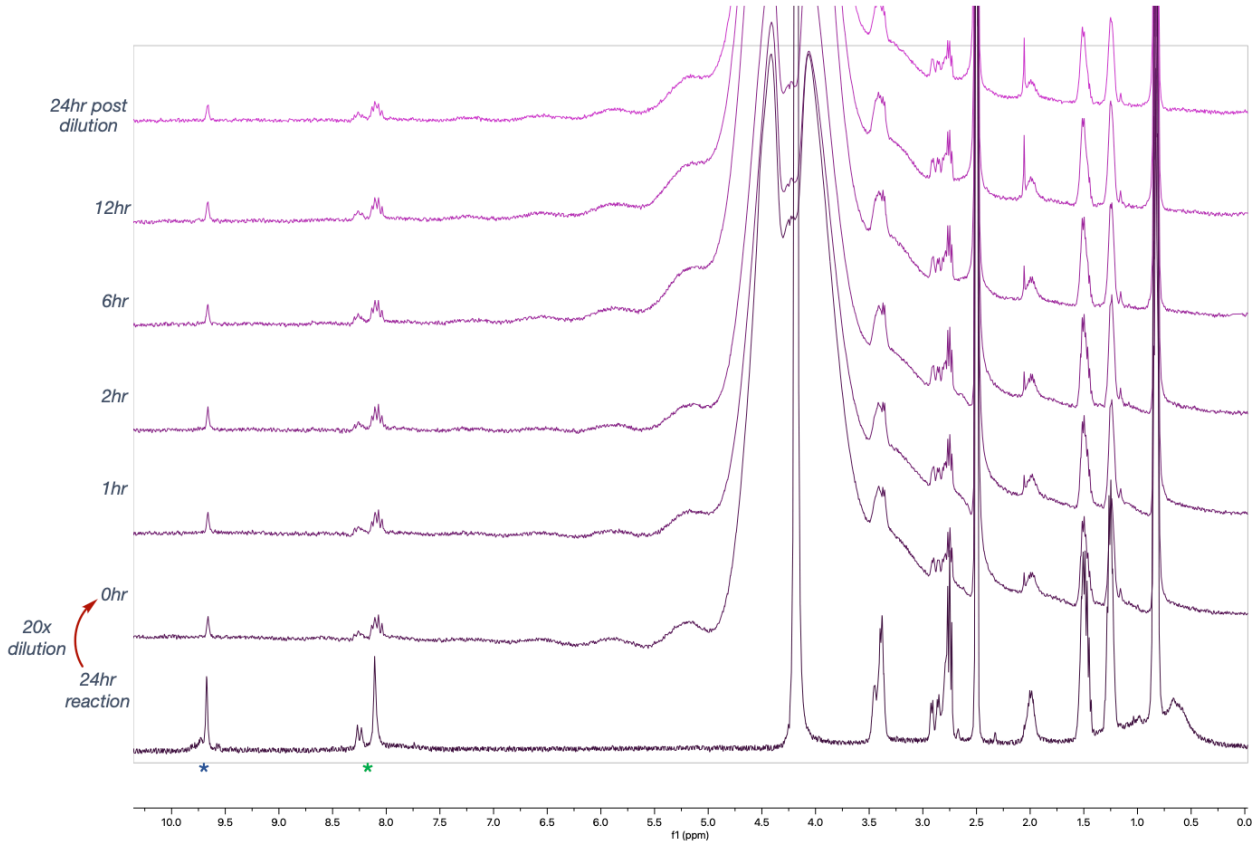

Supplementary Figure S10. ^{1}H-NMR time-course of dilution experiment for the reaction between jensenone and butylamine. The reaction of jensenone (10 mM) and butylamine (20 mM) was performed in DMSO-d_6:D_2O (3:1) mixture and allowed to react for 24 hours prior to a 20-fold dilution in a 3:1 mixture of DMSO-d_6:PBS. The peak corresponding to monoadduct (also see Supplementary Figure S2) is designated by the blue asterisk at 9.7 ppm, while the imine/enamine protons of the products are designated broadly by the green asterisk, at around 8.2 ppm. Similarly to the grandinol dilution analysis (also see **Supplementary Figure S9**) new tautomeric species arise due to the dilution conditions slightly altering the organic-to-aqueous solvent ratio and pH.[47-51] Integrations of the product are indicated on each corresponding spectral trace as percentages compared to the remaining aldehyde. Due to the presence of isomeric populations, only the peaks corresponding to the initial imine/enamine species prior to dilution were used to determine percentage of product remaining. Time points taken during the reaction are indicated to the left of each corresponding spectral trace. Due to the high concentration of water in the mixture, ^{1}H-NMR spectra post-dilution were acquired using WET 1F (1 frequency) solvent suppression, causing the large, broad signal around 4.25 ppm.

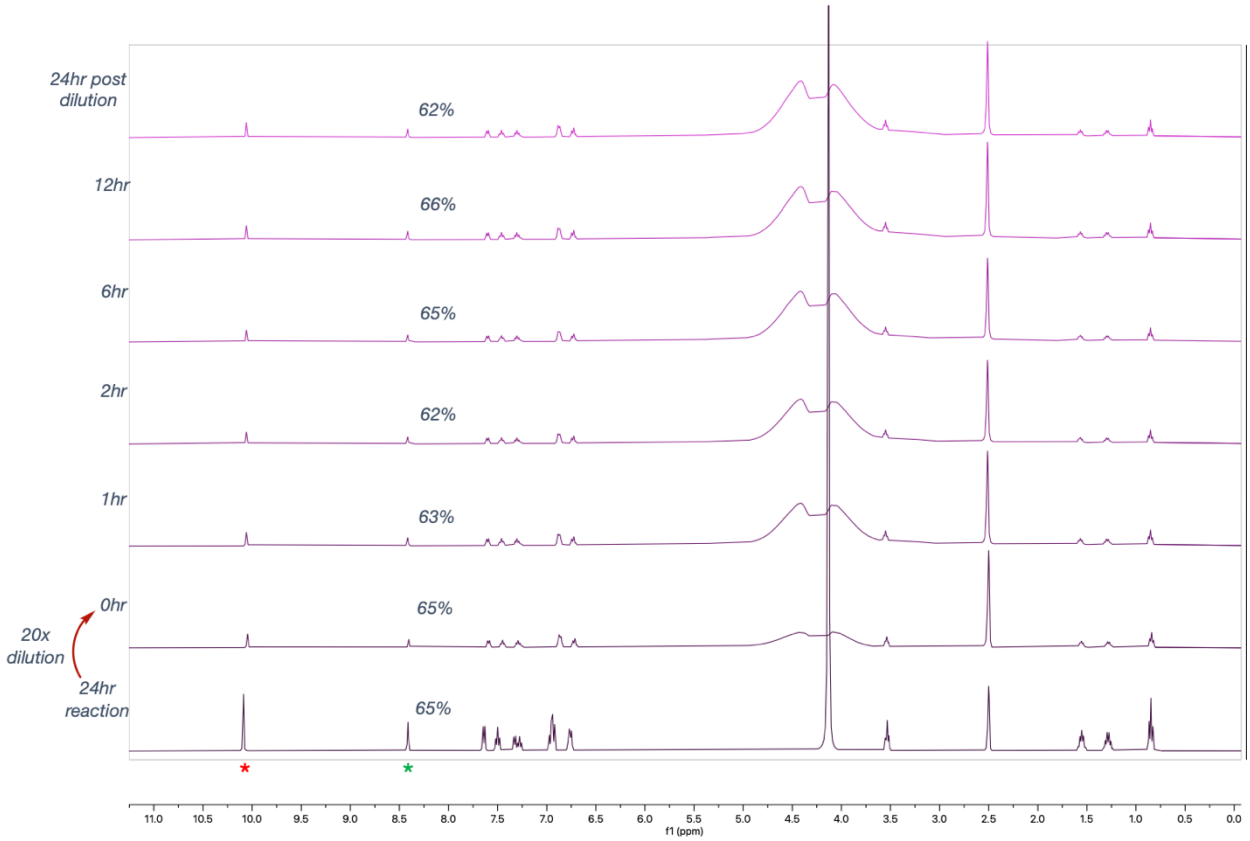

Supplementary Figure S11. ^{1}H-NMR time-course of dilution experiment for the reaction between salicylaldehyde and butylamine. The reaction of salicylaldehyde (10 mM) and butylamine (20 mM) was performed in DMSO-d_6:D_2O (3:1) mixture and allowed to react for 24 hours prior to a 20-fold dilution in a 3:1 mixture of DMSO-d_6:PBS. The peak of the aldehyde proton of salicyladehyde is designated by the red asterisk, at 10.1 ppm, while the imine proton of the product is designated by the green asterisk, at 8.4 ppm. Integrations of the product are indicated on each corresponding spectral trace as percentages compared to the remaining aldehyde. Time points taken during the reaction are indicated to the left of each corresponding spectral trace. Due to the high concentration of water in the mixture, ^{1}H-NMR spectra post-dilution were acquired using WET 1F (1 frequency) solvent suppression, causing the large, broad signal around 4.25 ppm.

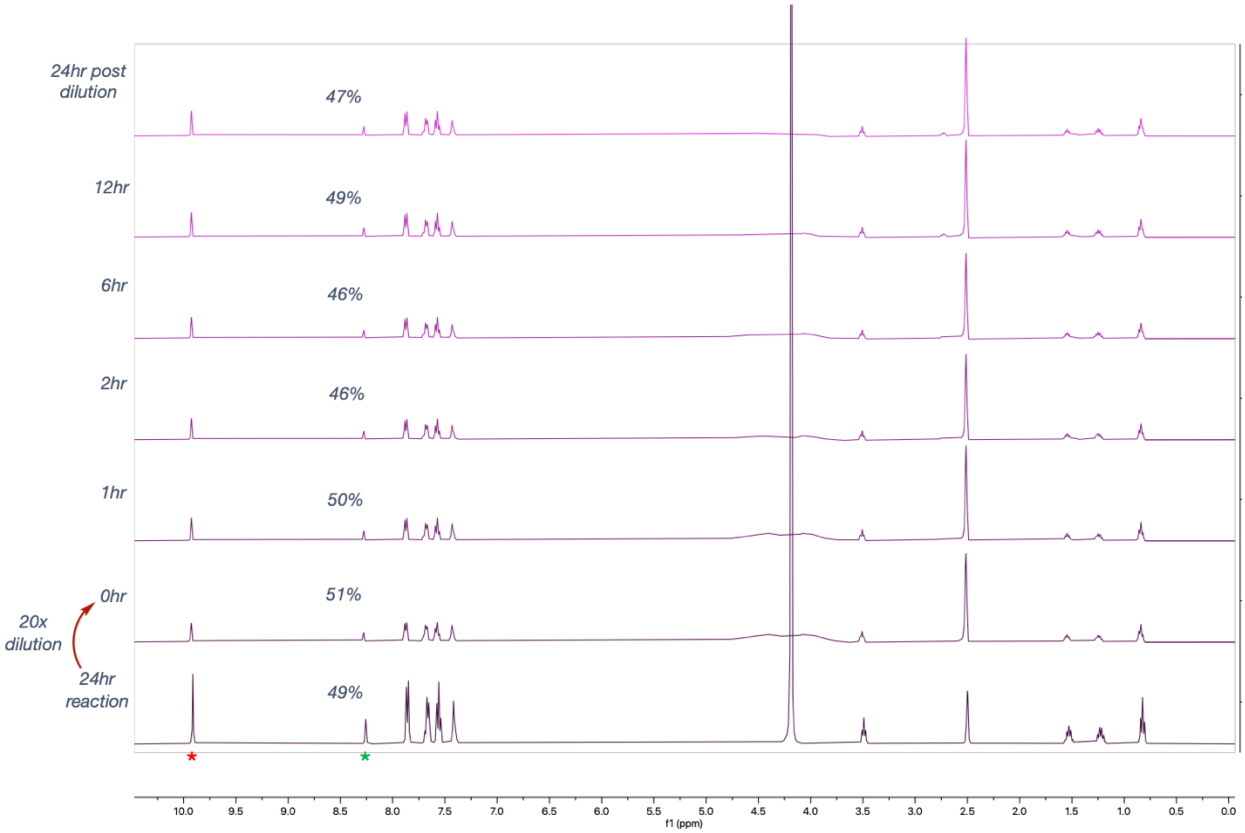

Supplementary Figure S12. ^{1}H-NMR time-course of dilution experiment for the reaction between benzaldehyde and butylamine. The reaction of benzaldehyde (10 mM) and butylamine (20 mM) was performed in DMSO-d_6:D_2O (3:1) mixture and allowed to react for 24 hours prior to a 20-fold dilution in a 3:1 mixture of DMSO-d_6:PBS. The peak of the aldehyde proton of benzaldehyde is designated by the red asterisk, at 9.9 ppm, while the imine proton of the product is designated by the green asterisk, at 8.25 ppm. Integrations of the product are indicated on each corresponding spectral trace as percentages compared to the remaining aldehyde. Time-points taken during the reaction are indicated to the left of each corresponding spectral trace. Due to the high concentration of water in the mixture, ^{1}H-NMR spectra post-dilution were acquired using WET 1F (1 frequency) solvent suppression, causing the large, broad signal around 4.25 ppm.

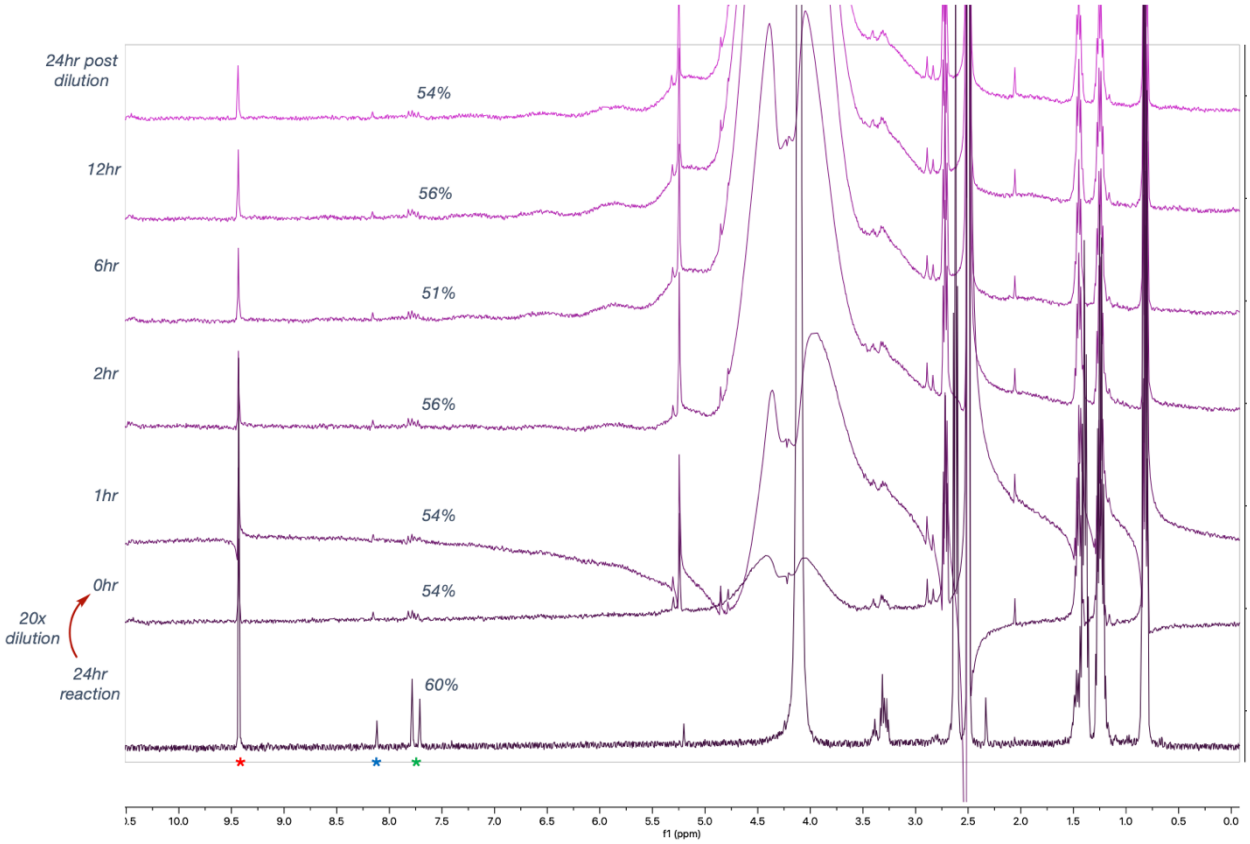

Supplementary Figure S13. ^{1}H-NMR time-course of dilution experiment for the reaction between phloroglucinaldehyde and butylamine. The reaction of phloroglucinaldehyde (10 mM) and butylamine (20 mM) was performed in DMSO-d_6:D_2O (3:1) mixture and allowed to react for 24 hours prior to a 20-fold dilution in a 3:1 mixture of DMSO-d_6:PBS. The peak of the aldehyde proton of phloroglucinaldehyde is designated by the red asterisk, at 9.4 ppm, while the imine proton of the product is designated by the green asterisk, at 7.75 ppm. The blue asterisk at 8.1 ppm represents the NH proton of the enamine tautomer, as determined in analysis of the HSQC seen in **Supplementary Figure S8**. As explained for the grandinol dilution analysis, new tautomeric species arise due to the dilution conditions used that slightly alter the organic-to-aqueous solvent ratio and pH.[47-51] Integrations of the product are indicated on each corresponding spectral trace as percentages compared to the remaining aldehyde. Due to the presence of new isomers, only the peaks corresponding to the initial imine/enamine species prior to dilution were used to determine percentage of product remaining. Time points taken during the reaction are indicated to the left of each corresponding spectral trace. Due to the high concentration of water in the mixture, ^{1}H-NMR spectra post-dilution were acquired using WET 1F (1 frequency) solvent suppression, causing the large, broad signal around 4.25 ppm.

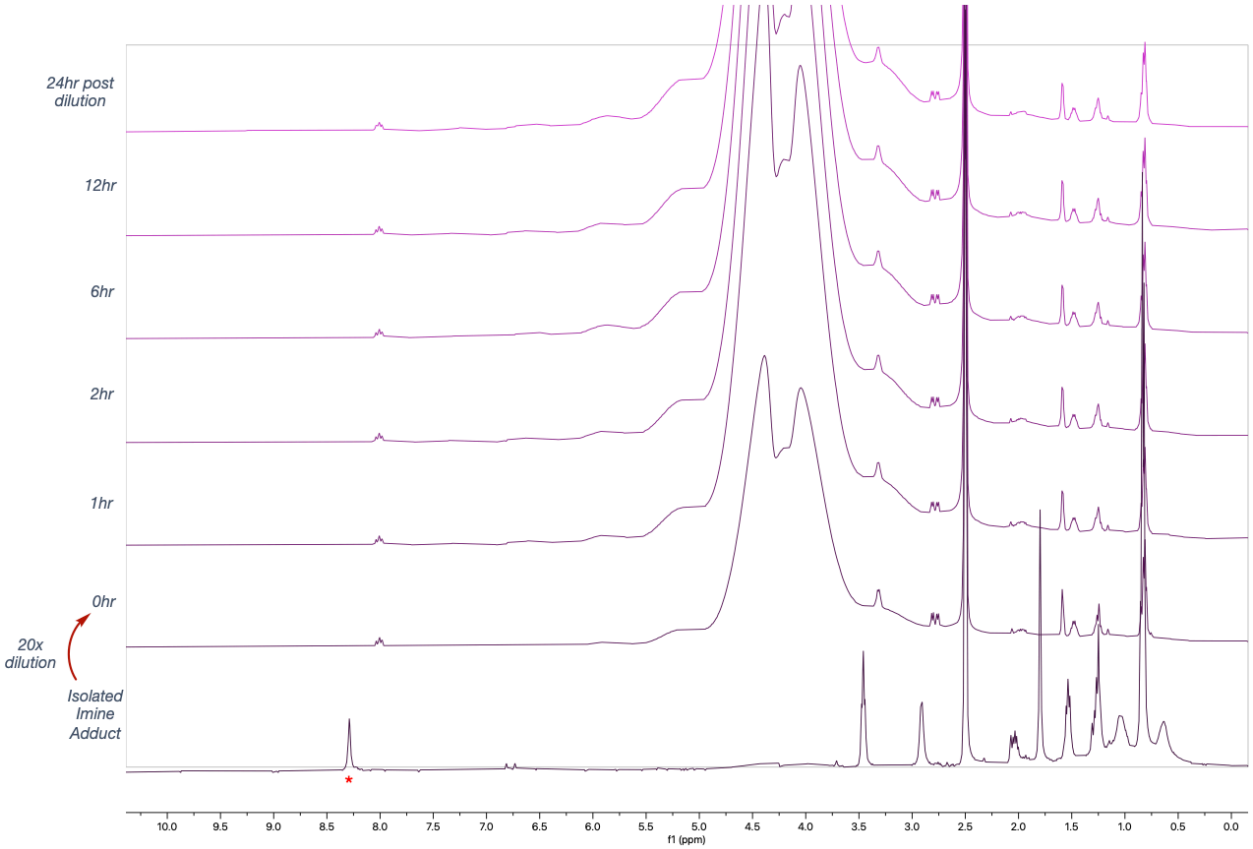

Supplementary Figure S14. ^{1}H-NMR time-course of dilution experiment for the isolated and purified grandinol-butylamine adduct. After isolating the grandinol-butylamine adduct, as described on page S85, the grandinol-butylamine adduct was dissolved in DMSO-d_6:D_2O (3:1) mixture at 10 mM final concentration and a reference ^{1}H-NMR spectrum was acquired (the imine proton of the starting material is designated by the red asterisk at 8.3 ppm). Then, the purified adduct was subjected to a 20-fold dilution in a 3:1 mixture of DMSO-d_6:PBS. Time points taken to monitor the reversibility during the dilution reaction are indicated to the left of each corresponding spectral trace. As explained for the grandinol dilution analysis, new tautomeric species arise due to the dilution conditions used that slightly alter the organic-to-aqueous solvent ratio and pH.[47-51] Due to the high concentration of water in the mixture, ^{1}H-NMR spectra post-dilution were acquired using WET 1F (1 frequency) solvent suppression, causing the large, broad signal around 4.25 ppm.

General Synthetic Procedures

Chemicals and reagents were purchased from a variety of vendors, including Sigma Aldrich, Acros, Fisher, Santa Cruz, AstaTech, Oakwood, TCI, Chem-Impex, Alfa Aesar, Click Chemistry Tools, Cayman, BroadPharm, and Cambridge Isotope Laboratories, and were used without further purification. Anhydrous solvents were obtained as commercially available pre-dried, oxygen-free formulations. Flash chromatography was carried out using 40-60 Å silica gel on XS 520Plus PuriFlash chromatography system (Advion, PFXSV1). All reactions were monitored by thin layer chromatography (TLC) carried out on silica gel plates (60F-254, Supelco) and visualized with UV light and Seebach stain. NMR spectra were recorded on Bruker AVIII-400, Bruker AVIII-500, or Varian INOVA-600 in the indicated solvent. Multiplicities are reported with the following abbreviations: s singlet; d doublet; t triplet; m multiplet; dd doublet of doublets; td triplet of doublets; br broad. Chemical shifts are reported in ppm relative to the residual solvent peak and *J* values are reported in Hz. Mass spectrometry data were collected on a DART-SVP (Direct Analysis in Real Time) ion source (IonSense, Saugus, MA) coupled to an Exactive Orbitrap mass spectrometer (ThermoScientific, Bremen, Germany). Optical rotation measurements were performed by NuMega Resonance Labs (San Diego, CA) on a Jasco P-2000 polarimeter with a 589-nm sodium lamp. The following molecules were purchased from commercial vendors: NHS-fluorescein (carboxyfluorescein succinimidyl ester) (**P1**) (ThermoScientific, 46410), ActivX™ TAMRA-FP serine hydrolase probe (ThermoScientific, 88318).

General Procedure (GP1) for the acylation of phloroglucinol compounds
The indicated compounds were prepared, with modifications, using a previously reported procedure.[52] Respective acid chlorides (1.5 equiv) were added dropwise over the course of 12 hours to a solution of phloroglucinol (1.0 equiv) in $MeSO_3$ (1.5 M). Reactions were stirred, open to air, for an additional 4 hours. Crude reactions were quenched with cold H_2O and extracted with EtOAc, washed with NaCl, and then dried with $MgSO_4$. EtOAc was removed by rotary evaporation, and then crude mixtures were redissolved in CH_2Cl_2, adsorbed onto silica gel (SiO_2, 12 g) by rotary evaporation, and purified on silica gel column (SiO_2, 50 µm, 220 g) using puriFlash® XS 520 Plus flash chromatography system.

General Procedure (GP2) for formylation of acylated phloroglucinol compounds
The indicated compounds were prepared, with modifications, using a previously reported procedure.[52] Under a nitrogen atmosphere, DMF (1.2 equiv) was cooled to –20 °C before the dropwise addition of $POCl_3$ (1.2 equiv) to the solution over the course of 2 hours completed the formation of the Vilsmeier-Haack reagent. The reagent was then added dropwise to a solution of precursor **S1** or **S5** (1.0 equiv) in EtOAc (0.5 M) under nitrogen, and the reaction was stirred for 16 hours at ambient temperature. Crude reactions were quenched with cold H_2O and stirred for an additional 1 hour at ambient temperature, prior to extracting with EtOAc, washing with NaCl, and then drying with $MgSO_4$. EtOAc was removed by rotary evaporation, and then crude mixtures were redissolved in CH_2Cl_2, adsorbed onto silica gel (SiO_2, 12 g) by rotary evaporation, and purified on silica gel column (SiO_2, 50 µm, 220 g) using puriFlash® XS 520 Plus flash chromatography system.

General Procedure (GP3) for the alkylation of phloroglucinol compounds
Similar to the previous report,[53] under nitrogen, KOH (3.0 equiv) was added to a solution of precursor **S2**, **S6**, or **S14** (1.0 equiv) in MeOH (0.1 M). Then, respective alkyl iodides (6.0 equiv)

were added to the solution, and the reaction was stirred at 80 °C for 16 hours. MeOH was removed by rotary evaporation, and the crude mixtures were redissolved in EtOAc, adsorbed onto silica gel (SiO_2, 12 g) by rotary evaporation, and purified on silica gel column (SiO_2, 50 μm, 220 g or 120 g) using puriFlash® XS 520 Plus flash chromatography system.

General procedure (GP4) for the synthesis of euglobals and their analogues

The indicated compounds were prepared according to previously reported procedures with modifications.[52,53] DDQ (1.2 equiv) was added to a solution of grandinol, **8** or **S18** (1.0 equiv) in $MeNO_2$ (0.2 M final concentration). Subsequently, respective terpenes (3.0 equiv.) were added to the solution. The reaction was heated for 16 hours with stirring at 50 °C, and $MeNO_2$ was removed by directing a constant stream of air into the flask for 30 minutes. The crude mixture was redissolved in CH_2Cl_2, adsorbed onto silica gel (SiO_2, 12 g) by rotary evaporation, and purified on silica gel column (SiO_2, 50 μm, 220 g) using puriFlash® XS 520 Plus flash chromatography system.

General procedure (GP5) for the synthesis of guadials and their analogues

The indicated compounds were prepared according to a previously reported procedure.[54] Intermediate **S16** (1.0 equiv) was mixed with respective terpenes (3.0 equiv) and heated to 90 °C for 16 hours with stirring. The crude mixture was dissolved in CH_2Cl_2, adsorbed onto silica gel (SiO_2, 12 g) by rotary evaporation, and purified on silica gel column (SiO_2, 50 μm, 80g) using puriFlash® XS 520 Plus flash chromatography system.

Characterization of synthetic compounds

3-methyl-1-(2,4,6-trihydroxyphenyl)butan-1-one (S1)

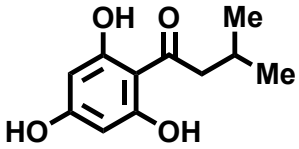

The title compound was synthesized according to the general procedure **GP1** using isovaleryl chloride. The desired product was afforded as a light yellow solid (1.33 g, 53%) following purification on silica gel column (SiO_2, 50 µm, 220 g) using puriFlash® XS 520 Plus flash chromatography system (6.4→56.5% of EtOAc in hexanes, 65 min, 46 mL/min). **TLC** (EtOAc:hexanes, 3:7 v/v) R_f = 0.14; visualized with 254-nm UV light. **^{1}H-NMR** (500 MHz, CD_3OD): δ 5.80 (s, 2H), 2.91 (d, *J* = 6.9 Hz, 2H), 2.20 (m,1H), 0.95 (d, *J* = 6.7 Hz, 6H). **^{13}C-NMR** (126 MHz, CD_3OD): δ 207.01, 165.96, 165.76, 105.58, 95.73, 53.69, 26.69, 23.26. **HRMS** (DART): exact mass calculated for $C_{11}H_{15}O_4$ $[M+H]^+$ m/z = 211.0965; found m/z = 211.0969.

2,4,6-trihydroxy-3-(3-methylbutanoyl)benzaldehyde (S2)

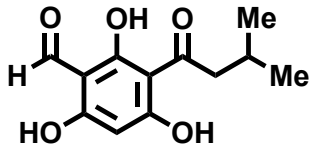

The title compound was synthesized according to the general procedure **GP2** using **S1**. The desired product was afforded as a light pink solid (1.55 g, 61%) following purification on silica gel column (SiO_2, 50 µm, 220 g) using puriFlash® XS 520 Plus flash chromatography system (6.4→56.5% of EtOAc in hexanes, 33 min, 127 mL/min). **TLC** (EtOAc:hexanes, 3:7 v/v) R_f = 0.28; visualized with 254-nm UV light. **^{1}H-NMR** (400 MHz, CD_3OD): δ 10.06 (s, 1H), 5.81 (s, 1H), 2.93 (d, *J* = 6.7 Hz, 2H), 2.22 (m, 1H), 0.97 (d, *J* = 6.7 Hz, 6H). **^{13}C-NMR** (126 MHz, CD_3OD): δ 207.18, 193.28, 172.98, 171.36, 169.05, 105.38, 104.68, 95.49, 53.77, 26.13, 23.09. **HRMS** (DART): exact mass calculated for $C_{12}H_{15}O_5$ $[M+H]^+$ m/z = 239.0914; found m/z = 239.0917.

2,4,6-trihydroxy-3-methyl-5-(3-methylbutanoyl)benzaldehyde (grandinol)

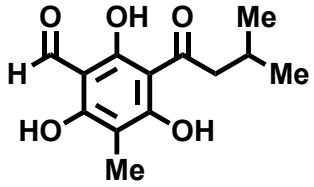

The title compound was synthesized according to the general procedure **GP3** using precursor **S2** and methyl-iodide. The desired product was afforded as an orange-red solid (944 mg, 28%) following purification on silica gel column (SiO_2, 50 µm, 220 g) using puriFlash® XS 520 Plus flash chromatography system (6.4→56.5% of EtOAc in hexanes, 33 min, 127 mL/min). To obtain high-purity material for biological applications, the desired product was further subjected to puriFlash 5.250 preparative HPLC system (0→100% of CH_3CN:0.1% TFA in H_2O:0.1% TFA, 60 min, 32 mL/min) using an Uptisphere® Strategy (C18-HQ, 5 µm, 250´ 30 mm) column. **TLC** (EtOAc:hexanes, 3:7 v/v) R_f = 0.15; visualized with 254-nm UV light. **^{1}H-NMR** (500 MHz, CD_3OD): δ 10.11 (s, 1H), 2.967 (d, *J* = 6.8 Hz, 2H), 2.27 – 2.19 (m, 1H), 1.98 (s, 3H), 0.978 (d, *J* = 6.7 Hz, 6H). **^{13}C-NMR** (126 MHz, CD_3OD): δ207.39, 193.69, 171.14, 168.89, 166.03, 105.50, 104.71, 103.62, 53.97, 26.21, 23.11, 7.09. **HRMS** (DART): exact mass calculated for $C_{13}H_{17}O_5^+$ $[M+H]^+$ m/z = 253.10705; found m/z = 253.10617.

(2*S*,4*R*,4a*S*,9a*R*)-6,8-dihydroxy-3,3,4a-trimethyl-7-(3-methylbutanoyl)-2,3,4,4a,9,9a-hexahydro-1*H*-2,4-methanoxanthene-5-carbaldehyde (euglobal G1)

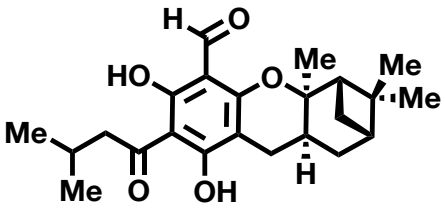

The title compound was synthesized according to the general procedure **GP4** using precursor grandinol and (+)-α-Pinene. The desired product was afforded as a colorless oil (90 mg, 11.7%) following purification on silica gel column (SiO_2, 50 µm, 220 g) using puriFlash® XS 520 Plus flash chromatography system (0→56.5% of DCM in hexanes, 45 min, 127 mL/min). However, we encountered challenges in separating this compound from an unidentified impurity that made up 20% of the mixture, ultimately leading us to omit this compound from our biological studies. **TLC** (DCM:hexanes, 3:7 v/v) R_f = 0.18; visualized with 254-nm UV light. **^{1}H-NMR** (500 MHz, $CDCl_3$): δ 15.44 (s, 1H), 13.14 (s, 1H), 10.21 (s, 1H), 3.01 (dd, *J* = 15.3, 6.1 Hz, 1H), 2.74 (m, 1H), 2.70-2.67 (m, 1H), 2.59 (dd, *J* = 15.3, 7.6 Hz, 1H), 2.41 (dd, *J* = 14.9, 5.7 Hz, 1H), 2.28 (t, *J* = 5.6 Hz, 1H), 2.22 (m, 1H), 2.15-2.10 (m, 2H), 1.90 (m, 1H), 1.51 (s, 3H), 1.33 (m, 1H), 1.31 (s, 3H), 1.10 (s, 3H), 0.99 (d, *J* = 6.6 Hz, 3H), 0.94 (d, *J* = 6.6 Hz, 3H), 0.80 (d, *J* = 10.7 Hz, 1H). **^{13}C-NMR** (126 MHz, $CDCl_3$): δ 205.93, 192.60, 170.60, 167.06, 166.31, 104.81, 104.15, 100.72, 89.43, 55.50, 52.81, 40.57, 40.44, 33.87, 32.44, 29.86, 29.30, 28.27, 27.73, 25.03, 23.18, 22.89, 22.57, 20.06. **HRMS** (DART): exact mass calculated for $C_{23}H_{31}O_5$ $[M+H]^+$ m/z = 387.21660; found m/z =387.21365.

(2*S*,4*R*,4a*S*,9a*R*)-6,8-dihydroxy-3,3,4a-trimethyl-5-(3-methylbutanoyl)-2,3,4,4a,9,9a-hexahydro-1*H*-2,4-methanoxanthene-7-carbaldehyde ((+)-euglobal G2)

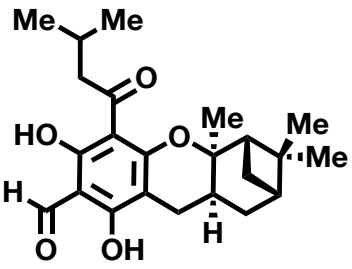

The title compound was synthesized according to the general procedure **GP4** using precursor grandinol and (+)-α-Pinene. The desired product was afforded as a colorless oil (68 mg, 8.9%) following purification on silica gel column (SiO_2, 50 µm, 220 g) using puriFlash® XS 520 Plus flash chromatography system (0→56.5% of DCM in hexanes, 45 min, 127 mL/min). **TLC** (DCM:hexanes, 3:7 v/v) R_f = 0.35; visualized with 254-nm UV light. $[a]_D^{20}$ = +87.2° (*c* 0.17, $CHCl_3$). **^{1}H-NMR** (500 MHz, $CDCl_3$): δ 15.35 (s, 1H), 14.35 (s, 1H), 9.93 (s, 1H), 3.00 – 2.97 (m, 2H), 2.73 – 2.70 (m, 2H), 2.47-2.43 (dd, *J* = 15.7, 6.4 Hz, 1H), 2.29 – 2.22 (m, 2H), 2.14 – 2.10 (m, 2H), 1.89 (m, 1H), 1.46 (s, 3H), 1.34 – 1.30 (m, 1H), 1.30 (s, 3H), 1.10 (s, 3H), 1.00 (d, *J* = 3 Hz, 3H), 0.98 (d, *J* = 3 Hz, 3H), 0.82 (d, *J* = 10.5 Hz, 1H).**^{13}C-NMR** (126 MHz, $CDCl_3$): δ 206.50, 191.83, 171.44, 168.37, 164.55, 103.86, 103.64, 101.00, 87.73, 55.01, 52.89, 40.79, 40.41, 34.27, 32.14, 28.92, 28.35, 28.04, 25.16, 22.96, 22.92, 22.89, 20.07. **HRMS** (DART): exact mass calculated for $C_{23}H_{31}O_5$ $[M+H]^+$ m/z = 387.21660; found m/z = 387.21394.

(2*R*,4*S*,4a*R*,9a*S*)-6,8-dihydroxy-3,3,4a-trimethyl-5-(3-methylbutanoyl)-2,3,4,4a,9,9a-hexahydro-1*H*-2,4-methanoxanthene-7-carbaldehyde ((–)-euglobal G2)

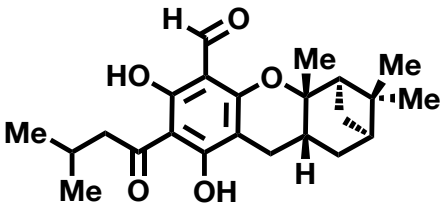

The title compound was synthesized according to the general procedure **GP4** using precursor grandinol and (–)-α-Pinene. The desired product was afforded as a colorless oil (93.9 mg, 13.5%) following purification on silica gel column (SiO_2, 50 µm, 220 g) using puriFlash® XS 520 Plus flash chromatography system (0→56.5% of DCM in hexanes, 45 min, 127 mL/min). **TLC** (DCM:hexanes, 3:7 v/v) R_f = 0.35; visualized with 254-nm UV light. $[a]_D^{20}$ = –84.7° (*c* 0.16, $CHCl_3$). **^{1}H-NMR** (500 MHz, $CDCl_3$): δ 15.35 (s, 1H), 14.36 (s, 1H), 9.93 (s, 1H), 3.03 – 2.93 (m, 2H), 2.73 – 2.68 (m, 2H), 2.45 (dd, *J* = 15.9, 6.5 Hz, 1H), 2.29 – 2.23 (m, 2H), 2.15 – 2.11 (m, 2H), 1.89 (m, 1H), 1.46 (s, 3H), 1.34 – 1.31 (m, 1H), 1.30 (s, 3H), 1.09 (s, 3H), 1.00 (d, *J* = 2.9 Hz, 3H), 0.98 (d, *J* = 2.9 Hz, 3H), 0.82 (d, *J* = 10.5 Hz, 1H). **^{13}C-NMR** (126 MHz, $CDCl_3$): δ 206.50, 191.83, 171.44, 168.37, 164.54, 103.86, 103.64, 101.00, 87.73, 55.01, 52.89, 40.79, 40.41, 34.27, 32.15, 28.92, 28.35, 28.04, 25.15, 22.96, 22.92, 22.89, 20.07. **HRMS** (DART): exact mass calculated for $C_{23}H_{31}O_5$ $[M+H]^+$ m/z = 387.21660; found m/z = 387.21562

(1*R*,2*R*,5*S*)-5',7'-dihydroxy-6,6-dimethyl-6'-(3-methylbutanoyl)spiro[bicyclo[3.1.1]heptane-2,2'-chromane]-8'-carbaldehyde ((–)-euglobal G3)

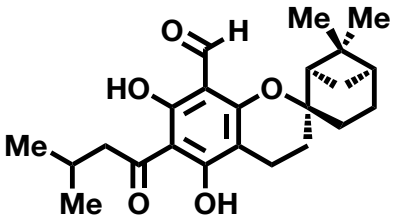

The title compound was synthesized according to the general procedure **GP4** using precursor grandinol and (–)-β-Pinene. The desired product was afforded as a colorless oil (102 mg, 13.3%) following purification on silica gel column (SiO_2, 50 µm, 220 g) using puriFlash® XS 520 Plus flash chromatography system (0→56.5% of DCM in hexanes, 45 min, 127 mL/min). **TLC** (DCM:hexanes, 3:7 v/v) R_f = 0.35; visualized with 254-nm UV light. $[a]_D^{20}$ = –16.5° (*c* 0.19, $CHCl_3$). **^{1}H-NMR** (500 MHz, $CDCl_3$): δ 15.37 (s, 1H), 14.42 (s, 1H), 10.01 (s, 1H), 2.966 (d, *J* = 6.7 Hz, 2H), 2.55 (t, *J* = 6.7 Hz, 2H), 2.27-2.22 (m, 2H), 2.16 (t, *J* = 5.4 Hz, 1H), 2.03 – 1.97 (m, 5H), 1.90-1.85 (m, 2H), 1.60 (d, *J* = 10.2 Hz, 1H), 1.29 (s, 3H), 1.02 (s, 3H), 0.98 (d, *J* = 6.7 Hz, 6H). **^{13}C-NMR** (126 MHz, $CDCl_3$): δ 206.51,191.89, 171.43, 168.42, 162.04, 104.49, 103.44, 101.28, 85.05, 52.83, 49.74, 40.74, 38.41, 32.01, 28.64, 27.65, 26.70, 25.26, 24.88, 23.41, 22.91, 22.90, 15.50. **HRMS** (DART): exact mass calculated for $C_{23}H_{31}O_5$ $[M+H]^+$ m/z = 387.21660; found m/z = 387.21394.

(1*R*,2*R*,5*S*)-5',7'-dihydroxy-6,6-dimethyl-8'-(3-methylbutanoyl)spiro[bicyclo[3.1.1]heptane-2,2'-chromane]-6'-carbaldehyde ((–)-euglobal G4)

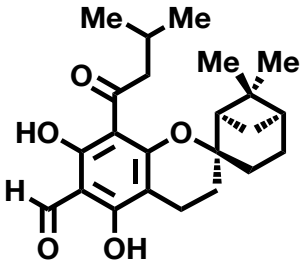

The title compound was synthesized according to the general procedure **GP4** using precursor grandinol and (–)-β-Pinene. The desired product was afforded as a colorless oil (107 mg, 14%) following purification on silica gel column (SiO_2, 50 µm, 220 g) using puriFlash® XS 520 Plus flash chromatography system (0→56.5% of DCM in hexanes, 45 min, 127 mL/min). **TLC** (DCM:hexanes, 3:7 v/v) R_f = 0.18; visualized with 254-nm UV light. $[a]_D^{20}$ = –8.4° (*c* 0.26, $CHCl_3$). **^{1}H-NMR** (500 MHz, $CDCl_3$): δ 15.36 (s, 1H), 13.17 (s, 1H), 10.17 (s, 1H), 2.94 (dd,

J = 6.8, 1.8 Hz, 2H), 2.56 (t, *J* = 6.7 Hz, 2H), 2.32 – 2.29 (m, 1H), 2.27 – 2.21 (m, 1H), 2.18 (t, *J* = 5.4 Hz, 1H), 2.04 – 1.98 (m, 5H), 1.91 – 1.85 (m, 2H), 1.63 (d, *J* = 10.1 Hz, 1H), 1.30 (s, 3H), 1.02 (s, 3H), 0.96 (d, *J* = 6.8 Hz, 3H), 0.947 (d, *J* = 6.8 Hz, 3H). **^{13}C-NMR** (126 MHz, $CDCl_3$): δ 205.79, 192.51, 170.05, 166.96, 163.44, 104.83, 104.35, 100.46, 86.78, 53.23, 49.52, 40.56, 38.40, 31.41, 28.78, 27.69, 27.44, 24.95, 24.75, 23.50, 22.90, 22.80, 15.29. **HRMS** (DART): exact mass calculated for $C_{23}H_{31}O_5$ $[M+H]^+$ m/z = 387.21660; found m/z = 387.21368.

6-bromo-1-(2,4,6-trihydroxyphenyl)hexan-1-one (S4)

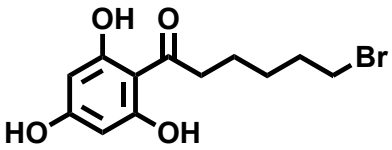

The title compound was synthesized according to the general procedure **GP1** using 6-bromohexanoyl chloride (1.0 equiv). The desired product was afforded as a light-yellow solid (2.53 g, 35%) following purification on silica gel column (SiO_2, 50 μm, 220 g) using puriFlash® XS 520 Plus flash chromatography system (9→100% of Et_2O in hexanes, 45 min, 127 mL/min). **TLC** (Et_2O:hexanes, 7:3 v/v) R_f = 0.45; visualized with 254-nm UV light. **^{1}H-NMR** (500 MHz, CD_3OD): δ 5.80 (s, 2H), 3.45 (t, *J* = 6.6 Hz, 2H), 3.05 (m, 2H), 1.89 (m, 2H), 1.69 (m, 2H), 1.51 (m, 2H). **^{13}C-NMR** (126 MHz, CD_3OD): δ 207.00, 166.06, 165.83, 105.29, 95.69, 44.57, 34.22, 33.89, 29.10, 25.26. **HRMS** (DART): exact mass calculated for $C_{12}H_{16}BrO_4$ $[M+H]^+$ m/z = 303.0226; found m/z = 303.0212.

6-azido-1-(2,4,6-trihydroxyphenyl)hexan-1-one (S5)

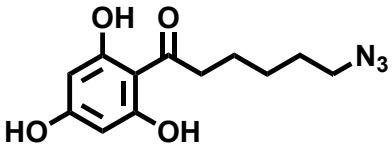

To a solution of 6-bromo-1-(2,4,6-trihydroxyphenyl)hexan-1-one **S4** (3.62 g, 12.0 mmol, 1.0 equiv) in DMF (120.0 mL, 0.1 M final concentration) was added sodium azide (7.8 g, 120 mmol, 10 equiv). The reaction was refluxed for 12 hours with stirring at 70 °C, and DMF was removed by a stream of air. The crude mixture was redissolved in EtOAc and extracted with EtOAc and H_2O to further remove the DMF. The EtOAc was then removed by rotary evaporation. The crude product was redissolved in EtOAc again, adsorbed into silica gel (SiO_2, 20 g) by rotary evaporation, and purified on silica gel column (SiO_2, 50 μm, 220 g) using puriFlash® XS 520 Plus flash chromatography system (4.6→75% of EtOAc in hexanes, 68 min, 127 mL/min) to deliver the desired product as a light yellow solid (2.60 g, 82%).**TLC** (EtOAc:hexanes, 4:6 v/v) R_f = 0.40; visualized with 254-nm UV light. **^{1}H-NMR** (500 MHz, CD_3OD): δ 5.80 (s, 2H), 3.29 (t, *J* = 6.4 Hz, 2H), 3.06 (m, 2H), 1.69 (m, 2H), 1.63 (m, 2H), 1.45 (m, 2H). **^{13}C-NMR** (126 MHz, CD_3OD): δ 207.03, 166.07, 165.83, 105.30, 95.70, 52.36, 44.60, 29.81, 27.70, 25.64. **HRMS** (DART): exact mass calculated for $C_{12}H_{16}N_3O_4$ $[M+H]^+$ m/z = 266.1135; found m/z = 266.1139.

3-(6-azidohexanoyl)-2,4,6-trihydroxybenzaldehyde (S6)

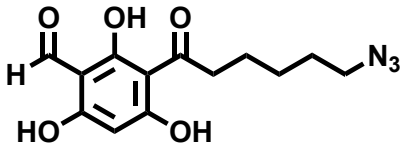

The title compound was synthesized according to the general procedure **GP2** using **S5** 6-azido-1-(2,4,6-trihydroxyphenyl)hexan-1-one. The desired product was afforded as a light yellow solid (1.30 g, 63%) following purification on silica gel column (SiO_2, 50 μm, 220 g) using puriFlash® XS 520 Plus flash chromatography system (6.1→93.5% of EtOAc in hexanes, 45 min, 127 mL/min). **TLC** (EtOAc:hexanes, 5:5 v/v) R_f = 0.34; visualized with 254-nm UV light. **^{1}H-NMR** (500 MHz, CD_3OD): δ 10.07 (s, 1H), 5.83 (s, 1H), 3.31 (m, 2H), 3.09 (t, *J* = 7.1 Hz, 2H), 1.71 (m,

2H), 1.64 (m, 2H), 1.46 (m, 2H). **^{13}C-NMR** (101 MHz, CD_3OD): δ 207.10, 193.14, 172.98, 171.28, 168.97, 105.34, 104.42, 95.50, 52.34, 44.79, 29.82, 27.52, 24.83. **HRMS** (DART): exact mass calculated for $C_{13}H_{16}N_3O_5$ $[M+H]^+$ m/z = 294.1084; found m/z = 294.1068.

3-(6-azidohexanoyl)-2,4,6-trihydroxy-5-methylbenzaldehyde (8)

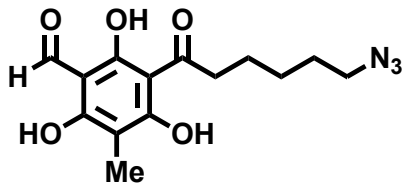

The title compound was synthesized according to the general procedure **GP3** using precursor **S6** and methyl-iodide. The desired product was afforded as an orange solid (480 mg, 36%) following purification on silica gel column (SiO_2, 50 µm, 220 g) using puriFlash® XS 520 Plus flash chromatography system (4.6→100% of EtOAc in hexanes, 55 min, 127 mL/min). **TLC** (EtOAc:hexanes, 4:6 v/v) R_f = 0.53; visualized with 254-nm UV light. **^{1}H-NMR** (500 MHz, CD_3OD): δ 10.09 (s, 1H), 3.31 (m, 2H), 3.10 (t, *J* = 7.2 Hz, 2H), 1.97 (s, 3H), 1.71 (m, 2H), 1.64 (m, 2H), 1.46 (m, 2H). **^{13}C-NMR** (126 MHz, CD_3OD): δ 207.48, 193.71, 171.22, 169.02, 166.12, 105.54, 104.53, 103.58, 52.36, 44.99, 29.85, 27.59, 25.09, 7.09. **HRMS** (DART): exact mass calculated for $C_{14}H_{18}N_3O_5$ $[M+H]^+$ m/z = 308.1241; found m/z = 308.1700.

(2*S*,4*R*,4a*S*)-5-(6-azidohexanoyl)-6,8-dihydroxy-3,3,4a-trimethyl-2,3,4,4a,9,9a-hexahydro-1*H*-2,4-methanoxanthene-7-carbaldehyde ((+)-9)

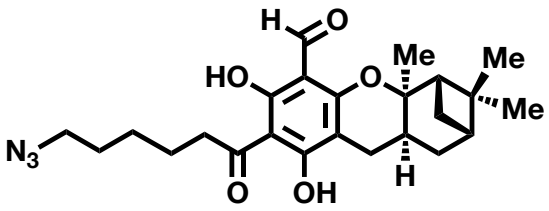

The title compound was synthesized according to the general procedure **GP4,** using precursor **8** and (+)-α-Pinene. The desired product was afforded as a colorless oil (32 mg, 4.6%) following purification on silica gel column (SiO_2, 50 µm, 220 g) using puriFlash® XS 520 Plus flash chromatography system (0→100% of EtOAc in hexanes, 55 min, 127 mL/min). **TLC** (EtOAc:hexanes, 0.5:9.5 v/v) R_f = 0.33; visualized with 254-nm UV light. **^{1}H-NMR** (500 MHz, $CDCl_3$): δ 15.19 (s, 1H), 14.38 (s, 1H), 9.93 (s, 1H), 3.29 (t, *J* = 6.9 Hz, 2H), 3.14-3.11 (m, 2H), 2.73-2.70 (m, 2H), 2.45 (dd, *J* = 16.0, 6.6 Hz, 1H), 2.25 (t, *J* = 5.6 Hz, 1H), 2.14-2.10 (m, 2H), 1.89 (m, 1H), 1.74-1.70 (m, 2H), 1.67-1.64 (m, 2H), 1.50-1.47 (m, 2H), 1.46 (s, 3H), 1.34-1.31 (m, 1H), 1.30 (s, 3H), 1.09 (s, 3H), 0.81 (d, *J* = 11.0 Hz, 1H). **^{13}C-NMR** (126 MHz, $CDCl_3$): δ 206.32, 191.88, 171.22, 168.38, 164.67, 103.86, 103.40, 101.04, 87.84, 54.98, 51.49, 43.91, 40.75, 40.42, 34.25, 32.12, 28.92, 28.91, 28.33, 28.01, 26.61, 24.01, 22.88, 20.04. **HRMS** (DART): exact mass calculated for $C_{24}H_{32}N_3O_5$ $[M+H]^+$ m/z = 442.23365 ; found m/z = 442.23393.

(2*R*,4*S*,4a*R*)-5-(6-azidohexanoyl)-6,8-dihydroxy-3,3,4a-trimethyl-2,3,4,4a,9,9a-hexahydro-1*H*-2,4-methanoxanthene-7-carbaldehyde ((–)-9)

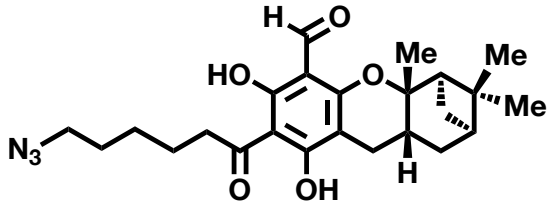

The title compound was synthesized according to the general procedure **GP4**, using precursor **8** and (–)-α-Pinene. The desired product was afforded as a colorless oil (38mg, 5.5%) following purification on silica gel column (SiO_2, 50 µm, 220 g) using puriFlash® XS 520 Plus flash chromatography system (0→100% of EtOAc in hexanes, 55 min, 127 mL/min). **TLC** (EtOAc:hexanes, 0.5:9.5 v/v) R_f = 0.33; visualized with 254-nm UV light. **^{1}H-NMR** (500 MHz, $CDCl_3$): δ 15.19 (s, 1H), 14.38 (s,

1H), 9.93 (s, 1H), 3.29 (t, *J* = 6.9 Hz, 2H), 3.14-3.11 (m, 2H), 2.73-2.70 (m, 2H), 2.45 (dd, *J* = 15.8, 6.6 Hz, 1H), 2.25 (t, *J* = 5.6 Hz, 1H), 2.14-2.10 (m, 2H), 1.89 (m, 1H), 1.75-1.70 (m, 2H), 1.68-1.64 (m, 2H), 1.50-1.47 (m, 2H), 1.46 (s, 3H), 1.34-1.31 (m, 1H), 1.30 (s, 3H), 1.09 (s, 3H), 0.81 (m, 1H). **^{13}C-NMR** (126 MHz, $CDCl_3$): δ 206.32, 191.88, 171.22, 168.38, 164.66, 103.86, 103.40, 101.04, 87.84, 54.98, 51.49, 43.91, 40.75, 40.42, 34.25, 32.12, 28.92, 28.91, 28.33, 28.01, 26.61, 24.01, 22.88, 20.04. **HRMS** (DART): exact mass calculated for $C_{24}H_{32}N_3O_5$ $[M+H]^+$ m/z = 442.23365 ; found m/z = 442.23422.

(1*R*,2*R*,5*S*)-6'-(6-azidohexanoyl)-5',7'-dihydroxy-6,6-dimethylspiro[bicyclo[3.1.1]heptane-2,2'-chromane]-8'-carbaldehyde ((–)-10)

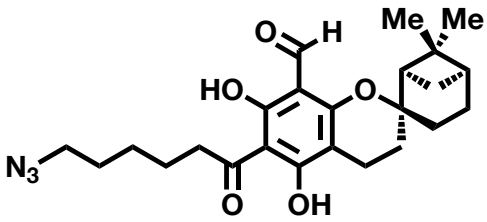

The title compound was synthesized according to the general procedure **GP4**, using precursor **8** and (–)-β-Pinene. The desired product was afforded as a colorless oil (96 mg, 7.5%) following purification on silica gel column (SiO_2, 50 µm, 220 g) using puriFlash® XS 520 Plus flash chromatography system (0→100% of EtOAc in hexanes, 55 min, 127 mL/min). **TLC** (EtOAc:hexanes, 0.5:9.5 v/v) R_f = 0.33; visualized with 254-nm UV light. **^{1}H-NMR** (500 MHz, $CDCl_3$): δ 15.21 (s, 1H), 14.45 (s, 1H), 10.01 (s, 1H), 3.29 (t, *J* = 6.9Hz, 2H), 3.11 (t, *J* = 7.4Hz, 2H), 2.55 (t, *J* = 6.8Hz, 2H), 2.27-2.23 (m, 1H), 2.15 (t, *J* = 5.4Hz, 1H), 2.03-1.96 (m, 5H), 1.9-1.83 (m, 2H), 1.73-1.70 (m, 2H), 1.67-1.64 (m, 2H), 1.60 (d, *J* = 10.2Hz, 1H), 1.48-1.45 (m, 2H), 1.29 (s, 3H), 1.02 (s, 3H). **^{13}C-NMR** (126 MHz, $CDCl_3$): δ 206.31, 191.95, 171.22, 168.42, 162.14, 104.51, 103.21, 101.31, 85.12, 51.49, 49.74, 43.85, 40.72, 38.41, 32.08, 28.91, 28.63, 27.64, 26.69, 26.60, 24.88, 24.05, 23.40, 15.48. **HRMS** (DART): exact mass calculated for $C_{24}H_{32}N_3O_5$ $[M+H]^+$ m/z = 442.23365 ; found m/z = 442.26679.

(1*R*,2*R*,5*S*)-8'-(6-azidohexanoyl)-5',7'-dihydroxy-6,6-dimethylspiro[bicyclo[3.1.1]heptane-2,2'-chromane]-6'-carbaldehyde ((–)-11).

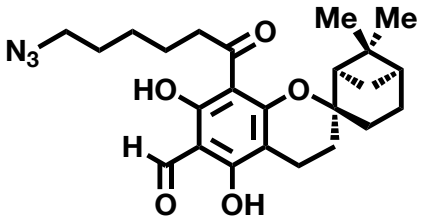

The title compound was synthesized according to the general procedure **GP4,** using precursor **8** and (–)-β-Pinene. The desired product was afforded as a colorless oil (80 mg, 6.3%) following purification on silica gel column (SiO_2, 50 µm, 220 g) using puriFlash® XS 520 Plus flash chromatography system (0→100% of EtOAc in hexanes, 55 min, 127 mL/min). **TLC** (EtOAc:hexanes, 0.5:9.5 v/v) R_f = 0.21; visualized with 254-nm UV light. **^{1}H-NMR** (500 MHz, $CDCl_3$): δ 15.29 (s, 1H), 13.19 (s, 1H), 10.18 (s, 1H), 3.3 (t, *J* = 6.9Hz, 2H), 3.1-3.06 (m, 2H), 2.57 (td, *J* = 7.0, 2.7 Hz, 2H), 2.32-2.28 (m, 1H), 2.19 (t, *J* = 5.4 Hz, 2H), 2.04-2.0 (m, 5H), 1.93-1.89 (m, 2H), 1.73-1.69 (m, 2H), 1.68-1.64 (m, 2H), 1.60 (d, *J* = 10.1 Hz, 1H), 1.46-1.43 (m, 1H), 1.30 (s, 3H), 1.03 (s, 3H). **^{13}C-NMR** (126 MHz, $CDCl_3$): δ 205.57, 192.57, 170.06, 167.08, 163.51, 104.58, 104.36, 100.53, 86.94, 51.45, 49.42, 44.22, 40.56, 38.46, 32.08, 29.04, 28.91, 27.69, 27.36, 26.55, 24.94, 23.85, 23.53, 15.33. **HRMS** (DART): exact mass calculated for $C_{24}H_{32}N_3O_5$ $[M+H]^+$ m/z = 442.23365; found m/z = 442.26702.

3-(hex-5-yn-1-yl)-2,4,6-trihydroxy-5-(3-methylbutanoyl)benzaldehyde (7)

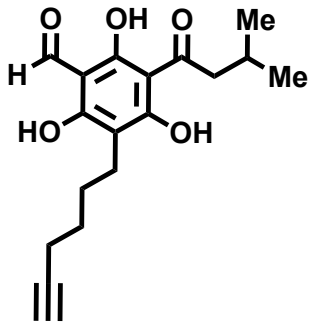

The title compound was synthesized according to the general procedure **GP3** using precursor **S2** and 6-iodo-1-hexyne. The desired product was afforded as a light pink solid (172 mg, 20%) following purification on silica gel column (SiO_2, 50 µm, 120 g) using puriFlash® XS 520 Plus flash chromatography system (3.8→56.5% of EtOAc in hexanes, 75 min, 46 mL/min. **TLC** (EtOAc:hexanes, 3:7 v/v) R_f = 0.28; visualized with 254-nm UV light. **^{1}H-NMR** (500 MHz, CD_3OD): δ 10.05 (s, 1H), 2.93 (d, *J* = 6.7 Hz, 2H), 2.53 (m, 2H), 2.21 (m, 1H), 2.18-2.15 (m, 2H), 1.54 (m, 4H), 0.96 (d, *J* = 6.7 Hz, 6H). **^{13}C-NMR** (126 MHz, CD_3OD): δ 207.54, 193.74, 171.45, 169.09, 165.91, 108.51, 105.62, 104.87, 85.04, 69.43, 54.00, 29.48, 29.09, 26.29, 23.12, 21.96, 19.03. **HRMS** (DART): exact mass calculated for $C_{18}H_{23}O_5$ $[M+H]^+$ m/z = 319.15400, found m/z = 319.15262.

2,4,6-trihydroxyisophthaladehyde (S14)

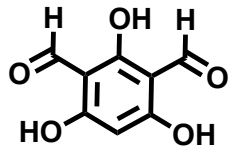

To a solution of anhydrous DMF (13.5 mL, 174 mmol, 2.2 equiv) under an inert atmosphere was added $POCl_3$ (16.5 mL, 174 mmol, 2.2 equiv) dropwise over a period of 30 min by syringe pump addition at 20 °C. The reaction was stirred for an additional 30 min before being transferred into an additional funnel. The Vilsmeier-Haack reagent was added dropwise to a solution of phloroglucinol (10 g, 79 mmol, 1.0 equiv) in anhydrous 1,4-dioxane (50 mL, 1.6 M) over 30 min. The reaction was stirred at 20 °C for an additional 12 hours. The crude mixture was quenched with 500 mL of an ice-water slurry while vigorously stirring and allowed to warm to 20 °C over a period of 4 hours. A beige precipitate was collected by vacuum filtration and washed well with H_2O. The precipitate was resuspended in 500 mL of H_2O and heated to 100 °C for 10 minutes and the solution immediately filtered while hot. The beige precipitate was dried by heating to 90 °C in a silicon oil bath under vacuum for 48 hours to deliver the desired product as a salmon pink solid (11.22 g, 78 %). **TLC** (MeOH:EtOAc, 1:9 v/v) R_f = 0.3 (steaking observed); visualized with 254-nm UV light. **^{1}H-NMR** (500 MHz, DMSO-d_6): δ 10.00 (s, 2H), 5.89 (s, 1H). **^{13}C-NMR** (126 MHz, DMSO-d_6): δ 191.39, 169.45, 169.05, 103.76, 94.08. **HRMS** (DART): exact mass calculated for $C_8H_5O_5$ $[M-H]^-$ m/z = 181.01425; found m/z = 181.01348.

5-(hex-5-yn-1-yl)-2,4,6-trihydroxyisophthalaldehyde (6)

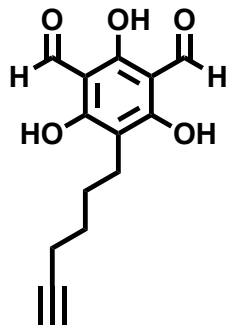

The title compound was synthesized according to the general procedure **GP3** using precursor **S14** and 6-iodo-1-hexyne. The desired product was afforded as a maroon solid (352 mg, 49%) following purification on silica gel column (SiO_2, 50 µm, 120 g) using puriFlash® XS 520 Plus flash chromatography system (4→100% of DCM in MeOH with 0.5% NH_4OH in DCM with 0.5% NH_4OH, 75 min, 46 mL/min). The product was then washed with 1 M HCl and water, collected by vacuum filtration, and redissolved in MeOH. The MeOH was removed by rotary evaporation, and the final product was dried under vacuum. **TLC** (DCM:MeOH, 8:2 v/v) R_f = 0.31; visualized with 254-nm UV light. **^{1}H-NMR** (500 MHz, CD_3OD): δ 10.14 (s, 2H), 2.57 (t, *J* = 7.0 Hz, 2H), 2.21-2.18 (m, 2H), 2.17-2.16 (m, 1H), 1.60 – 1.52 (m, 4H). **^{13}C-NMR** (126 MHz, CD_3OD): δ 191.97, 168.54, 168.07, 106.02, 104.69, 84.53, 71.15, 27.78, 27.54, 20.15, 17.62.

HRMS (DART): exact mass calculated for $C_{14}H_{15}O_5$ $[M+H]^+$ m/z = 263.0914; found m/z = 263.0896.

2,4,6-trihydroxy-5-(methoxy(phenyl)methyl)isophthalaldehyde (S16)

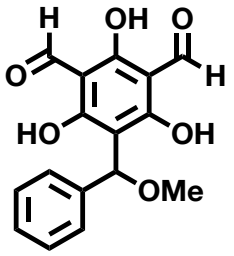

The title compound was synthesized according to previously reported methods.[54,55] Briefly, benzaldehyde (10.0 equiv, 5.6 mL), N,N,N′,N′-tetramethylethane-1,2-diamine (TMEDA) (0.2 equiv, 165 µL), and Et_3N (3.0 equiv, 2.3 mL) were added to a solution of **S14** in MeOH (5.49 mmol, 0.7 M). The mixture was stirred at 25 °C overnight before solvent and excess benzaldehyde were removed by rotary evaporation for several hours. Note: the compound degrades readily at ambient temperature, so any heating during purification and drying steps was avoided. The desired product was afforded as a colorless oil (513 mg, 31%) following purification on silica gel column (SiO_2, 50 µm, 120 g) using puriFlash® XS 520 Plus flash chromatography system (19→100% of DCM in hexanes, 50 min, 46 mL/min). The compound was immediately subjected to the subsequent reaction to prevent further loss of yield due to degradation. In the few hours post-purification, some free benzaldehyde had already been released (small peaks seen in ^{13}C-NMR spectrum taken overnight, though the ^{1}H-NMR spectrum taken immediately post-purification shows no free benzaldehyde). **TLC:** (DCM:hexanes 8:2 v/v) R_f = 0.34; visualized with 254-nm UV light and Seebach stain. **^{1}H-NMR** (500 MHz, CD_3OD): δ 10.13 (s, 2H), 7.44-7.42 (m, 2H), 7.36-7.33 (m, 2H), 7.31-7.28 (m, 1H), 5.82 (s, 1H), 3.50 (s, 3H). **^{13}C-NMR** (126 MHz, CD_3OD): δ 193.35, 169.76, 168.27, 140.75, 129.59, 129.37, 128.02, 105.52, 105.10, 81.25, 57.88.

(2*S*,4*R*,4a*R*,9*R*,9a*S*)-6,8-dihydroxy-3,3,4a-trimethyl-9-phenyl-2,3,4,4a,9,9a-hexahydro-1*H*-2,4-methanoxanthene-5,7-dicarbaldehyde ((+)-guadial B)

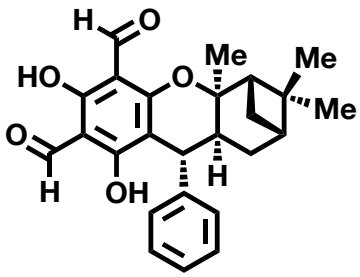

The title compound was synthesized according to the general procedure **GP5** using (+)-α-Pinene. The desired product was afforded as a colorless oil (92 mg, 13.3%) following purification on silica gel column (SiO_2, 50 µm, 80 g) using puriFlash® XS 520 Plus flash chromatography system (1% of Et_2O in hexanes, 60 min, 26 mL/min). After drying on high vacuum overnight, white crystals were obtained. **TLC** (Et_2O:hexanes 0.5:9.5 v/v) R_f = 0.14; visualized with 254-nm UV light and Seebach stain. $[\alpha]_D^{20}$ = +141.7° (*c* 0.18, $CHCl_3$). **^{1}H-NMR** (500 MHz, $CDCl_3$): δ 13.53 (s, 1H), 13.21 (s, 1H), 10.19 (s, 1H), 10.03 (s, 1H), 7.28 (m, 2H), 7.20 (m, 1H), 7.09 (m, 2H), 4.24 (s, 1H), 3.00 (t, *J* = 9.0Hz, 1H), 2.47 (m, 1H), 2.12-2.09 (m, 2H), 1.92 (m, 1H), 1.57-1.51 (m, 1H), 1.27 (s, 3H), 1.06 (s, 3H), 1.01 (s, 3H). **^{13}C-NMR** (126 MHz, $CDCl_3$): δ 192.27, 191.72, 169.51, 168.96, 166.51, 142.68, 128.78, 127.54, 126.83, 104.17, 103.85, 101.65, 89.07, 56.44, 41.31, 40.76, 40.35, 39.25, 36.67, 29.31, 28.04, 27.69, 23.00. **HRMS** (DART): exact mass calculated for $C_{25}H_{27}O_5$ $[M+H]^+$ m/z = 407.18530; found m/z = 407.18488.

(2*R*,4*S*,4a*S*,9*S*,9a*R*)-6,8-dihydroxy-3,3,4a-trimethyl-9-phenyl-2,3,4,4a,9,9a-hexahydro-1*H*-2,4-methanoxanthene-5,7-dicarbaldehyde ((–)-guadial B)

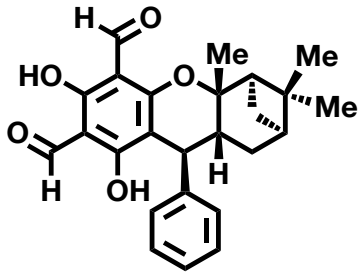

The title compound was synthesized according to the general procedure **GP5** using (–)-α-Pinene. The desired product was afforded as a colorless oil (46 mg, 8.3%) following purification on silica gel column (SiO_2, 50 µm, 80 g) using puriFlash® XS 520 Plus flash chromatography system (1% of Et_2O in hexanes, 60 min, 26 mL/min). After drying on high vacuum overnight, white crystals were obtained. **TLC** (Et_2O:hexanes 0.5:9.5 v/v) R_f = 0.14; visualized with 254-nm UV light and Seebach stain. $[\alpha]_D^{20}$ = –125.6° (*c* 0.15, $CHCl_3$). **^{1}H-NMR** (500 MHz, $CDCl_3$): δ 13.53 (s, 1H), 13.21 (s, 1H), 10.19 (s, 1H), 10.03 (s, 1H), 7.28 (m, 2H), 7.20 (m, 1H), 7.09 (m, 2H), 4.24 (s, 1H), 3.00 (t, *J* = 8.5Hz, 1H), 2.47 (m, 1H), 2.13-2.10 (m, 2H), 1.93 (m, 1H), 1.55-1.51 (m, 1H), 1.28 (s, 3H), 1.06 (s, 3H), 1.01 (s, 3H). **^{13}C-NMR** (126 MHz, $CDCl_3$): δ 192.30, 191.74, 169.51, 168.96, 166.52, 142.67, 128.79, 127.53, 126.84, 104.15, 103.84, 101.64, 89.08, 56.41, 41.30, 40.73, 40.35, 39.24, 36.67, 29.30, 28.03, 27.69, 23.00. **HRMS** (DART): exact mass calculated for $C_{25}H_{27}O_5$ $[M+H]^+$ m/z = 407.18530; found m/z = 407.18290

(1*R*,2*R*,4'*S*,5*S*)-5',7'-dihydroxy-6,6-dimethyl-4'-phenylspiro[bicyclo[3.1.1]heptane-2,2'-chromane]-6',8'-dicarbaldehyde ((+)-guadial C)

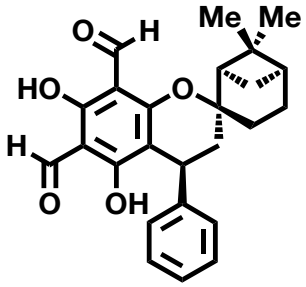

The title compound was synthesized according to the general procedure **GP5** using (–)-β-Pinene. The desired product was afforded as a colorless oil (81 mg, 15.8%) following purification on silica gel column (SiO_2, 50 µm, 80 g) using puriFlash® XS 520 Plus flash chromatography system (1% of Et_2O in hexanes, 60 min, 26 mL/min). After drying on high vacuum overnight, white crystals were obtained. **TLC** (Et_2O:hexanes 0.5:9.5 v/v) R_f = 0.14; visualized with 254-nm UV light and Seebach stain. $[\alpha]_D^{20}$ = +93.6° (*c* 0.24, $CHCl_3$). **^{1}H-NMR** (500 MHz, $CDCl_3$): δ 13.51 (s, 1H), 13.14 (s, 1H), 10.11 (s, 2H), 7.28 (t, *J* = 7.3 Hz 2H), 7.21 (t, *J* = 7.3Hz, 1H), 7.13 (d, *J* = 7.0 Hz, 2H), 3.99 (dd, *J* = 10.2, 6.9 Hz, 1H), 2.43 (dd, *J* = 14.4, 6.9 Hz, 1H), 2.30 (m, 1H), 2.22-2.18 (m, 1H), 2.11 (dd, *J* = 14.5, 10.2 Hz, 1H), 2.07 (m, 1H), 2.02-1.98 (m, 2H), 1.82-1.75 (m, 2H), 1.5 (d, *J* = 10.2 Hz, 1H), 1.30 (s, 3H), 1.00 (s, 3H). **^{13}C-NMR** (126 MHz, $CDCl_3$): δ 192.29, 191.65, 169.59, 168.72, 164.74, 144.50, 128.66, 126.89, 126.40, 104.57, 104.20, 103.09, 86.29, 47.70, 43.76, 40.67, 38.42, 35.18, 30.05, 27.64, 26.46, 24.69, 23.23. **HRMS** (DART): exact mass calculated for $C_{25}H_{27}O_5$ $[M+H]^+$ m/z = 407.18530; found m/z = 407.18330

2,4,6-trihydroxy-5-methylisophthalaldehyde (S18)

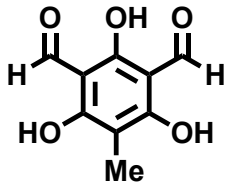

The title compound was synthesized according to the general procedure **GP3** using precursor **S14** and methyl iodide. The desired product was afforded as a brown solid (293 mg, 27%) following purification on silica gel column (SiO_2, 50 µm, 220 g) using puriFlash® XS 520 Plus flash chromatography system (16.5→100% of EtOAc in hexanes, 80 min, 127 mL/min). **TLC** (EtOAc:hexanes, 7:3 v/v) R_f = 0.25; visualized with 254-nm UV light. **^{1}H-NMR** (500 MHz, CD_3OD): δ 10.05 (s, 2H), 1.94 (s, 3H). **^{13}C-NMR** (126 MHz, CD_3OD): δ

191.45, 171.21, 169.38, 105.60, 99.97, 6.62. **HRMS** (DART): exact mass calculated for $C_9H_9O_5$ $[M+H]^+$ m/z = 197.04445; found m/z = 197.04352.

(2a*R*,4a*S*,10a*S*,13a*S*)-7,9-dihydroxy-2,2,4a-trimethyl-13-methylene-1,2,2a,3,4,4a,10,10a,11,12,13,13a-dodecahydrocyclobuta[6,7]cyclonona[1,2-*b*]chromene-6,8-dicarbaldehyde ((–)-cattleianal)

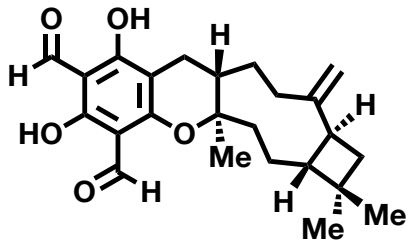

The title compound was synthesized according to the general procedure **GP4** using precursor **S18** and (–)-β-caryophyllene. The desired product was afforded as a colorless oil (110 mg, 11%) following purification on silica gel column (SiO_2, 50 µm, 220 g) using puriFlash® XS 520 Plus flash chromatography system (8.4→100% of DCM in hexanes, 45 min, 127 mL/min). **TLC** (DCM:hexanes, 6.5:3.5 v/v) R_f = 0.54; visualized with 254-nm UV light. $[a]_D^{20}$ = –25.9° (*c* 0.14, $CHCl_3$). **^{1}H-NMR** (500 MHz, $CDCl_3$): δ 13.42 (s, 1H), 13.24 (s, 1H), 10.14 (s, 1H), 10.02 (s, 1H), 4.91 (s, 1H), 4.87 (s, 1H), 2.64-2.62 (m, 1H), 2.49-2.44 (m, 1H), 2.43-2.40 (m, 1H), 2.21-2.17 (m, 1H), 2.16-2.13 (m, 1H), 2.08-2.07 (m, 1H), 2.06-2.04 (m, 1H), 1.97-1.94 (m, 1H), 1.90-1.87 (m, 1H), 1.76-1.73 (m, 1H), 1.72-1.70 (m, 1H), 1.70-1.69 (m, 1H), 1.64-1.62 (m, 1H), 1.60-1.58 (m, 1H), 1.47-1.43 (m, 1H), 1.21 (s, 3H), 0.99 (s, 3H), 0.98 (s, 3H). **^{13}C-NMR** (126 MHz, $CDCl_3$): δ 192.06, 191.77, 168.56, 168.32, 163.32, 152.01, 110.74, 104.18, 103.74, 100.95, 84.91, 53.56, 41.90, 38.15, 36.56, 35.38, 33.96, 33.89, 33.62, 30.38, 24.18, 22.62, 22.33, 21.35. **HRMS** (DART): exact mass calculated for $C_{24}H_{31}O_5$ $[M+H]^+$ m/z = 399.21660; found m/z = 399. 21518.

2,4,6-trihydroxy-5-(3-methylbutanoyl)isophthalaldehyde (jensenone)

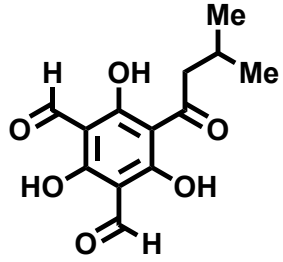

Formamidine acetate (2.48 g, 23.8 mmol, 5.0 equiv) and Ac_2O (4.5 mL, 47.6 mmol, 10.0 equiv) were added to a solution of **S1** in THF (1 g, 4.76 mmol, 0.07 M). The mixture was then stirred at 70 °C overnight, after which the solvent was removed by rotary evaporation at 50 °C. HCl (5 M, 100 mL) was then added, and the new mixture stirred at 20 °C overnight. The precipitate was collected and washed with H_2O and hexanes to afford an imine precursor to the title compound. LiOH (3 g/100 mL) was added and again, the mixture was left to stir overnight at 20 °C. Next, concentrated HCl was added until a pH of 3 was obtained for the solution, at which point the desired compound began to precipitate. It was collected and washed with H_2O and Et_2O to afford the final product as a salmon-orange solid without further purification (520 mg, 41%). **^{1}H-NMR** (500 MHz, $CDCl_3$): δ 15.10 (s, 1H), 14.09 (s, 1H), 10.16 (s, 1H), 10.12 (s, 1H), 2.98 (d, *J* = 6.7Hz, 2H), 2.25 (m, 1H), 0.99 (d, *J* = 6.7Hz, 6H). **^{13}C-NMR** (126 MHz, $CDCl_3$): δ 207.06, 192.93, 192.22, 176.55, 174.07, 172.63, 103.66, 102.83, 102.75, 52.75, 25.03, 22.83. **HRMS** (DART): exact mass calculated for $C_{13}H_{13}O_6$ $[M-H]^-$ m/z = 265.07176; found m/z = 265.06974.

Sodium 2,3,5,6-tetrafluoro-4-((6-((4R, 5S)-5-methyl-2-oxoimidazolidin-4-yl)hexanoyl)oxy)benzenesulfonate (desthiobiotin-tagged STP ester probe)

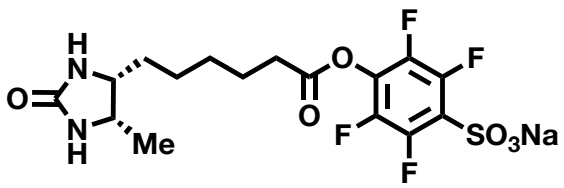

DCC (1.0 g, 4.85 mmol, 1.3 equiv) was added to a solution of desthiobiotin (800 mg, 3.73 mmol, 1.0 equiv) in DMF (15 mL, 0.25 M) under nitrogen. The mixture was stirred for 5 minutes, and then 2,3,5,6-tetrafluorophenol (1.0 g, 3.73 mmol, 1.0 equiv) was added. The reaction was stirred overnight at 20 °C, filtered, and then DMF was removed by a stream of air. The crude mixture was resuspended in DCM, mixed thoroughly, and filtered. Collected solid was then resuspended again in Et_2O, vortexed to mix, and again filtered. Next, the washed solid was transferred to a clean flask, 500 mL of MeCN was added, and the mixture was left to stir vigorously for 3 hours at 20 °C. Again, the remaining solid was collected by filtration and then was dried overnight on high vacuum. The final product yielded a white solid (720 mg, 42%), without further purification. **^{1}H-NMR** (500 MHz, DMSO-d_6): δ 6.32 (s, 1H), 6.12 (s, 1H), 3.62 (m, 1H), 3.52-3.47 (m, 1H), 2.77 (t, J = 7.3 Hz, 2H), 1.67 (m, 2H), 1.41-1.32 (m, 5H), 1.25-1.21 (m, 1H), 0.96 (d, J = 6.4 Hz, 3H). **^{13}C-NMR** (126 MHz, DMSO-d_6): δ 169.63, 162.85, 143.91, 141.93, 141.07, 140.90, 139.05, 138.92, 128.17, 128.05, 127.94, 124.67, 124.52, 124.37, 54.94, 50.24, 32.48, 29.43, 28.17, 25.39, 24.20, 15.51. **^{19}F-NMR** (470 MHz, DMSO-d_6): δ -139.41 (dd, J = 25.6, 9.8 Hz), -154.06 (dd, J = 25.5, 10.0 Hz).

Computational methods

All calculations were performed with the Gaussian 16 program.[5] Geometry optimizations of all minima and transition states involved were carried out using M06-2X[2] functional and SMD[3] solvation model in nitromethane solvent, the basis set was def2SVP.[4] Frequency calculations at the same level were performed to validate each structure as either a minimum (the number of imaginary frequencies = 0) or a transition state (the number of imaginary frequencies = 1) and to evaluate its zero-point energy and thermal corrections at 298 K. High level single point energies were computed by using ωB97xD[6] functional and SMD solvation model with def2QZVPP[7] basis set. It was labelled as ωB97xD/def2QZVPP/SMD($MeNO_2$)//M06-2X/def2SVP/SMD($MeNO_2$) level. Standard states are the hypothetical states at 1 mol/L. Orbital calculations were performed at the same level as geometry optimizations.

Computed energies of all the stationary points

Thermal correction to Enthalpy **TCH** (M06-2X/def2SVP/SMD($MeNO_2$) level), Thermal correction to Gibbs Free Energy **TCG** (M06-2X/def2SVP/SMD($MeNO_2$) level), Single point energies **E** (ωB97xD/def2QZVPP/SMD($MeNO_2$) level), Sum of electronic and thermal Free Energies **G**, delta Gibbs free Energies **ΔG**. Complete level of theory: ωB97xD/def2QZVPP/SMD($MeNO_2$)//M06-2X/def2SVP/SMD($MeNO_2$).

Table S4. Computed energies of all the stationary points

Compound	TCH	TCG	E	G	ΔG
ortho-quinone methide	0.151621	0.101948	-722.773352	-722.671404	
αα-caryophyllene	0.371682	0.314849	-586.083664	-585.768815	**-0.3**
αβ-caryophyllene	0.371597	0.313455	-586.07474	-585.761285	**4.5**
βα-caryophyllene	0.371717	0.31443	-586.082839	-585.768409	**0.0**
ββ-caryophyllene	0.371713	0.314601	-586.082478	-585.767877	**0.3**
TS-βα	0.524745	0.437241	-1308.858449	-1308.421208	**9.8**
cattleianal	0.529979	0.447157	-1308.92979	-1308.482633	**-28.8**
TS-ββ	0.524665	0.438748	-1308.856827	-1308.418079	**11.7**
4,10-*epi*-cattleianal	0.530168	0.448759	-1308.922961	-1308.474202	**-23.5**
TS-βα→ββ	0.370937	0.314933	-586.054934	-585.740001	**17.8**

FMO analysis of βα-caryophyllene and *ortho*-quinone methide

M06-2X/def2SVP/SMD($MeNO_2$)

βα-caryophyllene

HOMO –7.57 eV

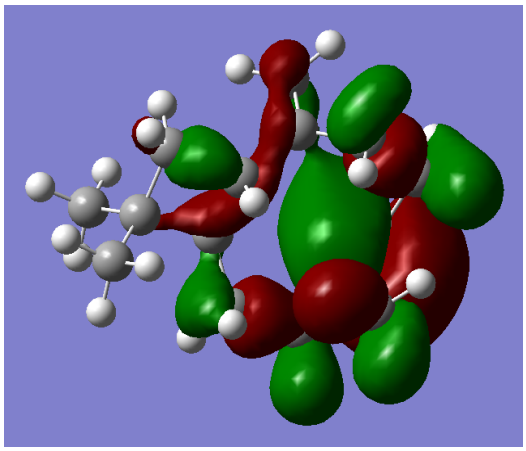

LUMO +1.27 eV

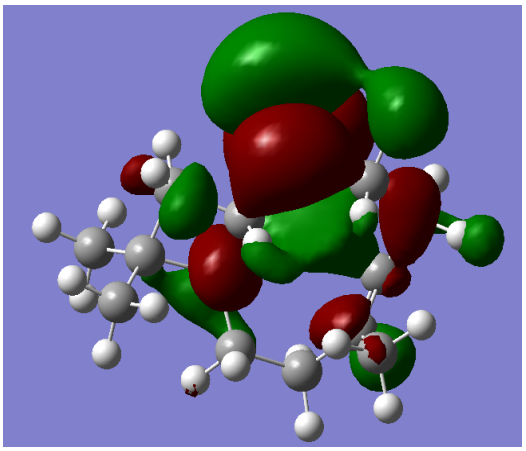

ortho-quinone methide

HOMO –7.88 eV

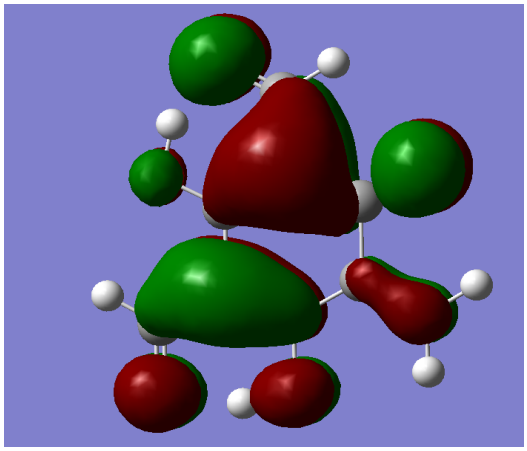

LUMO +1.92 eV

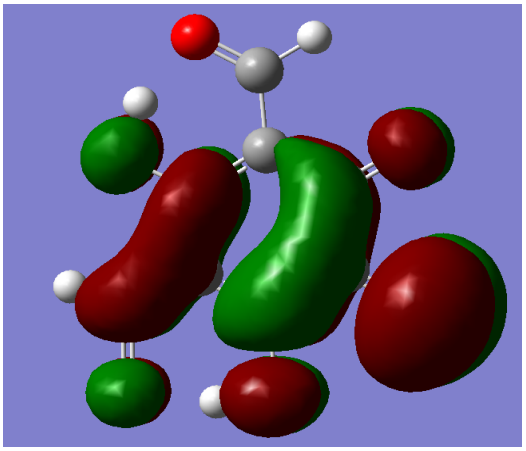

Based on these orbital peremeters, we can conclude that the Diels-Alder reaction is an inverse electron demand cycloaddition.

Cartesian coordinates of all computed structures

ortho-quinone methide
C 0.97734000 2.92385400 0.00031200
C 0.49877400 1.67060100 0.00011500
C -0.99080100 1.43451100 -0.00000200
C -1.42343100 0.04321200 0.00008500
C -0.49895100 -1.01395400 0.00014400
C 0.92357300 -0.78718000 0.00004400
C 1.40988500 0.52185900 0.00001500
C -2.81950200 -0.28223600 0.00002200
C 1.87103900 -1.87767900 -0.00007000
O -1.76477200 2.37476500 -0.00018700
O -3.24077300 -1.44685900 -0.00014300
O -0.91270000 -2.24727700 0.00007700
O 3.08846100 -1.68518300 -0.00033700
O 2.68479600 0.75691200 -0.00008600
H 2.05006300 3.12513500 0.00077600
H -3.53475300 0.56047100 -0.00012500
H 1.47597800 -2.90941600 -0.00002600
H -1.94120700 -2.19947800 0.00018200
H 3.14415300 -0.15651500 -0.00004200
H 0.27811000 3.76301500 0.00065900

αα-caryophyllene
C 0.93014500 0.40392100 -0.17873000
C 0.66599300 1.80040900 0.38195900
C -0.61965400 2.46650500 -0.16213400
C -1.75882700 1.48189300 -0.09993800
C -1.99034200 0.71177400 -1.17407000
C -2.63054200 -0.64277500 -1.19961400
C -1.51057200 -1.69011300 -0.98765500
C -0.87443500 -1.57081900 0.38630600
C 0.45070900 -0.86854000 0.57897300
C 1.73127000 -1.56939600 0.06053200
C 2.37509600 -0.17766800 -0.14799100
C 3.17469300 0.26132500 1.07593400
C 3.19063300 0.02142700 -1.41518600
C -2.39024600 1.30153200 1.25257300
C -1.48212700 -2.13019700 1.44143100
H 0.58543700 0.34766900 -1.22418700
H 0.62650500 1.74796500 1.48290400
H 1.52150600 2.45249400 0.13746100
H -0.44478200 2.76134000 -1.20858700
H -0.83050500 3.38168500 0.41413300
H -1.44525300 0.97051200 -2.09058000

H -3.12385800 -0.83218200 -2.16508500
H -3.38629600 -0.76505800 -0.40961700
H 0.57226200 -0.68296200 1.65799500
H 1.54519100 -2.06513100 -0.90553000
H 2.23112900 -2.27418900 0.74280500
H 3.46192600 1.32180600 1.00255800
H 4.09988900 -0.33129900 1.15608600
H 2.60873600 0.12808600 2.01020100
H 3.43563100 1.08680800 -1.55842900
H 4.13994800 -0.53649100 -1.36813600
H 2.63545300 -0.32227900 -2.30142600
H -2.83794600 2.25282900 1.58465800
H -1.63055000 1.03186600 2.00520700
H -3.16857000 0.52825700 1.26385400
H -2.41057300 -2.69892200 1.32780400
H -1.07347400 -2.03585300 2.45192500
H -1.93403600 -2.69917200 -1.10624000
H -0.74851900 -1.56345200 -1.77411000

αβ-caryophyllene
C -1.81441800 -1.54816000 -0.24336800
C -0.70214400 -2.26653700 -0.98888200
C 0.48468200 -1.32426100 -1.28023300
C 0.81026000 -0.36689100 -0.12305700
H 0.25979800 -0.66947500 0.78210000
C 2.27974100 -0.12059400 0.33702000
C 1.83993400 1.31932700 0.69807800
H 1.47894900 1.37024000 1.73771900
H 2.54971800 2.14082000 0.51567600
C 0.65701400 1.17091600 -0.29016300
H 1.01905400 1.43974400 -1.29484700
C -0.60570200 1.96845100 -0.03322400
C -2.25651400 -2.18248100 1.04529500
H -2.55295000 -3.23002300 0.87368200
H -3.09730700 -1.65972700 1.51876800
C -1.65703100 1.47841600 0.94618500
C -2.80793600 0.73484400 0.22104500
H -3.36670500 1.46218400 -0.38832700
H -3.50283300 0.32166400 0.96618800
C -2.18486900 -0.32398800 -0.63989000
H -1.75878800 0.04662700 -1.57995700
C 3.28699400 -0.12962800 -0.80951000
H 2.94312500 0.46503400 -1.66941600
H 3.47755700 -1.15502700 -1.16251100
H 4.24790200 0.28997300 -0.47172200

C 2.76639800 -1.00054600 1.47710800
H 2.85608800 -2.04895700 1.14742200
H 2.06789500 -0.96982800 2.32741900
H 3.75699600 -0.67672900 1.83566200
C -0.79277600 3.12662700 -0.68061800
H -1.66379500 3.75732900 -0.47710600
H -0.07885100 3.48375200 -1.42886900
H -1.41738600 -2.21204400 1.76237300
H -0.35291000 -3.10045500 -0.35927300
H -1.06055600 -2.72385900 -1.92595500
H 1.36893000 -1.93669400 -1.52076000
H 0.27746600 -0.73248700 -2.18661100
H -1.20395000 0.79190300 1.67980100
H -2.06925000 2.33306400 1.50382200

βα-caryophyllene
C -0.98617400 -0.31690000 -0.39615200
C -0.60701200 -1.79323500 -0.30149700
C 0.72940600 -2.19052100 -0.95002500
C 1.85211500 -1.41763900 -0.31285500
C 2.30344500 -0.30396100 -0.90511300
C 3.04474700 0.80354900 -0.20634800
C 2.08152000 1.49590200 0.78405800
C 0.69850600 1.71853500 0.18658400
C -0.42651600 0.77820800 0.58409200
C -1.85789400 1.35976600 0.65813600
C -2.42951800 0.05288300 0.06750300
C -2.96494000 -0.85759400 1.16931400
C -3.45205800 0.20061300 -1.04791800
C 2.24854900 -1.84007200 1.07586000
C 0.51463400 2.71829100 -0.68554600
H -0.84263100 0.04235100 -1.43098200
H -0.60645000 -2.10182100 0.75658100
H -1.41300300 -2.37247800 -0.78454500
H 0.68723200 -1.96730100 -2.02784600
H 0.87311000 -3.27762600 -0.83622500
H 1.92465900 -0.08015100 -1.90882500
H 3.39961300 1.53854200 -0.94347200
H 3.93078800 0.44051400 0.33841600
H 2.51104000 2.45839000 1.10247700
H 1.98749300 0.86922500 1.68383500
H -0.16484700 0.29441600 1.53863100
H -1.99188600 2.20423700 -0.03162700
H -2.21936600 1.65361000 1.65546200
H -3.19992500 -1.86345200 0.78868600

H -3.89082400 -0.43009300 1.58590900
H -2.24547100 -0.96485300 1.99550600
H -3.65878900 -0.77332800 -1.52146400
H -4.40603600 0.59480800 -0.66142700
H -3.08937400 0.88790900 -1.82768400
H 2.46639800 -2.91989200 1.09850700
H 1.42772000 -1.66977300 1.79277700
H 3.13289400 -1.30178000 1.44178800
H 1.34120800 3.38345500 -0.95475700
H -0.44642400 2.90814700 -1.17028300

ββ-caryophyllene
C -1.79183200 1.43881900 0.09372000
C -0.64118400 2.41702600 -0.06447700
C 0.63958400 1.72538100 -0.55579400
C 0.97823900 0.41877800 0.16096100
H 0.72607600 0.49588800 1.23397900
C 2.43362000 -0.12624900 0.04422600
C 1.83607000 -1.55175800 0.02566600
H 1.80379100 -1.98137900 1.03788600
H 2.28740900 -2.28153900 -0.66409500
C 0.46261800 -0.95887800 -0.36942000
H 0.39378200 -0.89429900 -1.46619200
C -0.79616700 -1.61974300 0.16000300
C -2.37733100 1.36079600 1.47690500
H -2.72039600 2.35937500 1.79462800
H -3.22093900 0.66510200 1.56088100
C -1.94693600 -1.83147600 -0.80833200
H -1.53976900 -1.98889700 -1.82001100
H -2.50709900 -2.73889400 -0.53685900
C -2.92273400 -0.62962200 -0.83872400
H -3.60499500 -0.74552400 -1.69541400
H -3.53543300 -0.64963400 0.07319700
C -2.12760500 0.63774500 -0.92748000
H -1.60529800 0.79253300 -1.88088300
C 3.09254000 0.21487200 -1.28981500
H 2.44283400 -0.03087200 -2.14356000
H 3.34524800 1.28456700 -1.35200800
H 4.02662900 -0.35789800 -1.40361900
C 3.35857100 0.21635500 1.20067400
H 3.57496500 1.29728000 1.22127600
H 2.90407600 -0.05817800 2.16502100
H 4.31962800 -0.31581400 1.11152200
C -0.90909300 -1.99290800 1.44084400
H -1.82055400 -2.47211500 1.81123700
H -0.10500000 -1.82781500 2.16465900
H -1.60289000 1.05407900 2.20058000
H -0.44220600 2.88672300 0.91174900

H -0.90465200 3.23803000 -0.75169200
H 1.48346300 2.42487000 -0.42760900
H 0.57116200 1.52958800 -1.63841000

TS-βα
O 1.79498900 -1.97918900 1.82858800
H 2.17819200 -1.74344900 2.73936800
O 3.10730000 -0.90610100 3.65673100
O 4.76610100 1.54846200 0.89840900
H 5.05639600 2.07989100 0.07694600
O 5.00496400 2.40149900 -1.41907100
O 2.21069400 -0.36009700 -2.57256800
C 2.36624600 -1.17715600 0.96775300
C 3.30353000 -0.21819200 1.42028700
C 3.89607300 0.66952900 0.46883700
C 3.55556400 0.62150600 -0.89605200
C 2.57737600 -0.33852300 -1.40050700
C 2.02624500 -1.29450200 -0.41433400
C 3.62101500 -0.15581700 2.82000800
H 4.35760500 0.60197300 3.14468400
C 4.17463600 1.55740900 -1.78491300
H 3.88168800 1.50317400 -2.85007000
C -0.86669000 -0.65320000 -1.47702300
C -0.46716200 0.72282600 -1.05243400
C -1.72772300 1.57304700 -0.80172600
C -2.69375700 1.09375000 0.27918400
H -2.13534300 0.77129900 1.17570000
C -3.78254600 2.12238900 0.71673100
C -4.76649200 0.94376100 0.87322200
H -4.80978200 0.60148300 1.91609900
H -5.79211800 1.09606900 0.50395900
C -3.84430800 0.05369000 0.01095100
H -4.13539300 0.13013200 -1.04923400
C -3.72263200 -1.41494500 0.37306500
C -1.13451200 -0.87434500 -2.93086000
H -0.20734600 -0.68094700 -3.49310000
H -1.88624500 -0.15047100 -3.28695400
C -3.37254300 -2.40748700 -0.72755400
H -3.57533600 -1.95107800 -1.70881700
H -4.00922100 -3.30102400 -0.64247300
C -1.89045900 -2.83149900 -0.67951000
H -1.62643600 -3.38441800 -1.59377200
H -1.72513700 -3.50537900 0.17418600
C -1.06211900 -1.59167600 -0.51208000
H -0.87059500 -1.27909800 0.52020500
C 1.11515800 -2.23879900 -0.84283300
H 0.79691700 -3.03656300 -0.17031100
C -4.22095300 3.05534200 -0.40924700
H -4.47100500 2.50044200 -1.32635600

H -3.43973900 3.79019800 -0.65678000
H -5.11983100 3.61144700 -0.09933400
C -3.46030600 2.91586300 1.97269500
H -2.62054600 3.60751000 1.79419300
H -3.18141400 2.24796200 2.80199900
H -4.32673100 3.51667800 2.29356000
C -3.89254900 -1.86397500 1.62318900
H -3.80229000 -2.93156600 1.84721200
H -4.11690500 -1.20376900 2.46378500
H -1.48847200 -1.88792700 -3.15584800
H 1.00169100 -2.40140300 -1.91542900
H -1.39112100 2.58437800 -0.51796500
H -2.27369300 1.68903000 -1.75209000
H 0.12843100 0.66647900 -0.12475300
H 0.14482800 1.20837900 -1.82641700

cattleianal
C 3.53290400 0.46814300 -0.41472600
C 2.93162300 1.37966300 0.65856700
C 1.42477100 1.66062800 0.55797300
C 0.38208900 0.75254800 1.23409200
C 0.47092600 -0.72027100 0.80010600
C 1.58858900 -1.47222600 1.53829700
C 2.17800500 -2.62040000 0.71732600
C 2.92838600 -2.11766300 -0.49197700
C 3.93300100 -1.02981600 -0.21037500
C 5.11969800 -0.77373300 -1.15916300
C 4.99958100 0.73977500 -0.86557800
C 5.90703600 1.15561000 0.28956200
C 5.16240600 1.68965300 -2.04058600
C 0.36926900 0.91937000 2.74744100
C 2.68344500 -2.59046800 -1.71987100
C -0.85291700 -1.46346800 1.00886900
C -2.01251800 -0.69138400 0.46305200
C -1.93358600 0.69632900 0.37707900
C -3.01477100 1.48361900 -0.12531800
C -4.20081600 0.83495100 -0.53919300
C -4.30559100 -0.57040800 -0.45693600
C -3.19944200 -1.31337500 0.04939500
C -2.93006000 2.92217700 -0.22184400
C -5.50553800 -1.25952000 -0.87228600
O -0.85716500 1.37081600 0.75046500
O -3.84960600 3.62075800 -0.65055800
O -5.21805000 1.53410900 -1.00585400
O -5.63473900 -2.48143200 -0.81589200
O -3.28291600 -2.62905700 0.13965500

H 2.90232800 0.51180800 -1.31999100
H 3.22508800 1.05910000 1.67141700
H 3.41650800 2.35962000 0.51831400
H 1.15528000 1.69818500 -0.50976600
H 1.22955700 2.66769700 0.95814100
H 0.68960300 -0.71577700 -0.28285800
H 1.18608000 -1.86324800 2.48554800
H 2.40211300 -0.79306900 1.82098000
H 1.39312000 -3.32877600 0.41089500
H 2.88426900 -3.17457800 1.35919900
H 4.31220300 -1.15426200 0.81675000
H 4.86000800 -0.98768700 -2.20588000
H 6.07282700 -1.26555200 -0.91293100
H 5.69411500 2.18510500 0.61640300
H 6.96055200 1.11801200 -0.02974400
H 5.79650000 0.49267800 1.16106700
H 4.86409300 2.71319500 -1.75951800
H 6.21136400 1.72821800 -2.37630200
H 4.54127100 1.37521700 -2.89312100
H 0.13955700 1.96403500 2.99934900
H 1.35082200 0.66933200 3.17238500
H -0.38881600 0.27185700 3.21297100
H 1.91793900 -3.35488600 -1.88099700
H 3.23033000 -2.24129900 -2.59928700
H -0.99824300 -1.65489200 2.08632400
H -1.98875000 3.39878500 0.10832500
H -6.33504500 -0.63629500 -1.25684900
H -4.93755800 2.49679000 -0.98157500
H -4.18472300 -2.88981200 -0.20048800
H -0.80150400 -2.44944600 0.52527500

TS-βα
C 0.86495400 -0.50331700 0.14458600
C 1.62500500 -1.68632000 0.68790200
C 3.09080200 -1.36166900 1.00618800
C 3.83344500 -0.63479500 -0.11219800
H 3.51853900 -1.03076300 -1.09458600
C 5.39046300 -0.61451500 -0.07328300
C 5.32677600 0.81728300 -0.65320600
H 5.39698700 0.80479100 -1.75093500
H 6.03445700 1.55874200 -0.25177200
C 3.85322100 0.92574000 -0.19364500
H 3.81946000 1.32193800 0.83268100
C 2.87686900 1.70556400 -1.05329100
C 0.10018000 -0.66608800 -1.12964800

H -0.08317600 -1.72409900 -1.35241900
H -0.86735400 -0.13694100 -1.08484100
C 1.93874400 2.67294900 -0.35498600
H 2.45634100 3.10172000 0.51792900
H 1.68760600 3.50640000 -1.02719800
C 0.62217100 2.01650500 0.12332900
H 0.11429100 2.70219000 0.81726600
H -0.04762300 1.86744700 -0.73608500
C 0.93163300 0.70282400 0.78121900
H 1.55117500 0.76224600 1.68321600
C 5.94917600 -0.61372300 1.34719300
H 5.46790400 0.14918200 1.97793000
H 5.81215500 -1.59210500 1.83310200
H 7.02910400 -0.39778900 1.32510500
C 6.08300500 -1.66897300 -0.92085200
H 5.91030100 -2.67705400 -0.50923600
H 5.70670900 -1.65418400 -1.95526800
H 7.17185800 -1.50121200 -0.95028100
C 2.83175600 1.55045100 -2.38213300
H 2.12876300 2.12390900 -2.99386700
H 3.48494700 0.84414700 -2.90380200
H 0.65957300 -0.22077200 -1.97001900
O -1.58194700 -2.28202700 0.97040500
O -2.60914200 2.31093800 1.17338900
O -4.64698900 3.15925200 0.01663200
O -5.47356600 -0.63334600 -1.11886900
H -5.51231600 -1.63365000 -1.31597400
H -3.33657800 2.91870800 0.80824300
C -4.39254600 -0.44975300 -0.40318900
C -4.07623600 0.88089300 0.01611000
C -2.91180900 1.09796500 0.78996600
C -2.06744100 0.01293800 1.18383300
C -2.35341000 -1.36130300 0.71466300
C -3.57073700 -1.54227600 -0.07165300
C -4.90609400 2.00223500 -0.33038300
H -5.81061700 1.80216100 -0.93363700
C -0.94618900 0.21532800 1.96399200
C -3.94218400 -2.84189800 -0.54350300
H -3.27276100 -3.68069900 -0.27577700
O -4.95756200 -3.05887200 -1.21987200
H -0.47473900 -0.65514200 2.42041800
H -0.76915600 1.19121800 2.41852300
H 1.11428800 -2.07356700 1.58644900
H 1.58311700 -2.49563000 -0.05604800
H 3.16186500 -0.77168400 1.93410000

H 3.60921600 -2.31334200 1.21125600

4,10-*epi*-cattleianal
C -3.71962300 0.57104700 0.07952300
C -2.91889000 1.25543600 -1.02077400
C -1.42840600 1.53908100 -0.78127000
C -0.44907700 0.49633200 -0.21481800
C -0.24691900 -0.75915700 -1.08527800
C -1.45927200 -1.65247600 -1.40550900
C -2.08582300 -2.55527200 -0.32912200
C -3.12714900 -1.97246100 0.60668200
C -4.06089500 -0.95192800 0.01783200
C -5.41099900 -0.60948000 0.67424900
C -5.25027200 0.84838300 0.17860400
C -5.91033500 1.05572200 -1.18187300
C -5.65481100 1.95330500 1.14045800
C -3.23252500 -2.40665700 1.86878000
C 0.91399700 -1.59196400 -0.53573900
C 2.10767100 -0.72724200 -0.25070600
C 1.97712000 0.65799800 -0.16101700
C 3.10310500 1.51048300 0.04877400
C 4.38666400 0.93352500 0.18110300
C 4.54295700 -0.46777700 0.11077400
C 3.39073400 -1.27746100 -0.10512000
C 2.96291000 2.94491100 0.14950700
C 5.84203300 -1.08706300 0.24578000
O 0.80288700 1.26553400 -0.28236500
O 3.91871700 3.70038100 0.32987000
O 5.44631400 1.69503300 0.37800100
O 6.01795900 -2.30262000 0.18455900
O 3.51810000 -2.59012700 -0.18258100
H -3.29081600 0.79106100 1.07068000
H -3.06974300 0.71734400 -1.96843900
H -3.36960400 2.24845000 -1.18604500
H -1.34884000 2.39760200 -0.09500500
H -0.99374500 1.87458000 -1.73581600
H -1.09423700 -2.33027900 -2.19272600
H -2.24345100 -1.05798600 -1.88958200
H -1.31056600 -3.07132300 0.25712000
H -2.61076700 -3.35107500 -0.88682700
H -4.23550600 -1.20833900 -1.04000000
H -5.35246300 -0.64878400 1.77162600
H -6.29444700 -1.17116100 0.33474400
H -5.63740300 2.03097900 -1.61371100
H -7.00623100 1.03299800 -1.07391900

H -5.62806800 0.27433700 -1.90339900
H -5.31907300 2.93570400 0.76934300
H -6.74988100 1.99609000 1.25635500
H -5.21120500 1.79470200 2.13520600
H -2.52137000 -3.13383900 2.27155400
H -4.02011800 -2.05669000 2.53987500
H 1.18866500 -2.36603100 -1.26844000
H 1.94341200 3.36288600 0.05986800
H 6.70503500 -0.41448700 0.41059800
H 5.11655900 2.64172000 0.40234700
H 4.48751200 -2.79846800 -0.06543500
H 0.60894500 -2.12885600 0.37790800
H 0.07719300 -0.35740300 -2.06141700
C -0.66059700 0.20202400 1.26467800
H -1.52554200 -0.44833000 1.42699600
H 0.22114000 -0.29895000 1.69042600
H -0.81677900 1.14207800 1.81313900

TS-βα→ββ
C 2.37910100 -1.22890800 0.14270100
C 1.19961100 -2.18069400 0.30493200
C -0.15356300 -1.72594300 -0.29569000
C -0.91215700 -0.48748800 0.24022000
H -0.72357200 -0.35867500 1.32124300
C -2.45473000 -0.45820800 0.01445700
C -2.35591000 1.07672300 -0.12445700
H -2.53113200 1.56497000 0.84456200
H -2.98378200 1.55667800 -0.89041700
C -0.85129400 0.94930500 -0.43426800
H -0.71233900 0.79401000 -1.51679300
C 0.11131400 2.05457600 0.00926500
C 3.76544800 -1.78947900 0.24538000
H 3.94701600 -2.53644100 -0.54440500
H 4.52926700 -1.00356800 0.16509900
C 1.41717600 2.27561000 -0.76510100
H 1.24983800 2.00928400 -1.82156900
H 1.68131500 3.34231400 -0.73382200
C 2.59555400 1.42218900 -0.22600100
H 3.46160100 1.46972300 -0.90452000
H 2.92352800 1.83847800 0.74239700
C 2.03289500 0.04639800 -0.04300900
H 0.96958300 0.12590000 -0.03226800
C -2.87998000 -1.10199800 -1.30345100
H -2.27773100 -0.74130200 -2.15101600
H -2.79238200 -2.19848700 -1.26611600

H -3.93356000 -0.85799000 -1.51224700
C -3.29344700 -0.99251700 1.16407400
H -3.14306500 -2.07791900 1.28568900
H -3.02357900 -0.50259200 2.11204800
H -4.36715300 -0.82190800 0.98350100
C -0.15311200 2.82825500 1.06974000
H 0.54237100 3.61724900 1.37188400
H -1.05508700 2.70886700 1.67461200
H 3.90314200 -2.31020000 1.20732800
H 1.06956300 -2.40767300 1.38003500
H 1.45448600 -3.14762000 -0.16137200
H -0.84012000 -2.57814000 -0.16010600
H -0.02965000 -1.61188000 -1.38650100

Structural assignment of (–)-cattleianal by 2D-NMR analysis

Discussion

We embarked on a comprehensive structural elucidation of (–)-cattleianal, leveraging 2D-NMR spectroscopy for analysis. Owing to the presence of multiple chemical species in the spectra reported from the initial isolation of (–)-cattleianal, coupled with insufficient resolution and poor quality in both 1D- and 2D-NMR spectra, a comparative analysis with our acquired data was impractical. Nonetheless, based on our spectral data, we ascertained that the synthesized compound conformed to the anticipated structural configuration initially proposed upon its isolation. Our hypothesis was underpinned by the expectation that we would discern a *trans*-configurational relationship between the methyl and proton moieties at the pyran-terpene ring fusion, as well as the protons at the site of cyclobutane ring attachment, a notion corroborated by literature pertaining to analogous natural products.[56-58] 2D-NMR techniques were deployed to validate the synthetic fidelity of (–)-cattleianal. It should be noted that the 2D-NMR spectra were not referenced relative to the 1D ^{1}H- and ^{13}C-NMR, leading to potential minor disparities in reported chemical shifts, expressed in ppm. Initially, HSQC was employed to delineate the proton-carbon one-bond correlations, particularly those of methyl (–CH_3), methylene (–CH_2), and sp^3 methine (–CH) groups. Additional validations for aldehyde and terminal ethylene (–CH_2) moieties were also acquired from HSQC spectra. Subsequently, HMBC and COSY were utilized to elucidate the broader bond connectivity landscape of the molecular structure. Pertinent correlations employed for assignment in both techniques are denoted by directional indicators, with associated crosspeaks illustrated in adjacent insets. Ultimately, NOESY was employed to ascertain the relative stereochemistry of the compound. Analogous to the HMBC and COSY methods, significant crosspeaks instrumental in stereochemical assignments are also displayed in insets, accompanied by arrows indicating the pertinent NOEs.

NOTE: For insets showing HMBC, COSY, and NOESY cross-peaks of CH_2 groups, each proton is designated by a 1 or 2 following the letter corresponding to the correlation arrow.

HSQC: Full spectrum

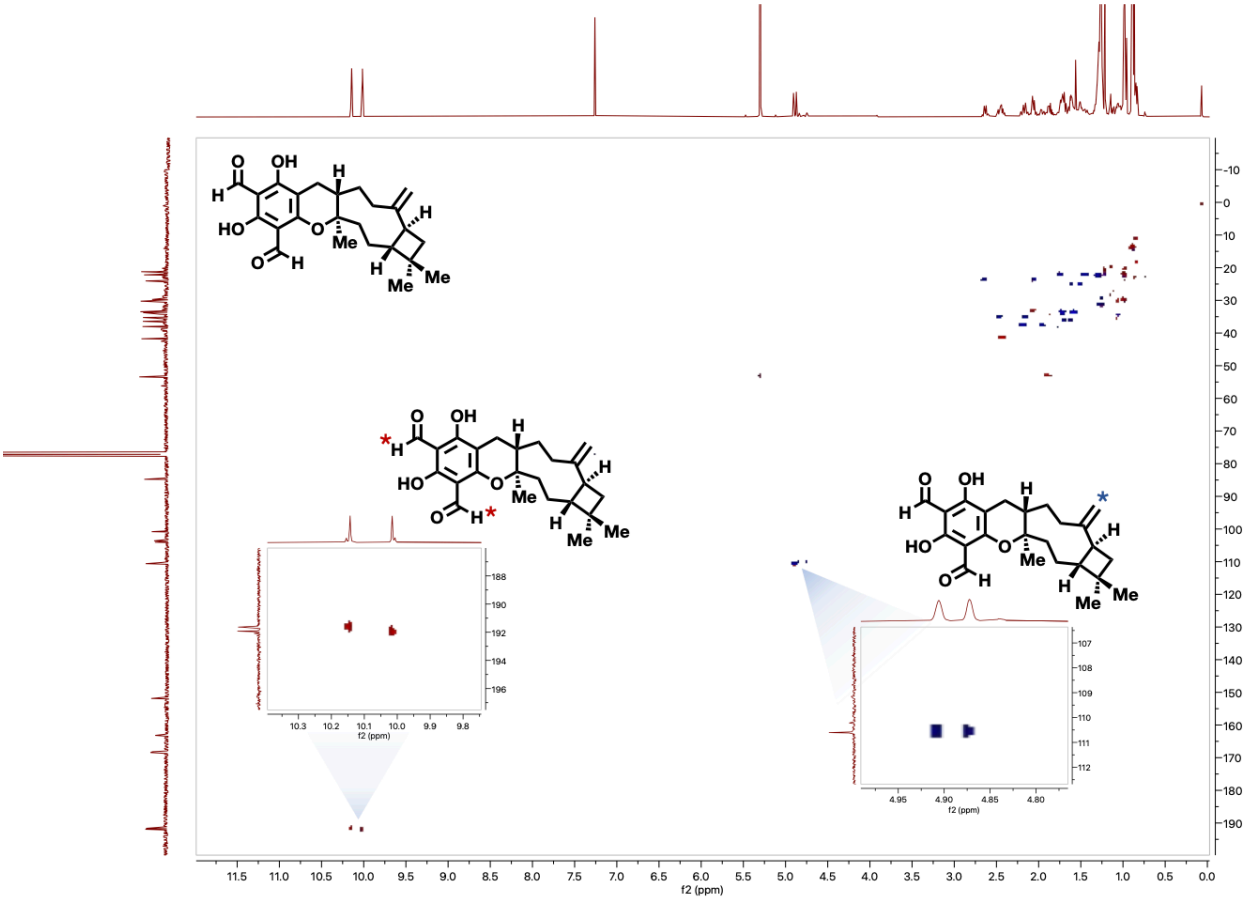

Aldehyde (–CHO) and terminal ethylene (–CH_2) single-bond correlations are shown in the inset windows, with the aldehyde cross-peaks (indicated by red asterisk) at 10.14 ppm, 192.06 ppm and 10.01 ppm, 191.77 ppm, and the alkene cross-peaks (indicated by blue asterisk) at 4.9 ppm, 110.78 ppm and 4.87 ppm, 110.78 ppm.

HSQC: Magnified view of the aliphatic –CH_2 and –CH region

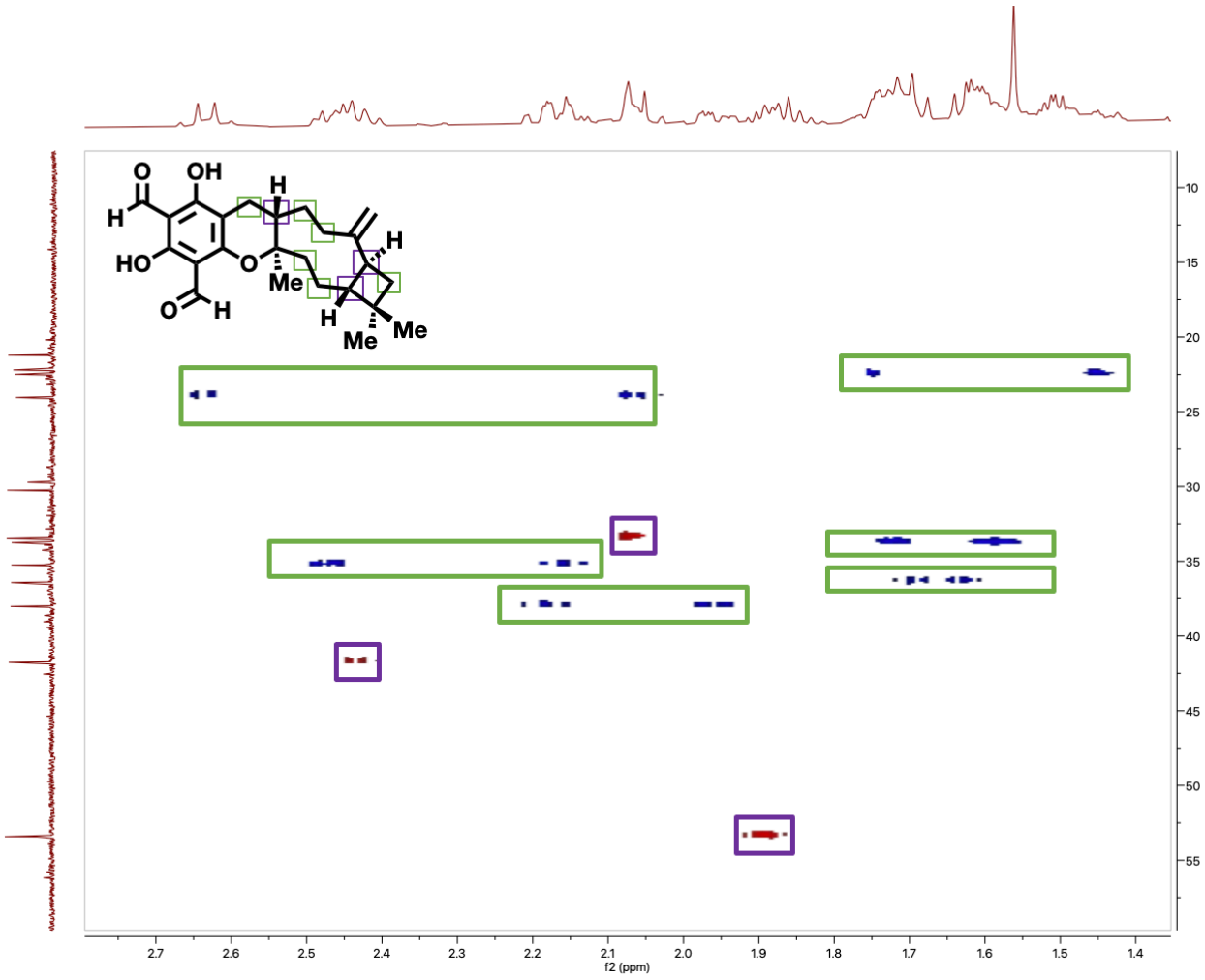

Identified methylene groups (–CH_2) are indicated in green boxes, while identified sp^3 methine (–CH) groups are indicated in purple boxes.

HSQC: Magnified view of the aliphatic –CH_3 region

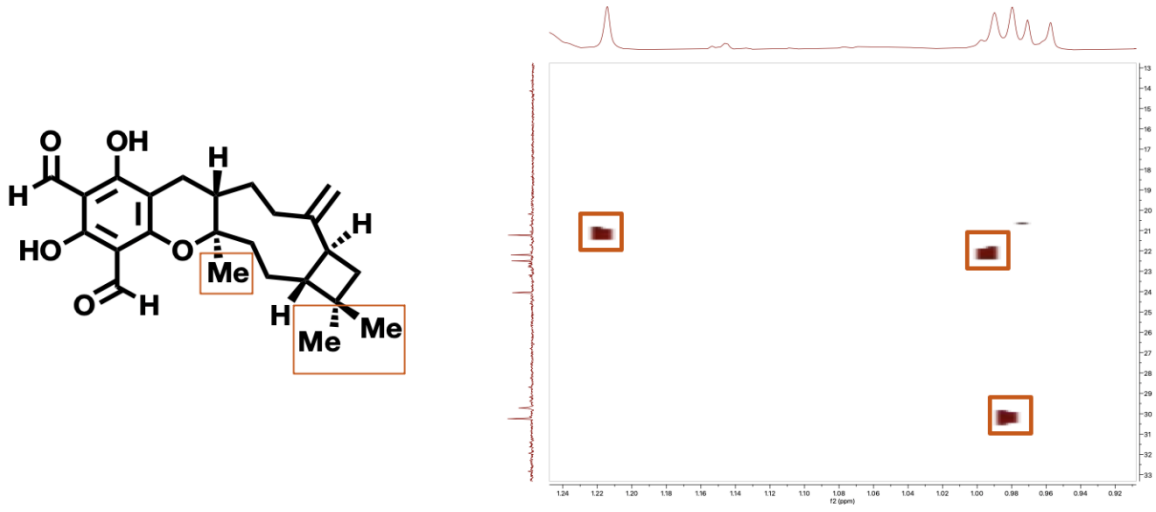

Identified methyl groups (–CH_3) are indicated in orange boxes.

HMBC: Full spectrum

NOTE: The size of correlation arrows shown does not indicate the strength of the coupling interaction.

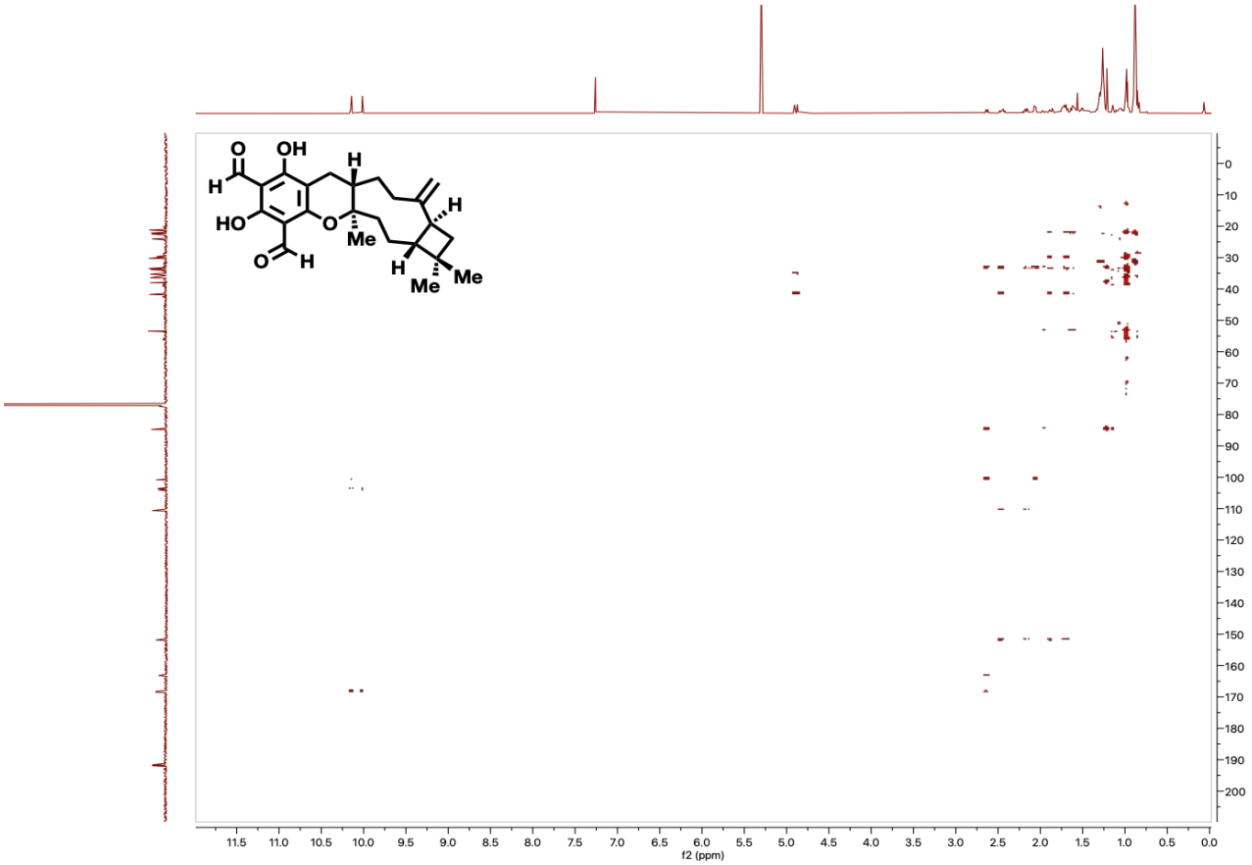

Significant HMBC correlations to the aldehydes:

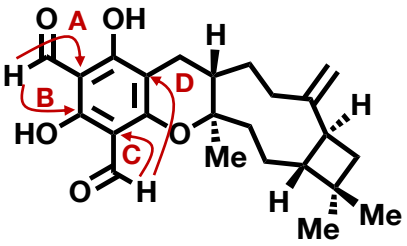

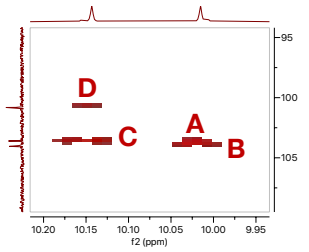

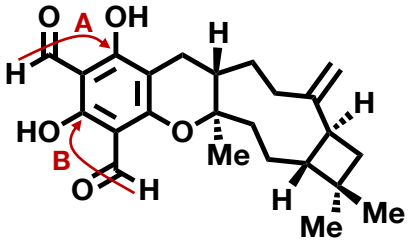

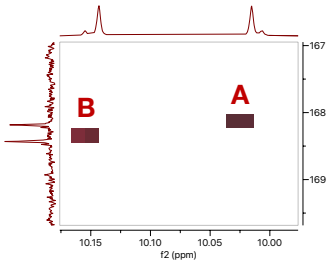

Significant HMBC correlations to the terminal alkene –CH_2:

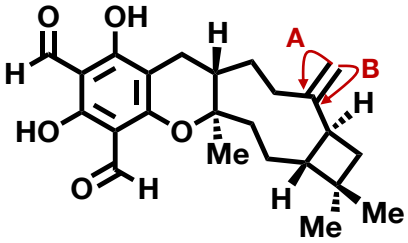

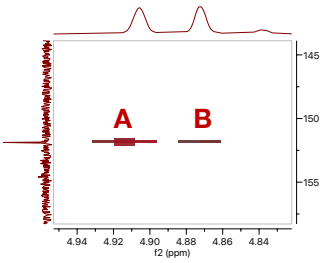

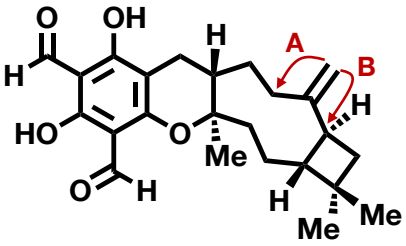

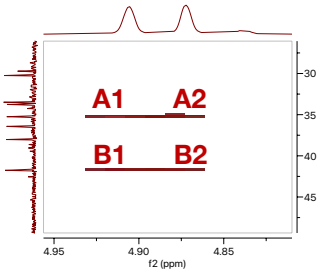

Significant HMBC correlations to the quaternary carbon of the terminal alkene:

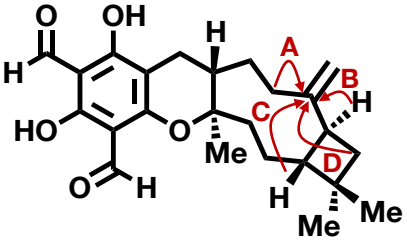

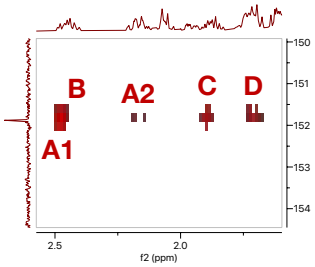

Significant HMBC correlations of the strained cyclobutane ring:

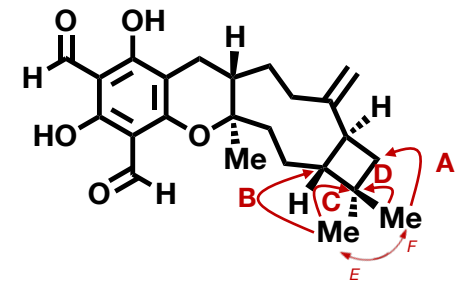

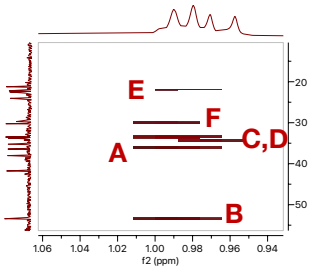

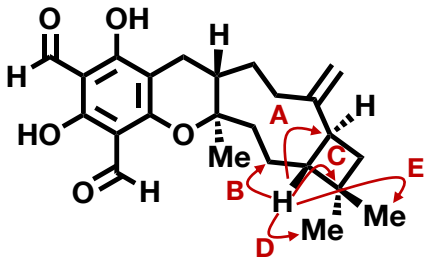

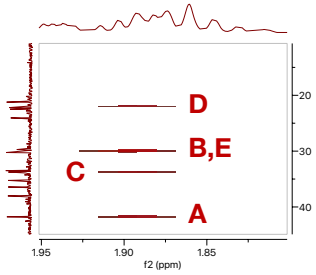

Significant HMBC correlations of the pyran system:

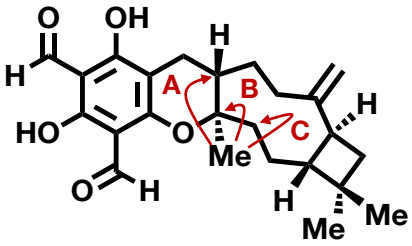

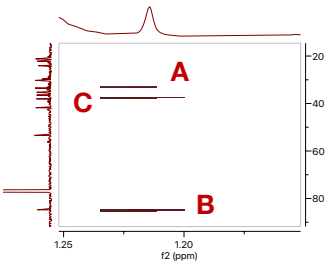

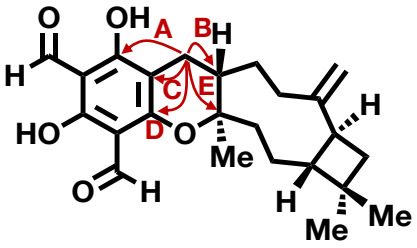

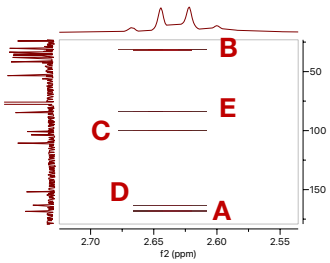

COSY: Full spectrum

NOTE: The size of correlation arrows shown does not indicate the strength of the coupling interaction

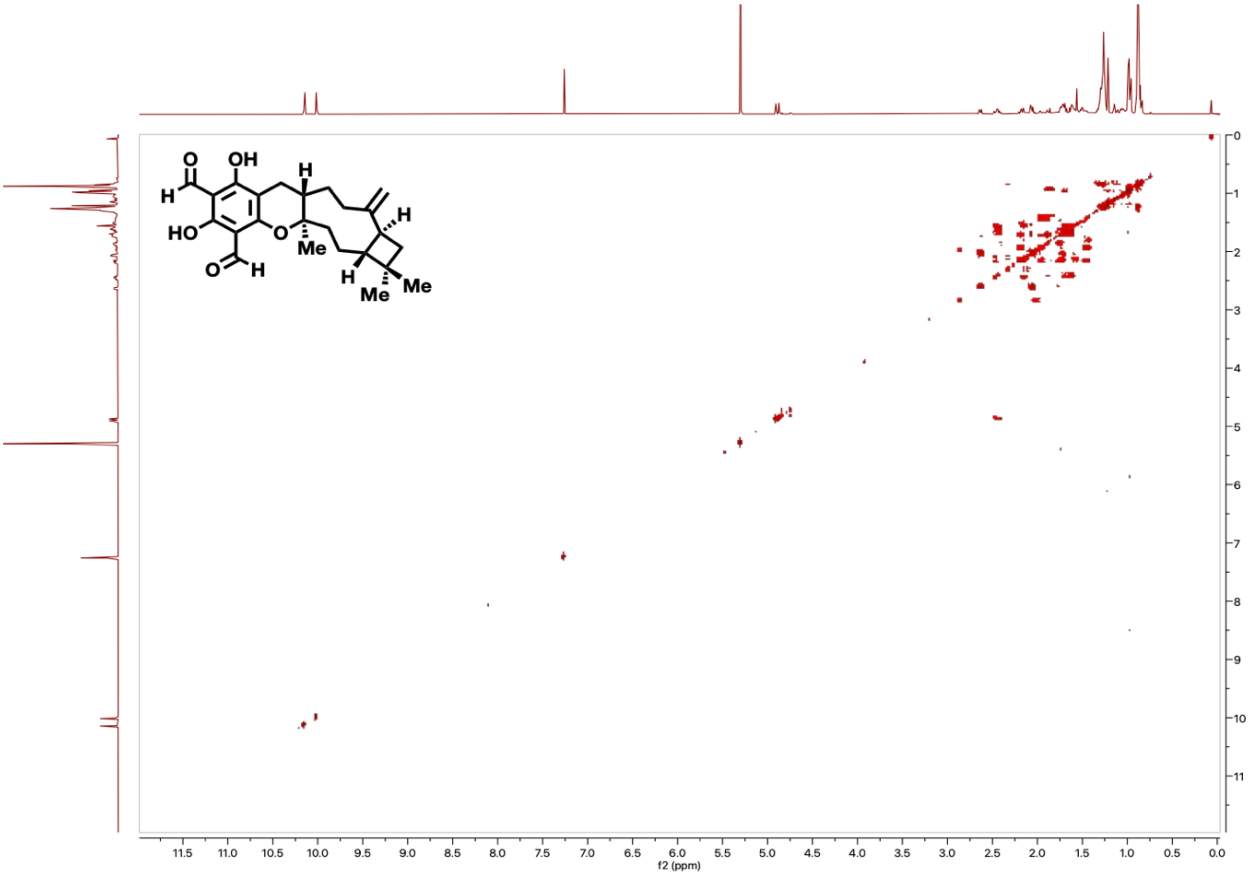

Significant COSY correlations of the aldehydes:

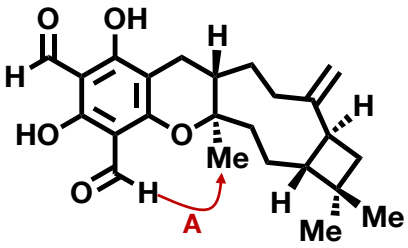

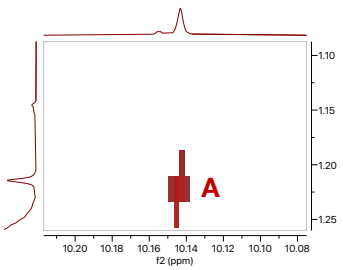

Significant COSY correlations of the methylenes:

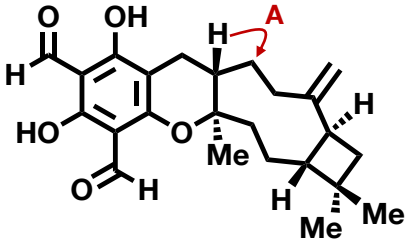

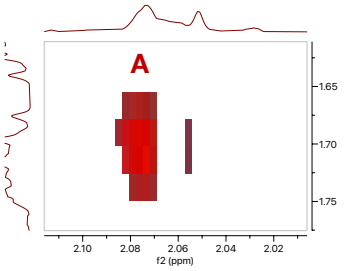

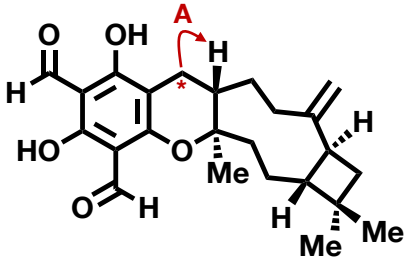

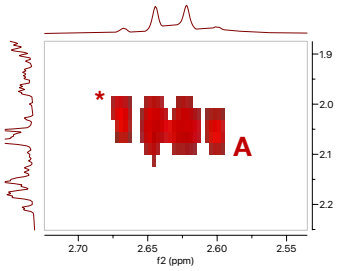

There is also geminal coupling overlapping here between the two hydrogens on the same carbon indicated with the red asterisk.

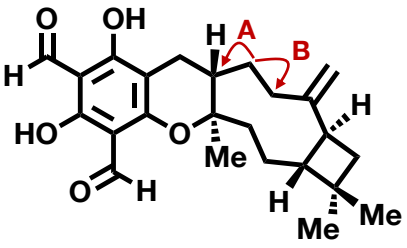

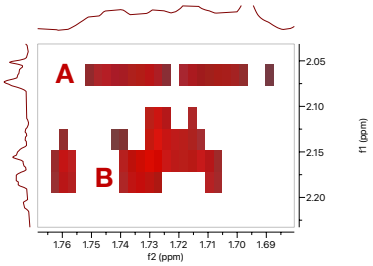

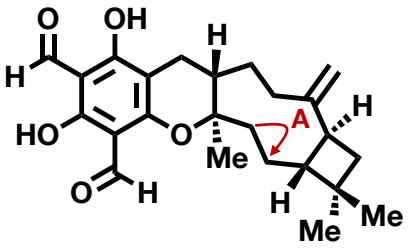

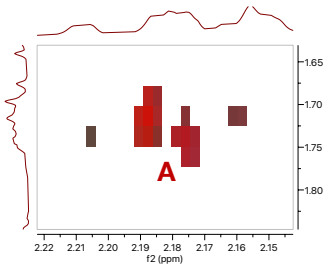

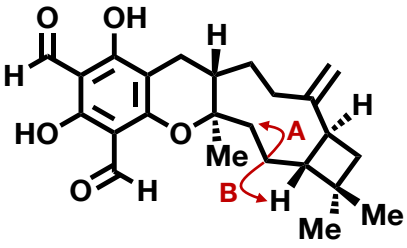

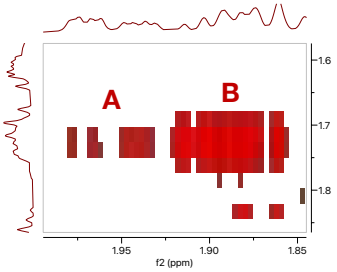

Significant COSY correlations of the terminal alkene:

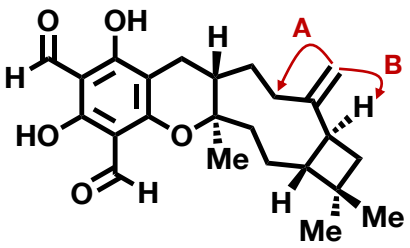

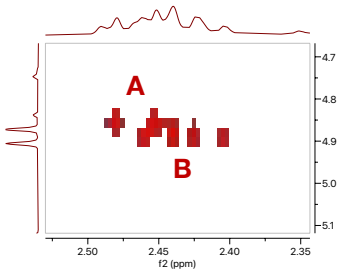

Significant COSY correlations of the strained cyclobutane ring:

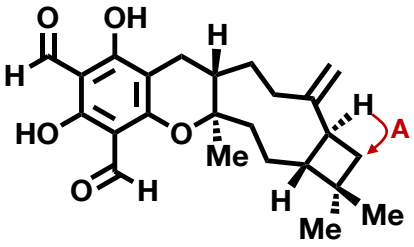

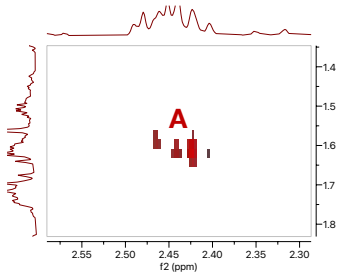

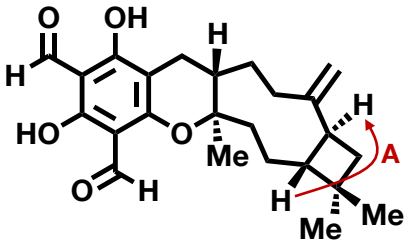

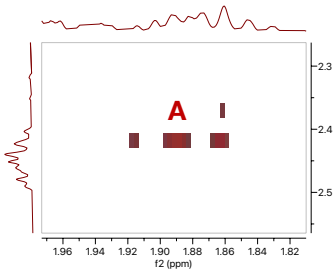

Significant COSY correlations of the strained cyclobutane ring:

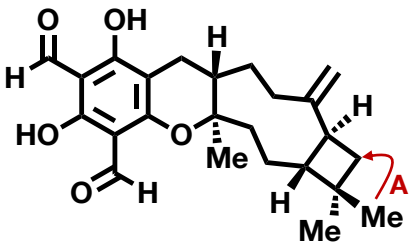

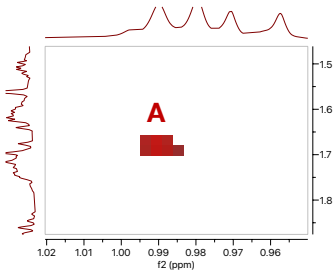

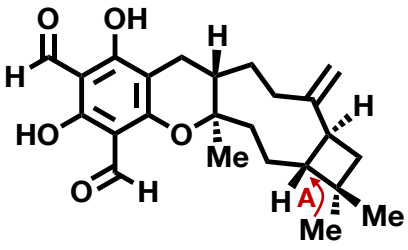

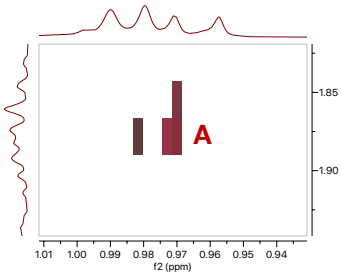

NOESY: Full spectrum

NOTE: The size of correlation arrows shown does not indicate the strength of the coupling interaction

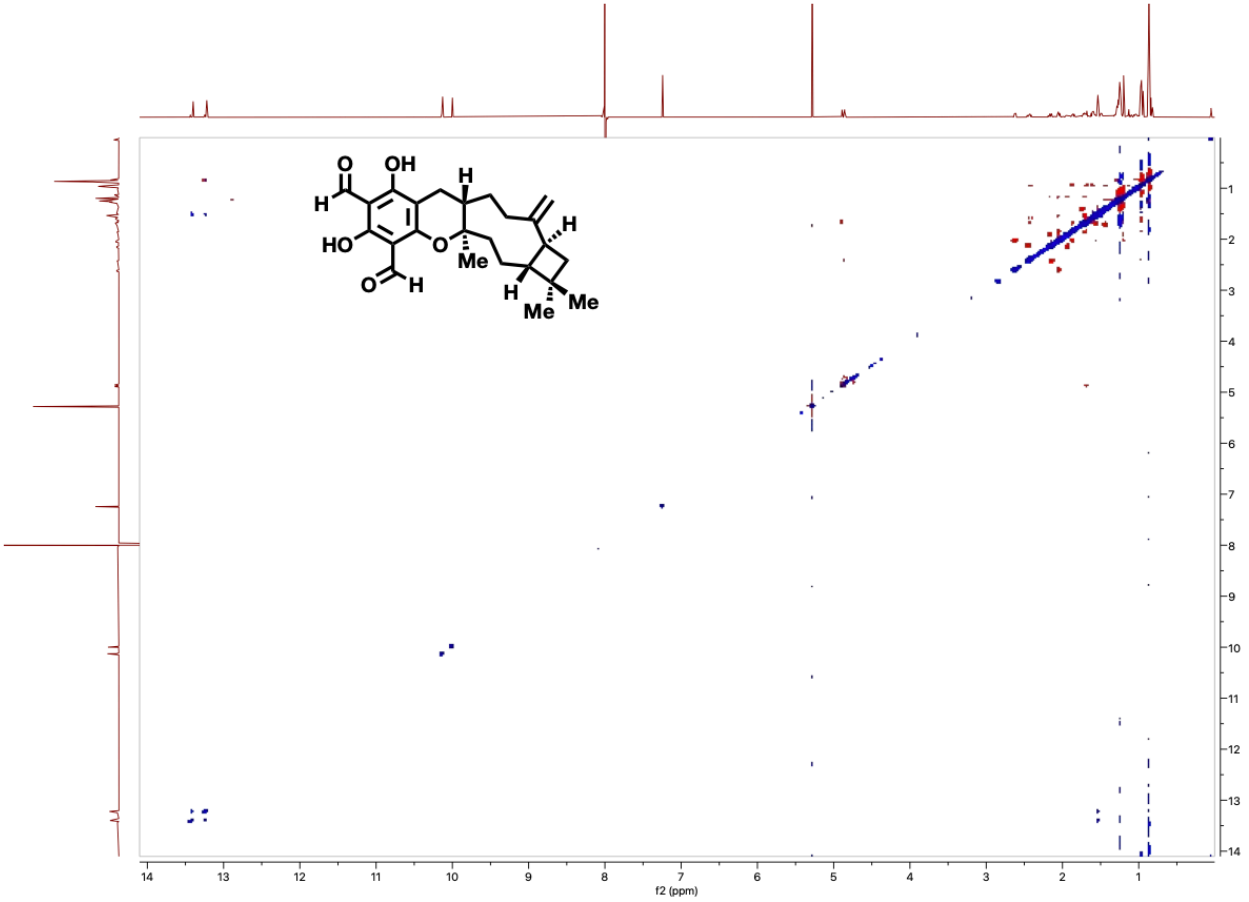

Significant NOESY correlations (interactions also seen in COSY are excluded) used to determine relative stereochemistry:

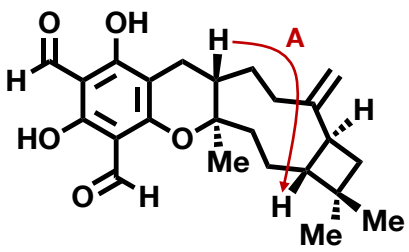

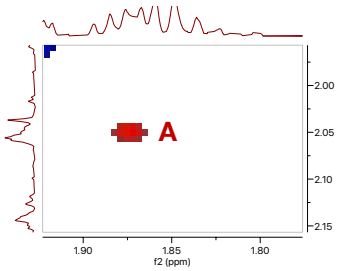

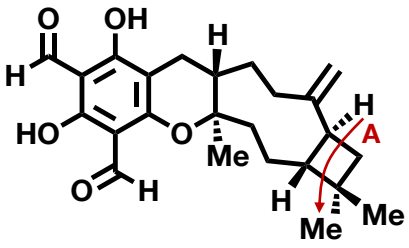

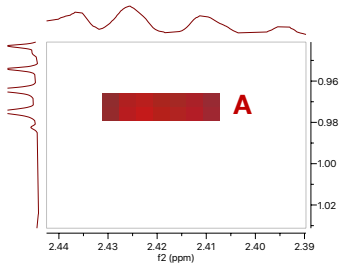

Structural assignment of (+)-guadial C by 2D-NMR

A comparative analysis was conducted on ^{1}H-NMR and ^{13}C-NMR spectral data derived from the primary isolation paper,[59] a preceding synthetic report,[54] and the current study (**Table S5**). Data were sourced verbatim from the mentioned references, hence potential inconsistencies in integration or shift might exist. Subsequently, two-dimensional NMR spectra were scrutinized to validate the identify of (+)-guadial C. It is noteworthy that minute discrepancies in ppm might manifest between the reported shifts of 1D and 2D spectra, since the latter was not referenced to ^{1}H-NMR and ^{13}C-NMR. In brief, HSQC was initially employed to pinpoint the identity of methyl ($-CH_3$), methylene ($-CH_2$), sp^3 methine (–CH) protons, and carbons. The hydrogens and carbons of aldehyde and phenyl groups were authenticated by HSQC. Upon deducing the proton-carbon one-bond correlations, HMBC and COSY were obtained to interpret the molecular bond connectivity. Key correlations instrumental for assignment in both spectra are demarcated with arrows, and the affiliated crosspeaks are illustrated in adjacent insets to the structure. Subsequently, NOESY correlations were assessed to elucidate the relative stereochemistry. Analogous to the HMBC and COSY, crosspeaks pivotal for stereochemical assignment are depicted in insets contrasted to the structure, with arrows indicating the pertinent NOE signals. Insets portraying HMBC, COSY, and NOESY crosspeaks of $-CH_2$ groups annotate each hydrogen with either “1” or “2” postfixed to the correlation arrow’s respective letter.

Table S5. Comparison of the ^{1}H-/^{13}C-NMR data for natural and synthetic guadial C

Signal	^{1}H-NMR (isolation)[59]	^{13}C-NMR (isolation)[59]	^{1}H-NMR (synthesis)[54]	^{13}C-NMR (synthesis)[54]	^{1}H-NMR (this work)	^{13}C-NMR (this work)
1	13.51 (s, 1H)		13.51 (s, 1H)		13.51 (s, 1H)	
2	13.13 (s, 1H)		13.13 (s, 1H)		13.14 (s, 1H)	
3	10.12 (s, 2H)	192.3, 191.7	10.11 (s, 2H)	192.28, 191.66	10.11 (s, 2H)	192.29, 191.65
4	7.28 (t, J=7.4Hz, 2H)	128.7	7.28 (t, J= 7.2Hz, 3H)	128.64	7.28 (t, J=7.3Hz, 2H)	128.66
5	7.21 (t, J=7.4Hz, 1H)	126.4	7.24-7.18 (m, 1H)	126.38	7.21 (t, J = 7.3Hz, 1H)	126.40
6	7.13 (d, J=7.4Hz, 2H)	126.9	7.13 (d, J=7.0Hz, 2H)	126.85	7.13 (d, J = 7.0Hz, 2H)	126.89
7	3.99 (dd, J=10.2, 7.0Hz, 1H)	35.2	3.99 (dd, J=10.2, 6.9Hz, 1H)	35.15	3.99 (dd, J = 10.2, 6.9 Hz, 1H)	35.18
8	2.43 (dd, J=14.5, 7.0Hz, 1H)	43.8	2.43 (dd, J=14.4, 6.9Hz, 1H)	43.74	2.43 (dd, J = 14.4, 6.9 Hz, 1H)	43.76
9	2.30 (dd, J=5.0, 4.8Hz, 1H)	47.7	2.32-2.27 (m, 1H)	47.63	2.30 (m, 1H)	47.70
10	2.20 (m, 1H)	26.5	2.25-2.16 (m, 1H)	26.42	2.22-2.18 (m, 1H)	26.46
11	2.12 (dd, J=14.5, 10.2Hz, 1H)	43.8	2.15-2.10 (m, 1H)	43.74	2.11 (dd, J = 14.5, 10.2 Hz, 1H)	43.76
12	2.08 (m, 1H)	30.1	2.07 (dd, J=14.4, 3.0Hz, 1H)	30.01	2.07 (m, 1H)	30.05
13	2.00 (m, 1H), 1.98 (m, 1H)	24.7, 40.7	2.03-1.97 (m, 2H)	24.65, 40.62	2.02-1.98 (m, 2H)	24.69, 40.67
14	1.83 (m, 1H), 1.80 (m, 1H)	30.1, 24.7	1.78 (ddd, J=13.8, 11.4, 2.6Hz, 2H)	30.01, 24.65	1.82-1.75 (m, 2H)	30.05, 24.69
15	1.50 (d, J=10.0Hz, 1H)	26.5	1.50 (d, J=10.2Hz, 1H)	26.42	1.50 (d, J = 10.2 Hz, 1H)	26.46
16	1.30 (s, 3H)	27.7	1.30 (s, 3H)	27.60	1.30 (s, 3H)	27.64
17	1.00 (s, 3H)	23.3	1.00 (s, 3H)	23.20	1.00 (s, 3H)	23.23
18		169.6		169.56		169.59
19		168.8		168.70		168.72
20		164.8		164.73		164.74
21		144.5		144.46		144.50
22		104.6		104.53		104.57
23		104.2		104.17		104.20
24		103.1		103.05		103.09
25		86.3		86.27		86.29
26		38.46		38.39		38.42

HSQC: Full spectrum

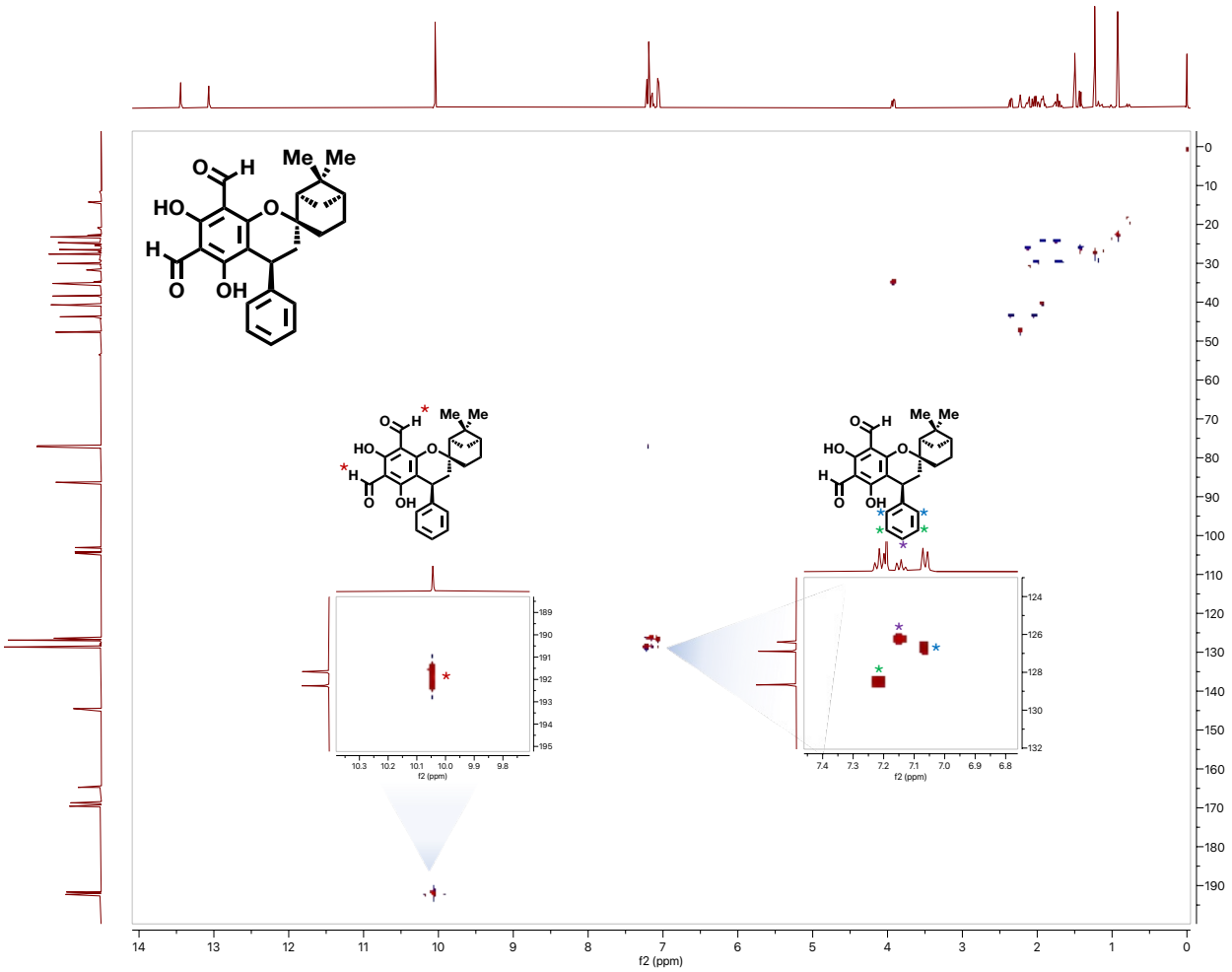

First, the aldehyde protons and carbons were identified, with the ^{1}H signals overlapping at 10.11 ppm, but carbons resolved at 192.2 and 191.65 ppm (left inset above, indicated with a red asterisk). The phenyl protons were also determined (right inset above) to match a singularly substituted benzene, with multiplicities for the three chemically distinct signals found to be two triplets (2H and 1H, indicated by the green and purple asterisks, respectively) and one doublet (2H, indicated by the blue asterisk) at 7.28 ppm, 7.21 ppm, and 7.13 ppm respectively. These protons correlated to carbons in the typical region of phenyl groups as well, with shifts of 128.66 ppm, 126.40 ppm, and 126.89 ppm respectively for the aforementioned ^{1}H signals.

HSQC: Magnified view of the aliphatic –CH_2 and –CH regions

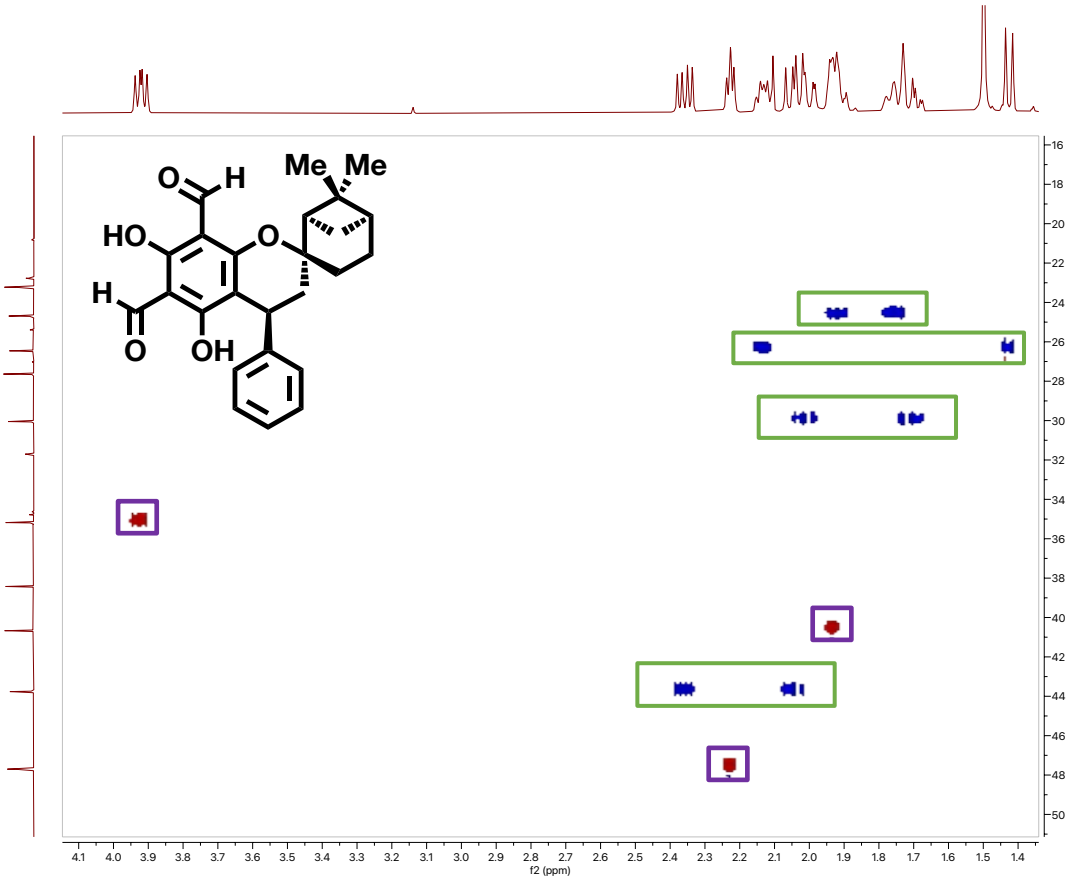

The identified methylene groups (–CH_2) are indicated in green boxes, while the identified sp^3 methine (–CH) groups are indicated in purple boxes.

HSQC: Magnified view of the aliphatic –CH_3 region

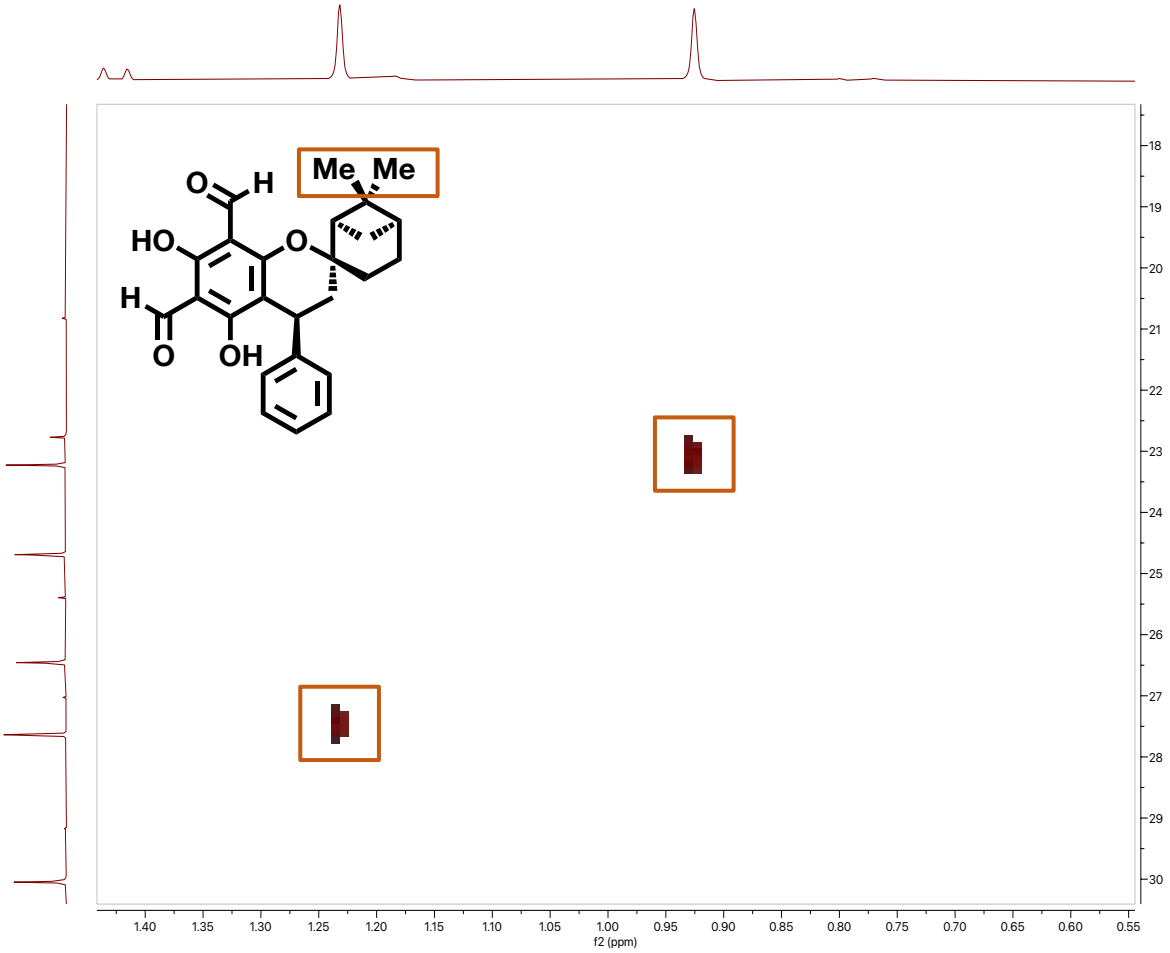

The identified methyl groups (–CH_3) are indicated in orange boxes.

HMBC: Full spectrum

NOTE: The size of correlation arrows shown does not indicate the strength of the coupling interaction

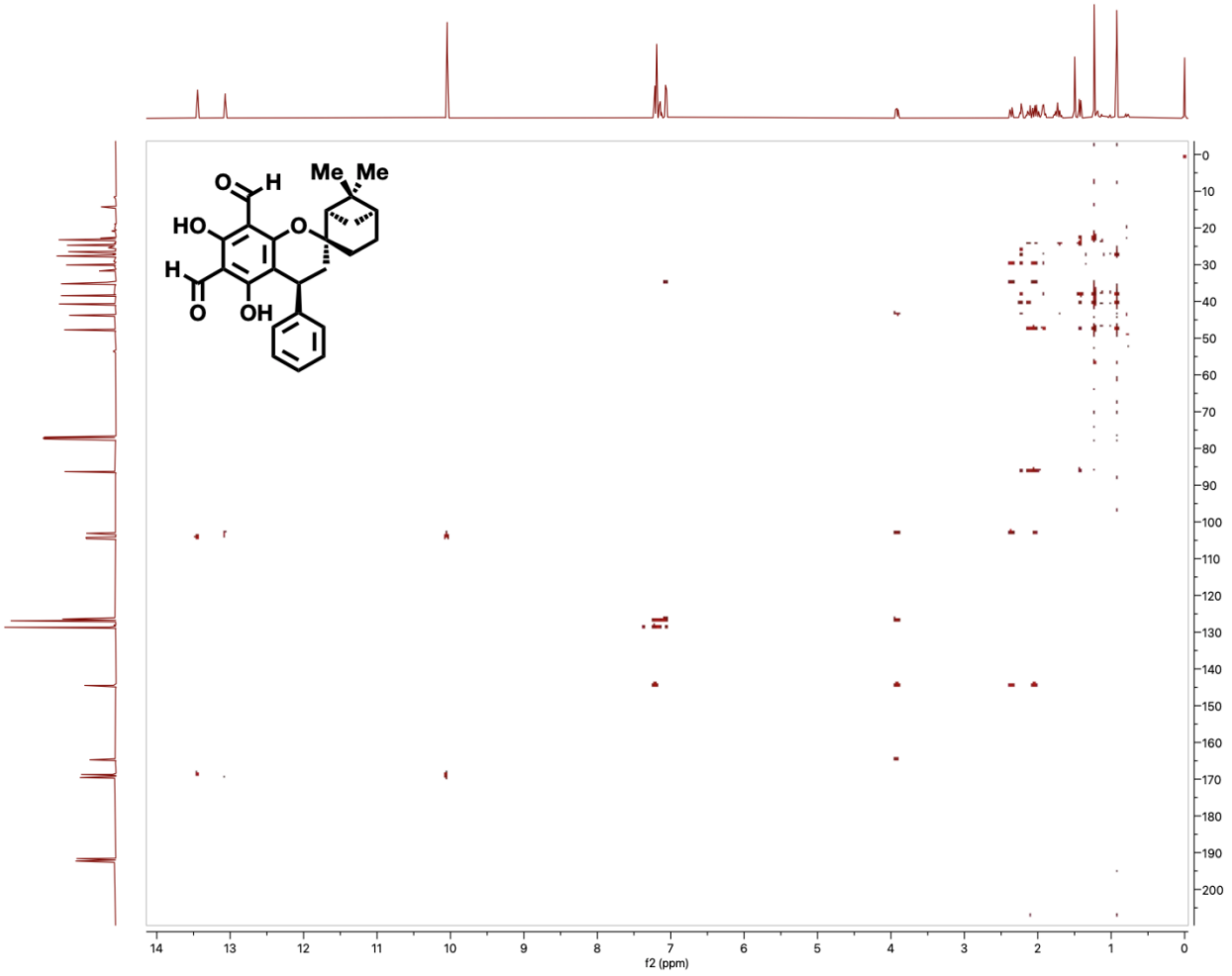

Significant HMBC correlations of the pyran methine (–CH):

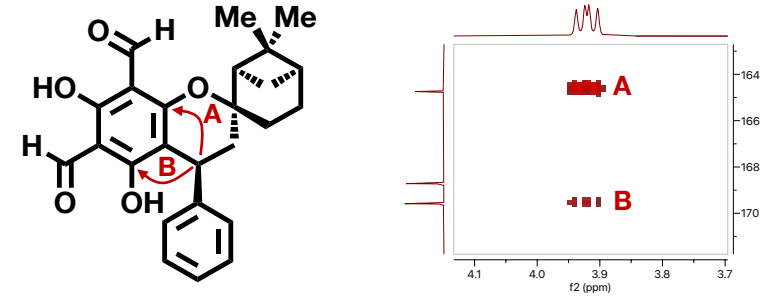

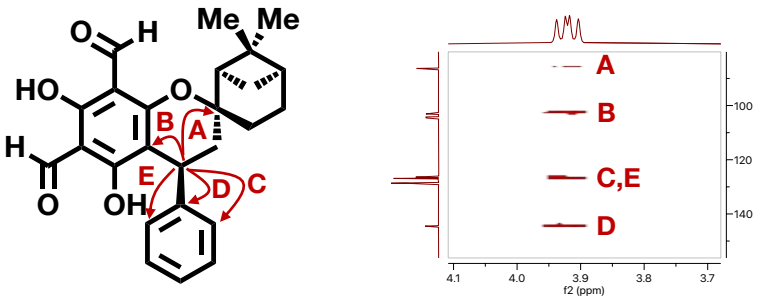

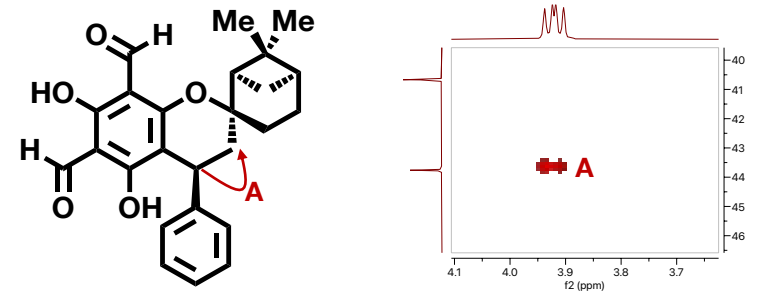

Additional significant HMBC correlations of the pyran system:

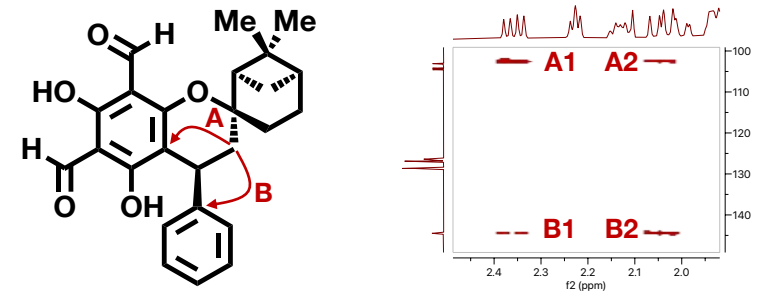

Significant HMBC correlations to the quaternary carbon joining the pyran and terpene rings

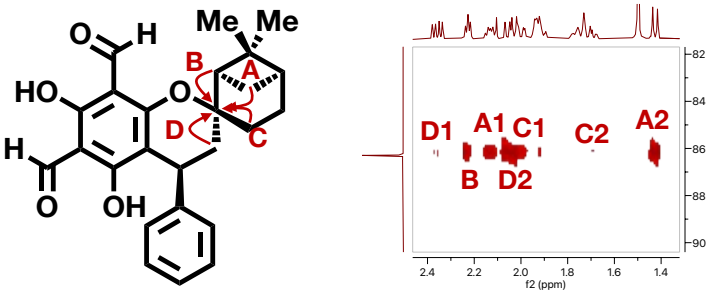

Significant HMBC correlations to the β-pinene methines (–CH):

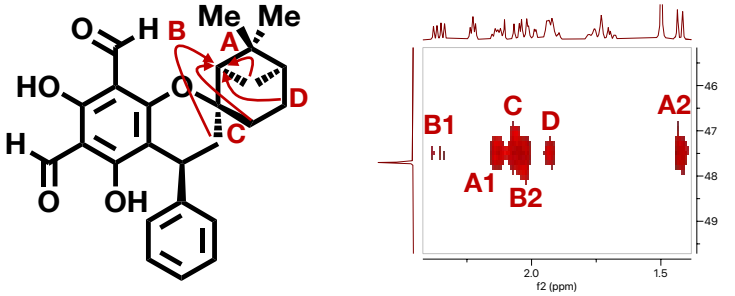

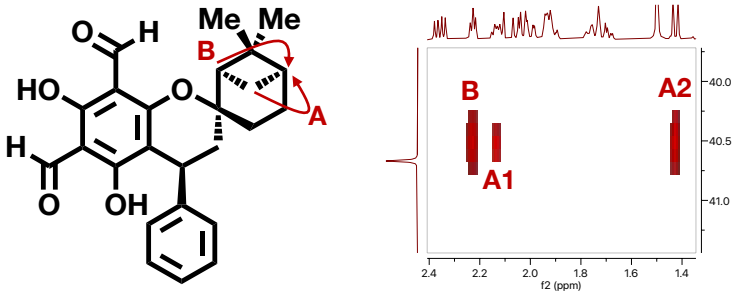

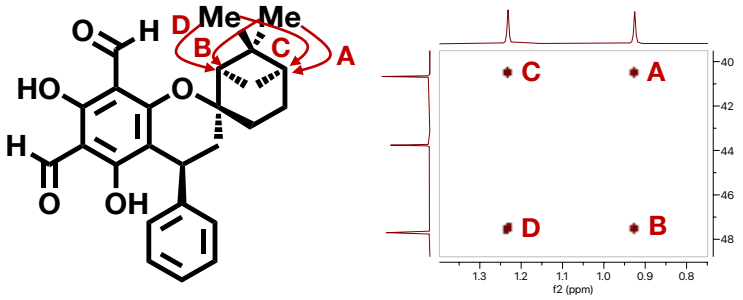

COSY: Full spectrum

NOTE: The size of correlation arrows shown does not indicate the strength of the coupling interaction

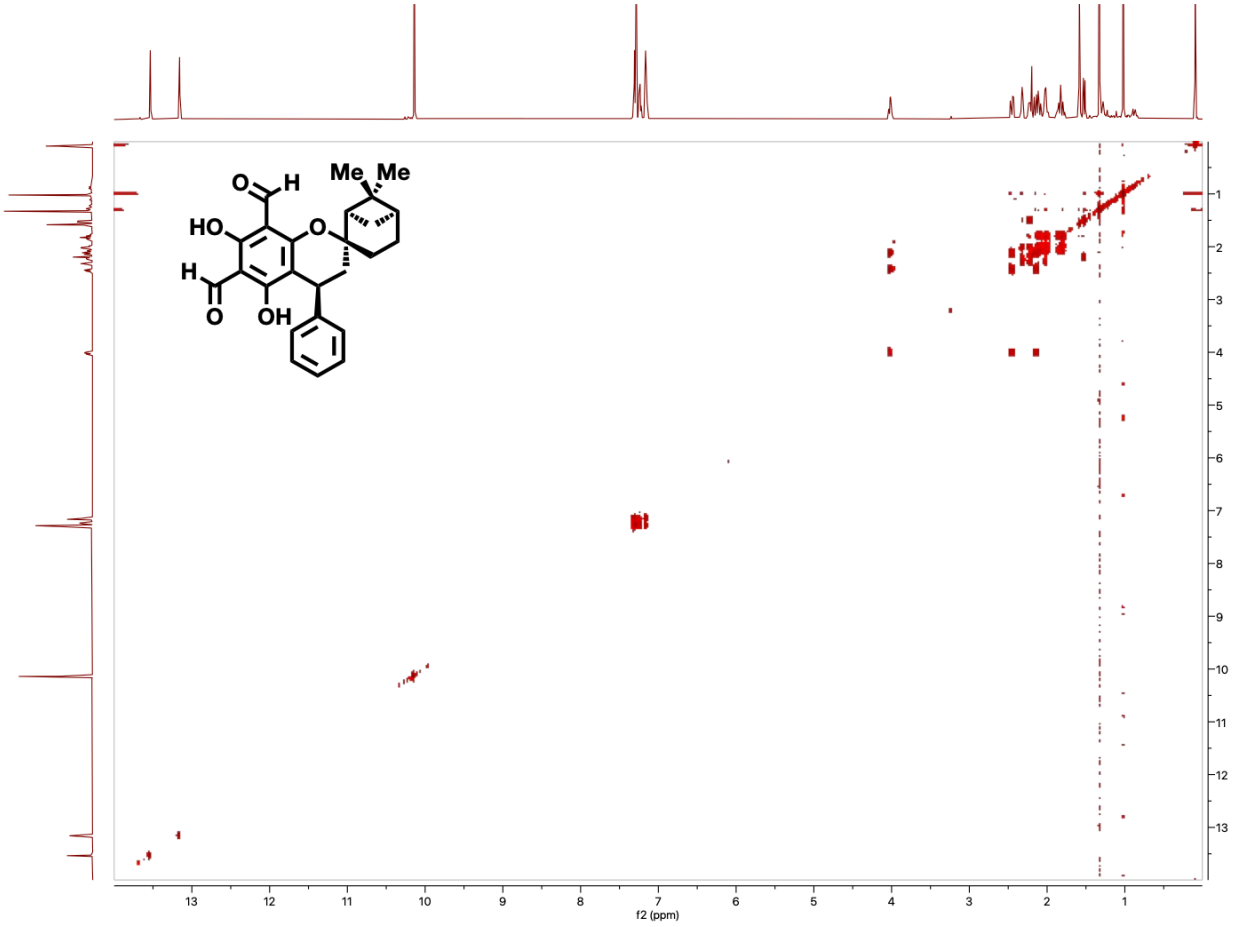

Significant COSY correlations of the pyran methine (–CH):

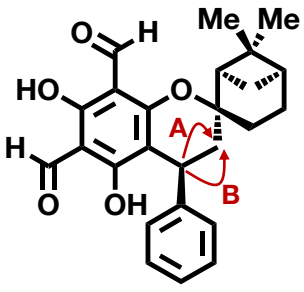

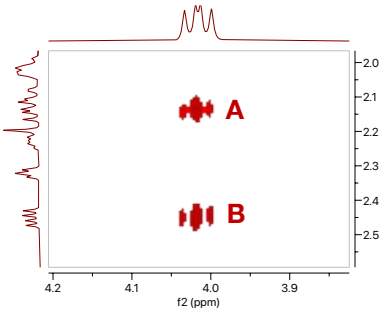

Significant COSY correlations of the β-Pinene (geminal –CH_2 couplings are excluded):

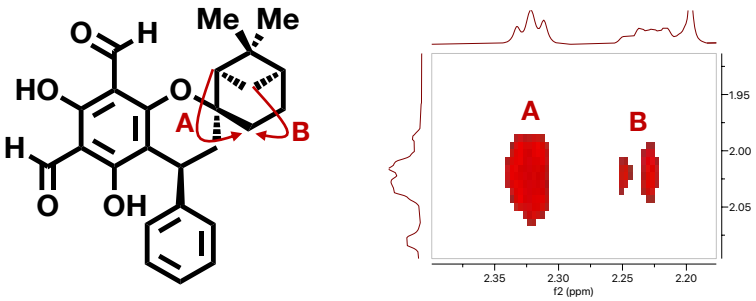

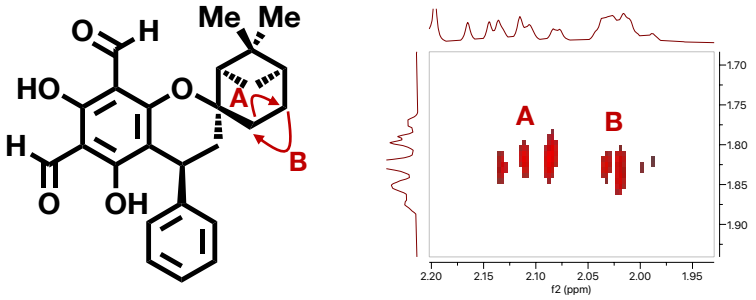

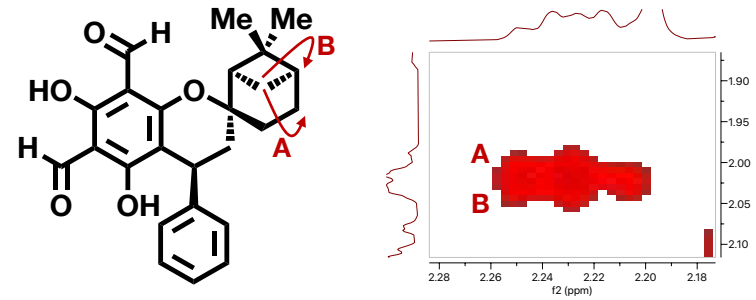

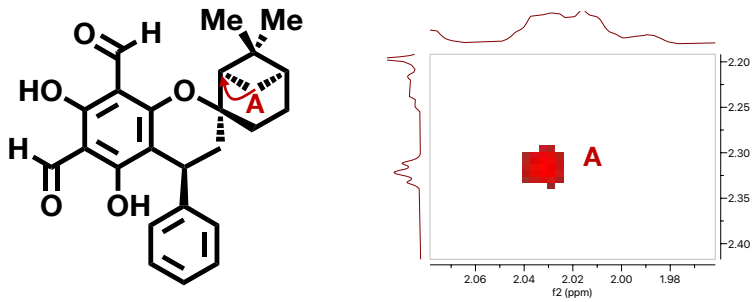

NOESY: Full spectrum

NOTE: The size of correlation arrows shown does not indicate the strength of the coupling interaction

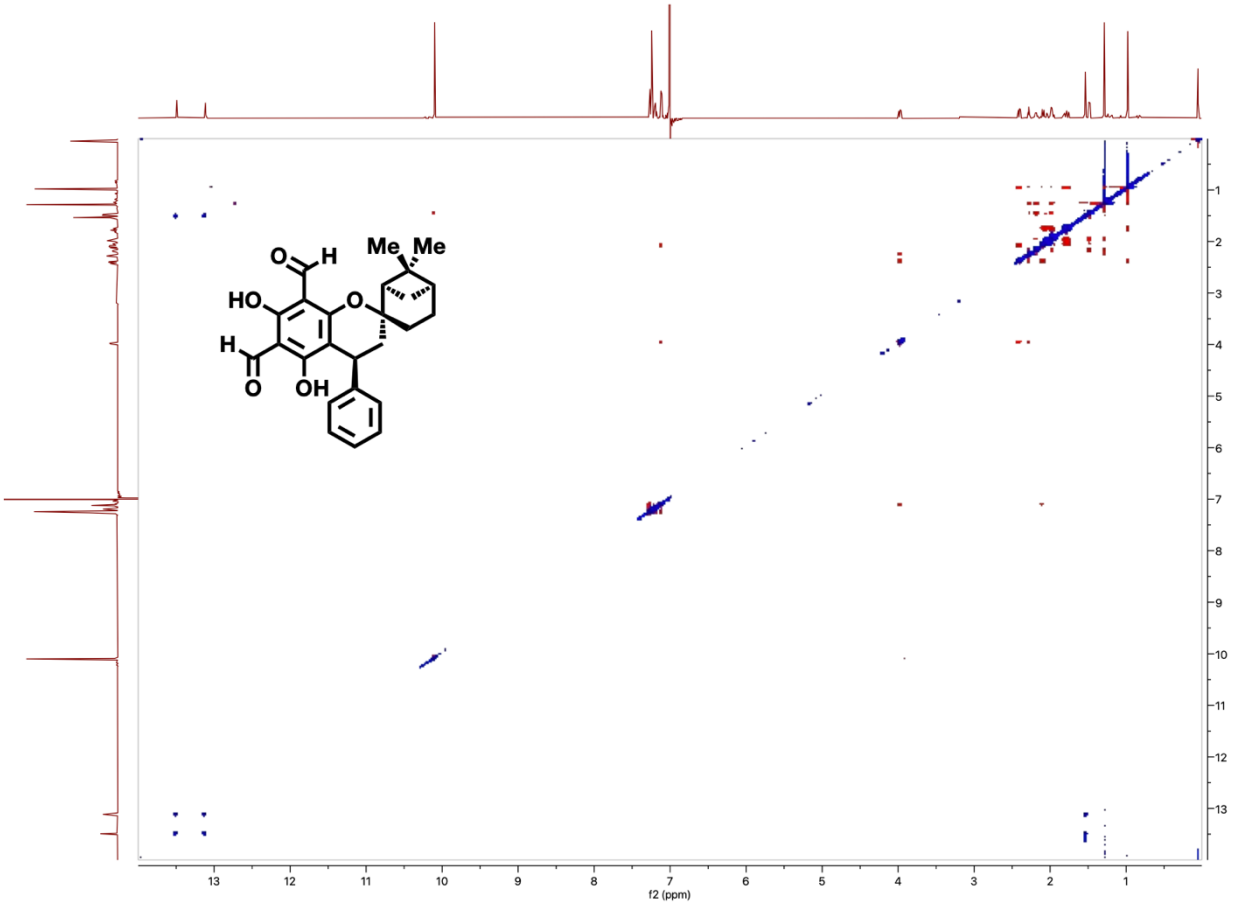

Significant NOESY correlations (interactions also seen in COSY are excluded) used to determine relative stereochemistry:

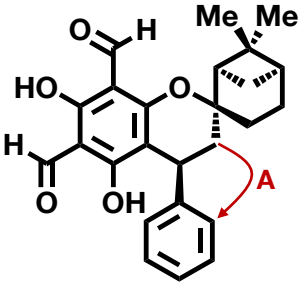

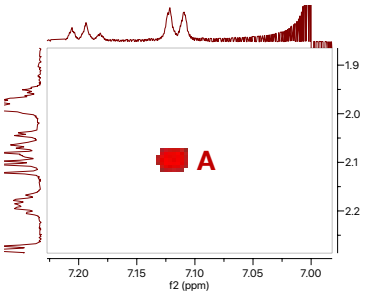

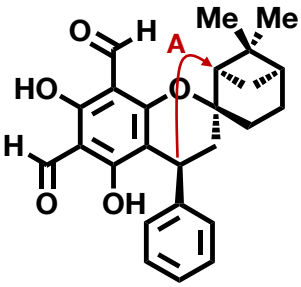

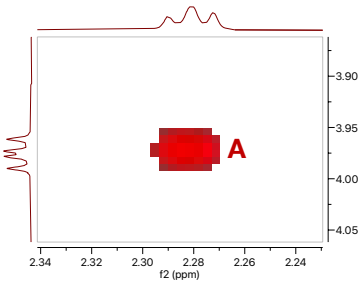

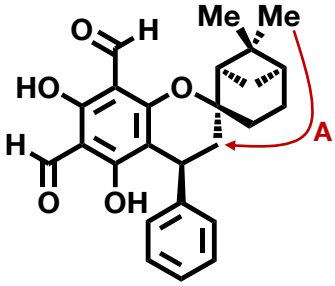

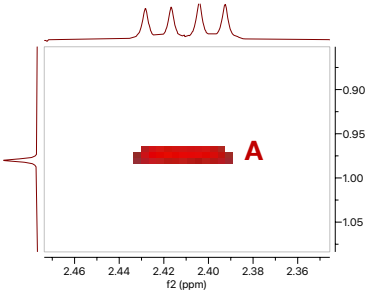

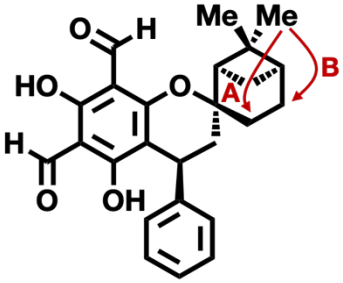

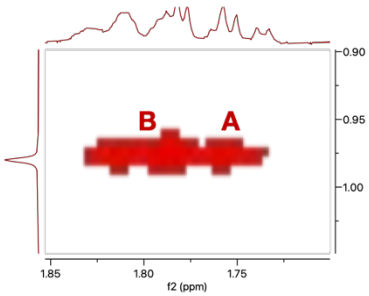

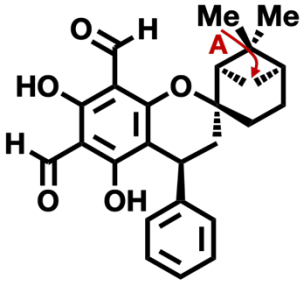

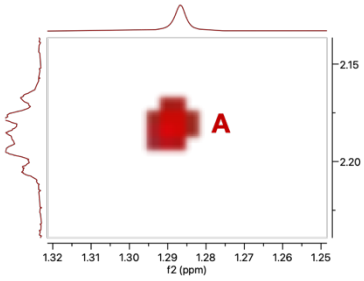

Synthesis and characterization of the isolated grandinol-butylamine monoadduct

(*E*)-1-(3-((butylimino)methyl)-2,4,6-trihydroxy-5-methylphenyl)-3-methylbutan-1-one (12)

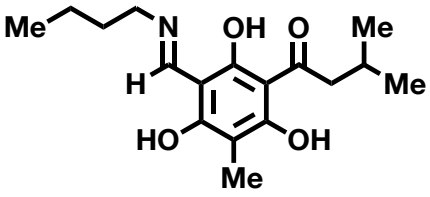

Butylamine (0.221 mL, 2.24 mmol, 1 equiv) was added to a solution of grandinol in MeOH (524 mg, 2.24 mmol, 0.1M). The mixture was stirred overnight at 25 °C before the MeOH was removed by rotary evaporation. The crude mixture was redissolved in EtOAc, adsorbed onto silica gel (SiO_2, 12 g) by rotary evaporation, and purified on silica gel column (SiO_2, 50 µm, 80 g) using puriFlash® XS 520 Plus flash chromatography system (6.1→100% of EtOAc in hexanes, 40 min, 34 mL/min to deliver the desired product as a crystalline solid (433 mg, 63%). **TLC** (EtOAc:hexanes, 3:7 v/v) R_f = 0.28; visualized with 254-nm UV light. **^{1}H-NMR** (500 MHz, CD_3OD): δ 8.37 (s, 1H), 3.56 (br t, *J* = 7.2 Hz, 2H), 2.83 (d, *J* = 7 Hz, 2H), 2.11 (m, 1H), 1.68 (m, 2H), 1.44-1.40 (m, 2H), 1.29 (s, 3H), 1.00-0.96 (m, 9H). **^{13}C-NMR** (126 MHz, CD_3OD): δ 206.47, 181.64, 177.13, 165.06, 159.01, 109.02, 103.14, 98.36, 81.23, 52.41, 51.14, 33.54, 23.28, 20.76, 13.95, 7.38. **HRMS** (DART): exact mass calculated for $C_{17}H_{26}NO_4$ $[M+H]^+$ m/z = 308.18563; found m/z = 308.18353.

^{1}H-NMR spectrum (500 MHz) of **12** in CD_3OD

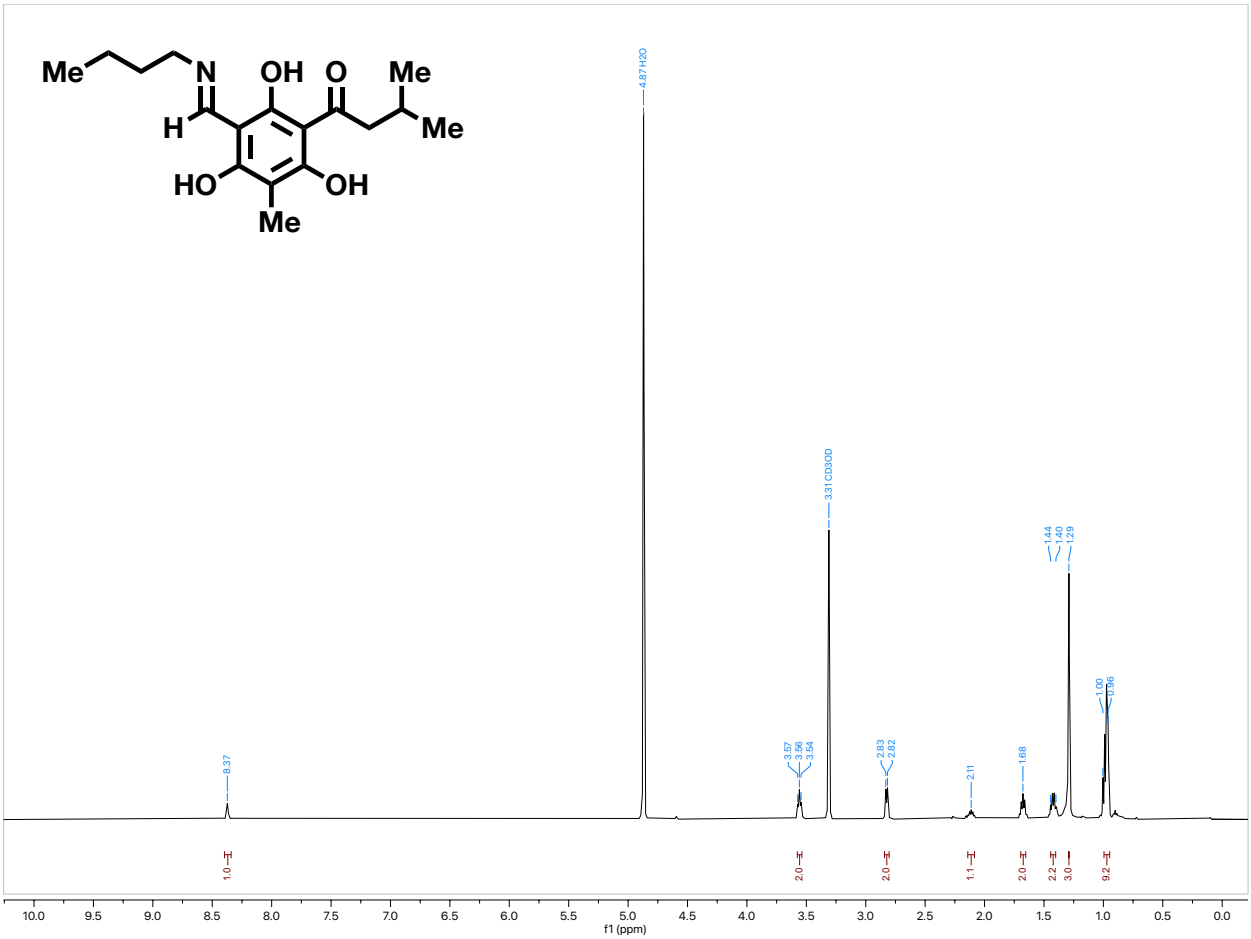

^{13}C-NMR spectrum (126 MHz) of **12** in CD_3OD

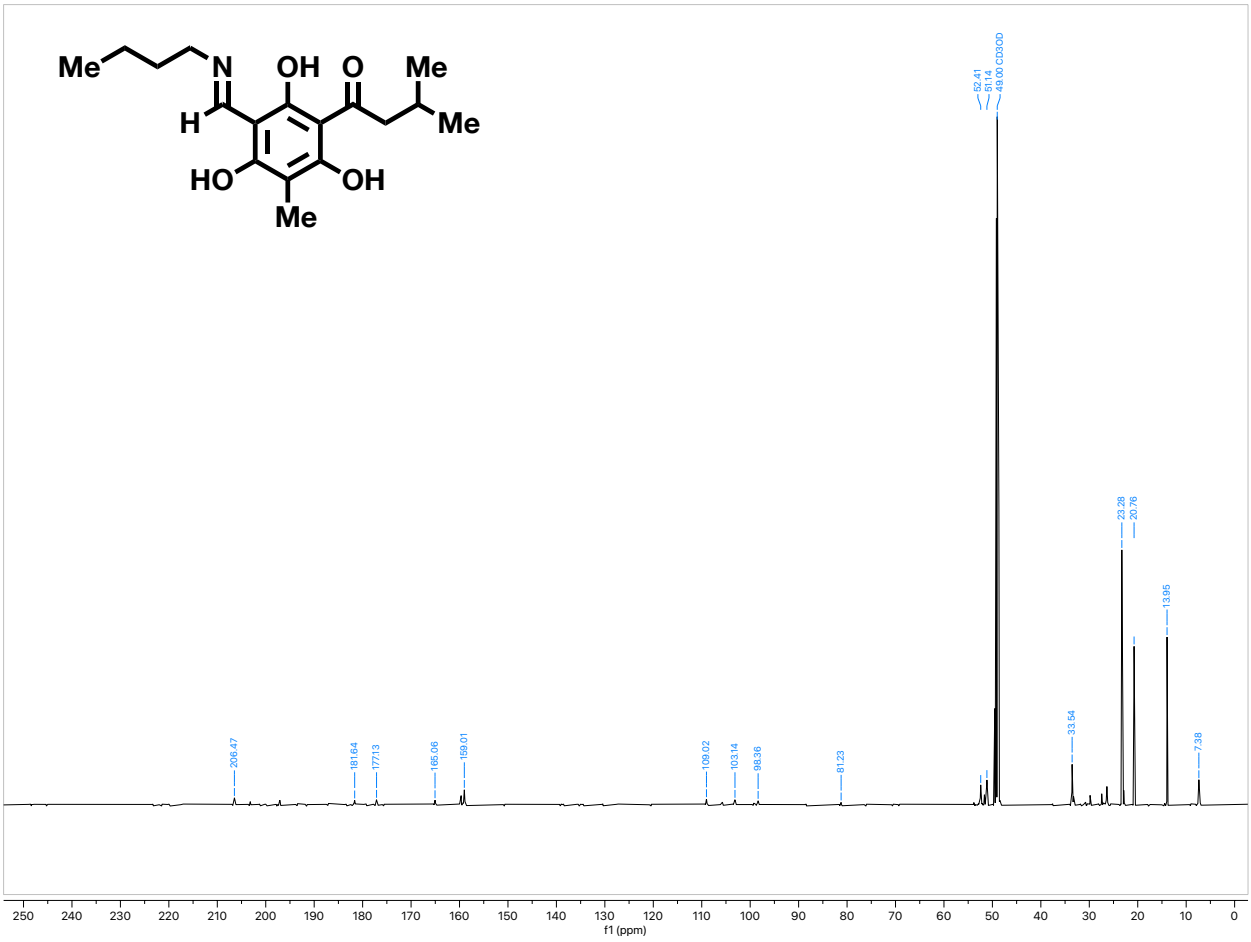

Characterization of the isolated jensenone-butylamine bisadduct by 2D-NMR

1-(3,5-bis((*E*)-(butylimino)methyl)-2,4,6-trihydroxyphenyl)-3-methylbutan-1-one (13)

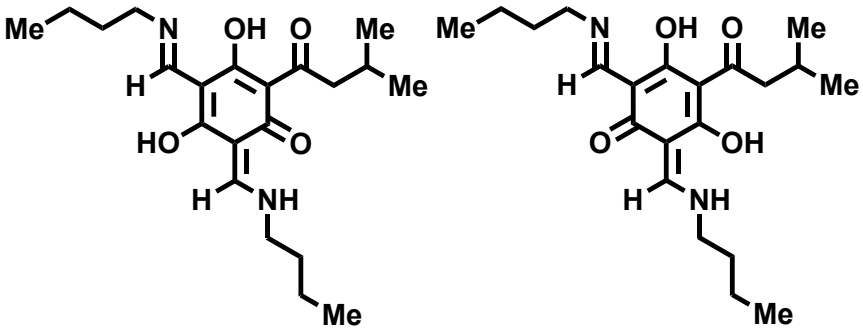

Butylamine (0.093 mL, 0.94 mmol, 5 equiv) was added to a solution of jensenone in MeOH (50 mg, 0.188 mmol, 0.1 M). The mixture was stirred overnight at 25 °C before the MeOH was removed by rotary evaporation. The crude mixture was redissolved in EtOAc, adsorbed onto silica gel (SiO_2, 12 g) by rotary evaporation, and purified on silica gel column (SiO_2, 50 μm, 12 g) using puriFlash® XS 520 Plus flash chromatography system (9→100% of EtOAc in hexanes, 30 min, 15 mL/min to deliver the desired product as a crystalline solid (37 mg, 53%). **TLC** (EtOAc:hexanes, 7:3 v/v) R_f = 0.53; visualized with 254-nm UV light. **HRMS** (DART): exact mass calculated for $C_{21}H_{33}N_2O_4$ $[M+H]^+$ m/z = 377.24348; found m/z = 377.24369.

Tautomer 1: **^{1}H-NMR** (500 MHz, CD_3OD): δ 8.30 (s, 1H), 8.20 (s, 1H), 3.54-3.46 (m, 4H), 2.99 (dd, *J* = 12.4, 6.9 Hz, 2H), 2.21-2.14 (m, 1H), 1.66 (m, 4H), 1.44-1.40 (m, 4H), 0.99-0.95 (m, 12H). **^{13}C-NMR** (126 MHz, CD_3OD): δ 205.63, 185.72, 183.70, 181.83, 160.04, 158.73, 106.97, 106.88, 99.91, 51.29, 51.17, 50.97, 33.68, 33.48, 26.74, 23.26, 20.72, 13.97.

Tautomer 2: **^{1}H-NMR** (500 MHz, CD_3OD): δ 8.32 (s, 1H), 8.21 (s, 1H), 3.54-3.46 (m, 4H), 2.99 (dd, *J* = 12.4, 6.9 Hz, 2H), 2.21-2.14 (m, 1H), 1.66 (m, 4H), 1.44-1.40 (m, 4H), 0.99-0.95 (m, 12H). **^{13}C-NMR** (126 MHz, CD_3OD): δ 206.19, 185.72, 184.16, 181.58, 159.39, 159.30, 106.92, 106.74, 99.91, 51.5, 51.17, 51.08, 33.71, 33.54, 26.84, 23.26, 20.74, 13.97.

^{1}H-NMR spectrum (500 MHz) of **13** in CD_3OD

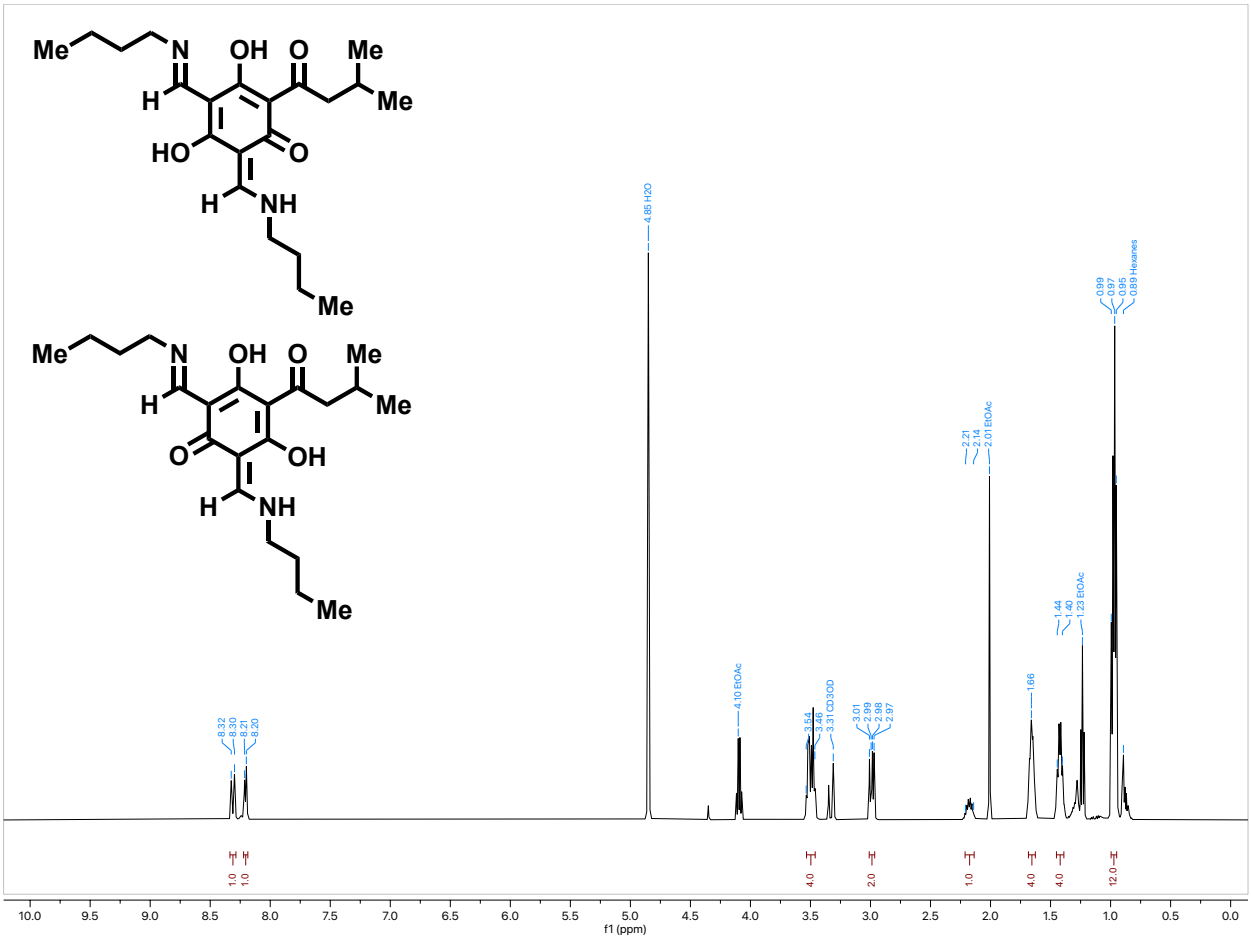

^{13}C-NMR spectrum (126 MHz) of **13** in CD_3OD

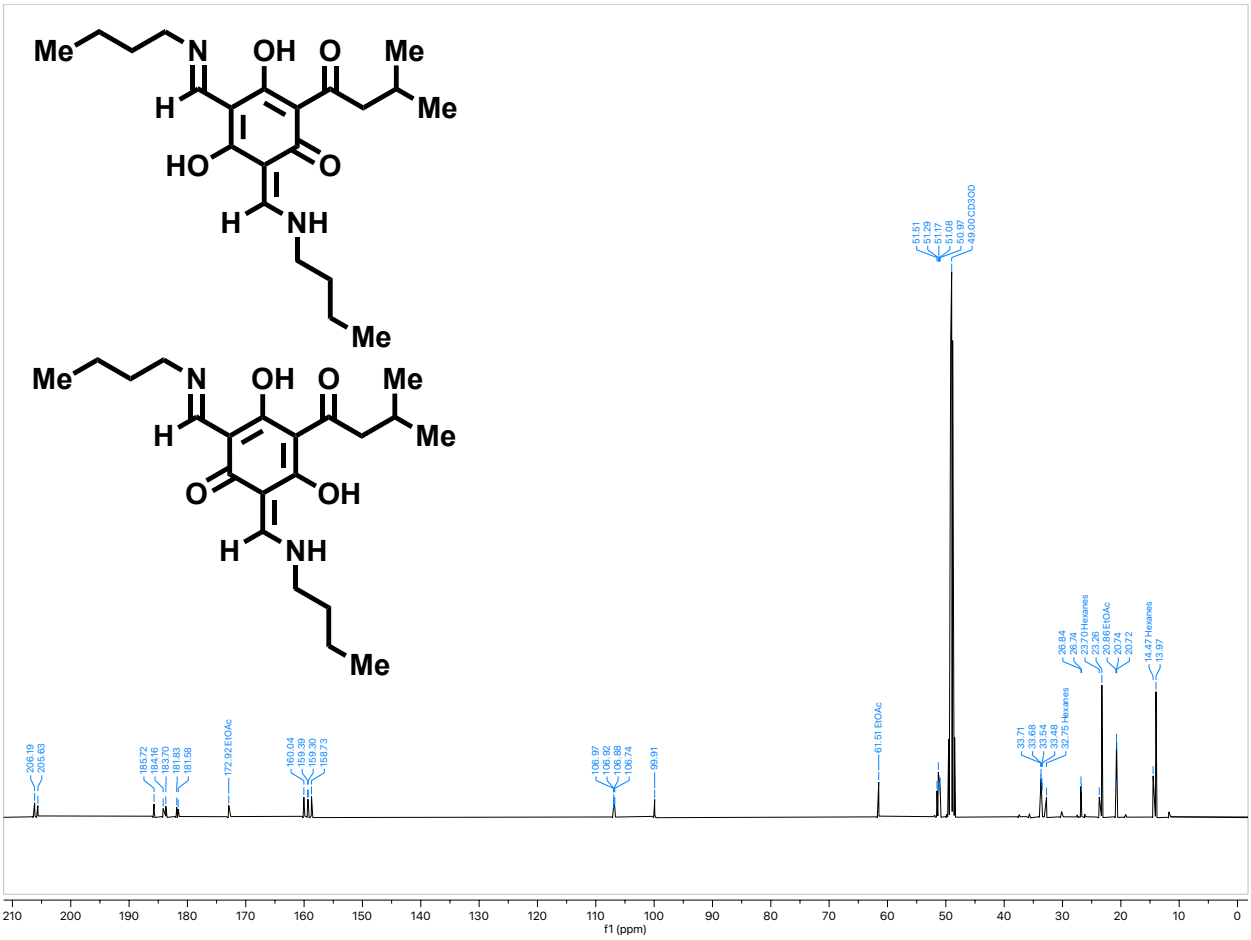

Structural assignment of the jensenone-butylamine bisadduct

Two-dimensional NMR was employed to corroborate the structure of the synthesized bisadduct. It should be noted that the chemical shifts reported in the 2D-NMR spectra were not cross-referenced with those obtained from one-dimensional ^{1}H-NMR and ^{13}C-NMR spectra; therefore, minor discrepancies in the observed chemical shifts, measured in ppm, may exist between the 1D- and 2D-NMR datasets. In brief, HSQC spectroscopy was initially employed to ascertain the identities of the anticipated imine(s), butylamine- and isovaleryl-derived carbon chain hydrogens and carbons within the molecular scaffold. Subsequently, HMBC and COSY spectra were used to elucidate the connectivity of bonds throughout the molecular structure. Salient correlations instrumental in spectral assignments are denoted by arrows, and the corresponding cross-peaks are depicted in insets adjacent to the molecular structure representation.

HSQC: Full spectrum

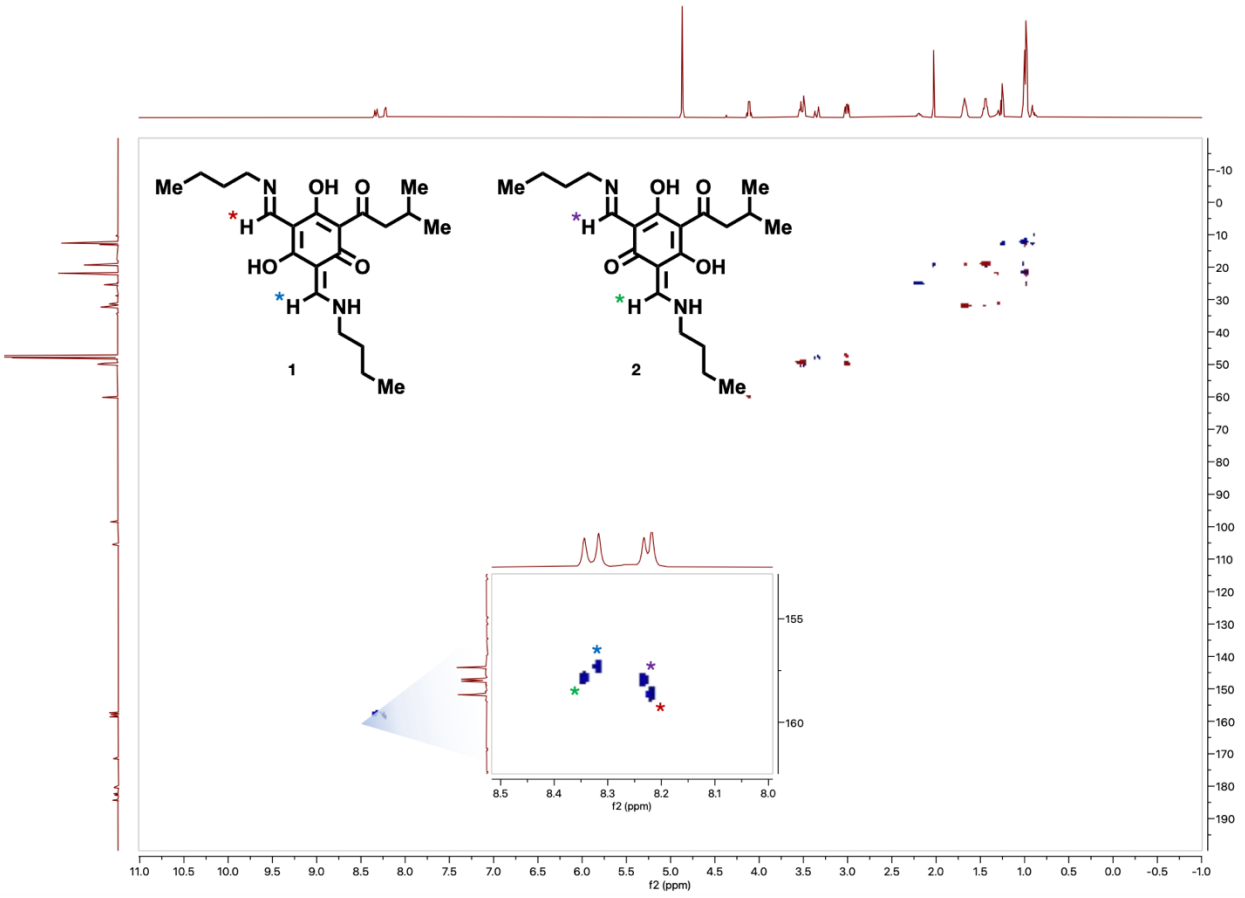

Analysis of the HSQC data revealed the presence of four discrete sets of hydrogens and carbons, as delineated in the accompanying HSQC spectral inset. These correspond to the region of the ^{1}H-NMR spectrum anticipated for the emergent imine moiety. Distinctive color-coded asterisks were employed to differentiate between the hydrogen atoms associated with the imine and enamine functional groups. This observation provided the initial empirical evidence for the existence of chemically distinct imine and enamine tautomeric species within the sample.

Upon examination of the aliphatic region within the HSQC spectrum, it was observed that hydrogens distal to the phloroglucinol core — specifically, those belonging to methyl groups (–CH_3) and isovaleryl methine (–CH) — exhibit spectral signals that are highly congruent or overlapping, indicating similarity in the chemical environment of these peripheral constituents.

HSQC: Magnified view of the aliphatic region

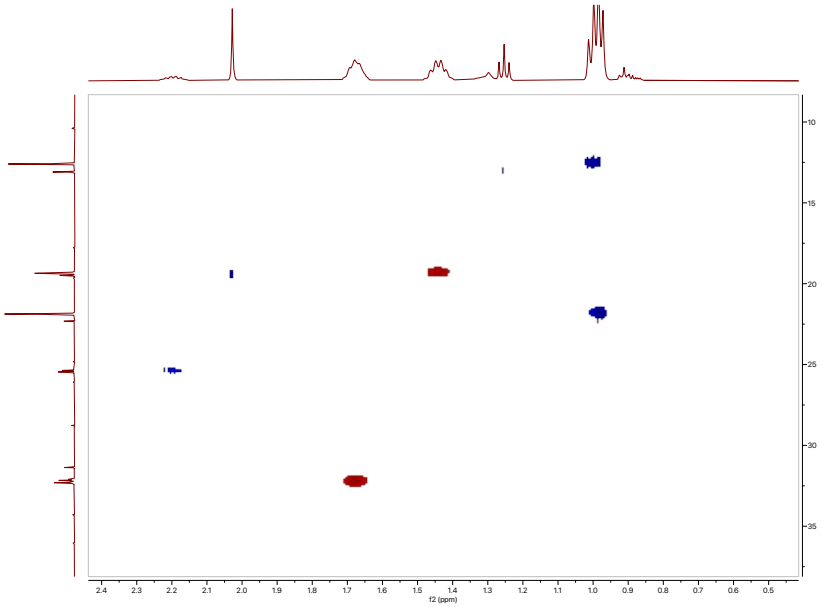

The observed conservation of symmetry suggests that the structural isomerism between the tautomers predominantly arises from variations in connectivity within the phloroglucinol moiety, rather than alterations in the aliphatic side chains. NMR data reveal pronounced chemical shift perturbations for the hydrogen and carbon nuclei proximal to this core, thereby lending empirical support to this hypothesis.

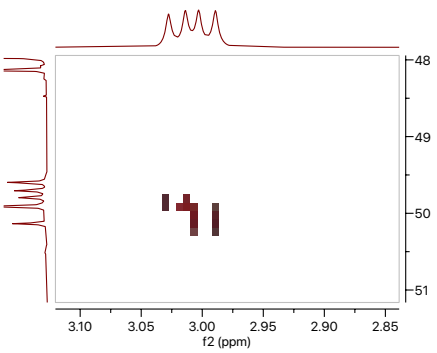

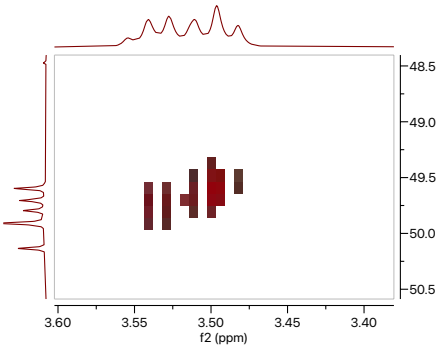

In the depicted left inset above, two distinct sets of methylene groups are evident in the isovaleryl moiety, characterized by overlapping ^{1}H-NMR doublet peaks, yet displaying disparate chemical shift values for their corresponding carbons. In addition, the methylene group adjacent to the nitrogen atom manifests distinct chemical shift disparities between hydrogens and carbons, as illustrated in the right inset. One set of resonances manifests as a triplet at 3.5 ppm, while another

appears as an undefined multiplet at 3.54 ppm. The latter is suggestive of an additional coupling interaction, most likely attributable to an N–H hydrogen of an enamine moiety. Cumulatively, these spectral features are indicative of four chemically unique butylamine chains, corroborated by the presence of four distinct carbon resonances corresponding to the two hydrogen signals.

HMBC: Full spectrum

NOTE: The size of correlation arrows shown does not indicate the strength of the coupling interaction

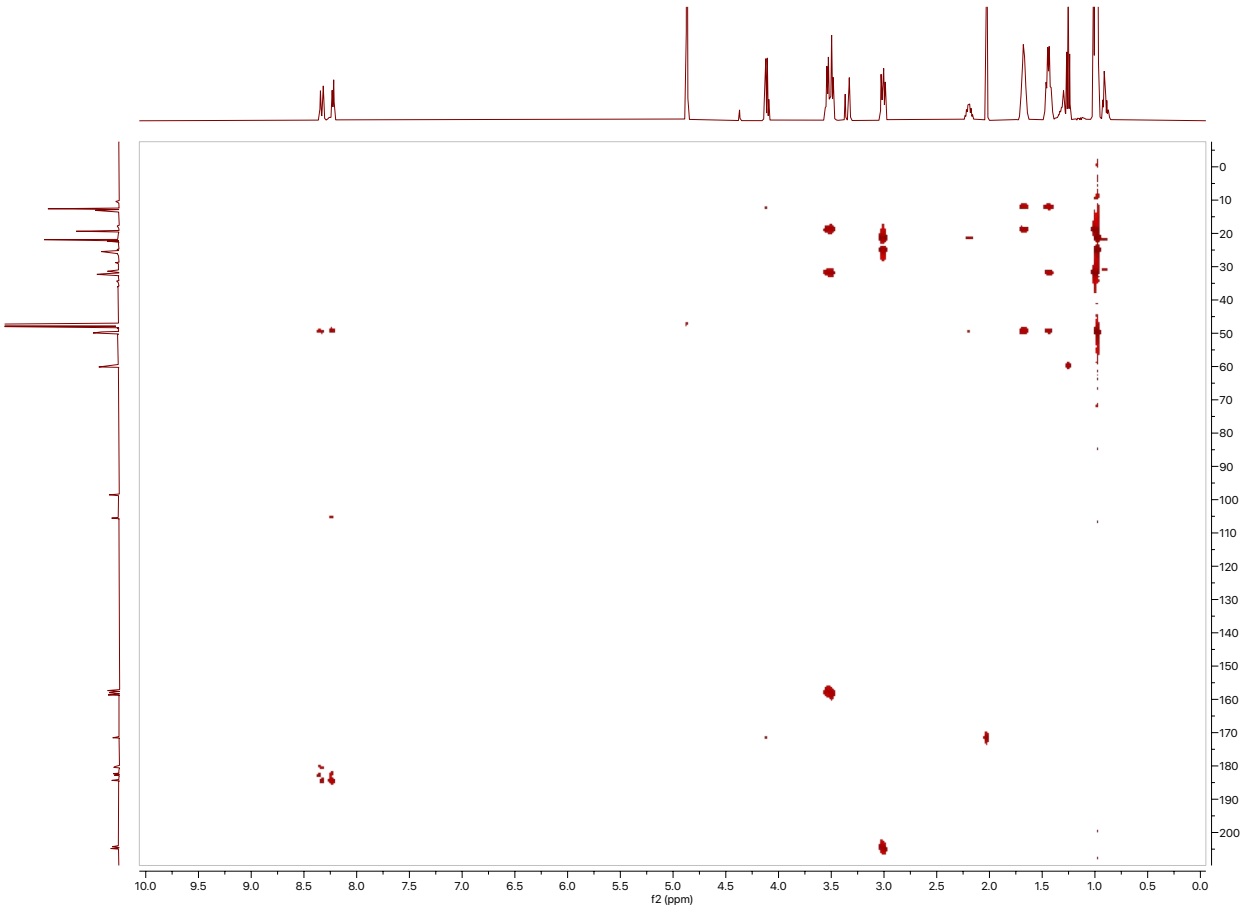

Significant HMBC correlations of the imine/enamine species:

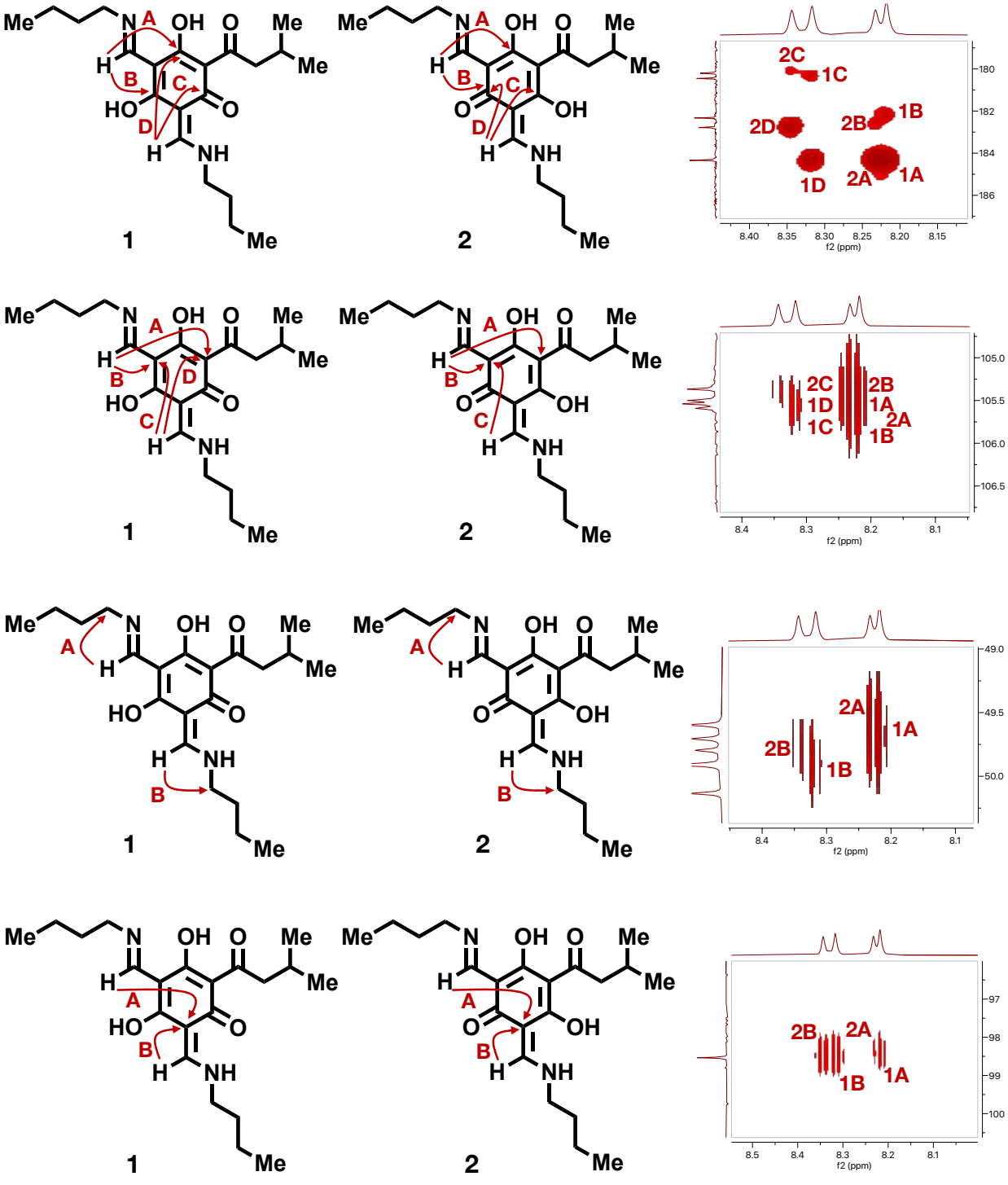

Significant HMBC correlations of the butylamine-derived carbon chain:

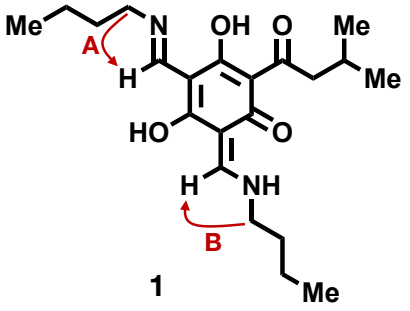

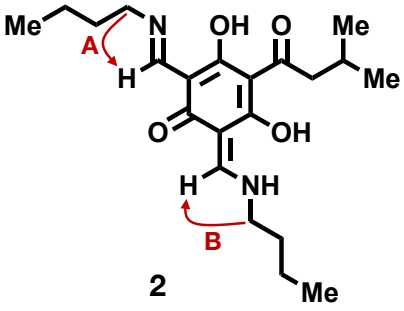

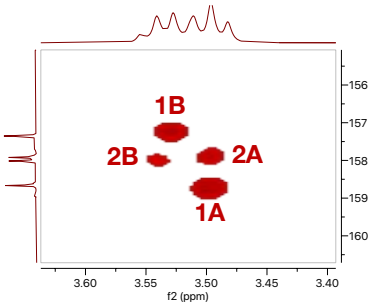

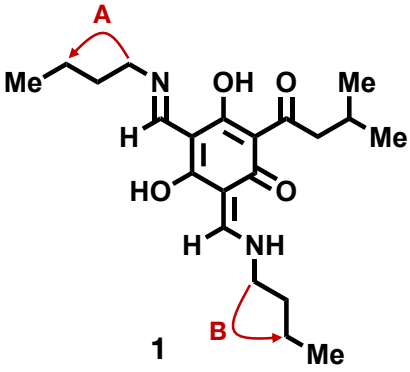

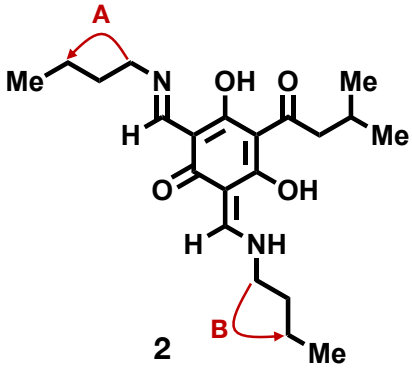

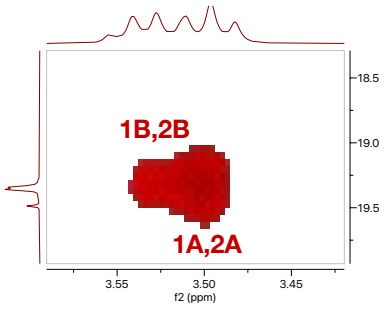

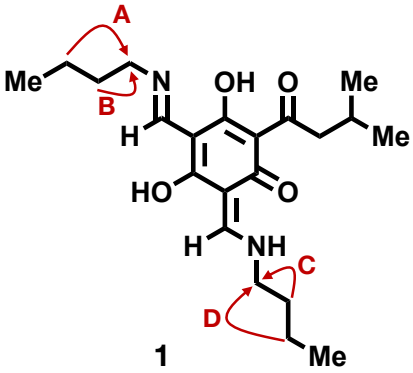

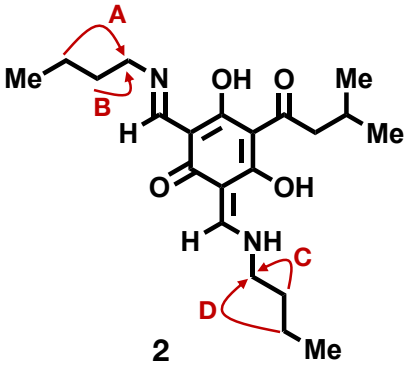

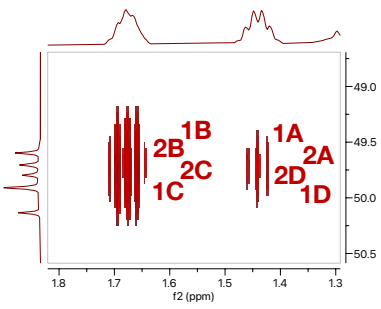

Significant HMBC correlations of the butylamine-derived carbon chain (continued):

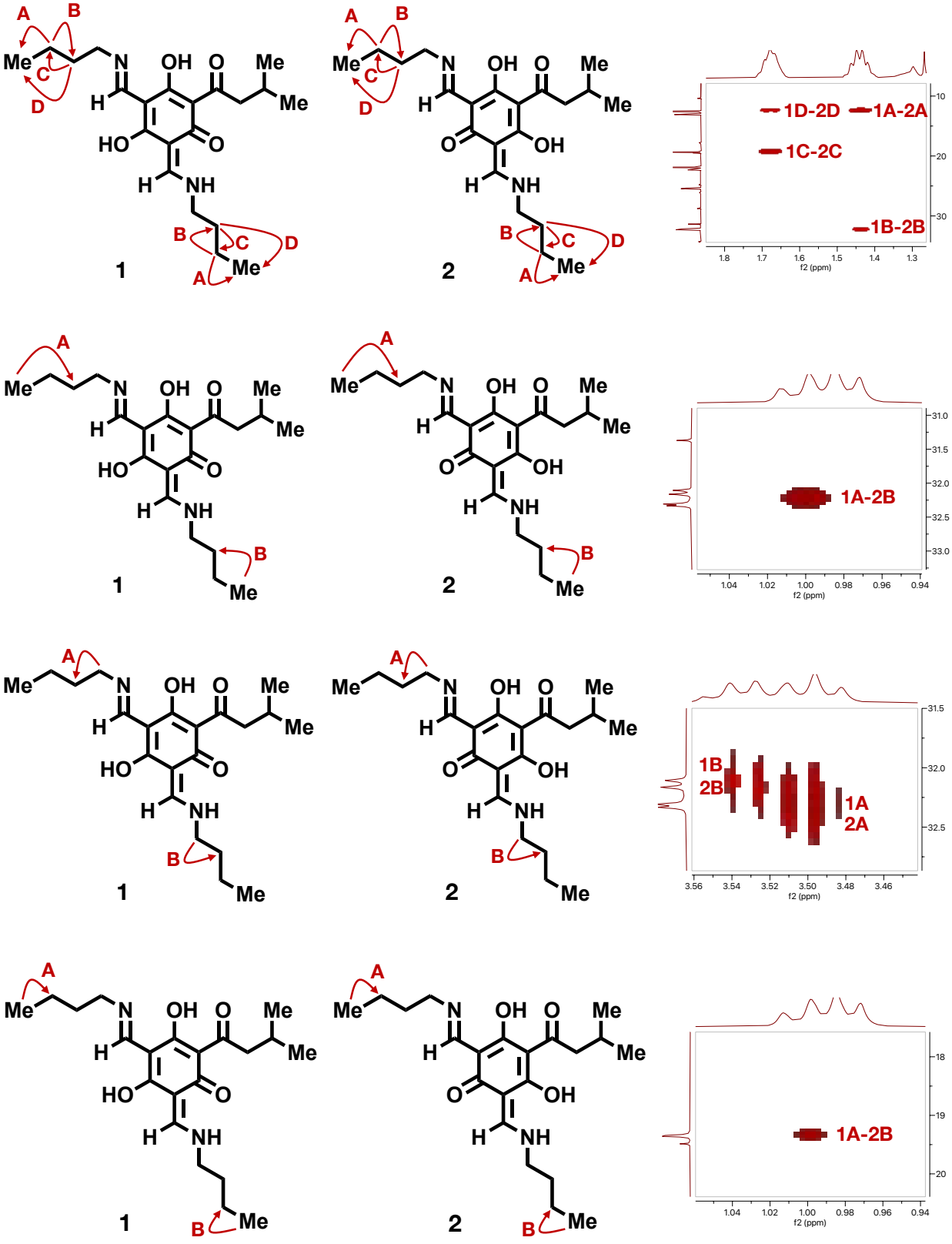

Significant HMBC correlations of the isovaleryl carbon chain:

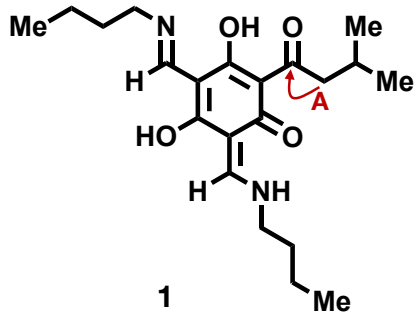

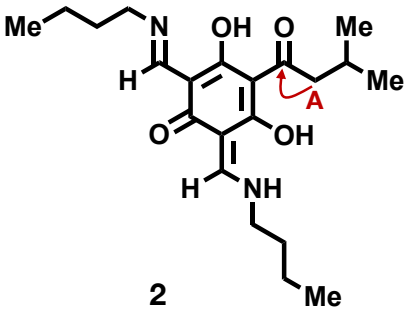

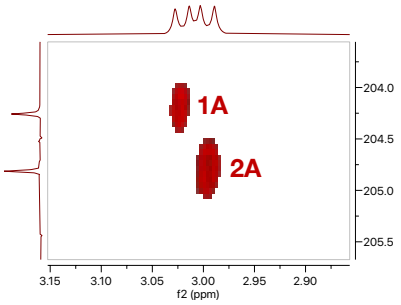

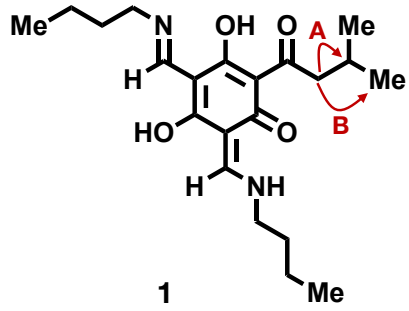

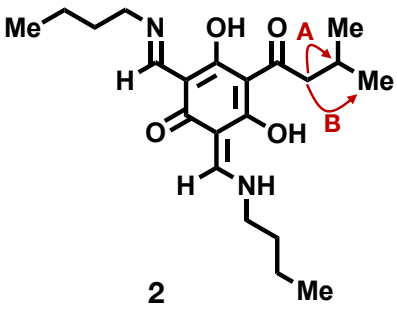

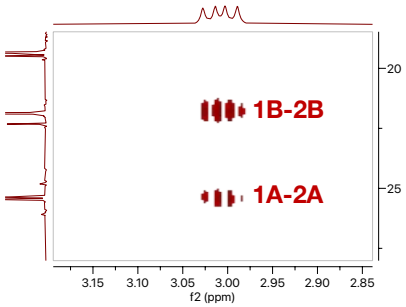

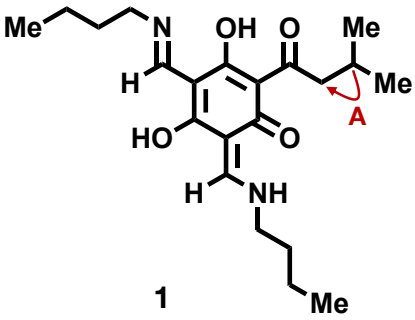

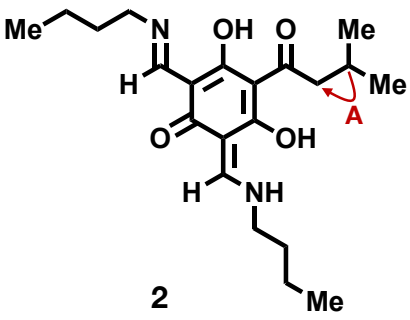

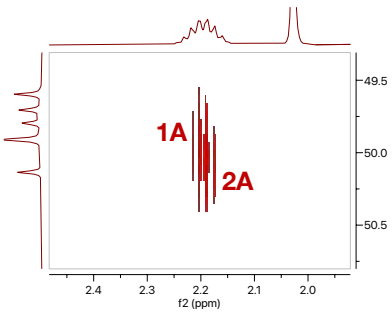

Significant HMBC correlations of the isovaleryl carbon chain (continued):

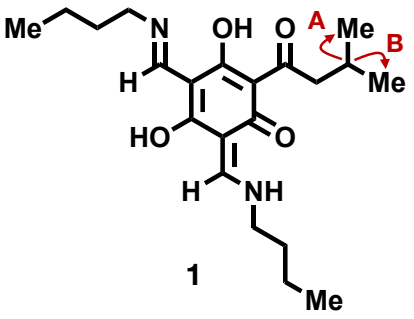

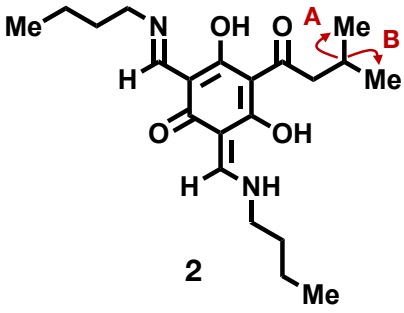

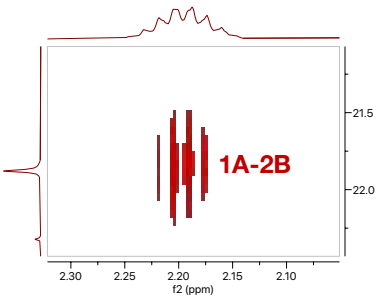

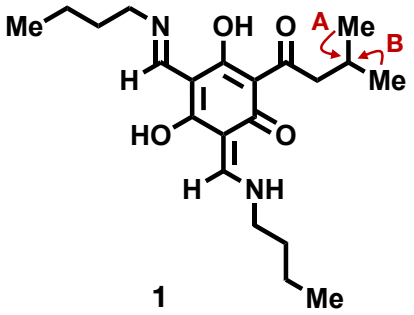

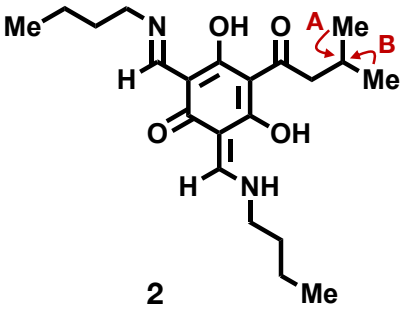

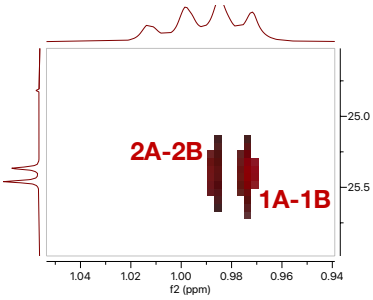

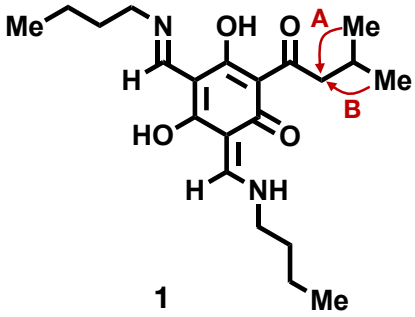

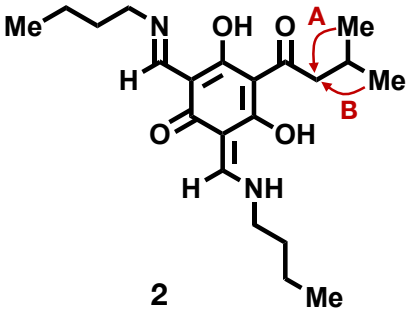

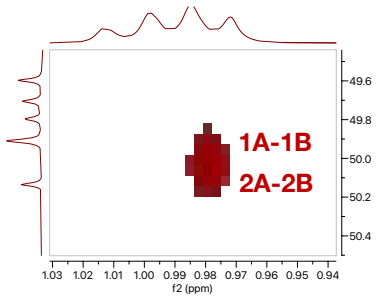

COSY: Full spectrum

NOTE: The size of correlation arrows shown does not indicate the strength of the coupling interaction

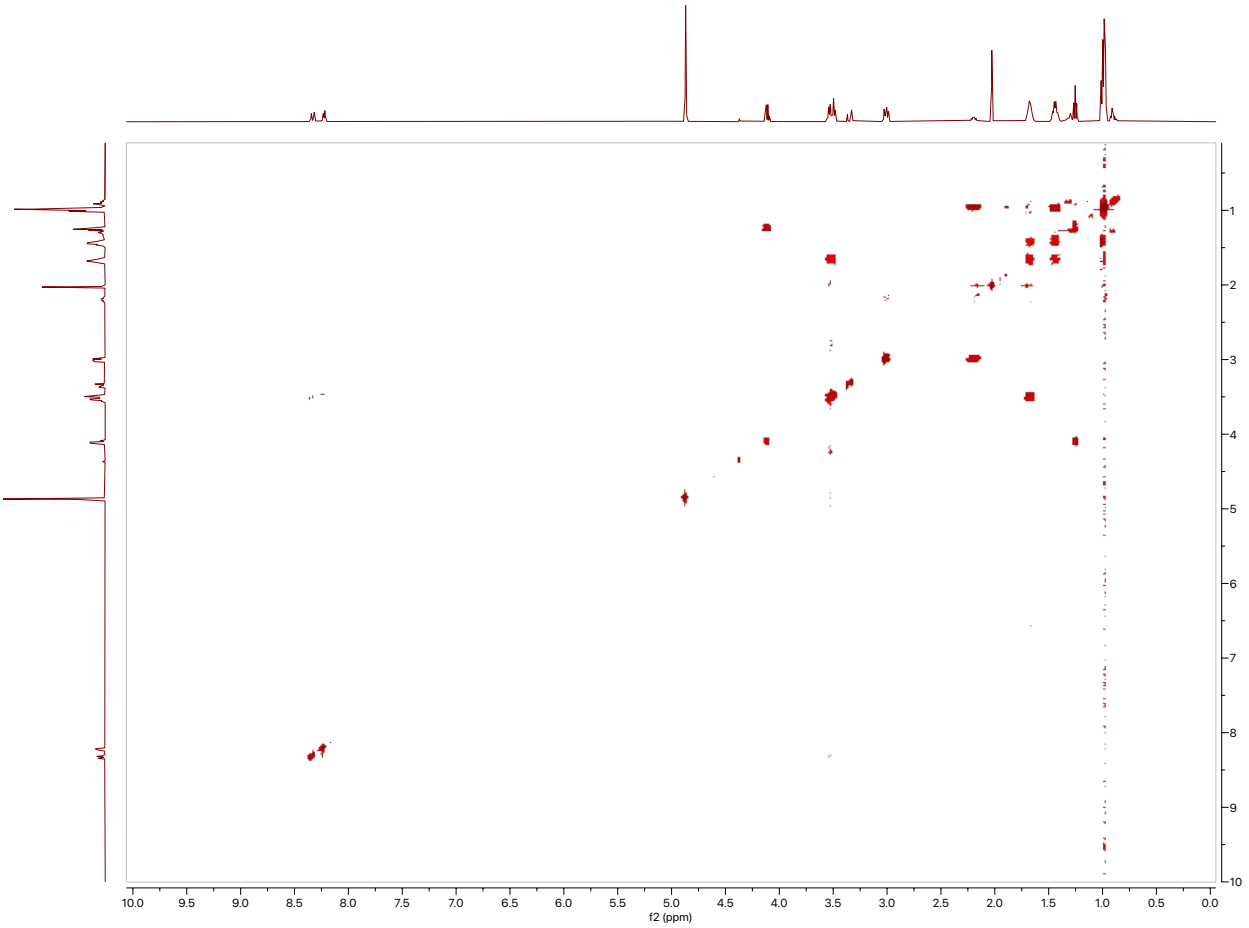

Significant COSY correlations of the imine/enamine species:

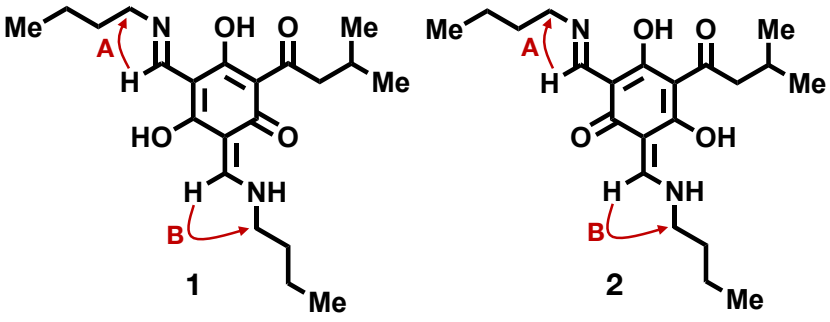

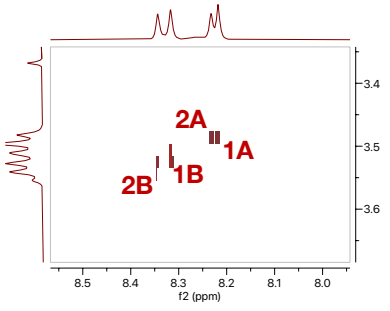

Significant COSY correlations of the butylamine-derived carbon chain:

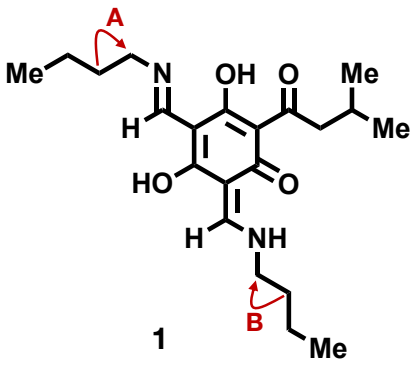

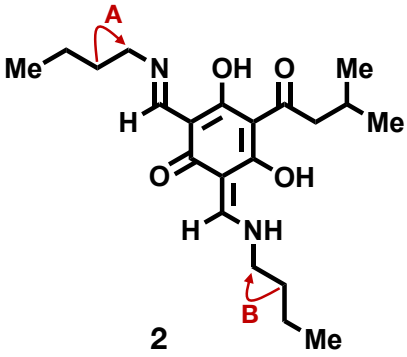

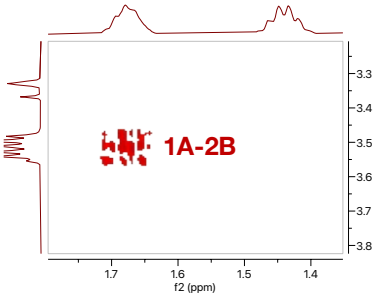

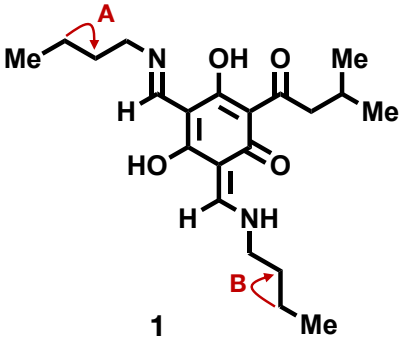

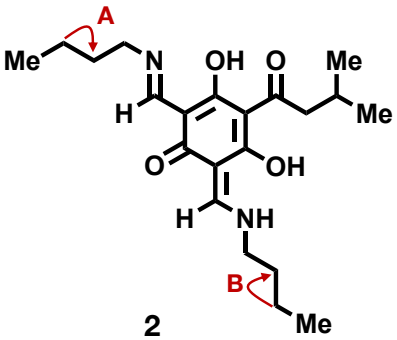

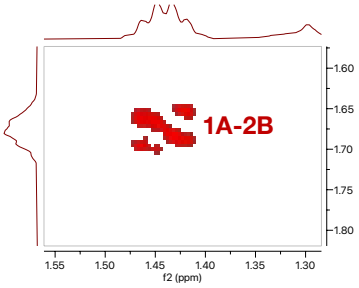

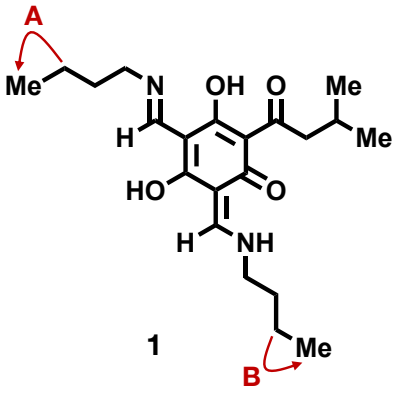

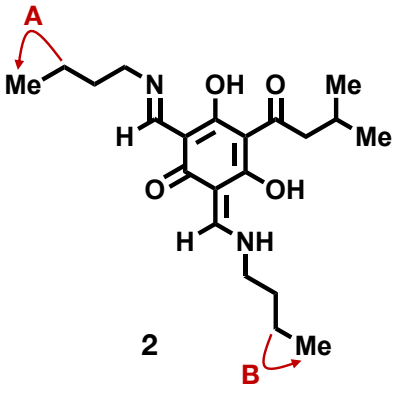

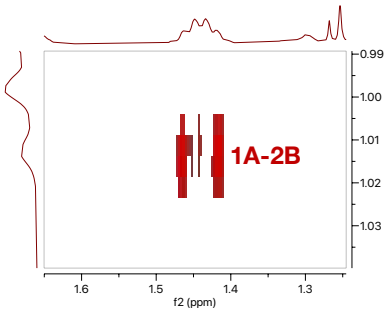

Significant COSY correlations of the isovaleryl carbon chain:

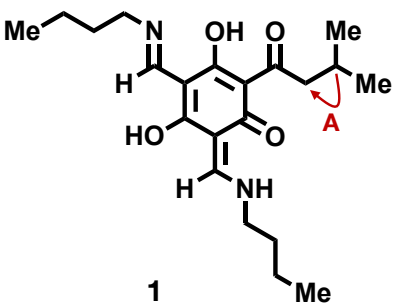

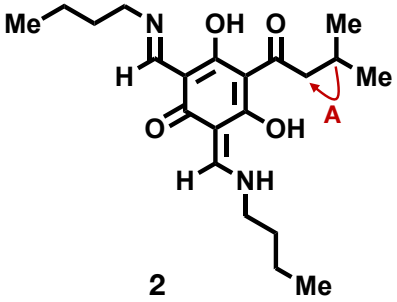

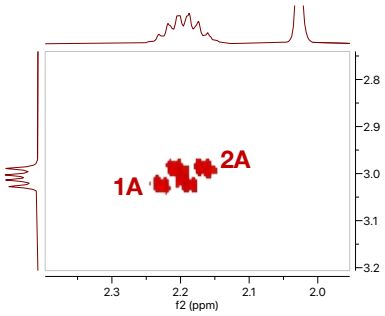

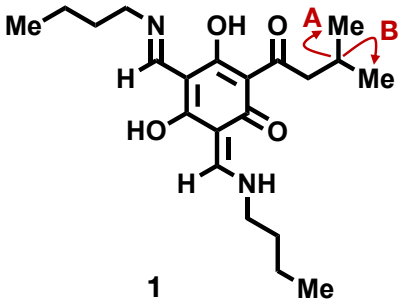

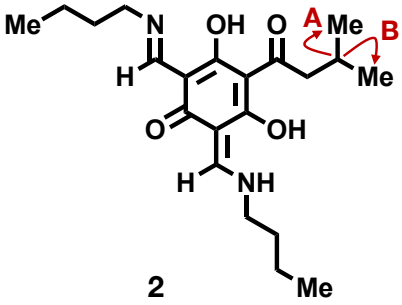

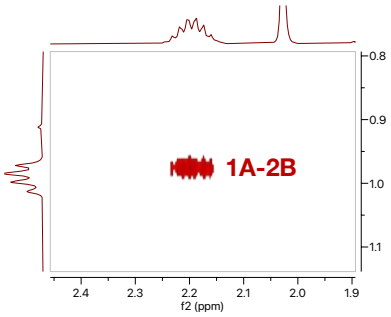

^{1}H-, ^{13}C-, and ^{19}F-NMR spectra

^{1}H-NMR spectrum (500 MHz) of **S1** in CD_3OD

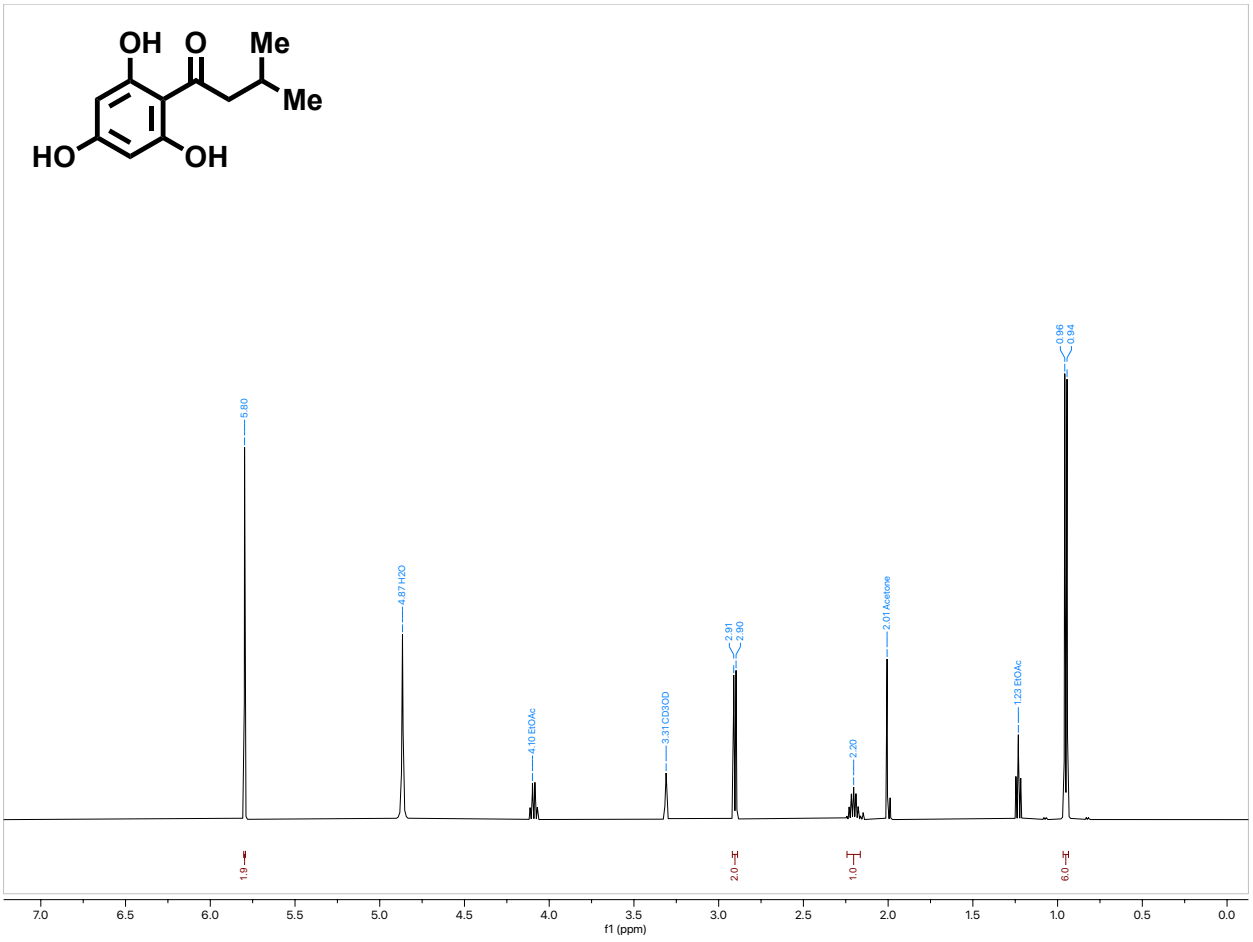

^{13}C-NMR spectrum (126MHz) of **S1** in CD_3OD

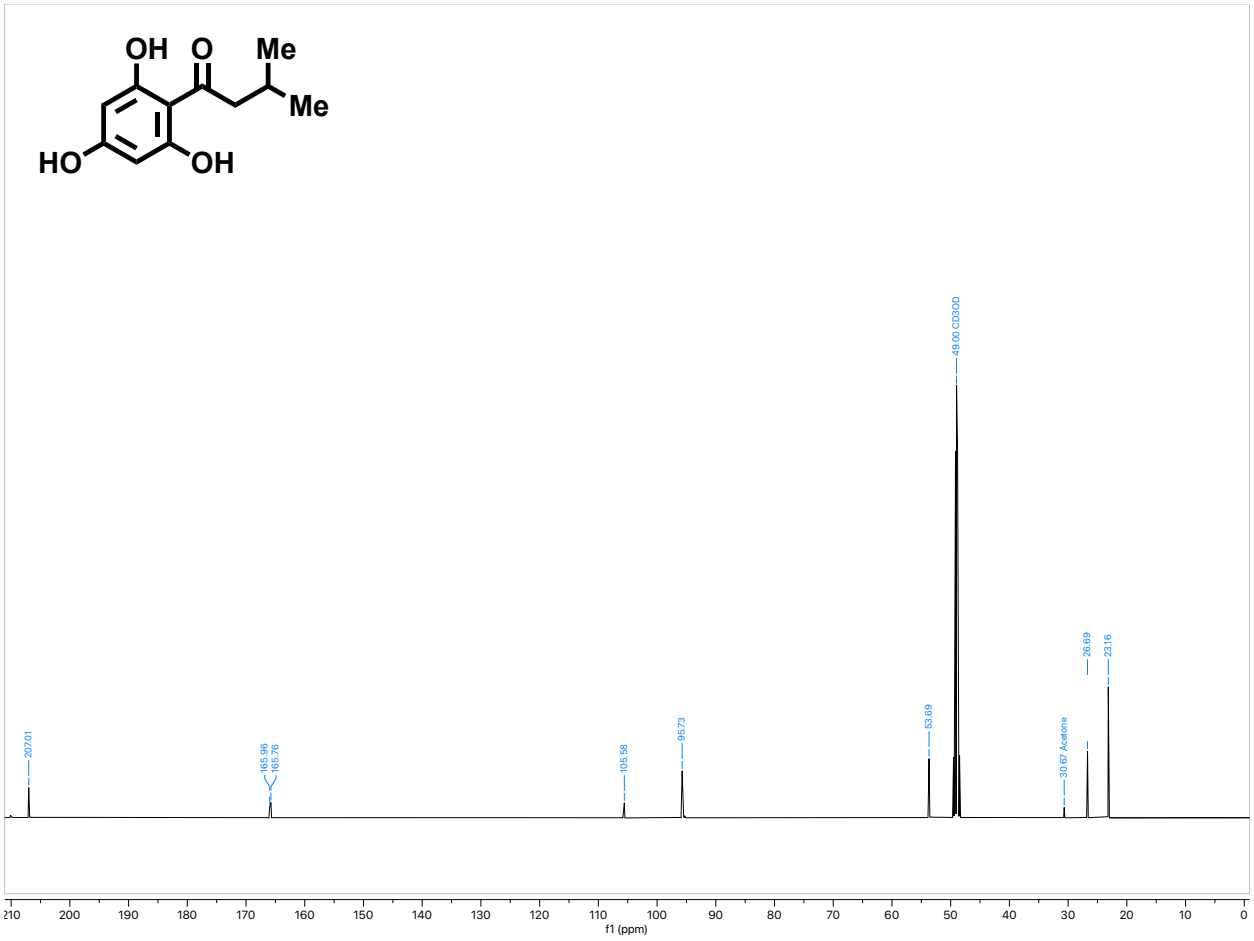

^{1}H-NMR spectrum (500 MHz) of **S2** in CD_3OD

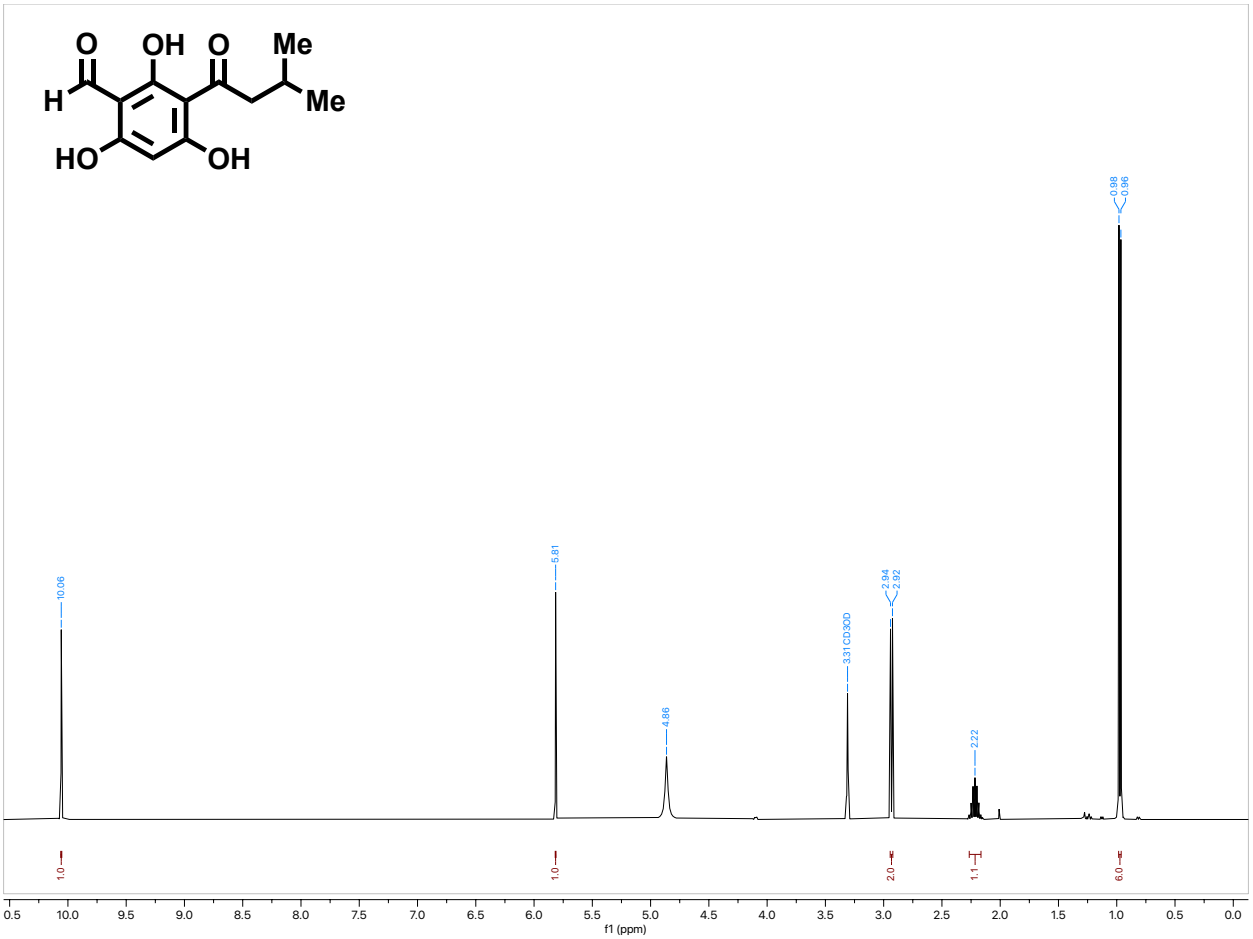

^{13}C-NMR spectrum (126 MHz) of **S2** in CD_3OD

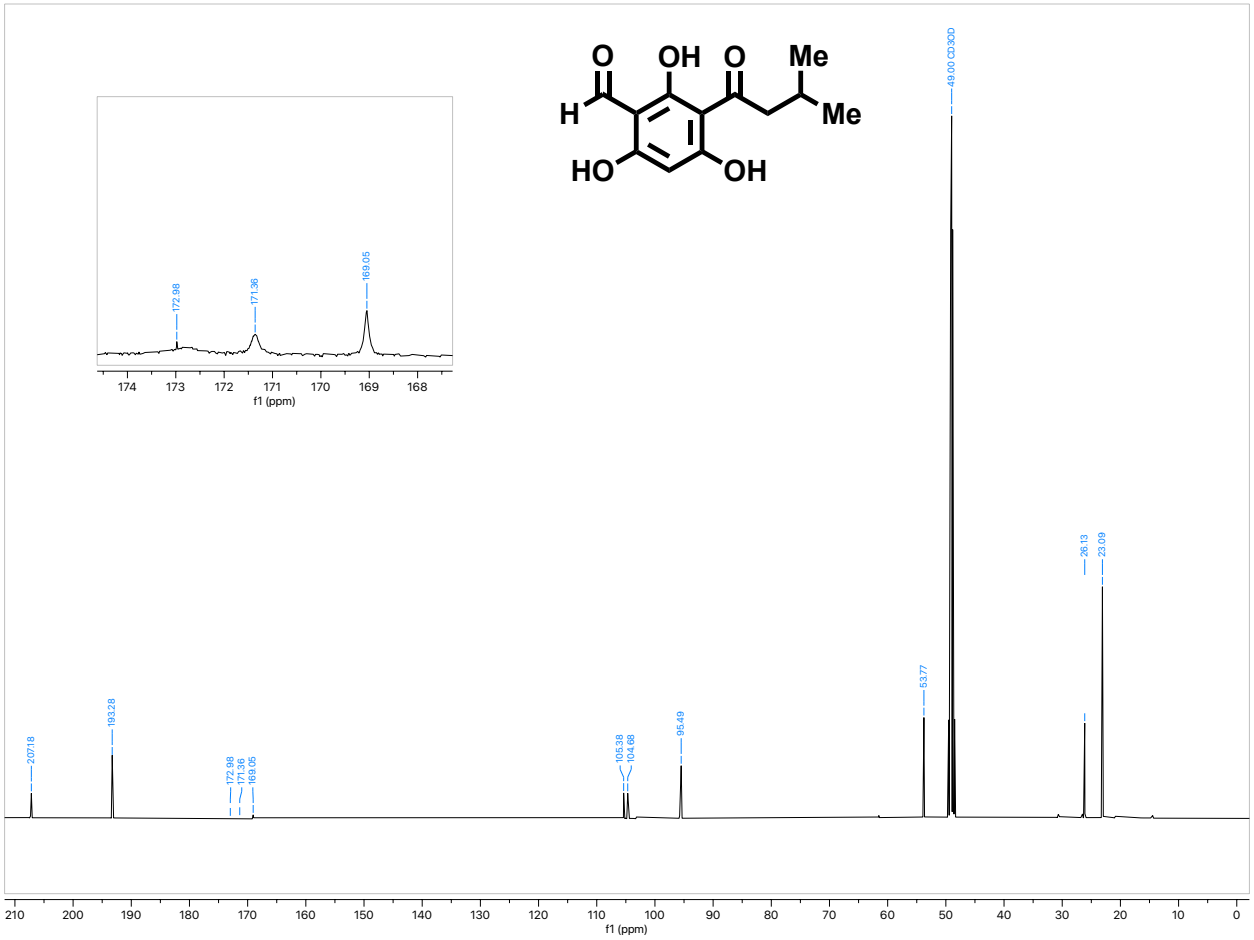

^{1}H-NMR spectrum (500 MHz) of **grandinol** in CD_3OD

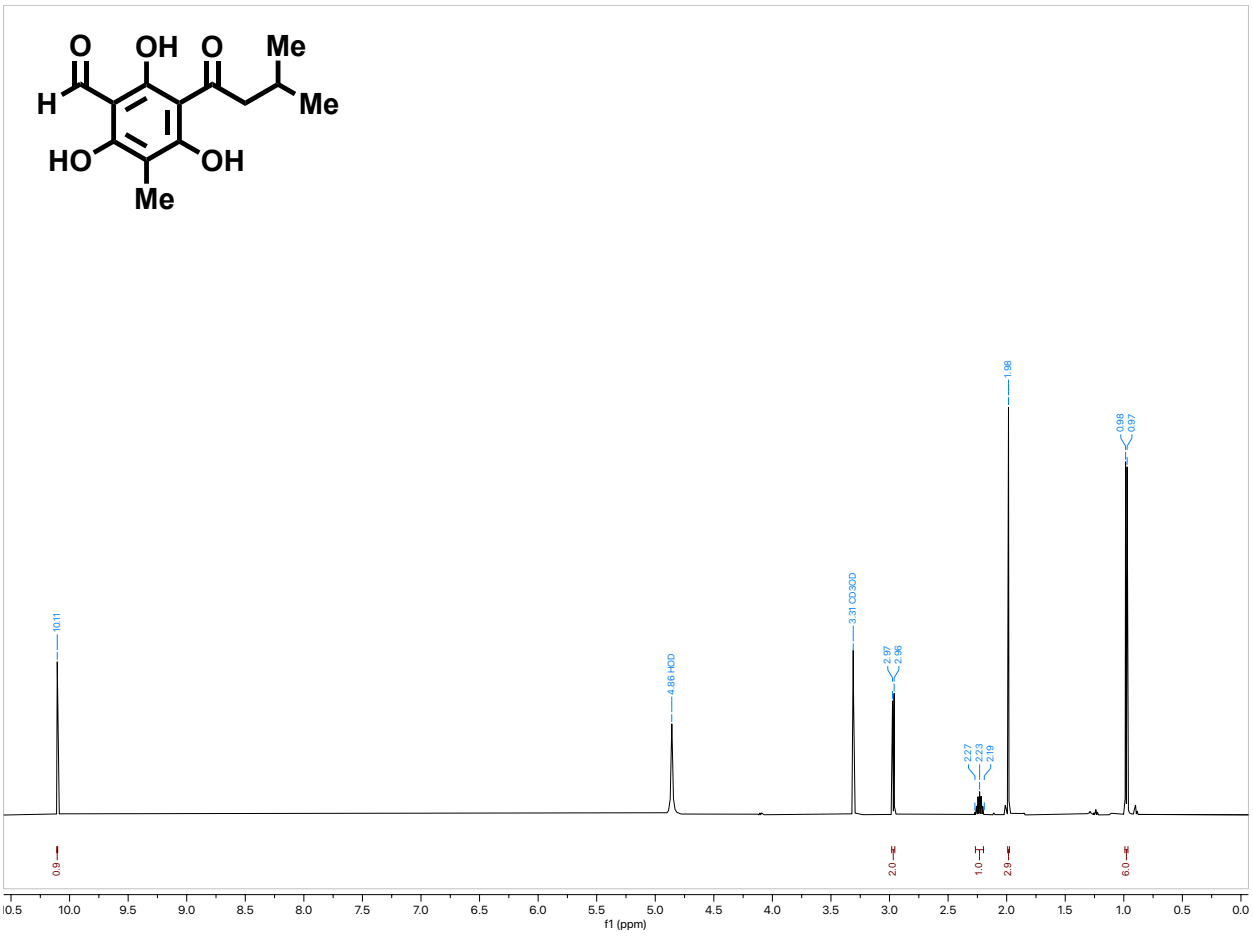

^{13}C-NMR spectrum (126 MHz) of **grandinol** in CD_3OD

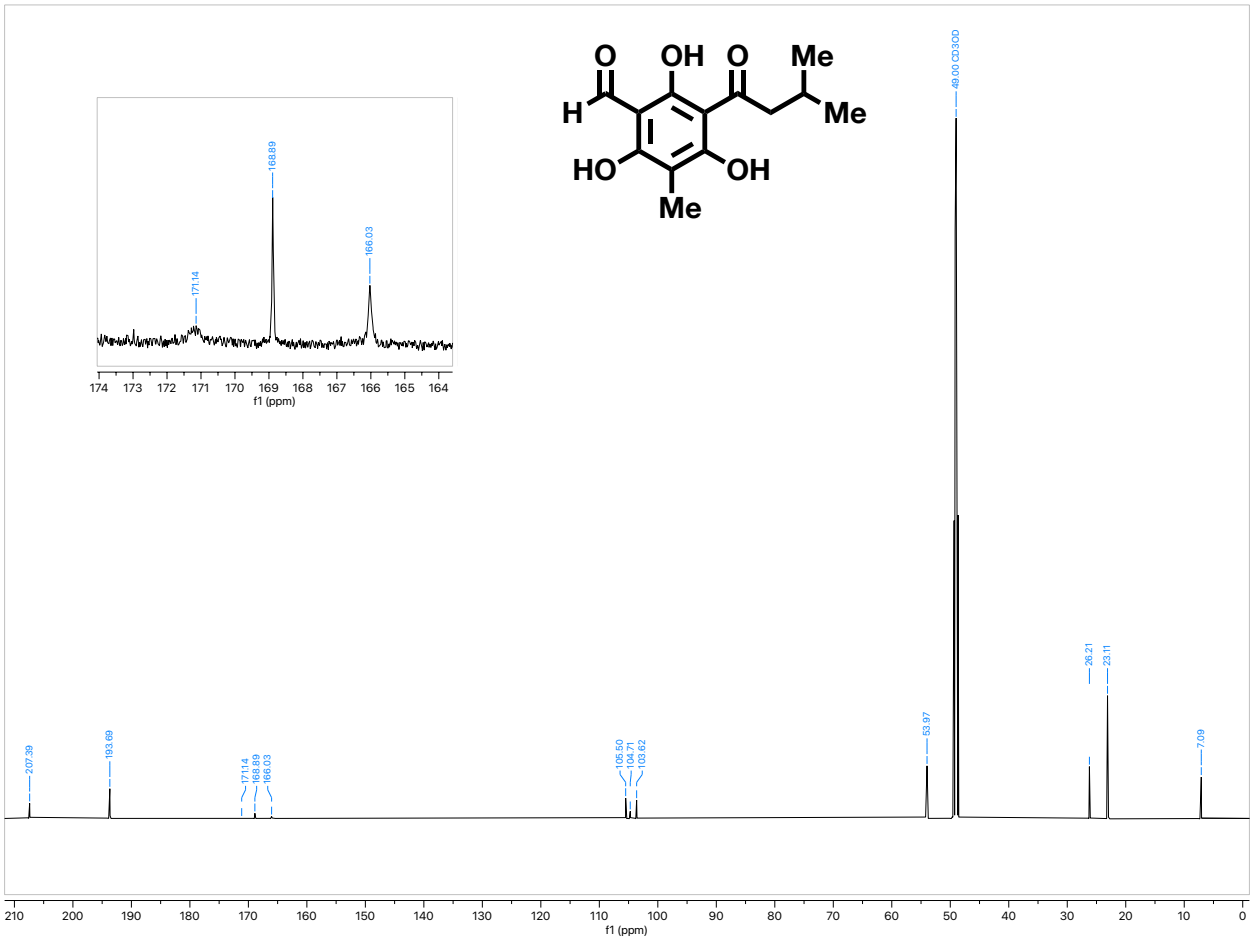

^{1}H-NMR spectrum (500 MHz) of **euglobal G1** in $CDCl_3$

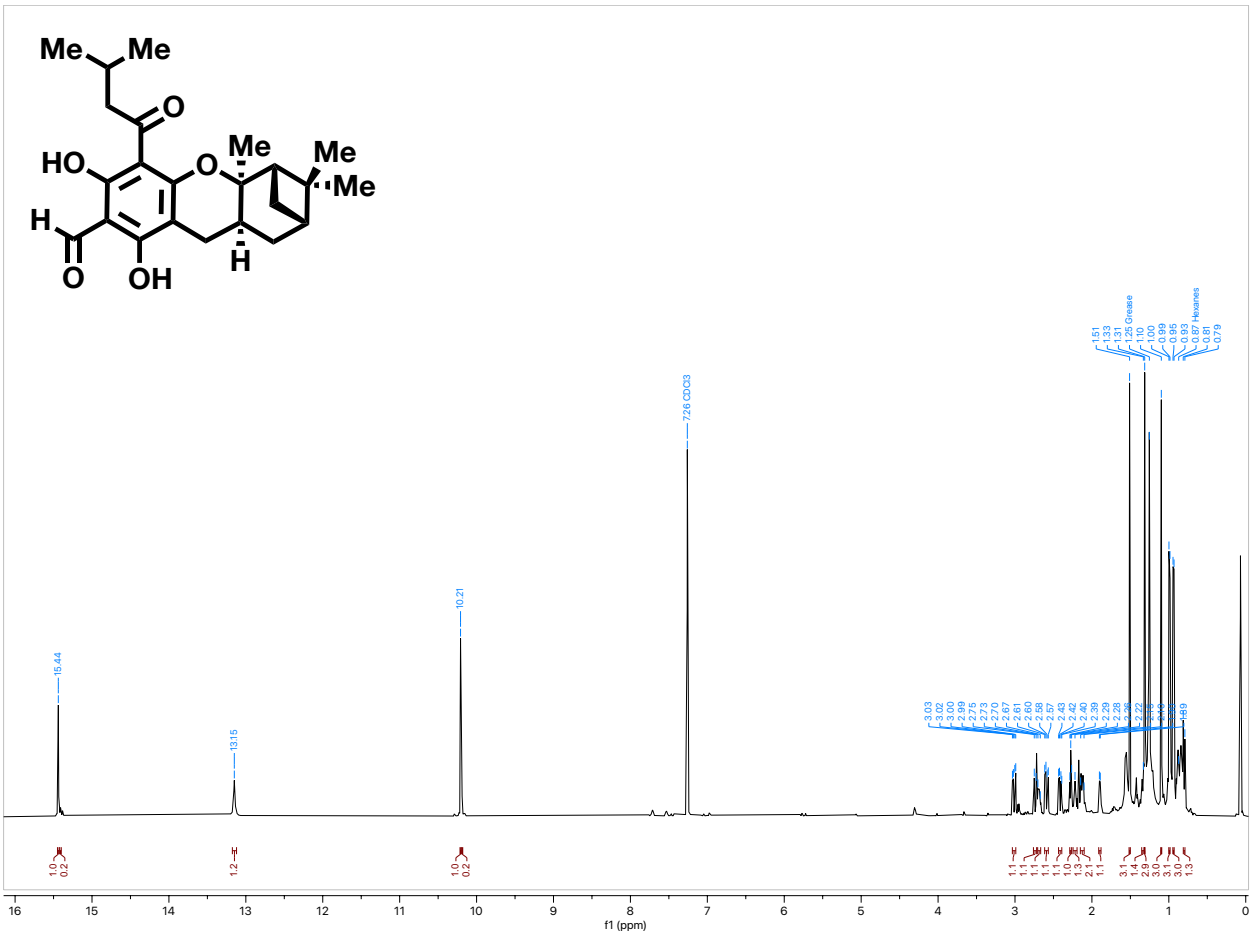

^{13}C-NMR spectrum (126 MHz) of **euglobal G1** in $CDCl_3$

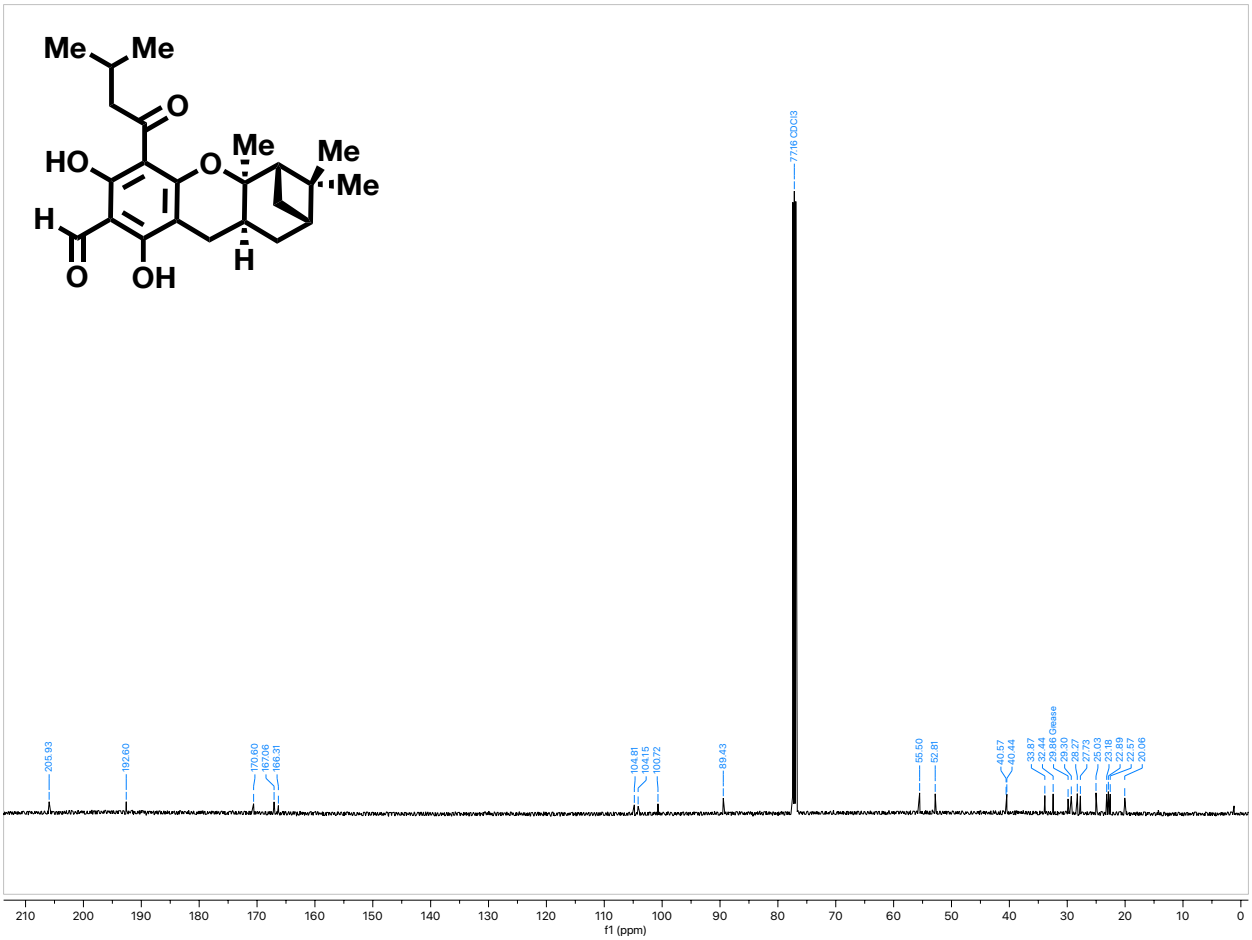

^{1}H-NMR spectrum (500 MHz) of **(+)-euglobal G2** in $CDCl_3$

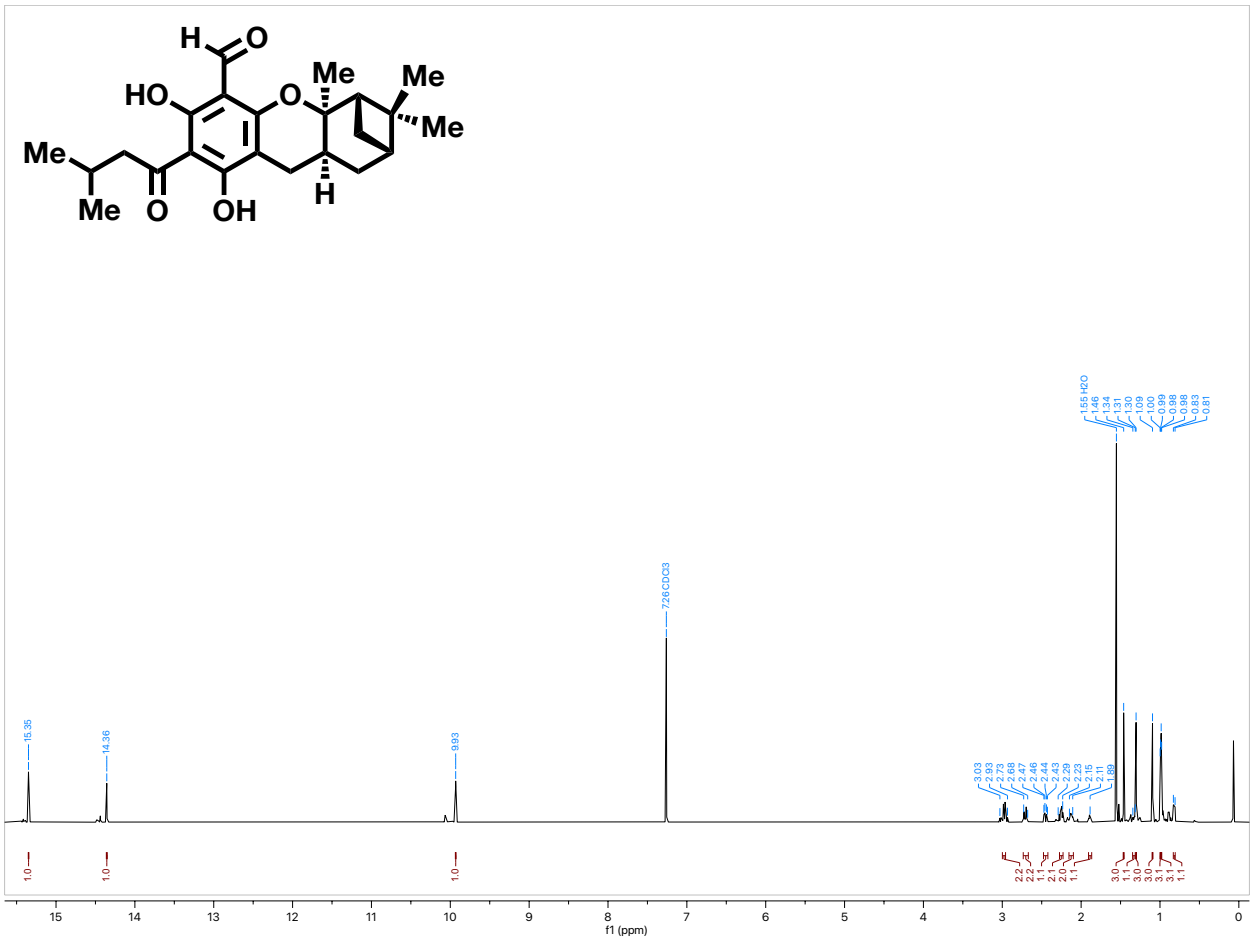

^{13}C-NMR spectrum (126 MHz) of **(+)-euglobal G2** in $CDCl_3$

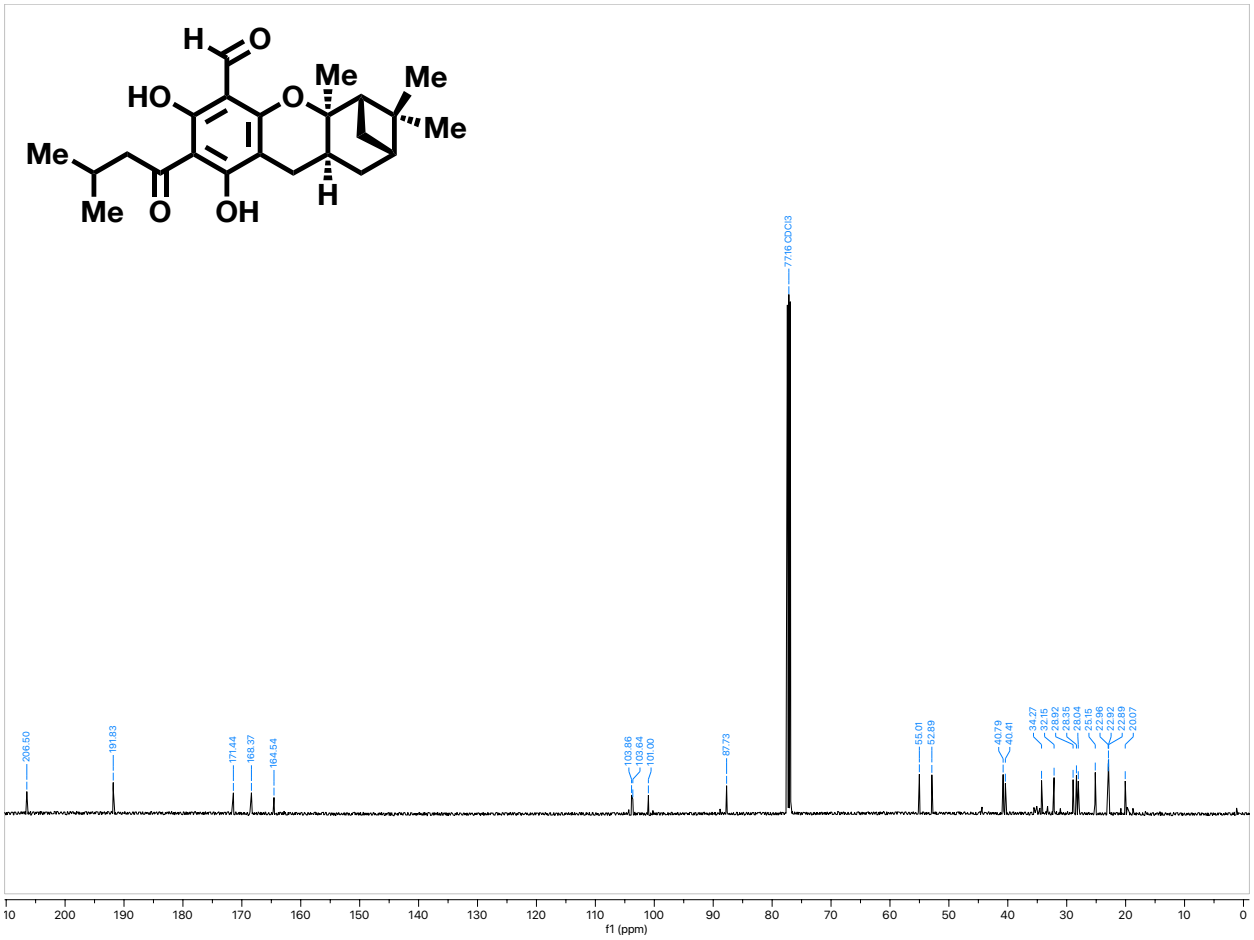

^{1}H-NMR spectrum (500 MHz) of **(–)-euglobal G2** in $CDCl_3$

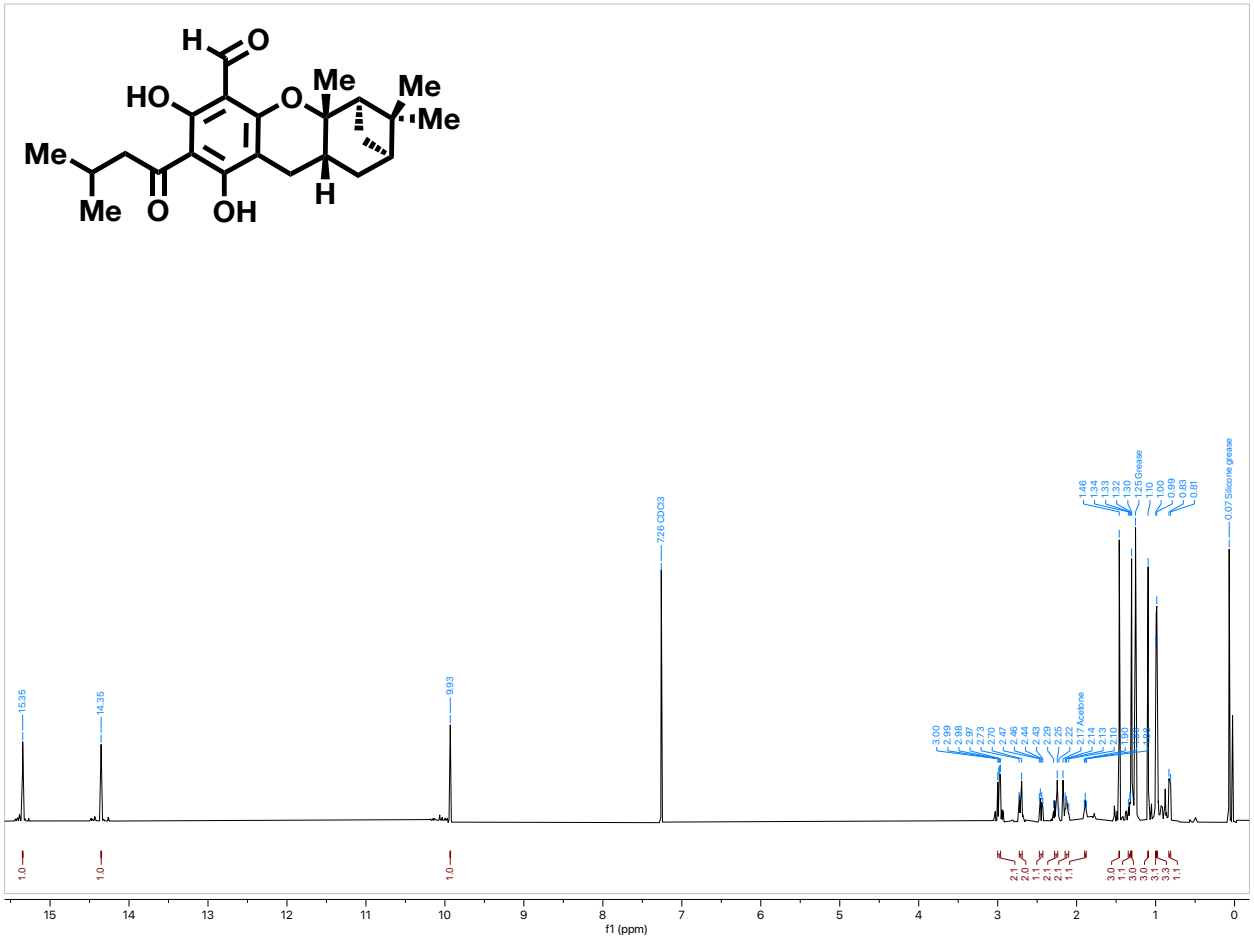

^{13}C-NMR spectrum (126 MHz) of **(–)-euglobal G2** in $CDCl_3$

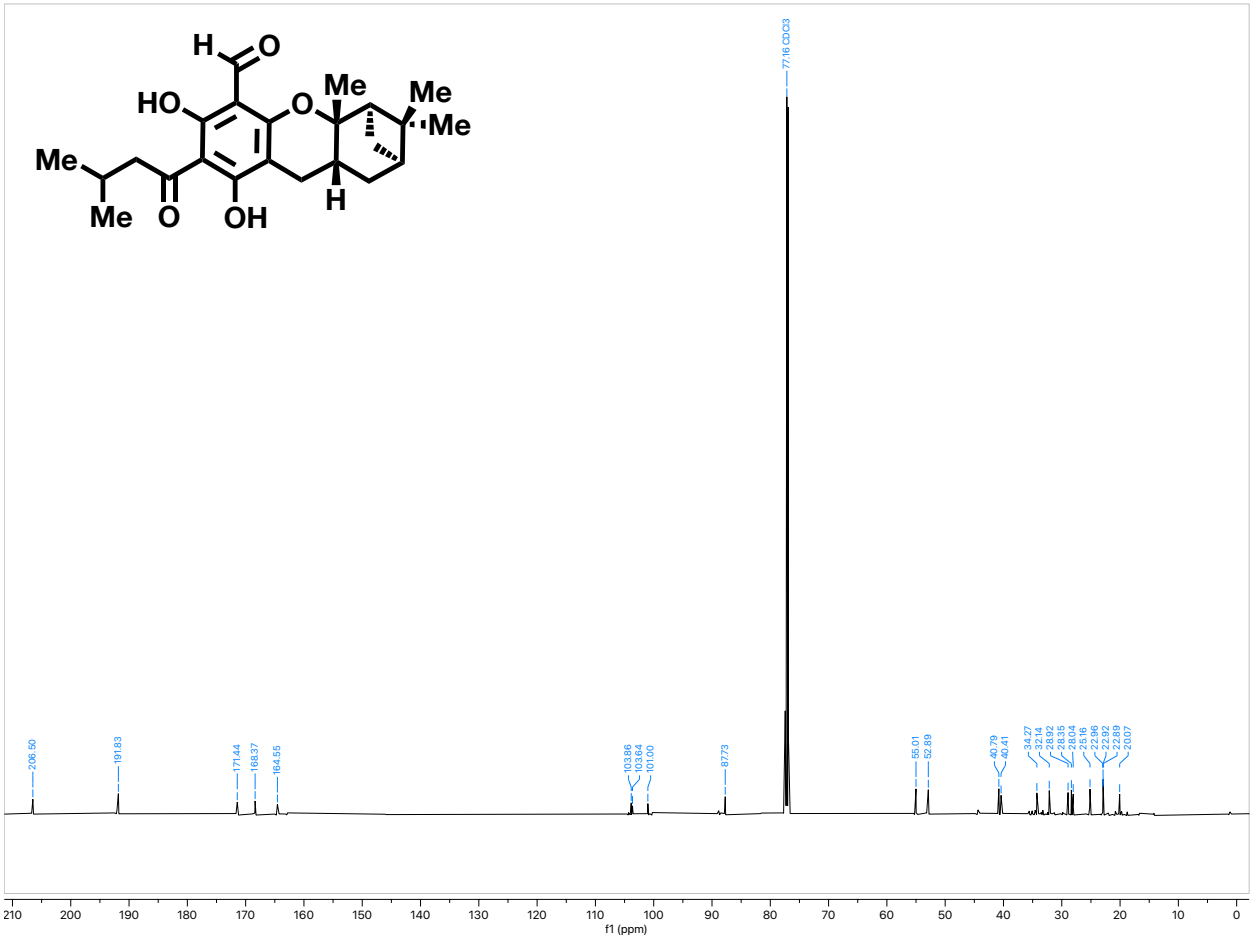

^{1}H-NMR spectrum (500 MHz) of **(–)-euglobal G3** in $CDCl_3$

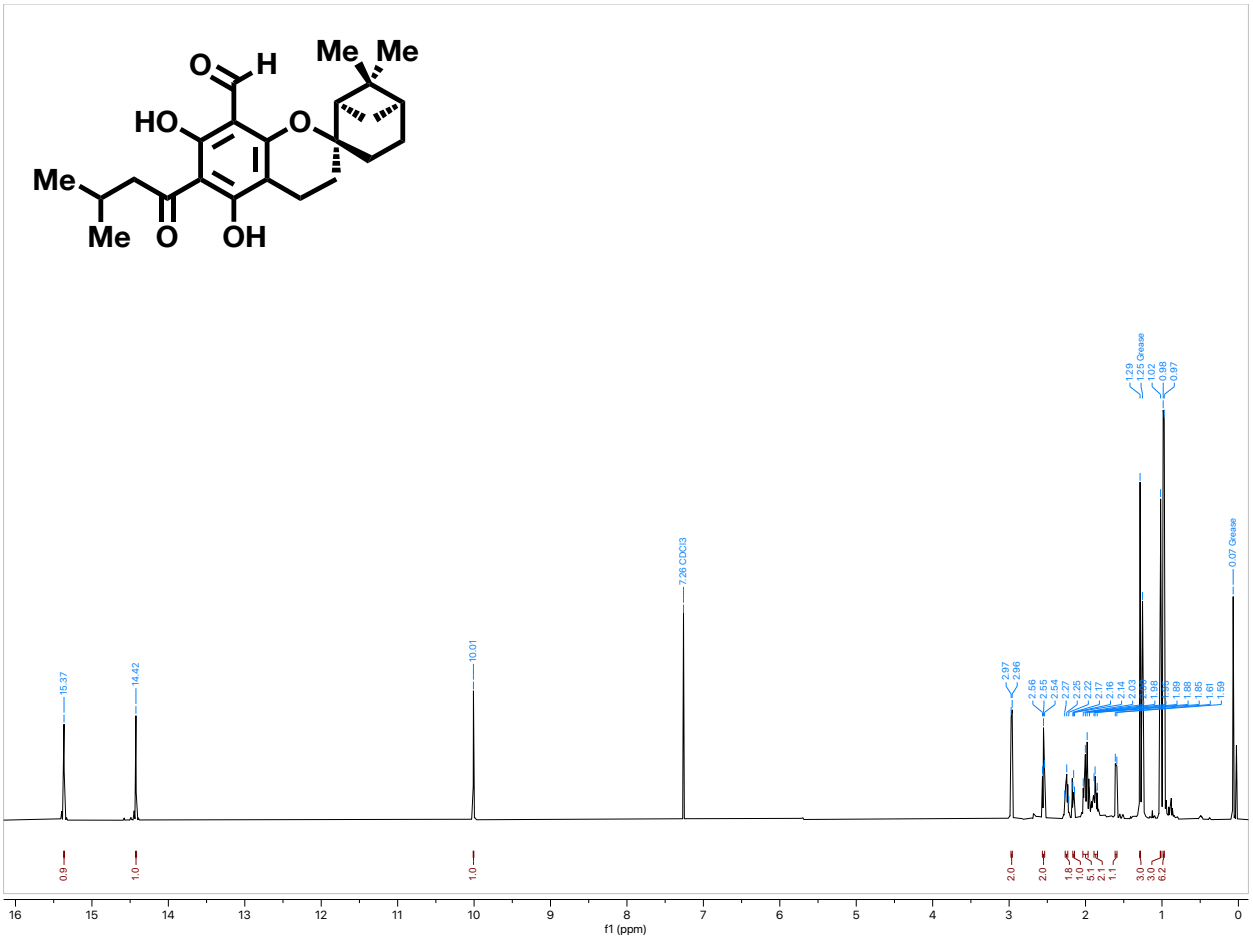

^{13}C-NMR spectrum (126 MHz) of **(–)-euglobal G3** in $CDCl_3$

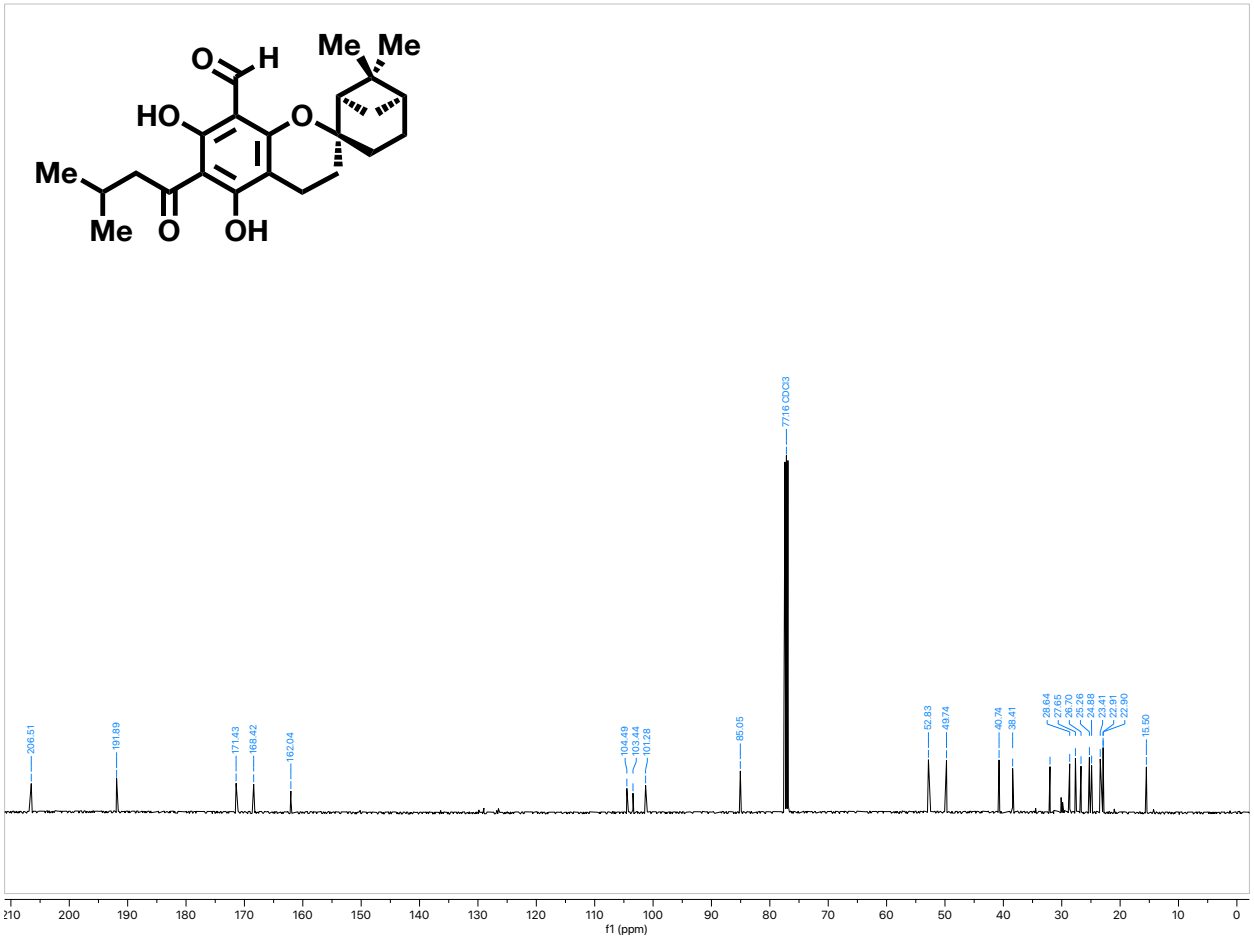

^{1}H-NMR spectrum (500 MHz) of **(–)-euglobal G4** in $CDCl_3$

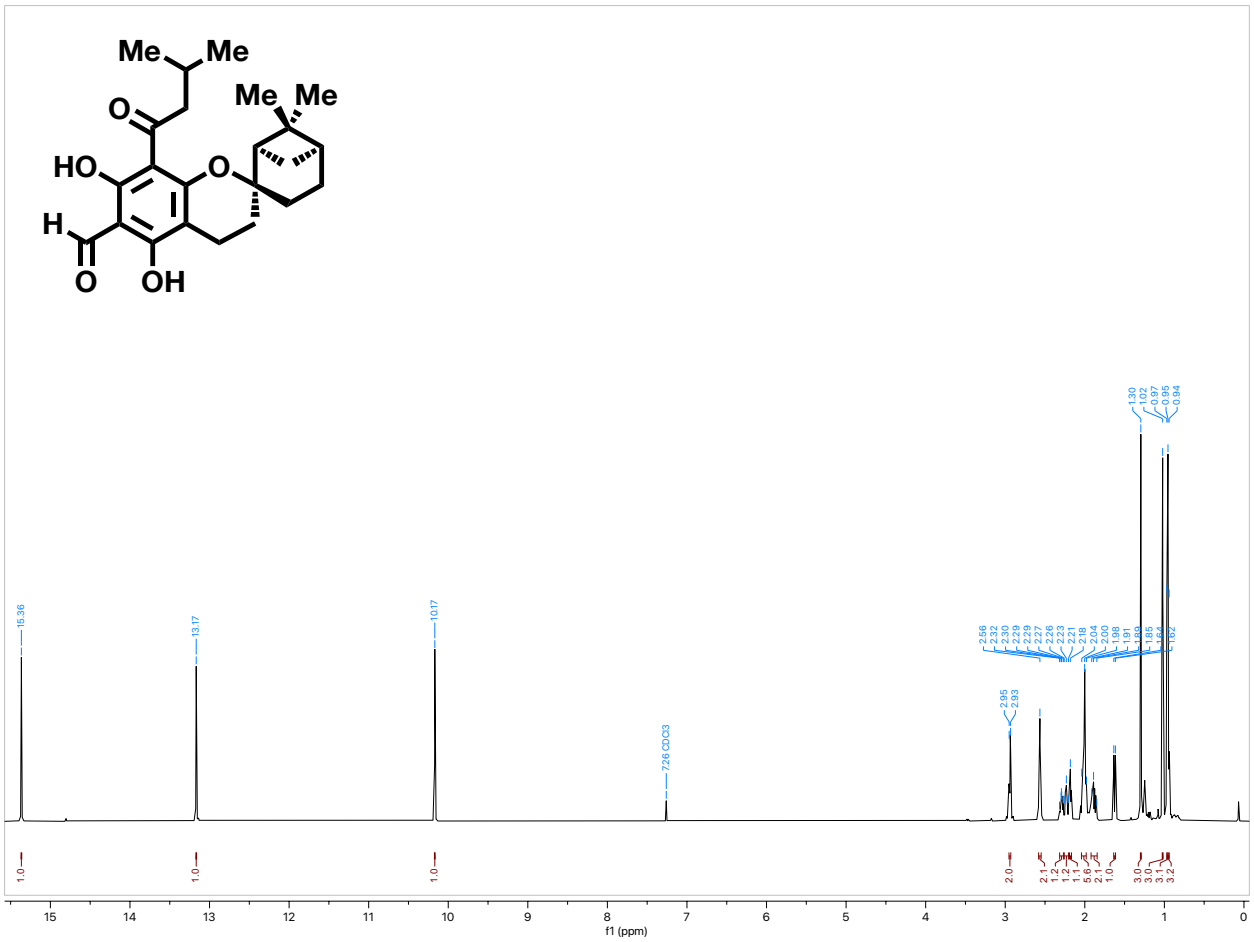

^{13}C-NMR spectrum (126 MHz) of **(–)-euglobal G4** in $CDCl_3$

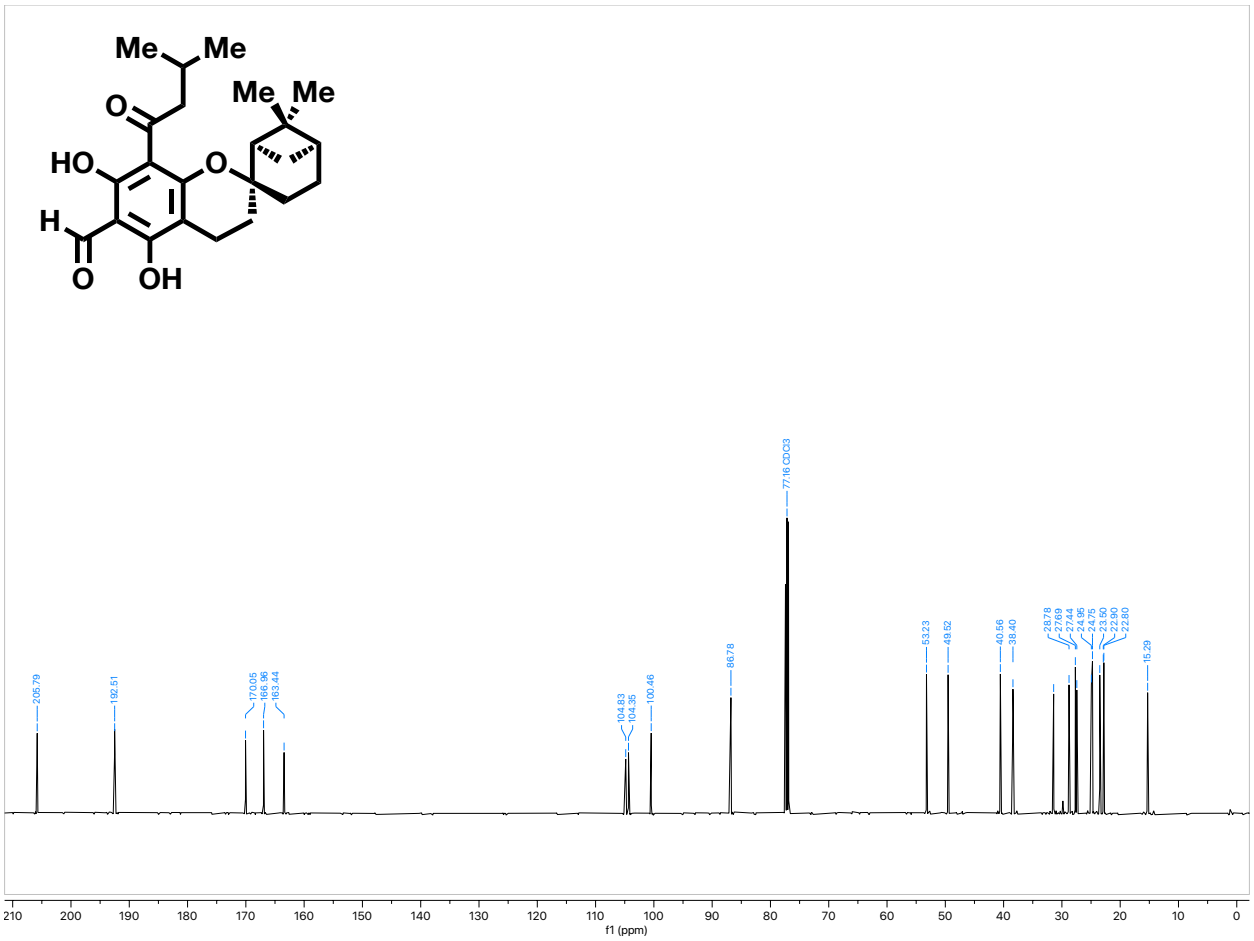

^{1}H-NMR spectrum (500 MHz) of **S4** in CD_3OD

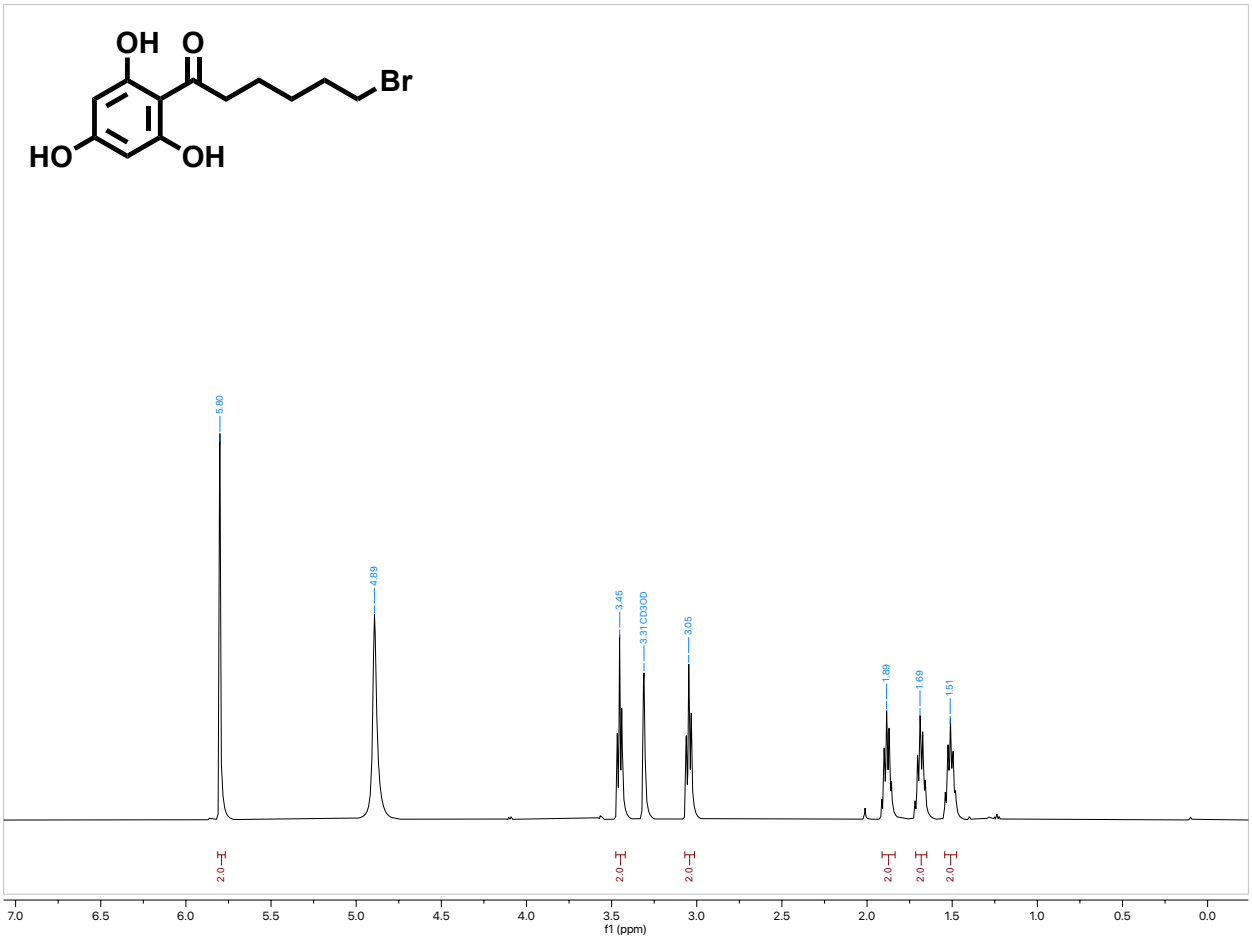

^{13}C-NMR spectrum (126 MHz) of **S4** in CD_3OD

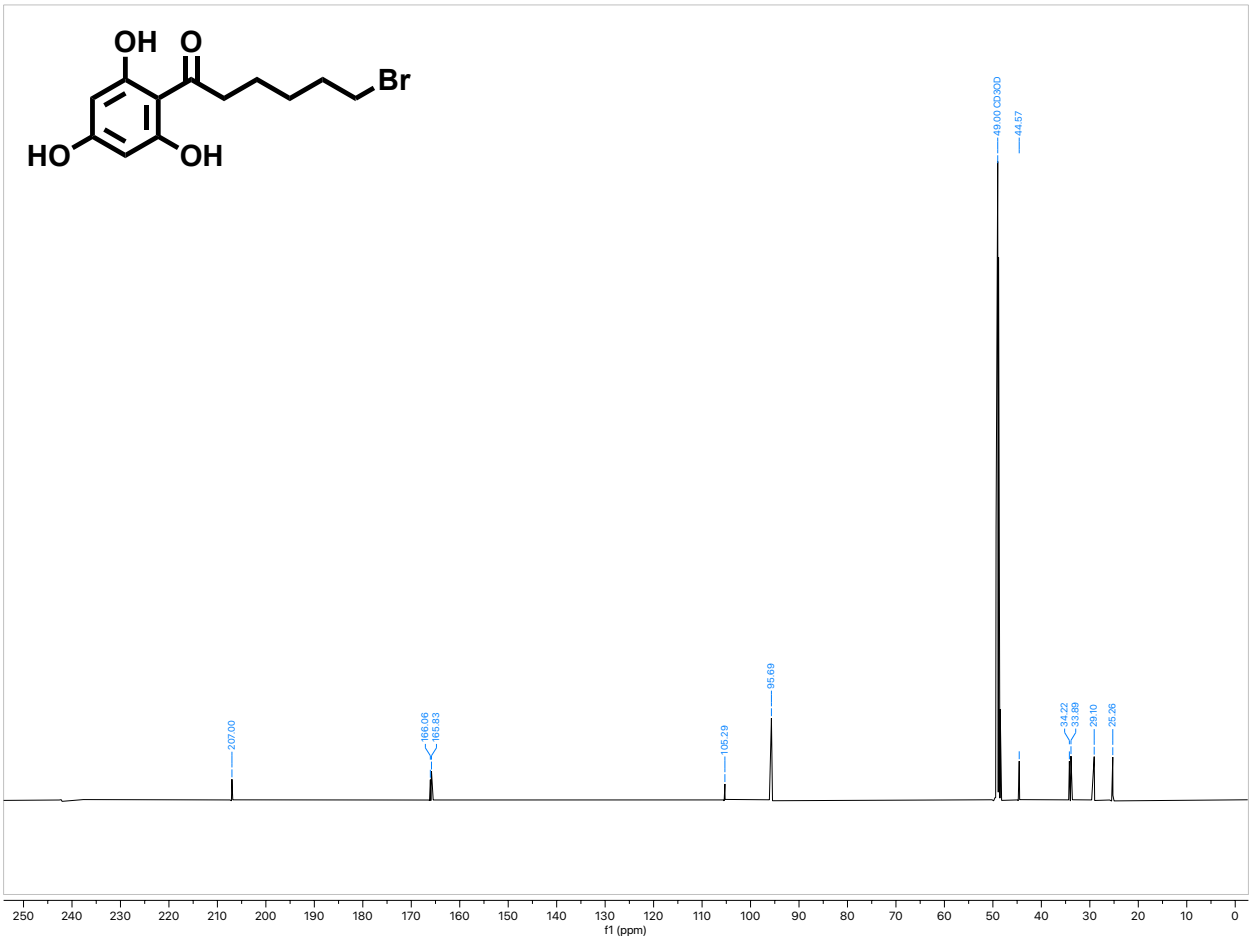

^{1}H-NMR spectrum (500 MHz) of **S5** in CD_3OD

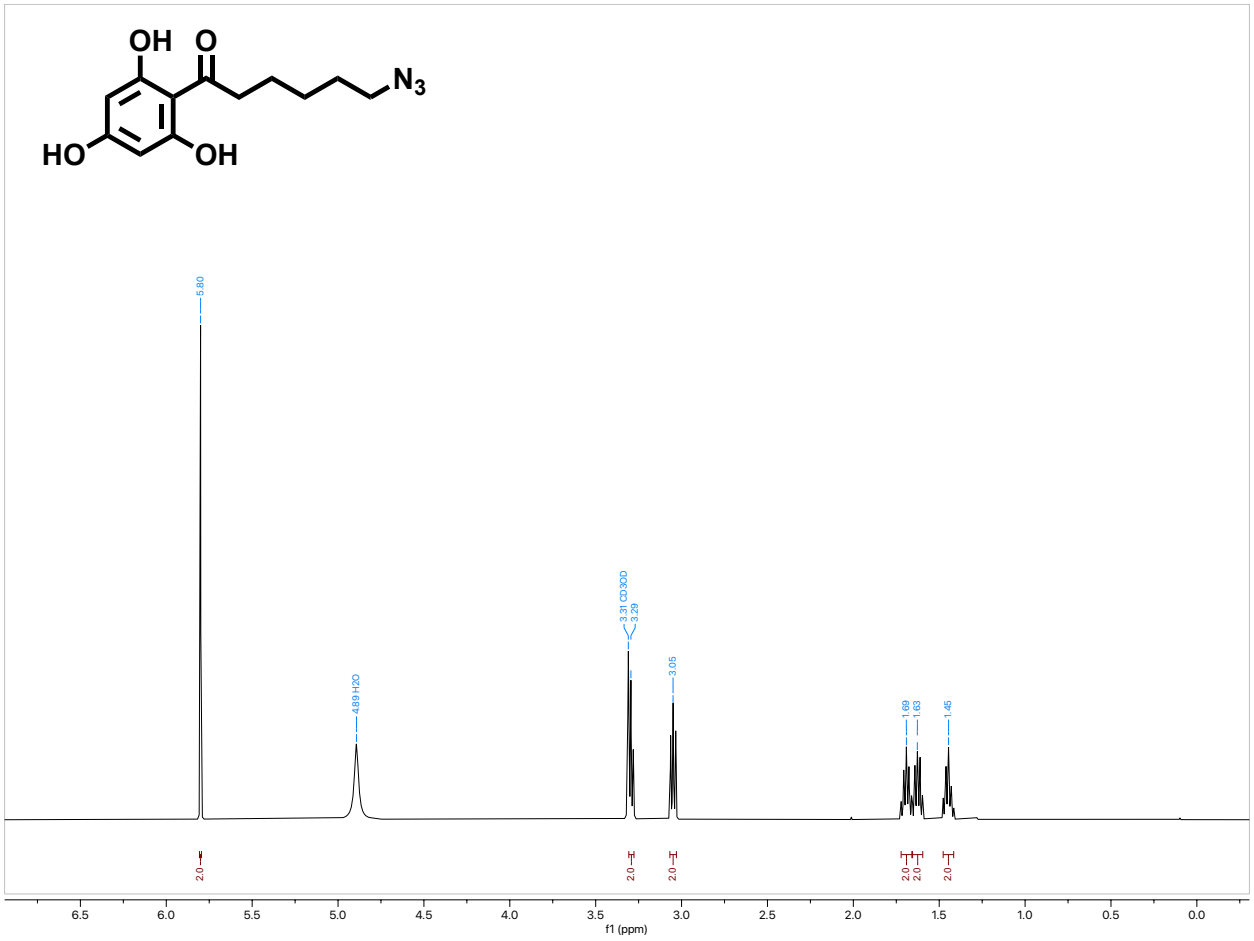

^{13}C-NMR spectrum (126 MHz) of **S5** in CD_3OD

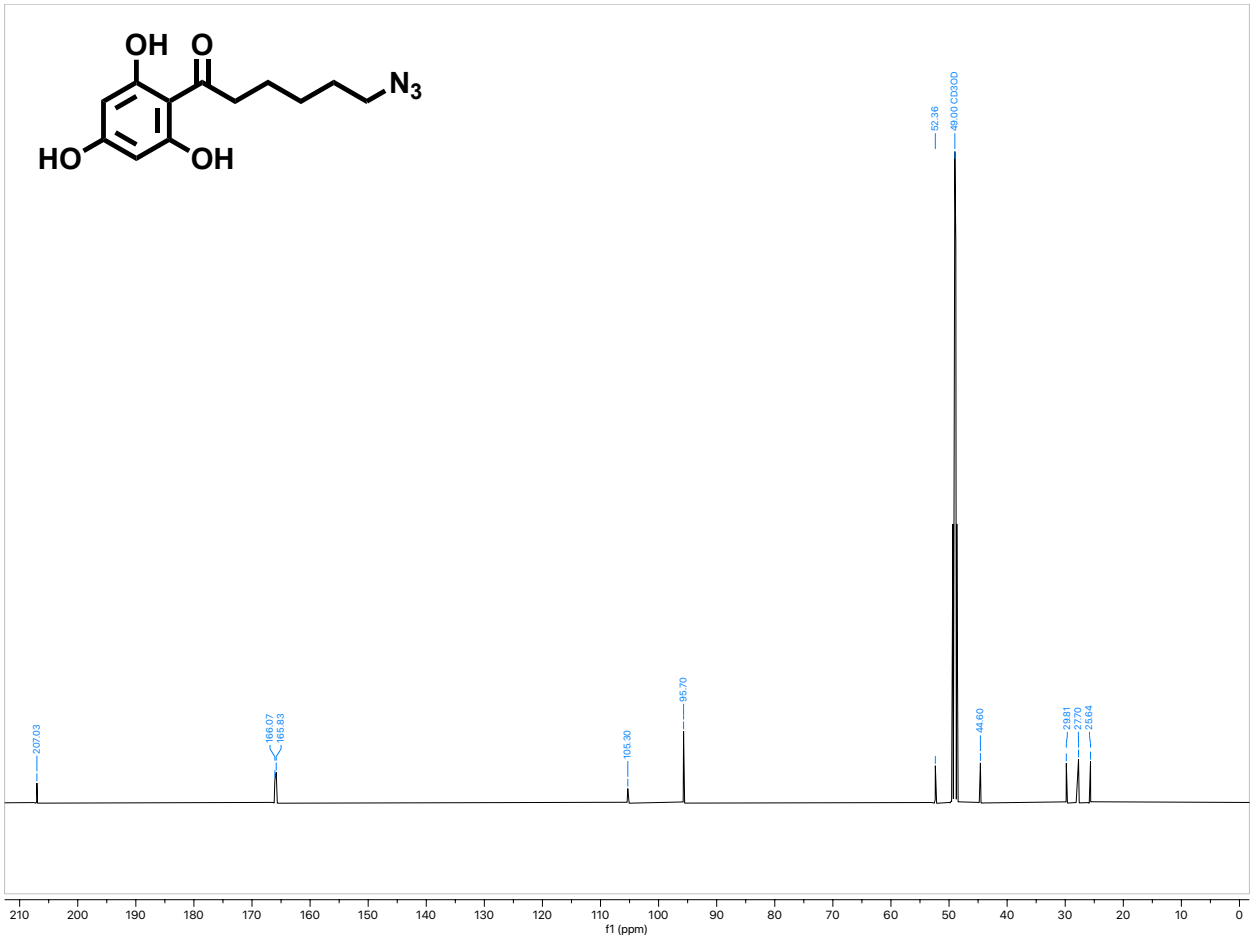

^{1}H-NMR spectrum (500 MHz) of **S6** in CD_3OD

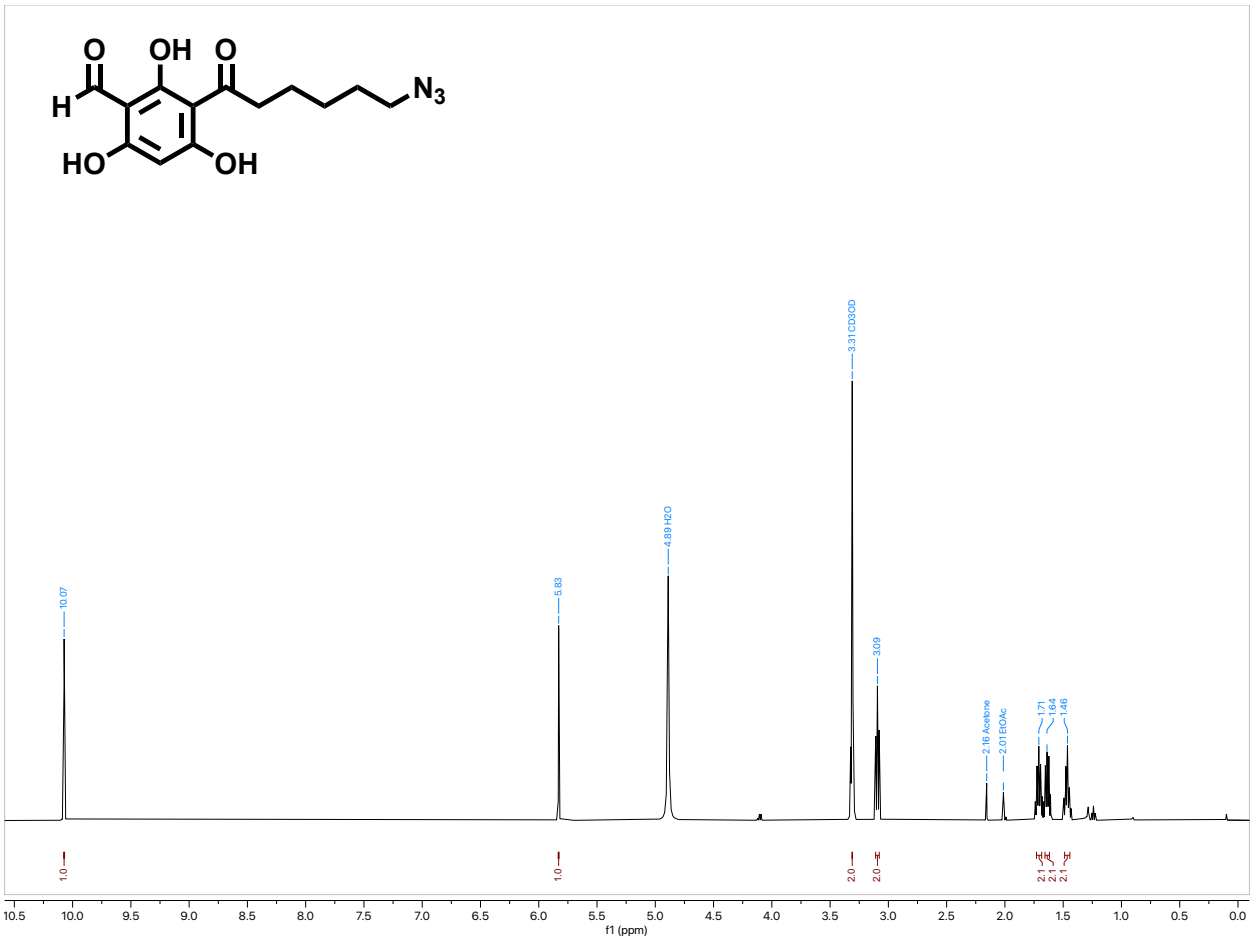

^{13}C-NMR spectrum (126 MHz) of **S6** in CD_3OD

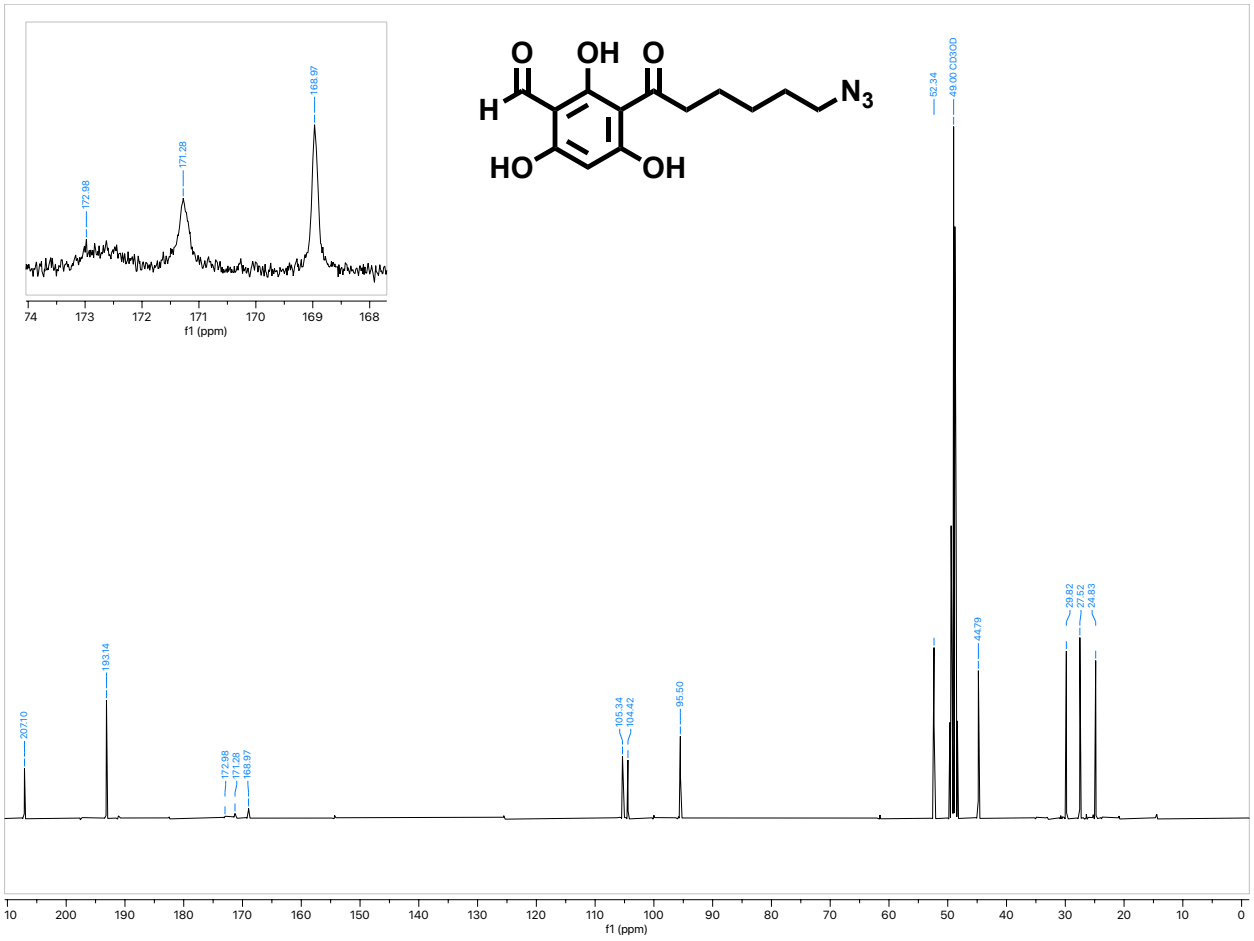

^{1}H-NMR spectrum (500 MHz) of **S7** in CD_3OD

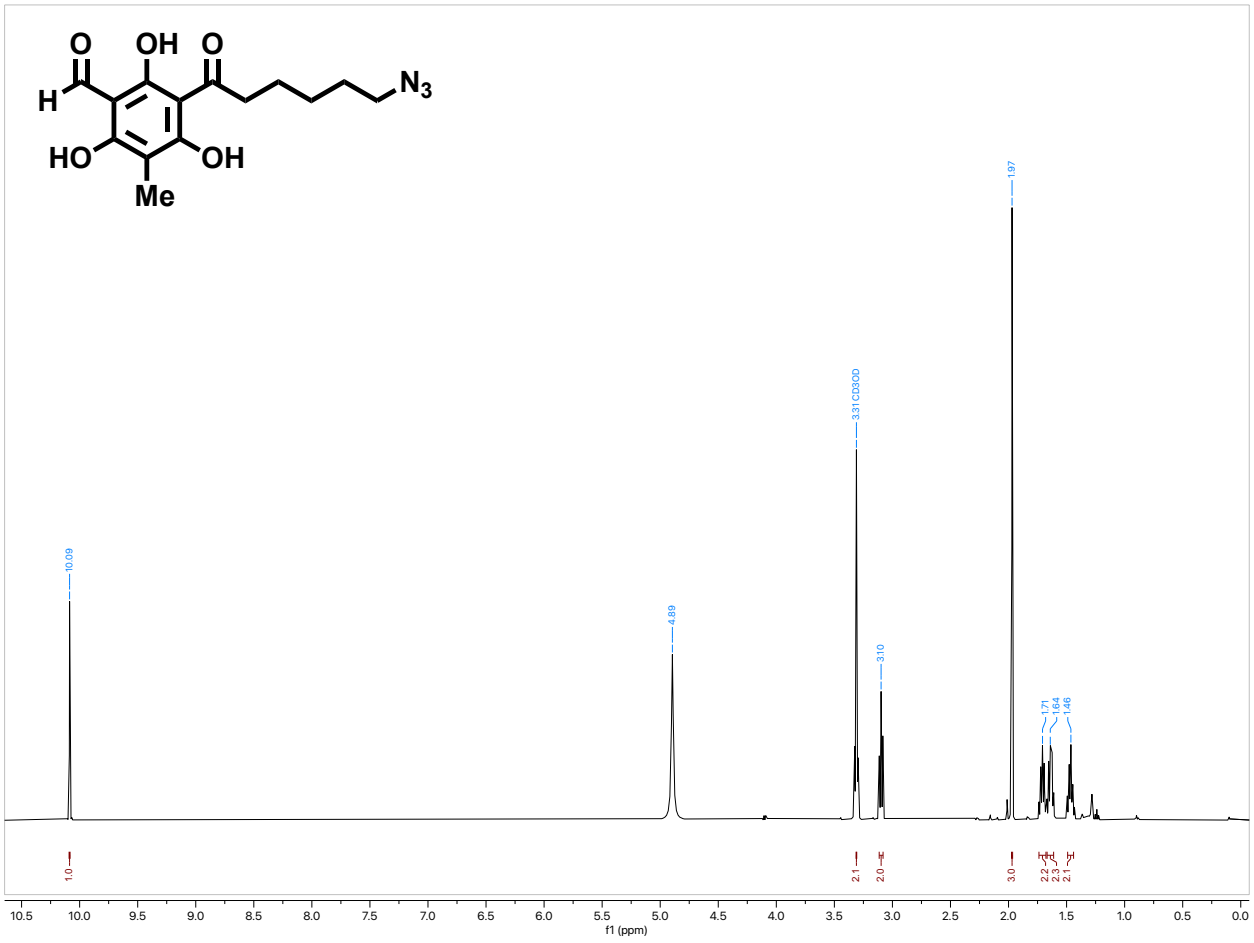

^{13}C-NMR spectrum (126 MHz) of **S7** in CD_3OD

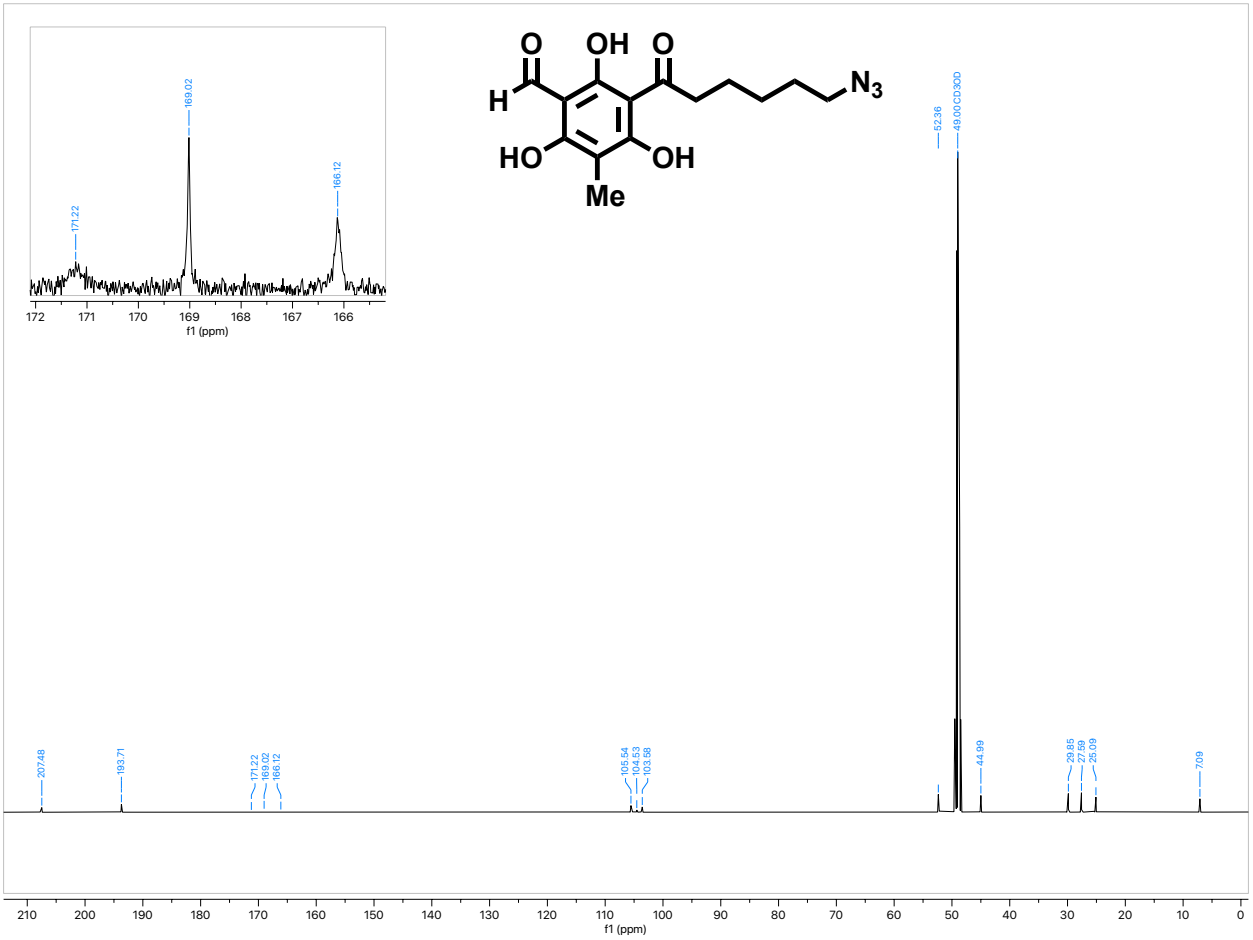

^{1}H-NMR spectrum (500 MHz) of **(+)-9** in $CDCl_3$

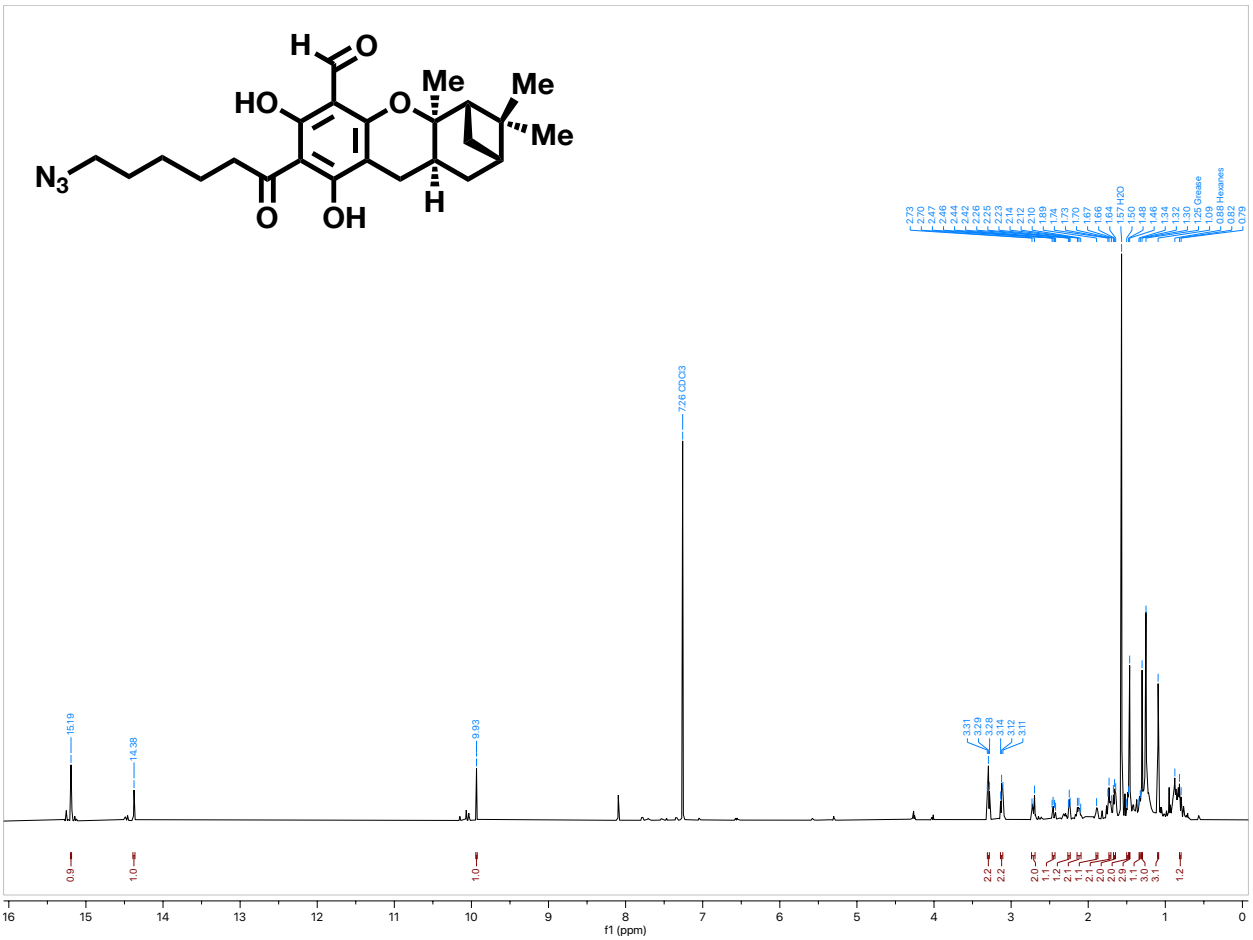

^{13}C-NMR spectrum (126 MHz) of **(+)-9** in $CDCl_3$

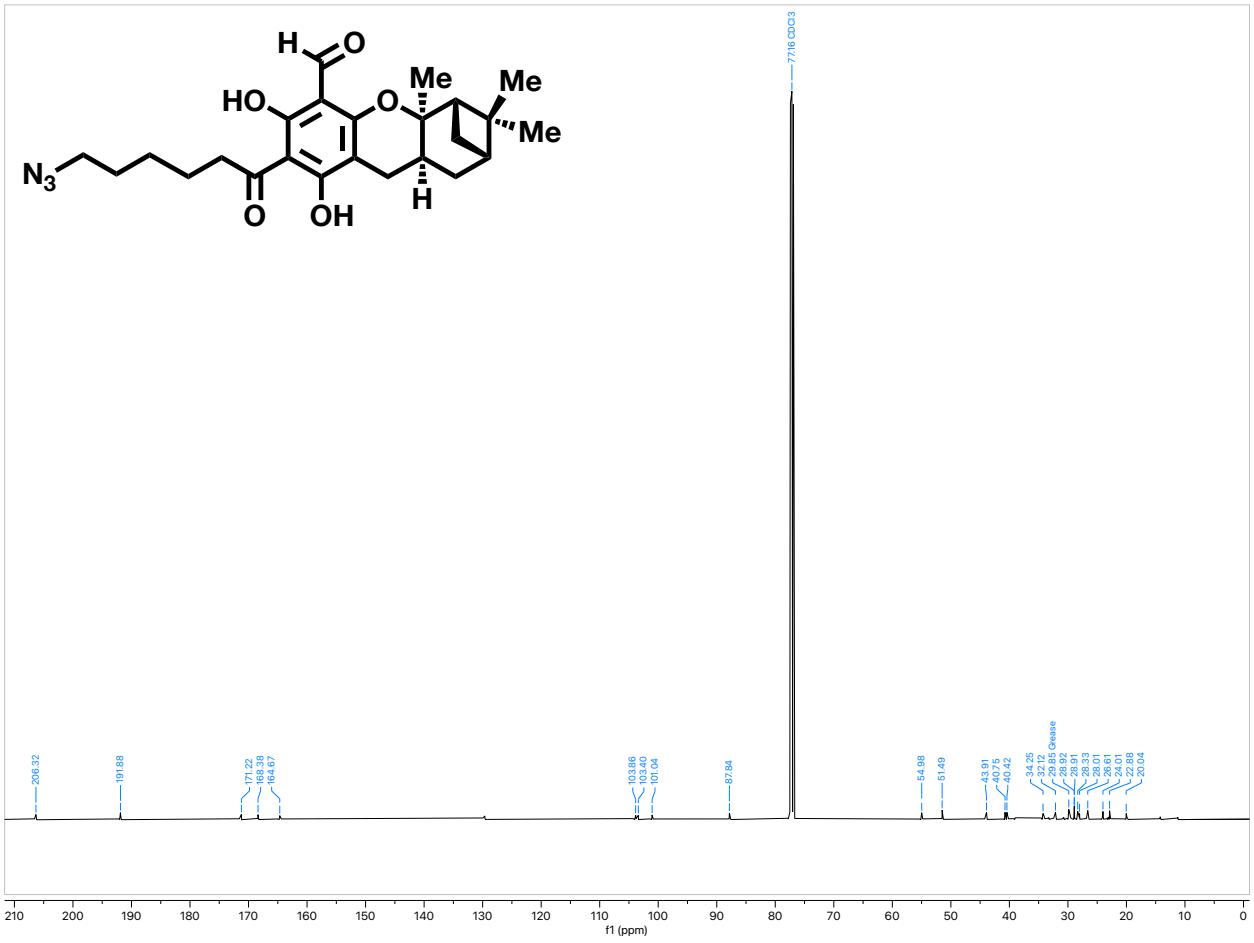

^{1}H-NMR spectrum (500 MHz) of **(–)-9** in $CDCl_3$

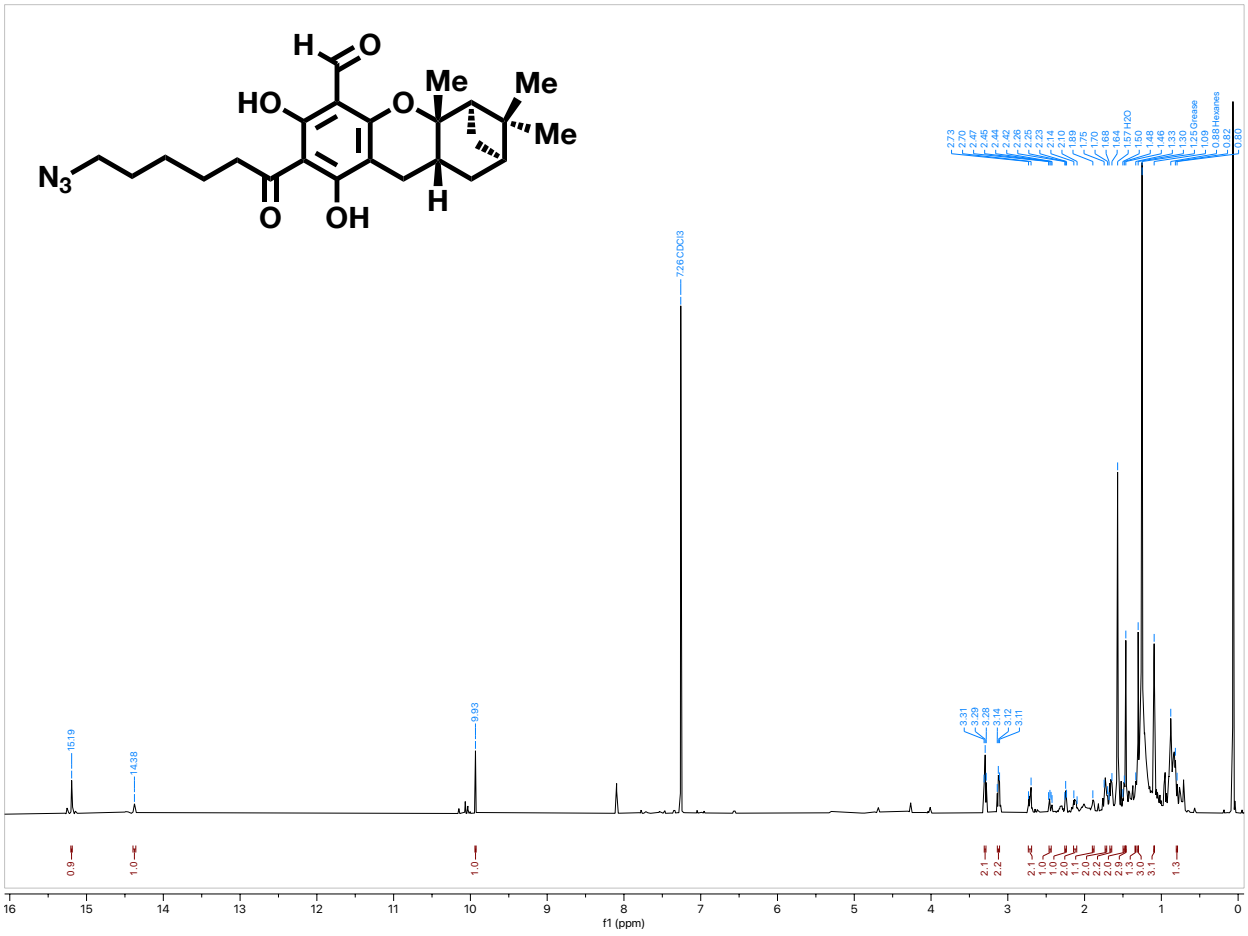

^{13}C-NMR spectrum (126 MHz) of **(–)-9** in $CDCl_3$

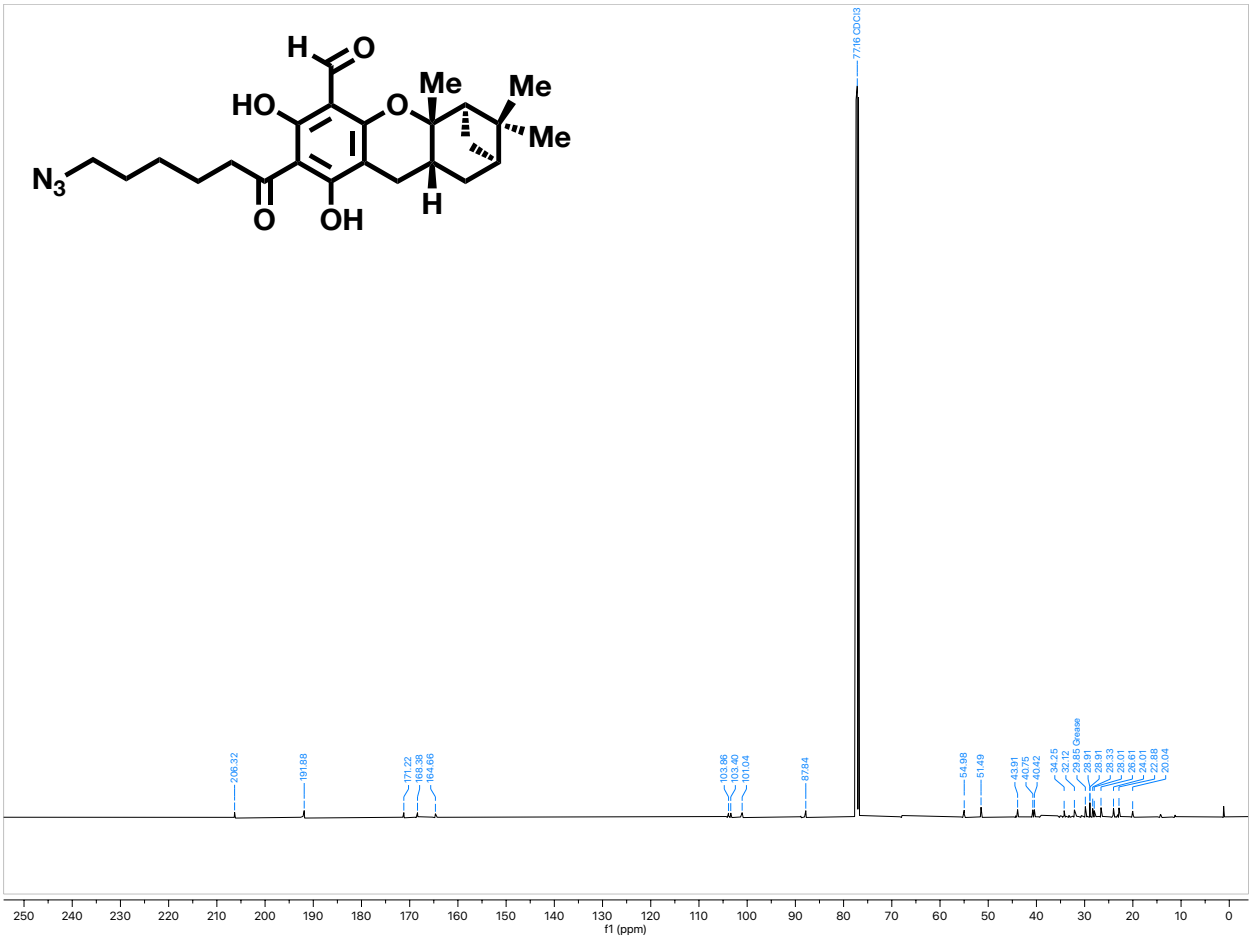

^{1}H-NMR spectrum (500 MHz) of **(–)-10** in $CDCl_3$

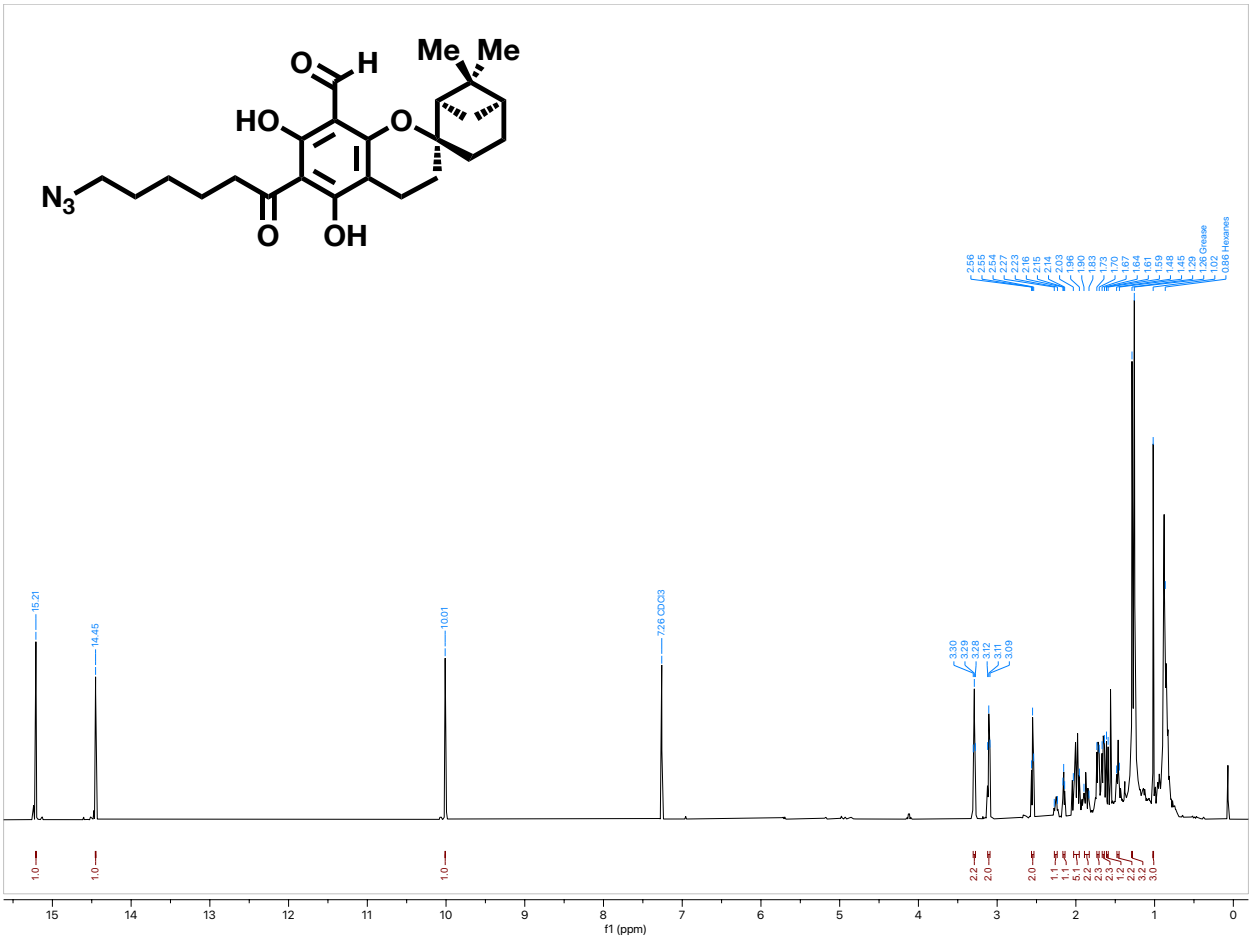

^{13}C-NMR spectrum (126 MHz) of **(–)-10** in $CDCl_3$

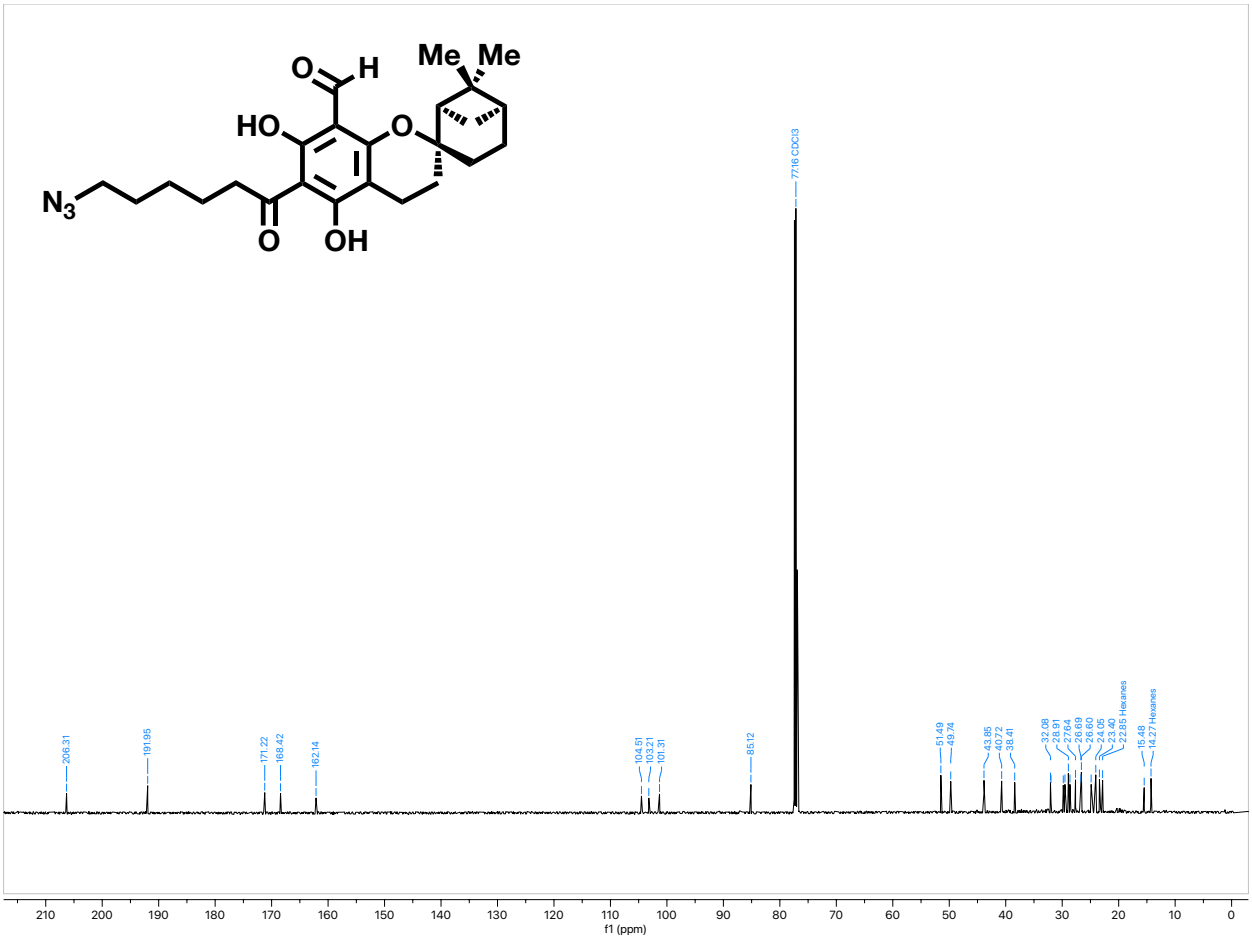

^{1}H-NMR spectrum (500 MHz) of **(–)-11** in $CDCl_3$

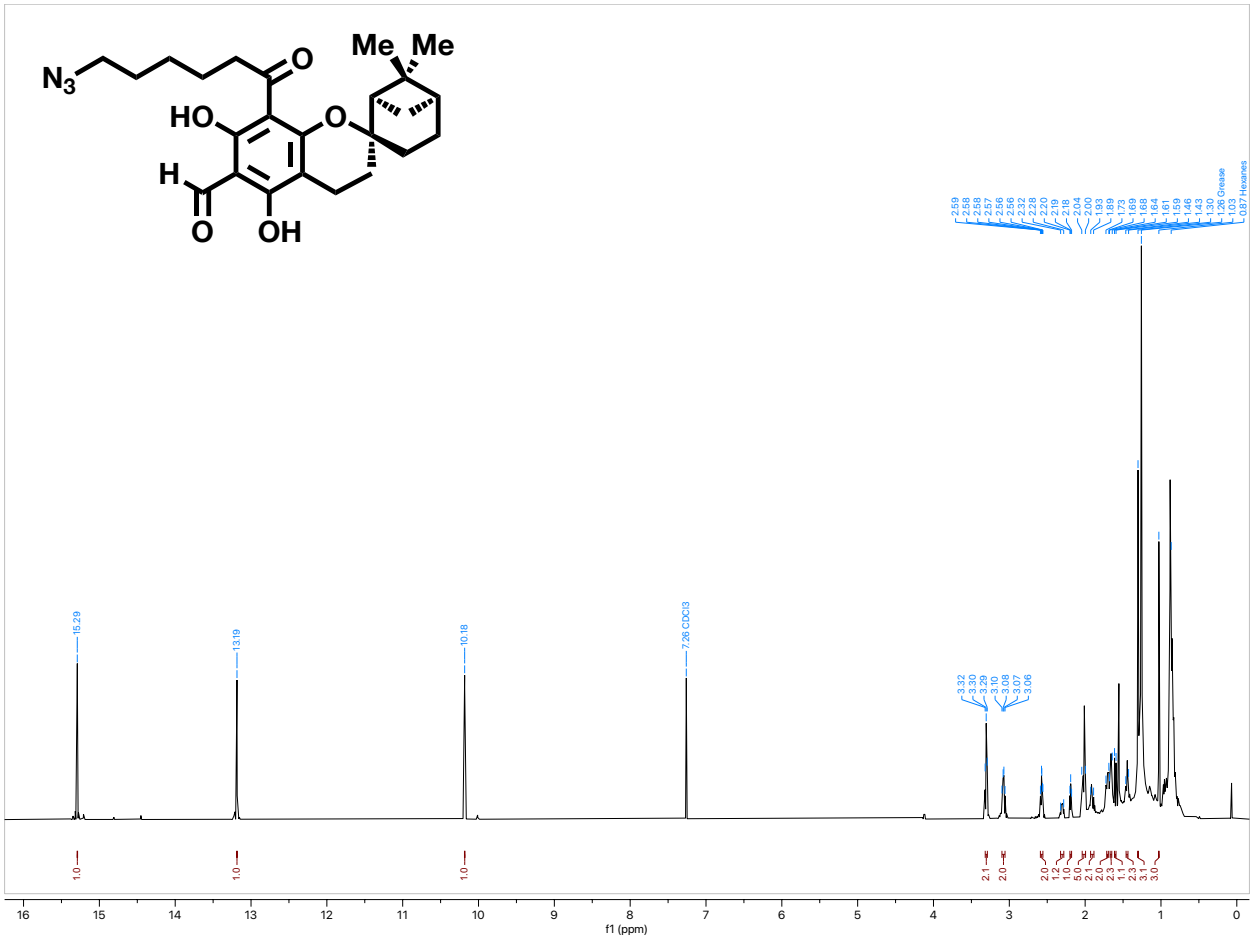

^{13}C-NMR spectrum (126 MHz) of **(–)-11** in $CDCl_3$

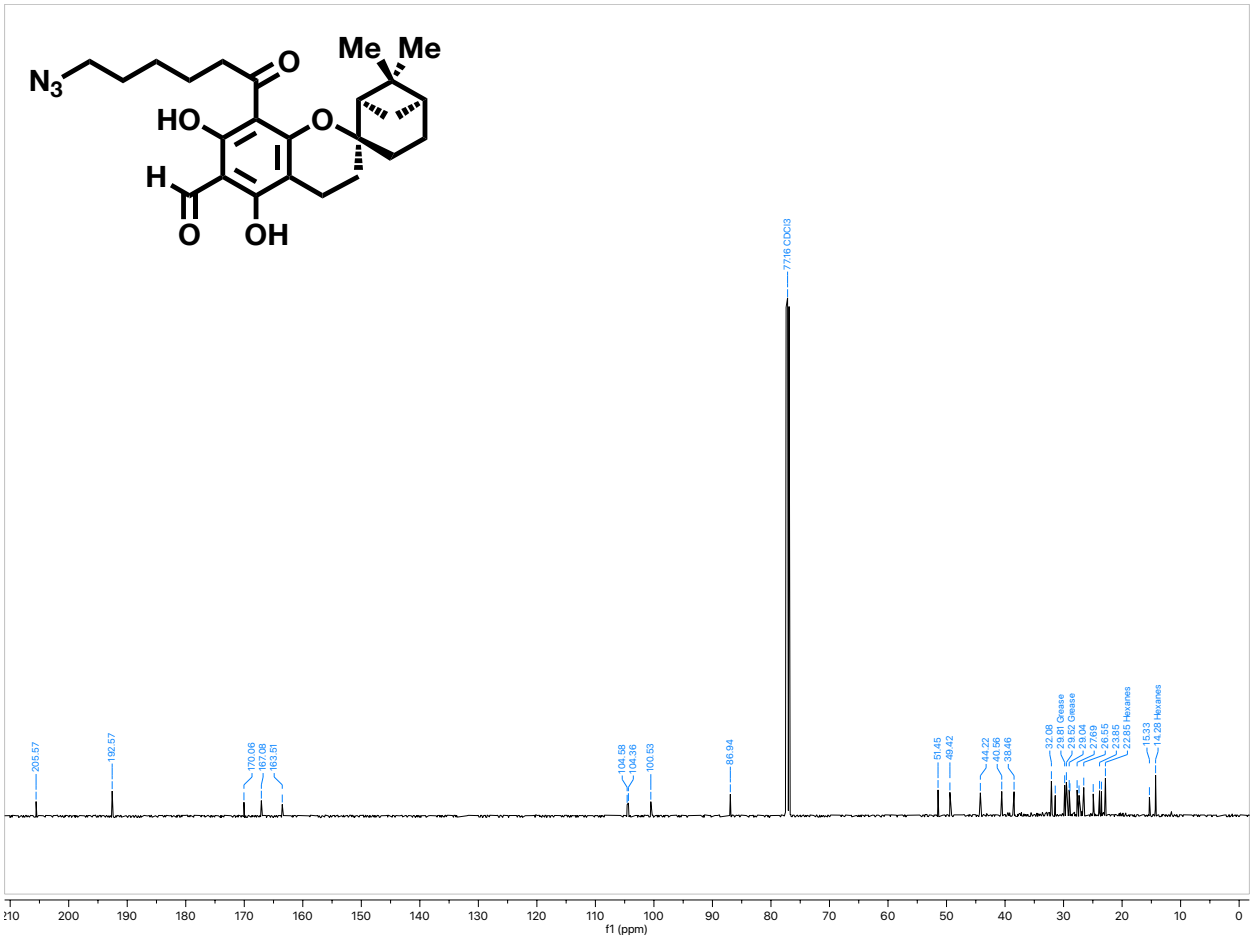

^{1}H-NMR spectrum (500 MHz) of **7** in CD_3OD

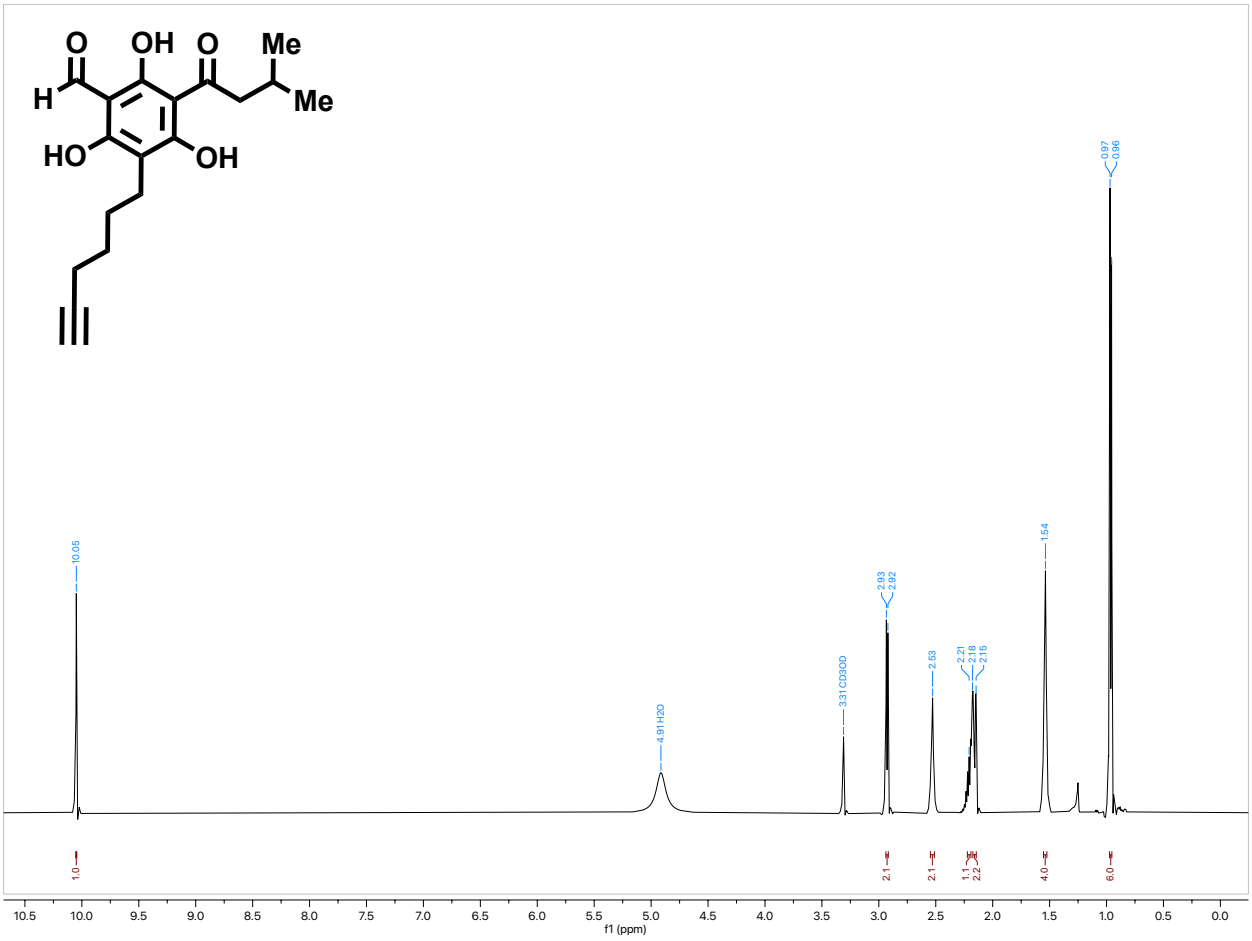

^{13}C-NMR spectrum (126 MHz) of **7** in CD_3OD

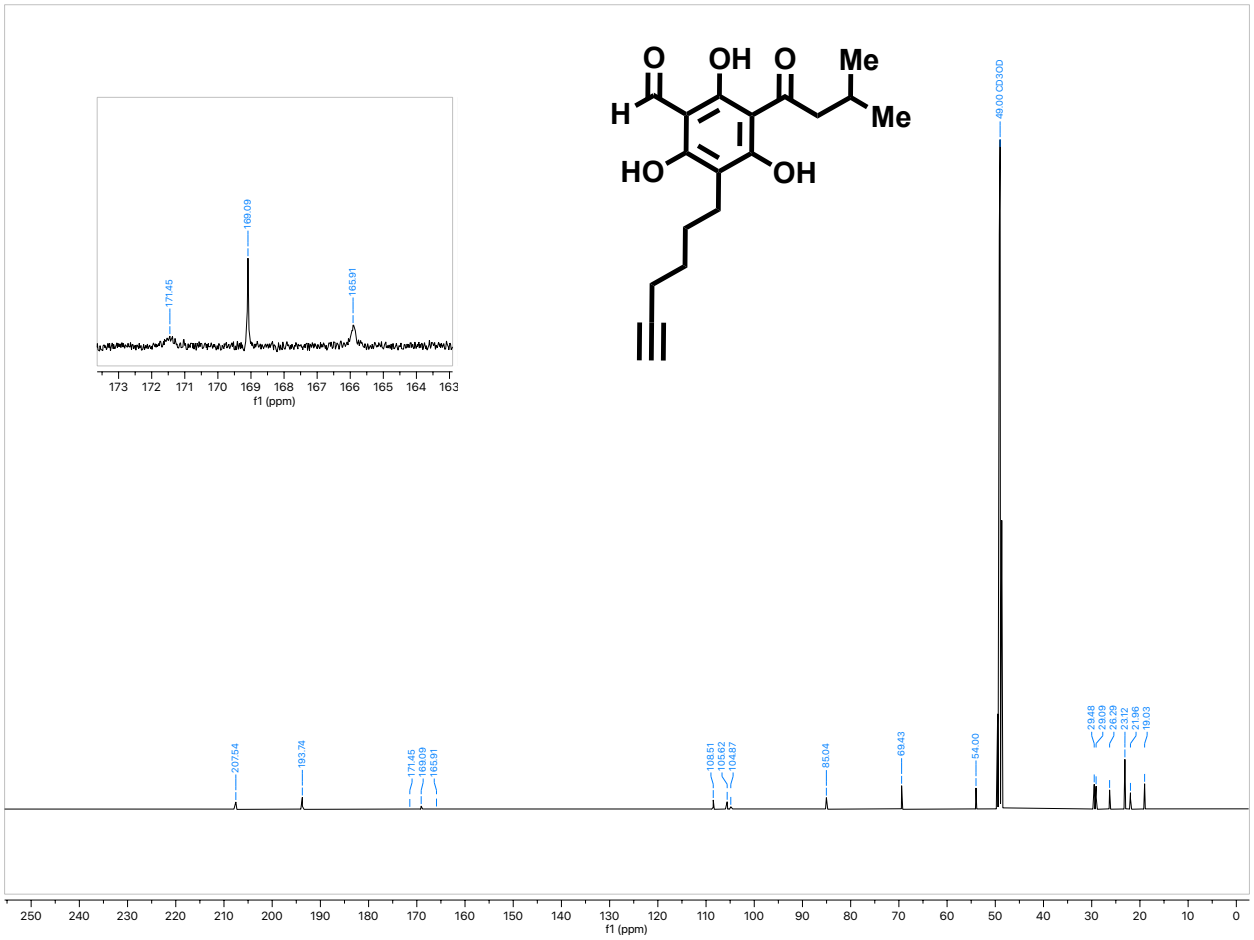

^{1}H-NMR spectrum (500 MHz) of **S14** in DMSO-d_6

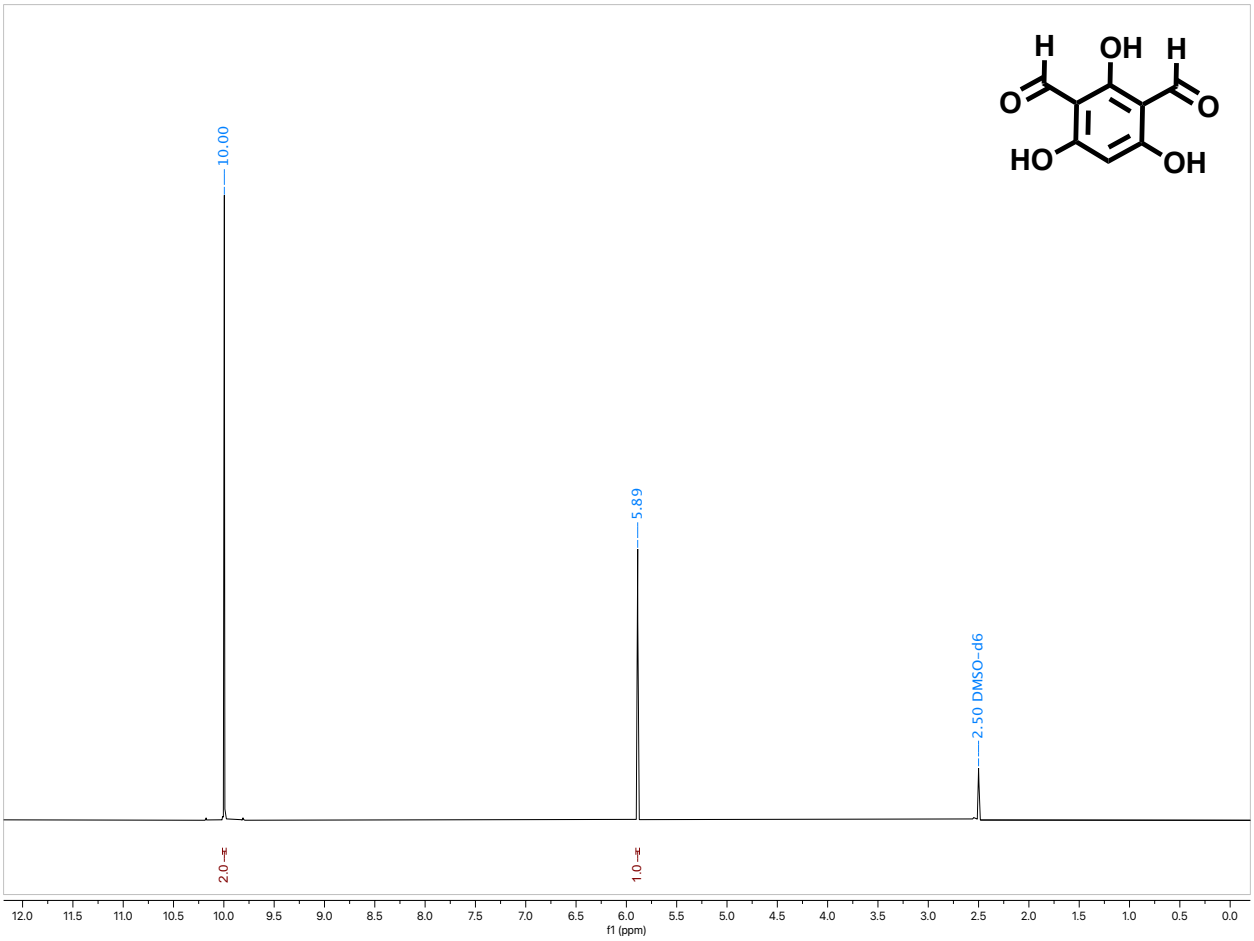

^{13}C-NMR spectrum (126 MHz) of **S14** in DMSO-d_6

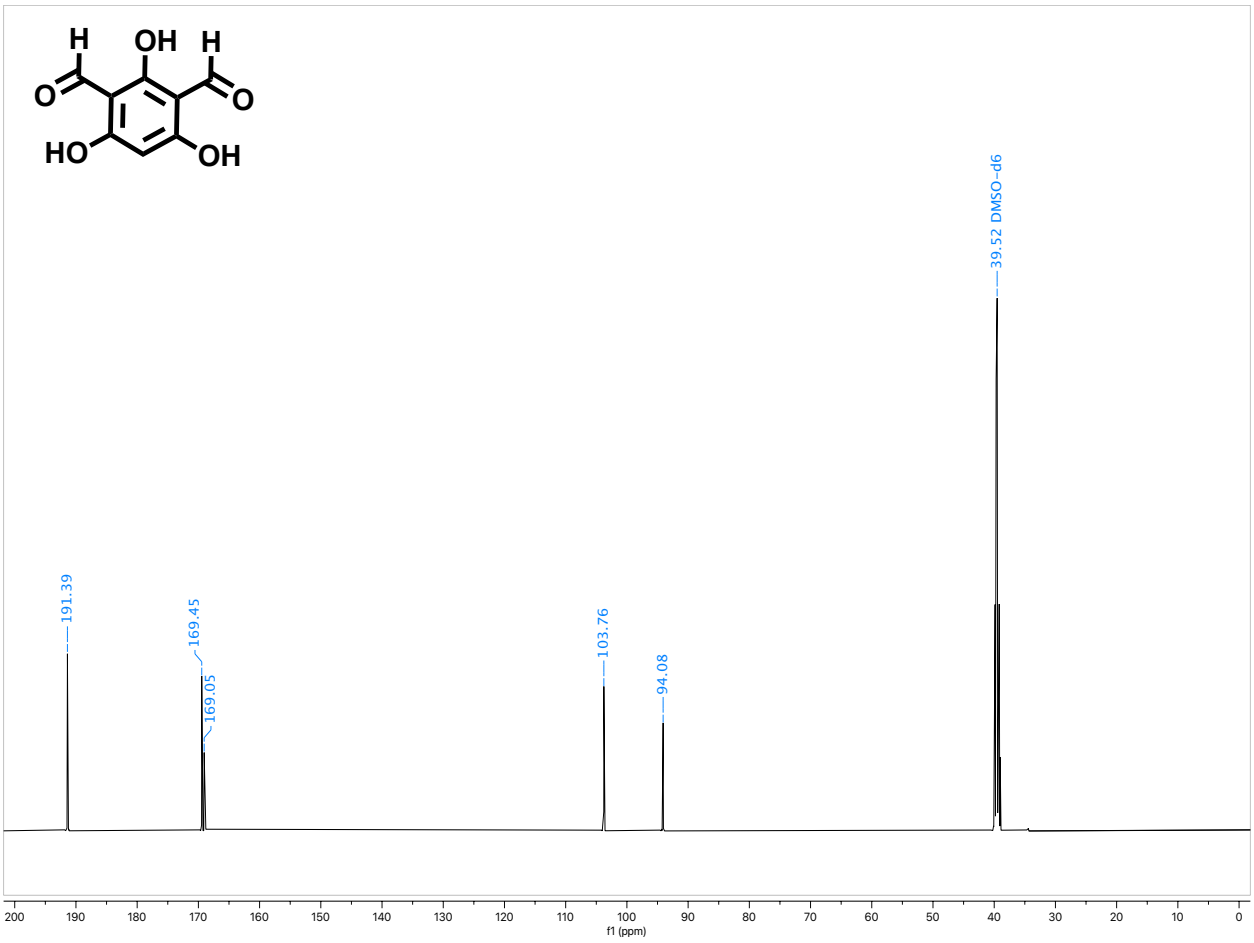

^{1}H-NMR spectrum (500 MHz) of **6** in CD_3OD

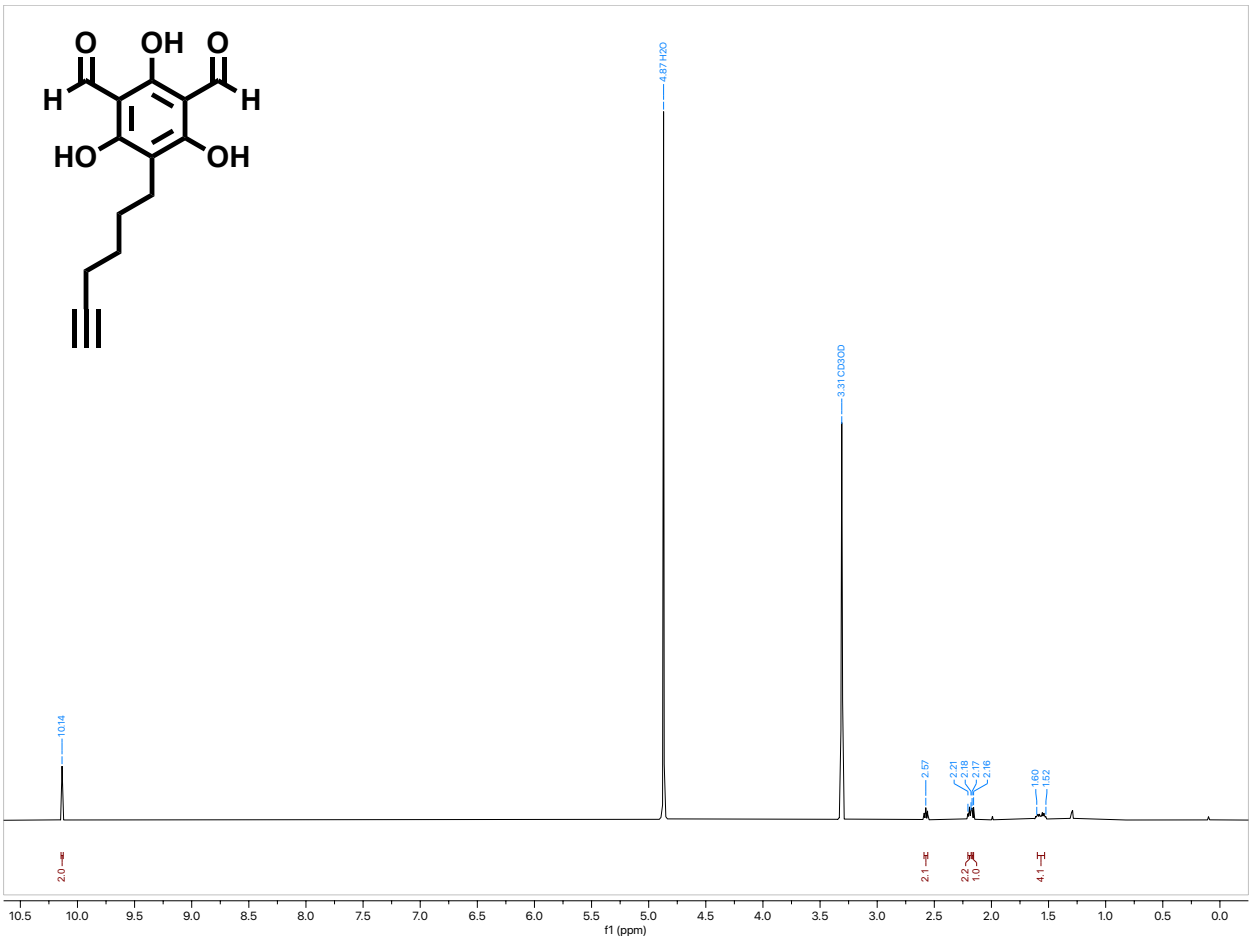

^{13}C-NMR spectrum (126 MHz) of **6** in CD_3OD

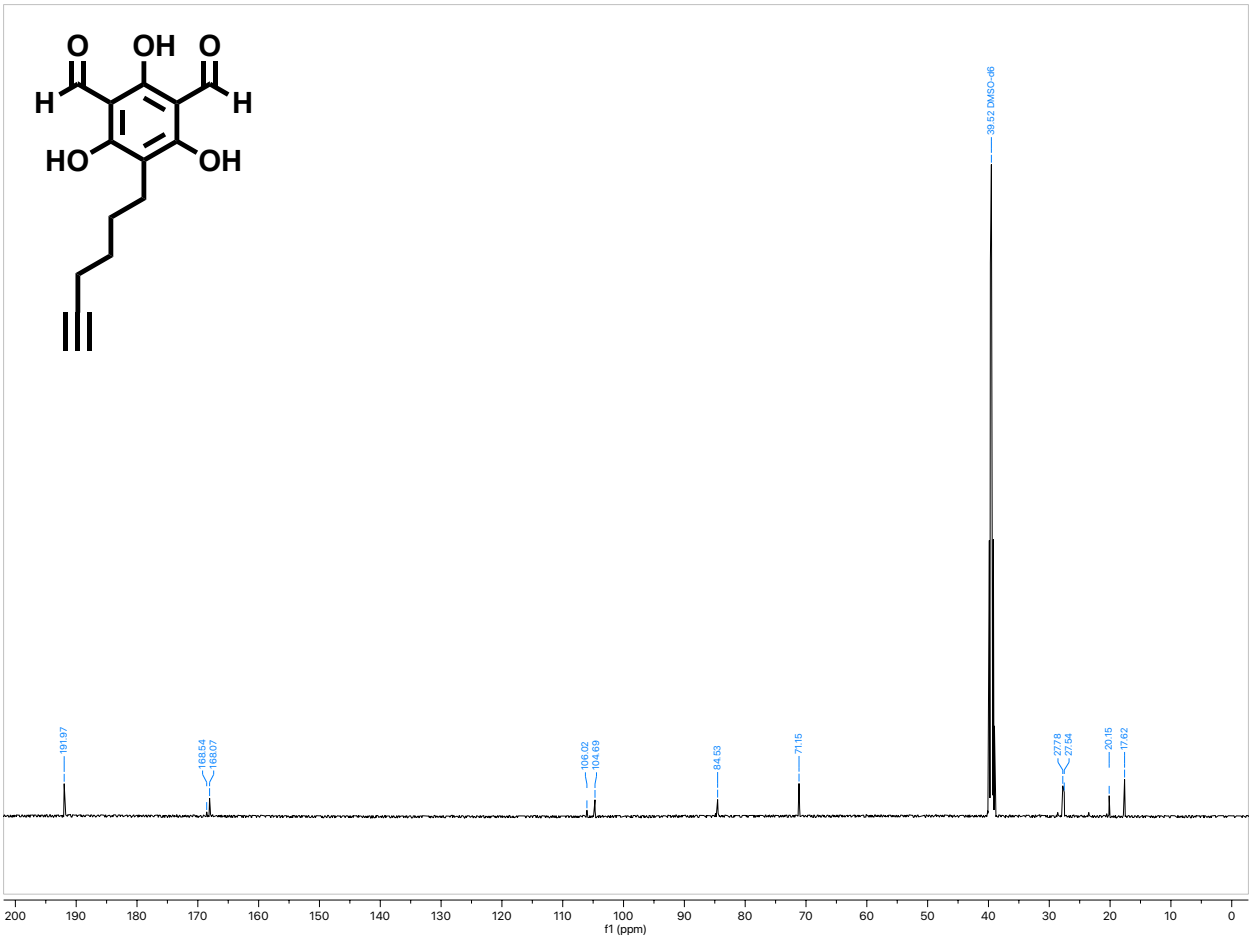

^{1}H-NMR spectrum (500 MHz) of **S16** in CD_3OD

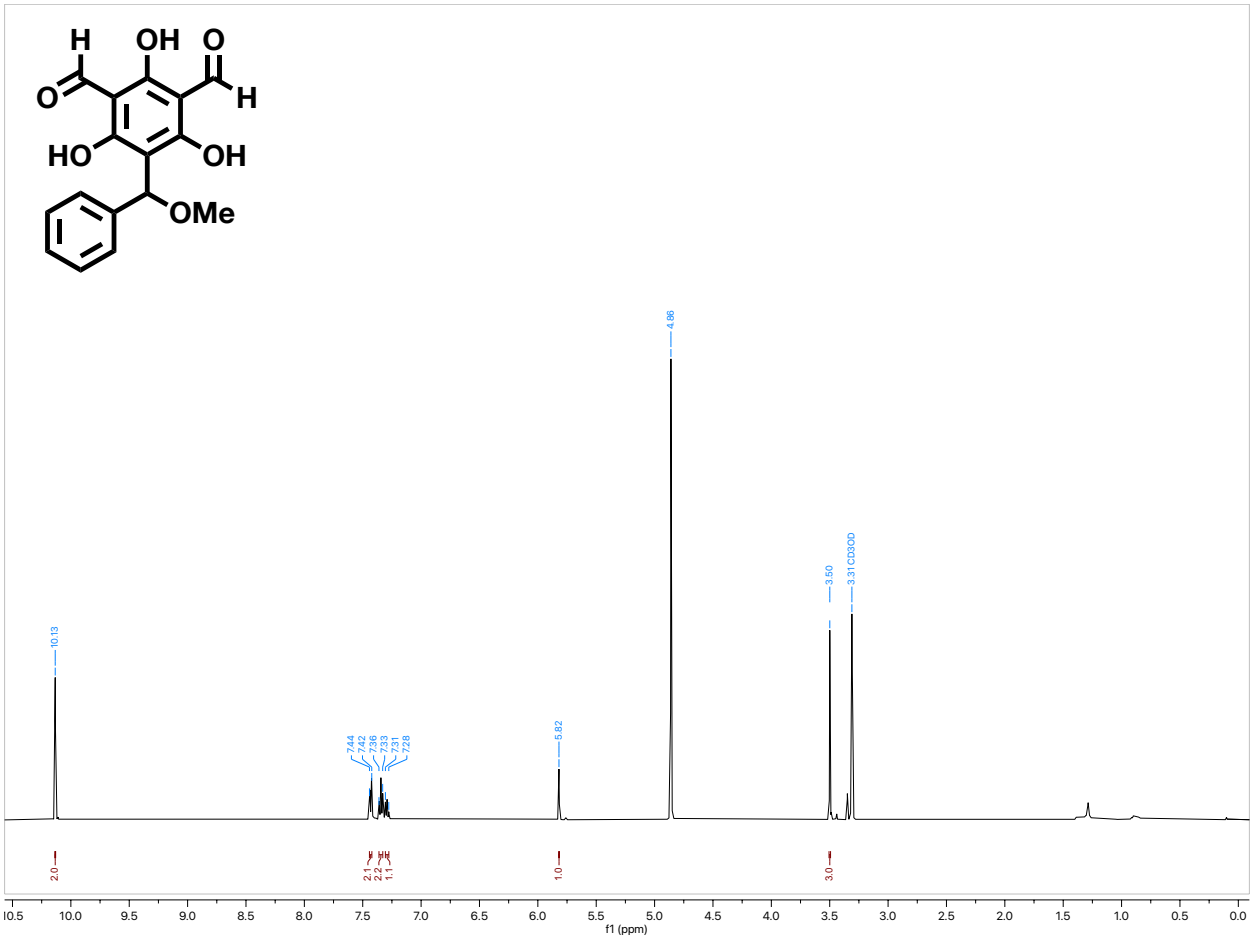

^{13}C-NMR spectrum (126 MHz) of **S16** in CD_3OD

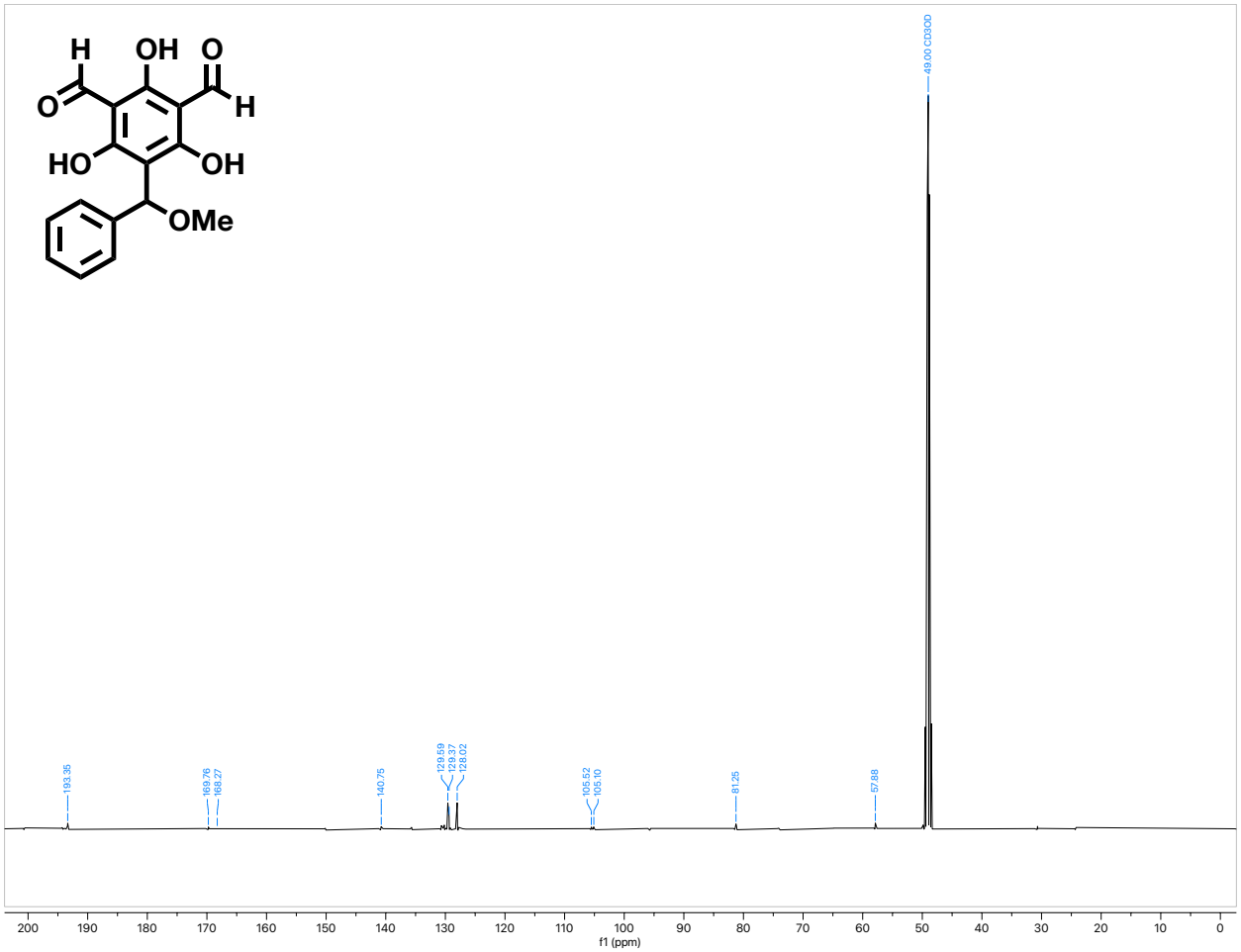

^{1}H-NMR spectrum (500 MHz) of **(+)-guadial B** in $CDCl_3$

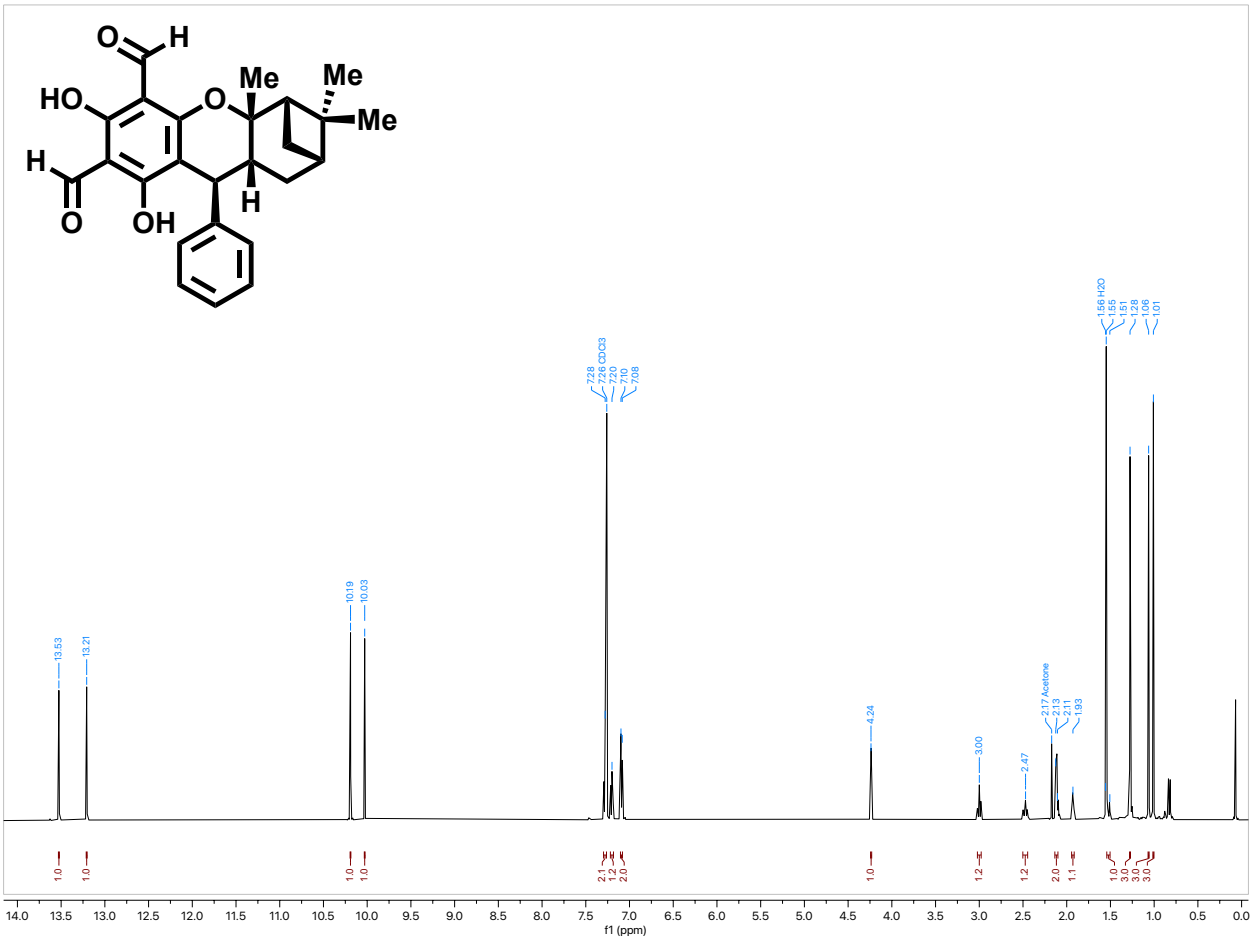

^{13}C-NMR spectrum (126 MHz) of **(+)-guadial B** in $CDCl_3$

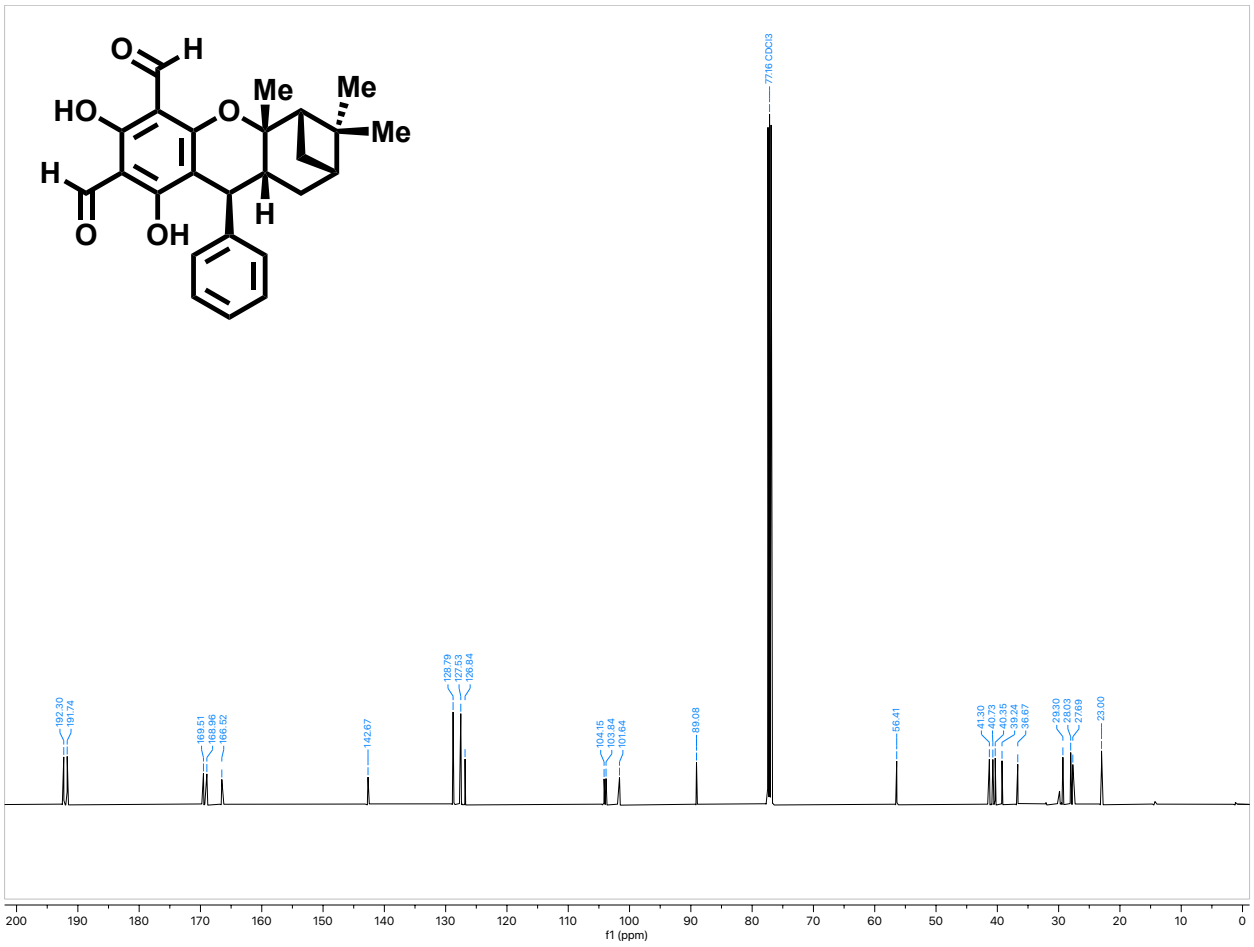

^{1}H-NMR spectrum (500 MHz) of **(–)-guadial B** in $CDCl_3$

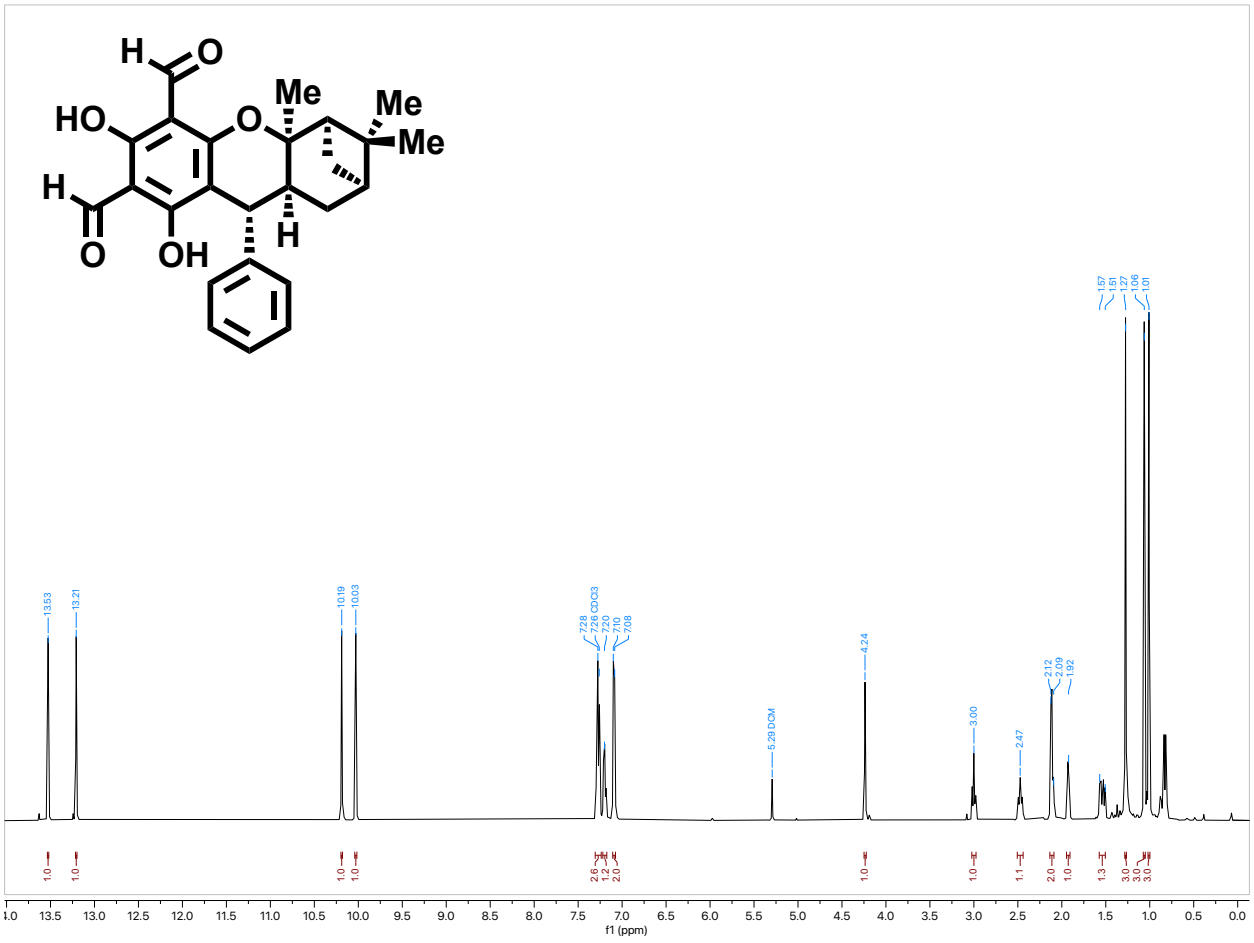

^{13}C-NMR spectrum (126 MHz) of **(–)-guadial B** in $CDCl_3$

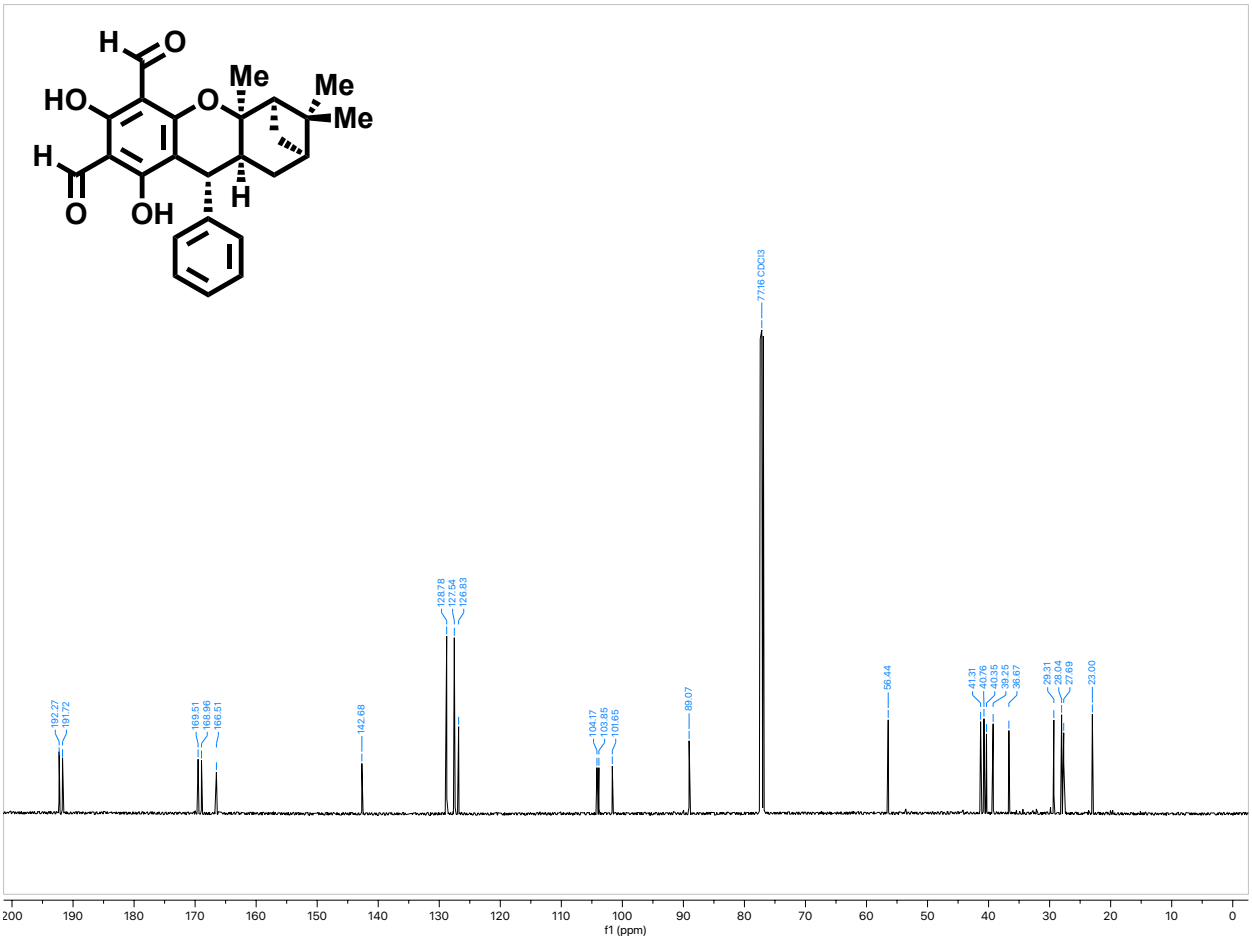

^{1}H-NMR spectrum (500 MHz) of **(+)-guadial C** in $CDCl_3$

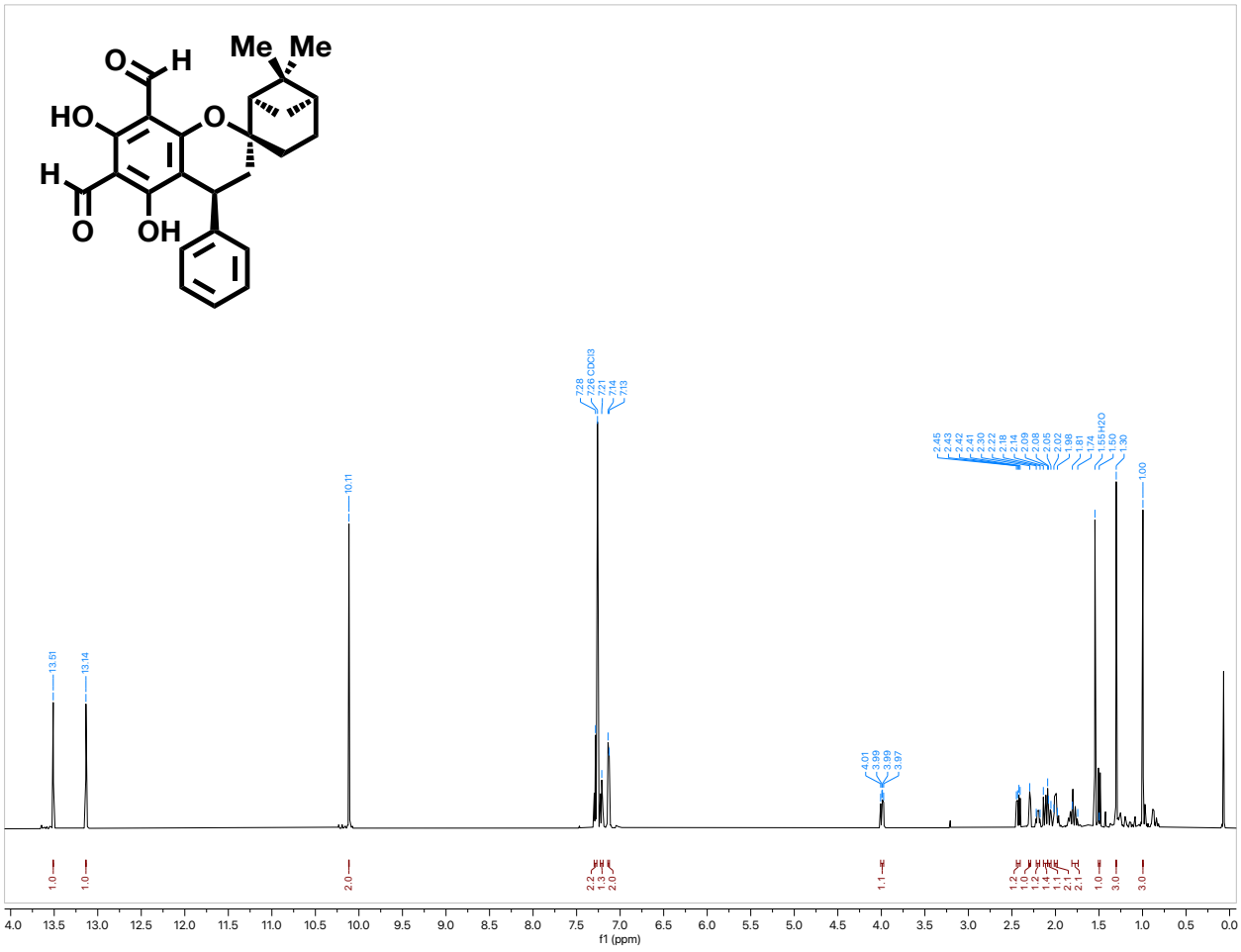

^{13}C-NMR spectrum (126 MHz) of **(+)-guadial C** in $CDCl_3$

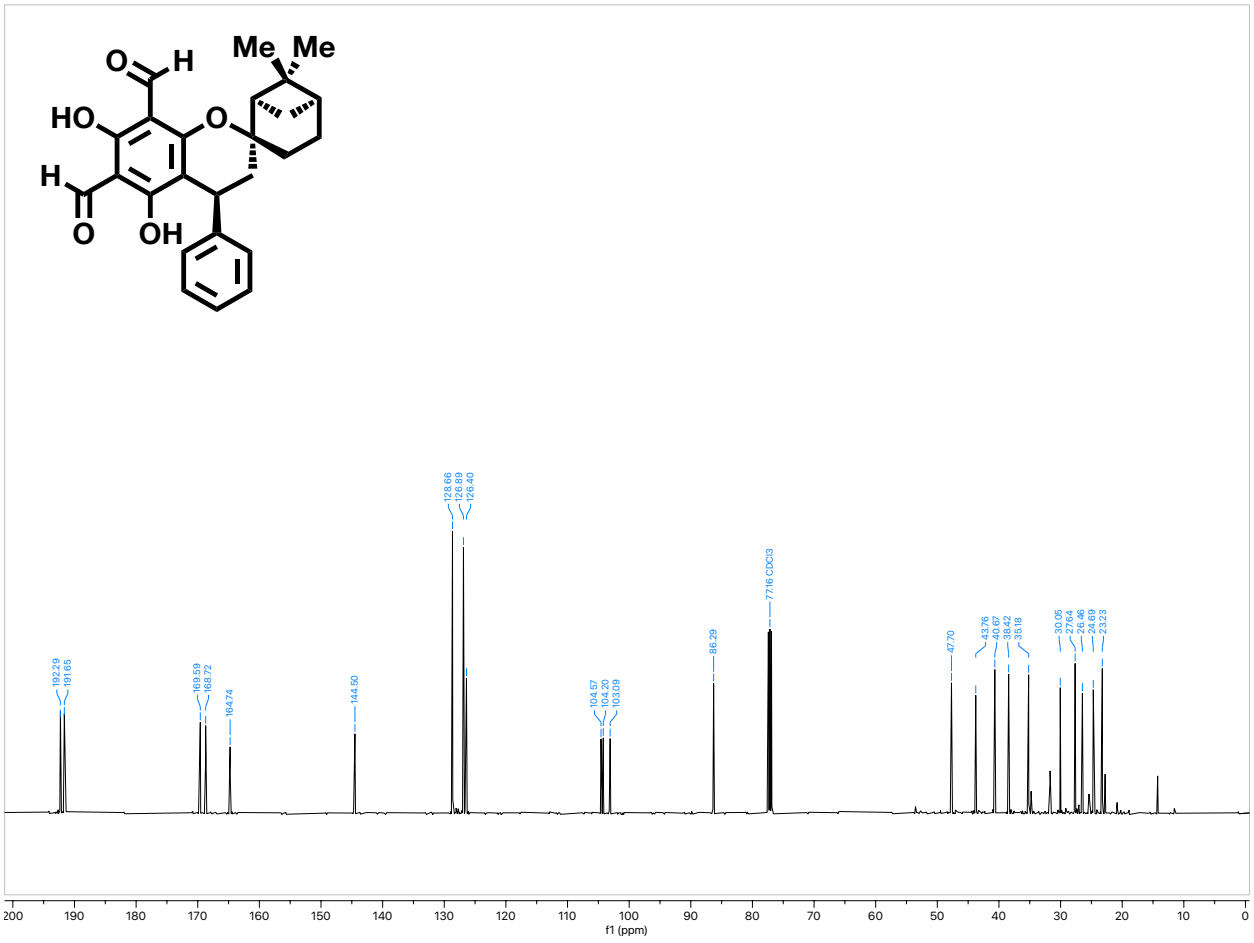

^{1}H-NMR spectrum (500 MHz) of **S18** in CD_3OD

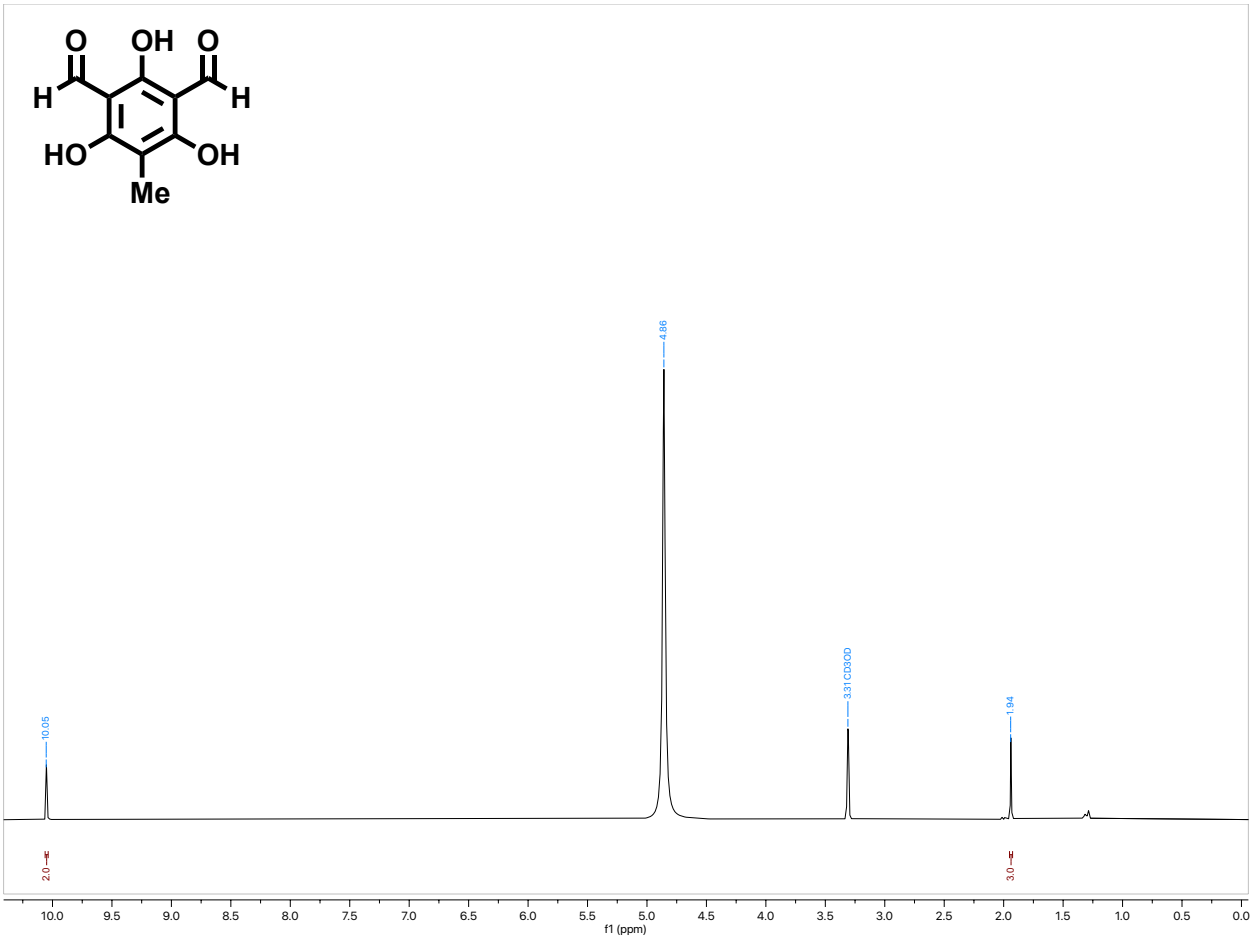

^{13}C-NMR spectrum (126 MHz) of **S18** in CD_3OD

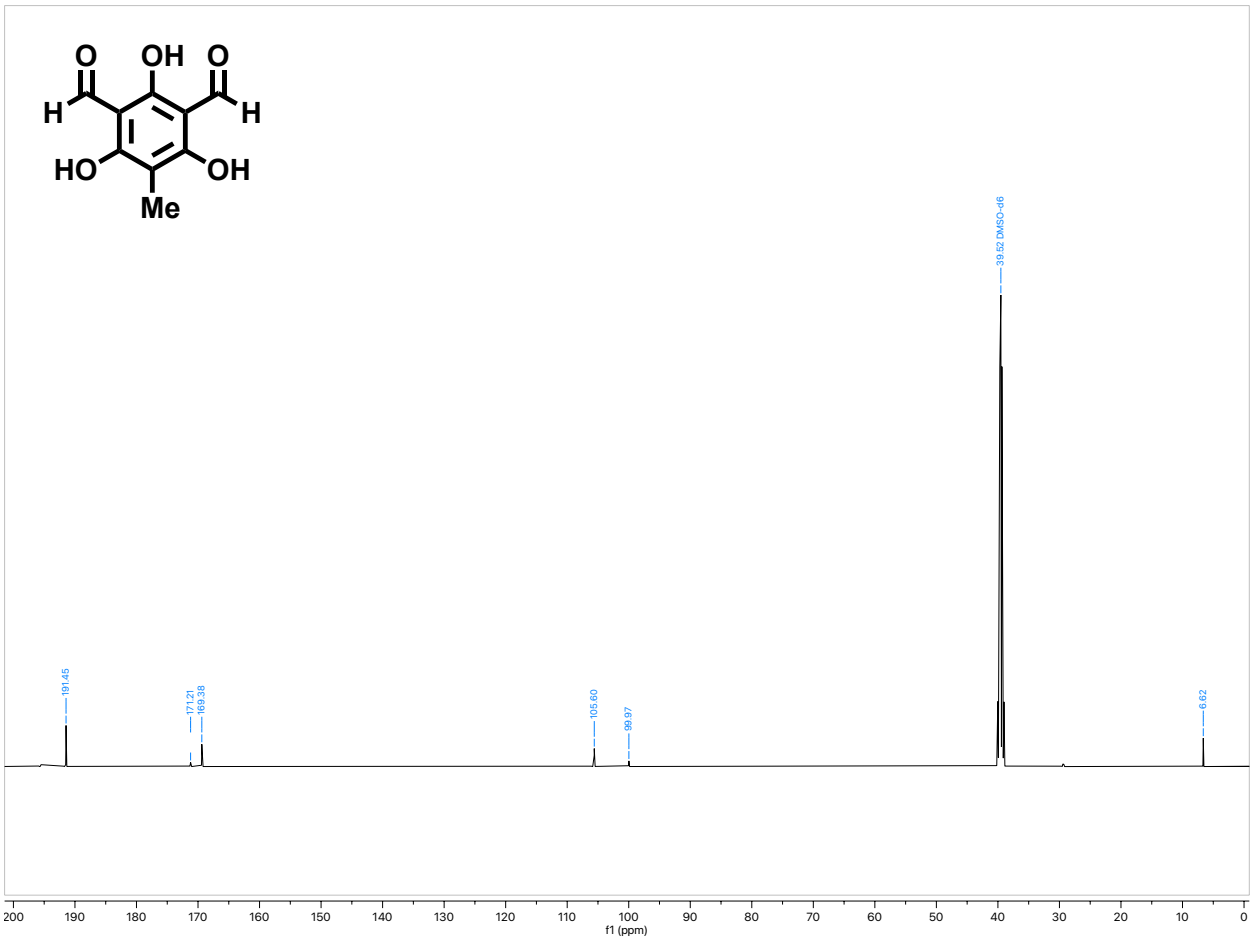

^{1}H-NMR spectrum (500 MHz) of **(–)-cattleianal** in $CDCl_3$

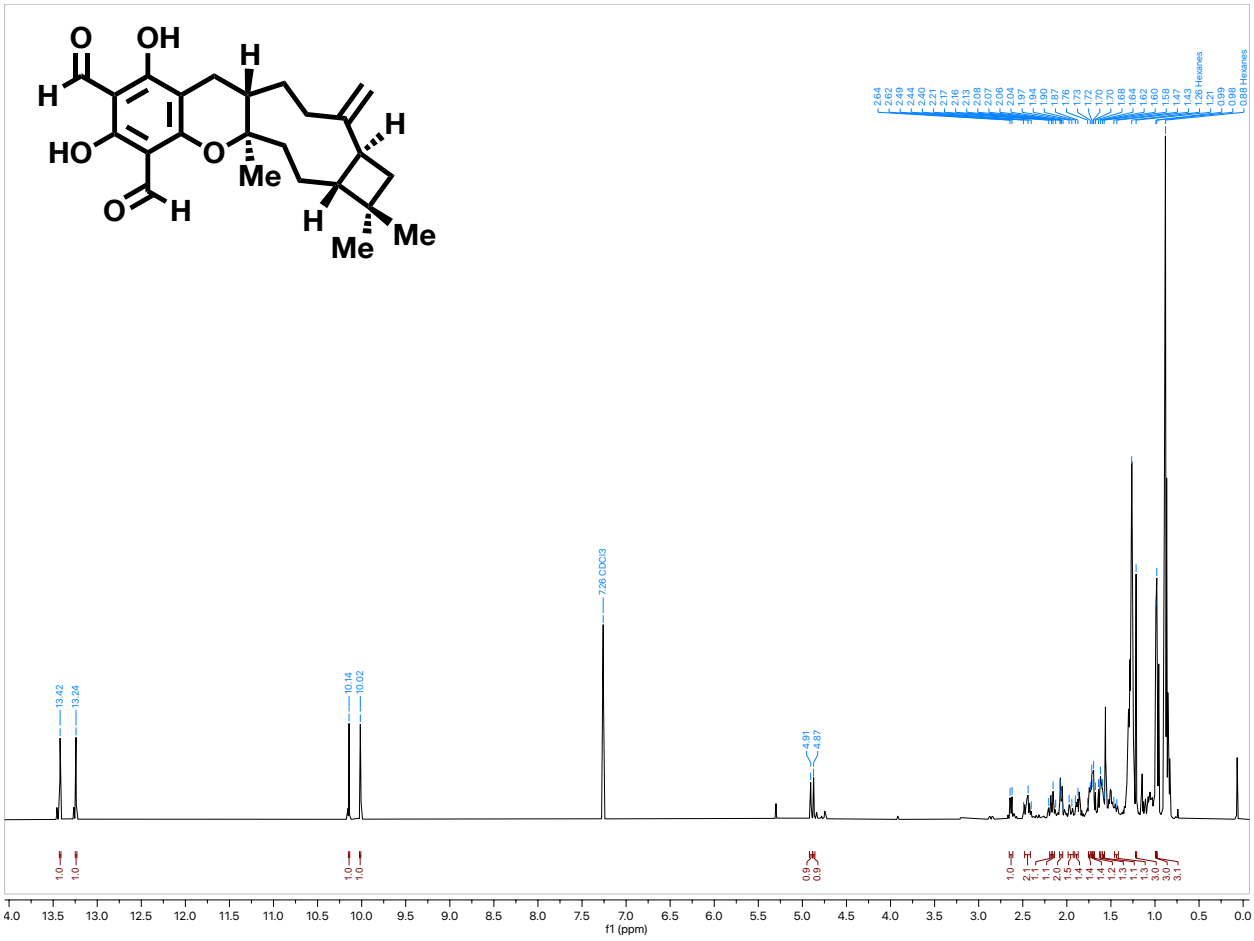

^{13}C-NMR spectrum (126 MHz) of **(–)-cattleianal** in $CDCl_3$

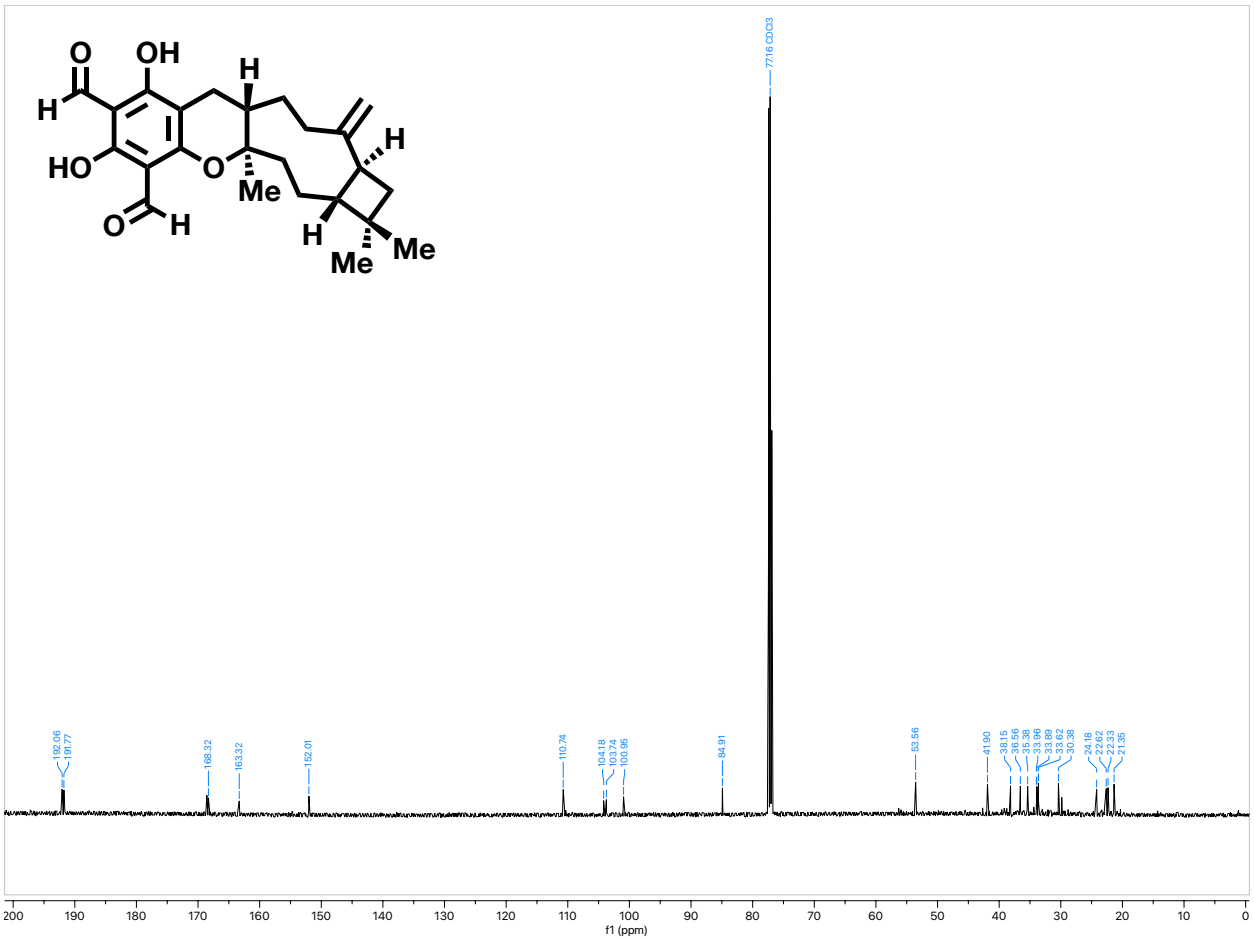

^{1}H-NMR spectrum (500 MHz) of **jensenone** in $CDCl_3$

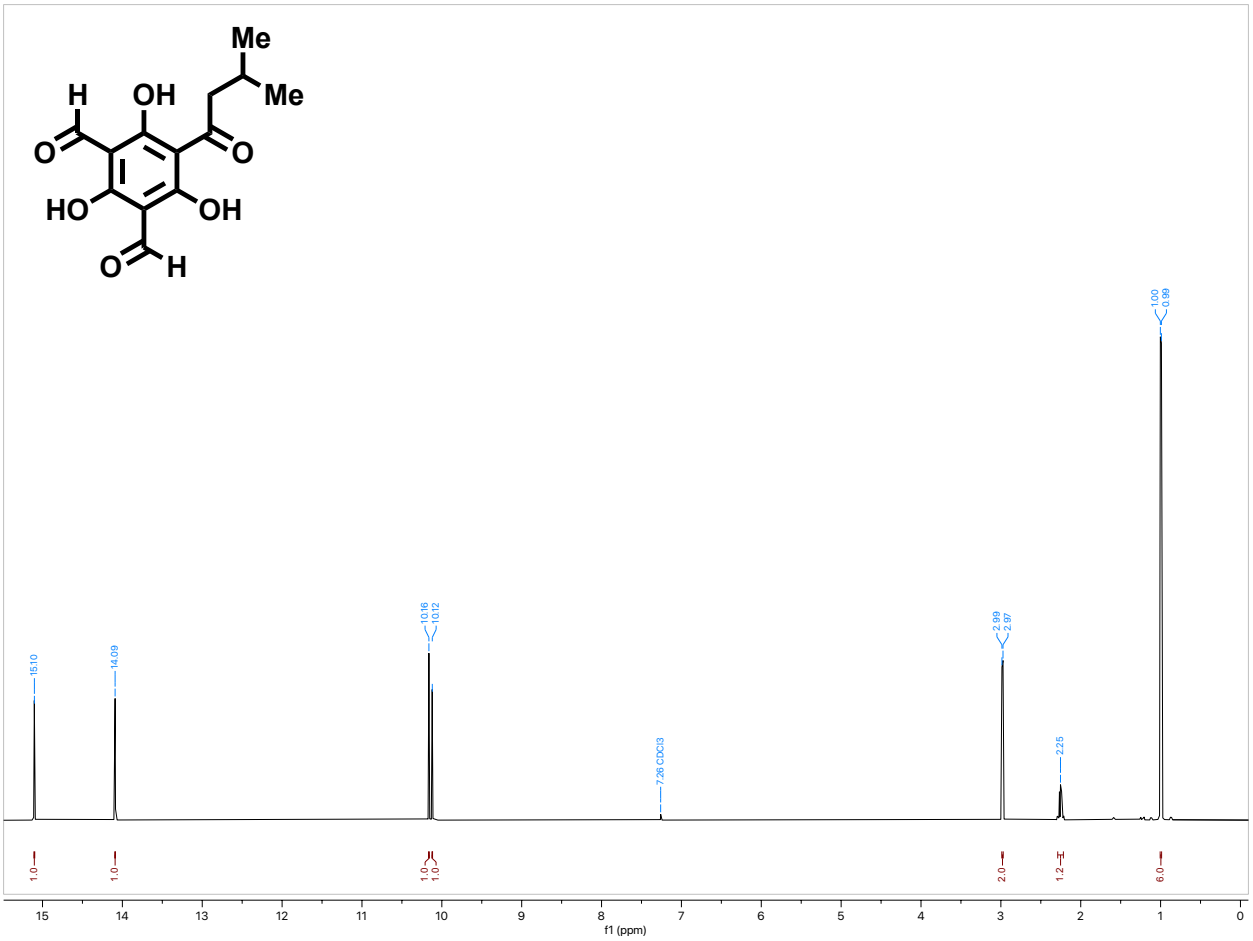

^{13}C-NMR spectrum (126 MHz) of **jensenone** in $CDCl_3$

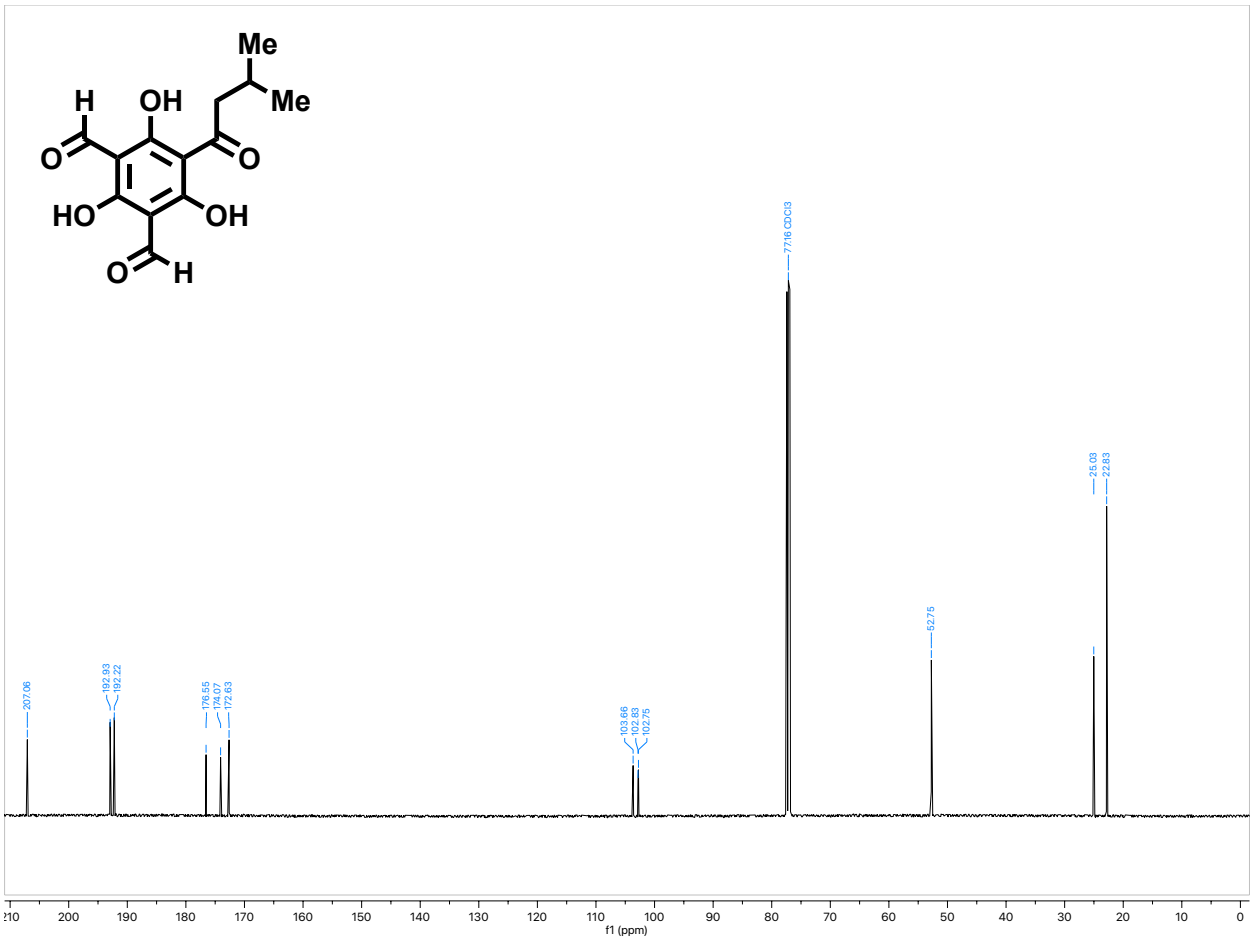

^{1}H-NMR spectrum (500 MHz) of **desthiobiotin-tagged STP ester probe** in DMSO-d_6

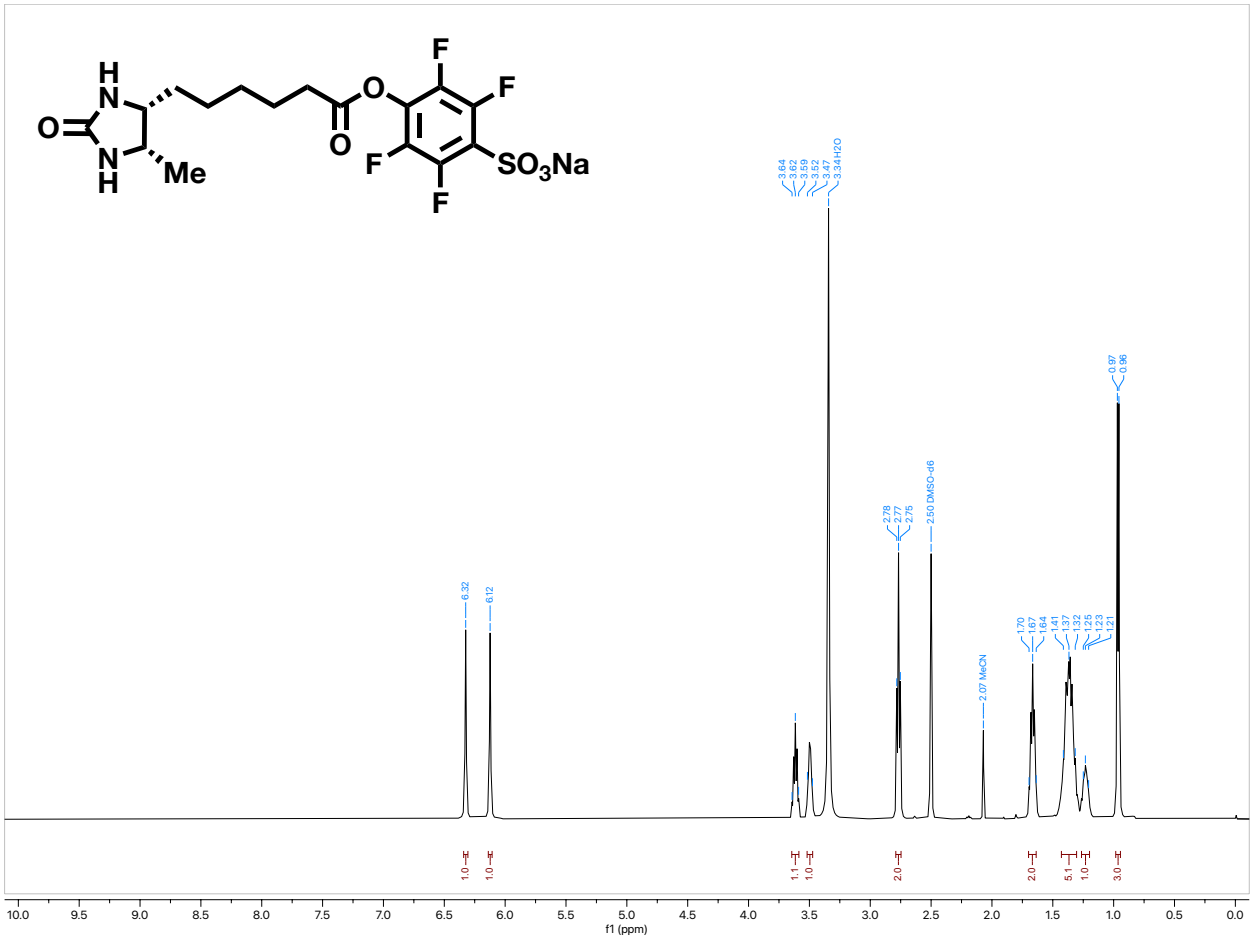

^{13}C-NMR spectrum (126 MHz) of **desthiobiotin-tagged STP ester probe** in DMSO-d_6

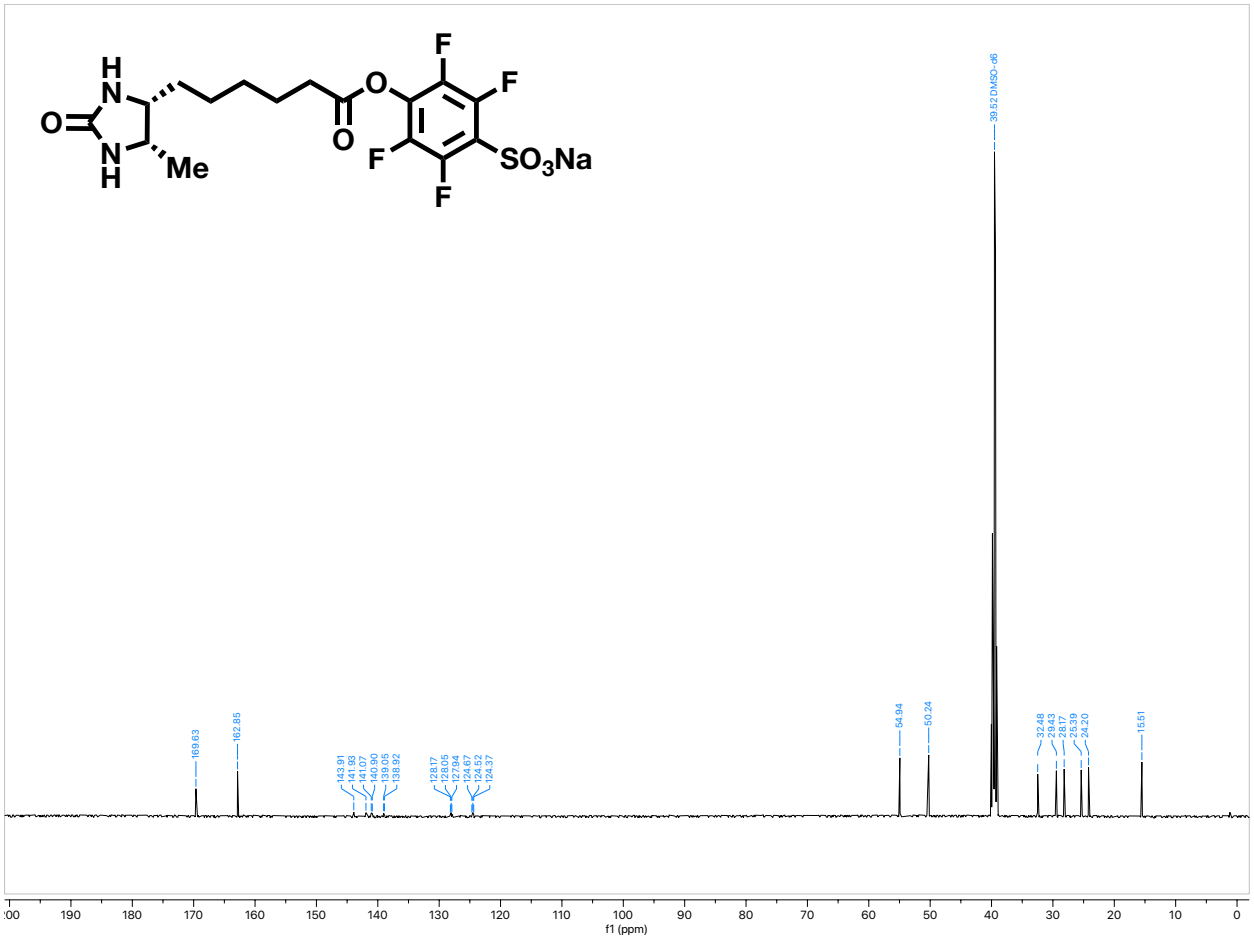

^{19}F-NMR spectrum (470 MHz) of **desthiobiotin-tagged STP ester probe** in DMSO-d_6

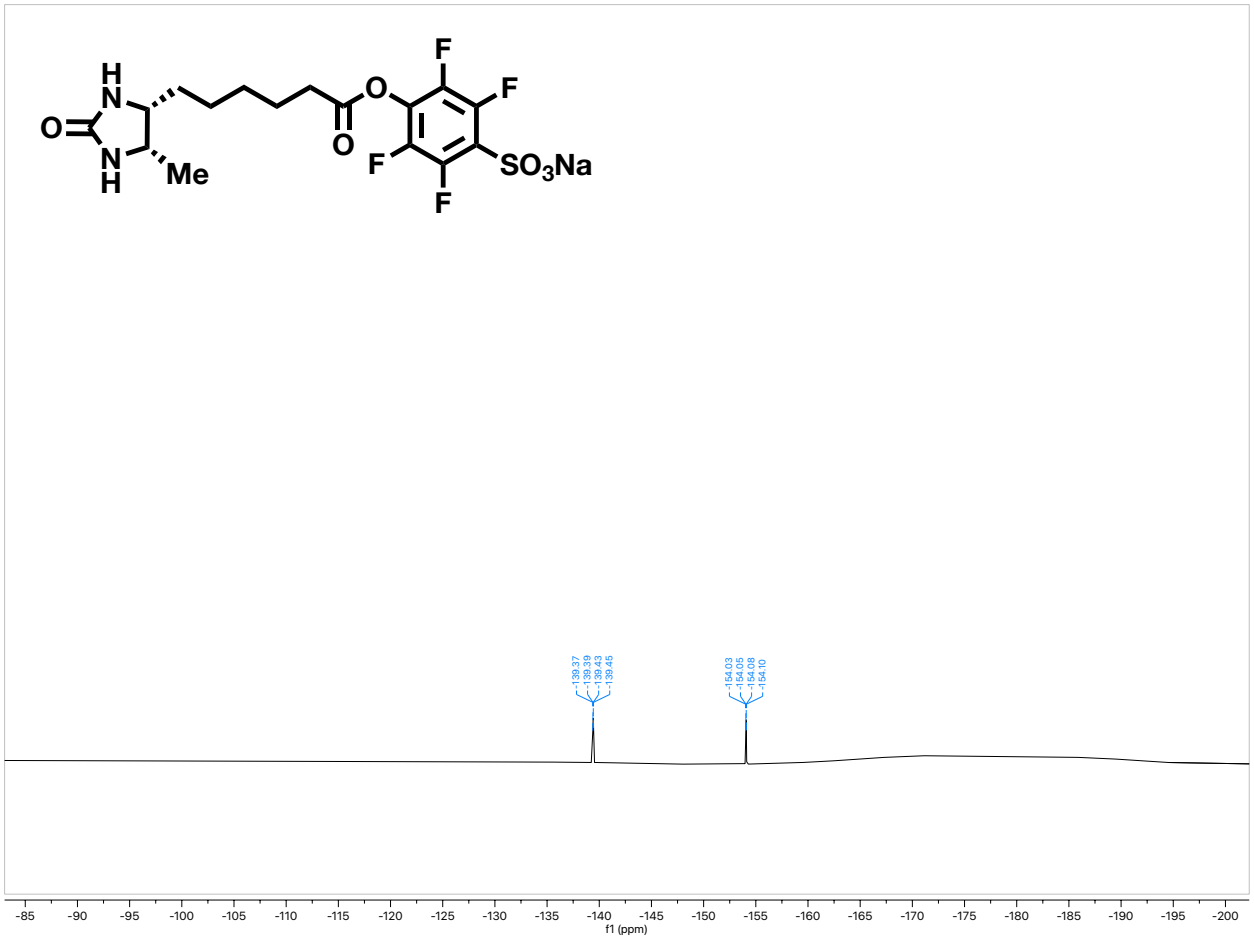

Bibliography

(1) Hübner, M.; Rissom, B.; Fitjer, L. Conformation and Dynamics of (–)-β-Caryophyllene. *Helv. Chim. Acta* **1997**, *80* (6), 1972-1982. DOI: 10.1002/hlca.19970800615.
(2) Zhao, Y.; Truhlar, D. G. The M06 suite of density functionals for main group thermochemistry, thermochemical kinetics, noncovalent interactions, excited states, and transition elements: two new functionals and systematic testing of four M06-class functionals and 12 other functionals. *Theor. Chem. Acc.* **2008**, *120* (1), 215-241. DOI: 10.1007/s00214-007-0310-x.
(3) Marenich, A. V.; Cramer, C. J.; Truhlar, D. G. Universal solvation model based on solute electron density and on a continuum model of the solvent defined by the bulk dielectric constant and atomic surface tensions. *J. Phys. Chem. B* **2009**, *113* (18), 6378-6396. DOI: 10.1021/jp810292n.
(4) Weigend, F.; Ahlrichs, R. Balanced basis sets of split valence, triple zeta valence and quadruple zeta valence quality for H to Rn: Design and assessment of accuracy. *Phys. Chem. Chem. Phys.* **2005**, *7* (18), 3297-3305. DOI: 10.1039/B508541A.
(5) Gaussian 16, R. C., Frisch, M. J.; Trucks, G. W.; Schlegel, H. B.; Scuseria, G. E.; Robb, M. A.; Cheeseman, J. R.; Scalmani, G.; Barone, V.; Petersson, G. A.; Nakatsuji, H.; Li, X.; Caricato, M.; Marenich, A. V.; Bloino, J.; Janesko, B. G.; Gomperts, R.; Mennucci, B.; Hratchian, H. P.; Ortiz, J. V.; Izmaylov, A. F.; Sonnenberg, J. L.; Williams-Young, D.; Ding, F.; Lipparini, F.; Egidi, F.; Goings, J.; Peng, B.; Petrone, A.; Henderson, T.; Ranasinghe, D.; Zakrzewski, V. G.; Gao, J.; Rega, N.; Zheng, G.; Liang, W.; Hada, M.; Ehara, M.; Toyota, K.; Fukuda, R.; Hasegawa, J.; Ishida, M.; Nakajima, T.; Honda, Y.; Kitao, O.; Nakai, H.; Vreven, T.; Throssell, K.; Montgomery, J. A., Jr.; Peralta, J. E.; Ogliaro, F.; Bearpark, M. J.; Heyd, J. J.; Brothers, E. N.; Kudin, K. N.; Staroverov, V. N.; Keith, T. A.; Kobayashi, R.; Normand, J.; Raghavachari, K.; Rendell, A. P.; Burant, J. C.; Iyengar, S. S.; Tomasi, J.; Cossi, M.; Millam, J. M.; Klene, M.; Adamo, C.; Cammi, R.; Ochterski, J. W.; Martin, R. L.; Morokuma, K.; Farkas, O.; Foresman, J. B.; Fox, D. J. *Gaussian, Inc.*, Wallingford CT, **2016**.
(6) Chai, J.-D.; Head-Gordon, M. Long-range corrected hybrid density functionals with damped atom–atom dispersion corrections. *Phys. Chem. Chem. Phys.* **2008**, *10* (44), 6615-6620. DOI: 10.1039/B810189B.
(7) Weigend, F. Accurate Coulomb-fitting basis sets for H to Rn. *Phys. Chem. Chem. Phys.* **2006**, *8* (9), 1057-1065. DOI: 10.1039/B515623H.
(8) Manallack, D. T. The $pK_{(a)}$ Distribution of Drugs: Application to Drug Discovery. *Perspect. Med. Chem.* **2007**, *1*, 25-38.
(9) Fischer, H.; Gottschlich, R.; Seelig, A. Blood-brain barrier permeation: molecular parameters governing passive diffusion. *J. Membr. Biol.* **1998**, *165* (3), 201-211. DOI: 10.1007/s002329900434.
(10) Bruyneel, W.; Charette, J. J.; De Hoffmann, E. Kinetics of Hydrolysis of Hydroxy and Methoxy Derivatives of N-Benzylidene-2-aminopropane. *J. Am. Chem. Soc.* **1966**, *88* (16), 3808-3813. DOI: 10.1021/ja00968a024.
(11) Godoy-Alcántar, C.; Yatsimirsky, A. K.; Lehn, J. M. Structure-stability correlations for imine formation in aqueous solution. *J. Phys. Org. Chem.* **2005**, *18* (10), 979-985. DOI: 10.1002/poc.941.
(12) Herscovitch, R.; Charette, J. J.; De Hoffmann, E. Physicochemical properties of Schiff bases. III. Substituent effects on the kinetics of hydrolysis of N-salicylidene-2-aminopropane derivatives. *J. Am. Chem. Soc.* **1974**, *96* (15), 4954-4958. DOI: 10.1021/ja00822a037.

(13) Kulchat, S.; Chaur, M. N.; Lehn, J.-M. Kinetic Selectivity and Thermodynamic Features of Competitive Imine Formation in Dynamic Covalent Chemistry. *Chem. Eur. J.* **2017**, *23* (46), 11108-11118. DOI: 10.1002/chem.201702088.
(14) Seoane, A.; Brea, R. J.; Fuertes, A.; Podolsky, K. A.; Devaraj, N. K. Biomimetic Generation and Remodeling of Phospholipid Membranes by Dynamic Imine Chemistry. *J. Am. Chem. Soc.* **2018**, *140* (27), 8388-8391. DOI: 10.1021/jacs.8b04557.
(15) Hoelm, M.; Adamczyk, J.; Wzgarda-Raj, K.; Palusiak, M. Effect of a Substituent on the Properties of Salicylaldehyde Hydrazone Derivatives. *J. Org. Chem.* **2023**, *88* (4), 2132-2139. DOI: 10.1021/acs.joc.2c02547.
(16) Rostovtsev, V. V.; Green, L. G.; Fokin, V. V.; Sharpless, K. B. A Stepwise Huisgen Cycloaddition Process: Copper(I)-Catalyzed Regioselective "Ligation" of Azides and Terminal Alkynes. *Angew. Chem. Int. Ed.* **2002**, *41* (14), 2596-2599. DOI: https://doi.org/10.1002/1521-3773(20020715)41:14<2596::AID-ANIE2596>3.0.CO;2-4.
(17) Antoniou, A.; Pharoah, P. D.; Narod, S.; Risch, H. A.; Eyfjord, J. E.; Hopper, J. L.; Loman, N.; Olsson, H.; Johannsson, O.; Borg, A.; et al. Average risks of breast and ovarian cancer associated with BRCA1 or BRCA2 mutations detected in case Series unselected for family history: a combined analysis of 22 studies. *Am. J. Hum. Genet.* **2003**, *72* (5), 1117-1130. DOI: 10.1086/375033.
(18) Begg, C. B.; Haile, R. W.; Borg, A.; Malone, K. E.; Concannon, P.; Thomas, D. C.; Langholz, B.; Bernstein, L.; Olsen, J. H.; Lynch, C. F.; et al. Variation of breast cancer risk among BRCA1/2 carriers. *JAMA* **2008**, *299* (2), 194-201. DOI: 10.1001/jama.2007.55-a.
(19) Gabai-Kapara, E.; Lahad, A.; Kaufman, B.; Friedman, E.; Segev, S.; Renbaum, P.; Beeri, R.; Gal, M.; Grinshpun-Cohen, J.; Djemal, K.; et al. Population-based screening for breast and ovarian cancer risk due to BRCA1 and BRCA2. *Proc. Natl. Acad. Sci.* **2014**, *111* (39), 14205-14210. DOI: 10.1073/pnas.1415979111.
(20) Kuchenbaecker, K. B.; Hopper, J. L.; Barnes, D. R.; Phillips, K. A.; Mooij, T. M.; Roos-Blom, M. J.; Jervis, S.; van Leeuwen, F. E.; Milne, R. L.; Andrieu, N.; et al. Risks of Breast, Ovarian, and Contralateral Breast Cancer for BRCA1 and BRCA2 Mutation Carriers. *JAMA* **2017**, *317* (23), 2402-2416. DOI: 10.1001/jama.2017.7112.
(21) Elias, A. D. Triple-negative breast cancer: a short review. *Am. J. Clin. Oncol.* **2010**, *33* (6), 637-645. DOI: 10.1097/COC.0b013e3181b8afcf.
(22) Couch, F. J.; Hart, S. N.; Sharma, P.; Toland, A. E.; Wang, X.; Miron, P.; Olson, J. E.; Godwin, A. K.; Pankratz, V. S.; Olswold, C.; et al. Inherited mutations in 17 breast cancer susceptibility genes among a large triple-negative breast cancer cohort unselected for family history of breast cancer. *J. Clin. Oncol.* **2015**, *33* (4), 304-311. DOI: 10.1200/jco.2014.57.1414.
(23) Foulkes, W. D.; Stefansson, I. M.; Chappuis, P. O.; Bégin, L. R.; Goffin, J. R.; Wong, N.; Trudel, M.; Akslen, L. A. Germline BRCA1 mutations and a basal epithelial phenotype in breast cancer. *J. Natl. Cancer. Inst.* **2003**, *95* (19), 1482-1485. DOI: 10.1093/jnci/djg050.
(24) Bayraktar, S.; Gutierrez-Barrera, A. M.; Liu, D.; Tasbas, T.; Akar, U.; Litton, J. K.; Lin, E.; Albarracin, C. T.; Meric-Bernstam, F.; Gonzalez-Angulo, A. M.; et al. Outcome of triple-negative breast cancer in patients with or without deleterious BRCA mutations. *Breast Cancer Res. Treat.* **2011**, *130* (1), 145-153. DOI: 10.1007/s10549-011-1711-z.
(25) Leventis, P. A.; Grinstein, S. The distribution and function of phosphatidylserine in cellular membranes. *Annu. Rev. Biophys.* **2010**, *39*, 407. DOI: 10.1146/annurev.biophys.093008.131234.

(26) Kamat, S. S.; Camara, K.; Parsons, W. H.; Chen, D. H.; Dix, M. M.; Bird, T. D.; Howell, A. R.; Cravatt, B. F. Immunomodulatory lysophosphatidylserines are regulated by ABHD16A and ABHD12 interplay. *Nat. Chem. Biol.* **2015**, *11* (2), 164-171. DOI: 10.1038/nchembio.1721.
(27) Nguyen, T. T.; Voeltz, G. K. An ER phospholipid hydrolase drives ER-associated mitochondrial constriction for fission and fusion. *Elife* **2022**, *11*. DOI: 10.7554/eLife.84279.
(28) Fiskerstrand, T.; H'mida-Ben Brahim, D.; Johanssond, S.; M'zahem, A.; Haukanes, B. I.; Drouot, N.; Zimmermann, J.; Cole, A. J.; Vedeler, C.; Bredrup, C.; et al. Mutations in ABHD12 Cause the Neurodegenerative Disease PHARC: An Inborn Error of Endocannabinoid Metabolism. *Am. J. Hum. Genet.* **2010**, *87* (3), 410-417. DOI: 10.1016/j.ajhg.2010.08.002.
(29) Tucker, E. J.; Compton, A. G.; Thorburn, D. R. Recent advances in the genetics of mitochondrial encephalopathies. *Curr. Neurol. Neurosci. Rep.* **2010**, *10* (4), 277-285. DOI: 10.1007/s11910-010-0112-8.
(30) Krüger, D. M.; Neubacher, S.; Grossmann, T. N. Protein-RNA interactions: structural characteristics and hotspot amino acids. *RNA* **2018**, *24* (11), 1457-1465. DOI: 10.1261/rna.066464.118.
(31) Ma, K.; Chen, G.; Li, W.; Kepp, O.; Zhu, Y.; Chen, Q. Mitophagy, mitochondrial homeostasis, and cell fate. *Front. Cell Dev. Biol.* **2020**, *8*, 467. DOI: 10.3389/fcell.2020.00467.
(32) Chen, Q.; Lei, J. H.; Bao, J.; Wang, H.; Hao, W.; Li, L.; Peng, C.; Masuda, T.; Miao, K.; Xu, J.; et al. BRCA1 deficiency impairs mitophagy and promotes inflammasome activation and mammary tumor metastasis. *Adv. Sci.* **2020**, *7* (6), 1903616. DOI: 10.1002/advs.201903616.
(33) Miyahara, K.; Takano, N.; Yamada, Y.; Kazama, H.; Tokuhisa, M.; Hino, H.; Fujita, K.; Barroga, E.; Hiramoto, M.; Handa, H.; et al. BRCA1 degradation in response to mitochondrial damage in breast cancer cells. *Sci. Rep.* **2021**, *11* (1), 8735. DOI: 10.1038/s41598-021-87698-7.
(34) Dang, L.; White, D. W.; Gross, S.; Bennett, B. D.; Bittinger, M. A.; Driggers, E. M.; Fantin, V. R.; Jang, H. G.; Jin, S.; Keenan, M. C.; et al. Cancer-associated IDH1 mutations produce 2-hydroxyglutarate. *Nature* **2009**, *462* (7274), 739-752. DOI: 10.1038/nature08617.
(35) Ogasawara, D.; Ichu, T.-A.; Vartabedian, V. F.; Benthuysen, J.; Jing, H.; Reed, A.; Ulanovskaya, O. A.; Hulce, J. J.; Roberts, A.; Brown, S.; et al. Selective blockade of the lyso-PS lipase ABHD12 stimulates immune responses in vivo. *Nat. Chem. Biol.* **2018**, *14* (12), 1099-1108. DOI: 10.1038/s41589-018-0155-8.
(36) Hacker, S. M.; Backus, K. M.; Lazear, M. R.; Forli, S.; Correia, B. E.; Cravatt, B. F. Global profiling of lysine reactivity and ligandability in the human proteome. *Nat. Chem.* **2017**, *9* (12), 1181-1190. DOI: 10.1038/nchem.2826.
(37) Yi, W.; Clark, P. M.; Mason, D. E.; Keenan, M. C.; Hill, C.; Goddard, W. A.; Peters, E. C.; Driggers, E. M.; Hsieh-Wilson, L. C. Phosphofructokinase 1 Glycosylation Regulates Cell Growth and Metabolism. *Science* **2012**, *337* (6097), 975-980. DOI: 10.1126/science.1222278.
(38) Amara, N.; Cooper, M. P.; Voronkova, M. A.; Webb, B. A.; Lynch, E. M.; Kollman, J. M.; Ma, T.; Yu, K.; Lai, Z.; Sangaraju, D.; et al. Selective activation of PFKL suppresses the phagocytic oxidative burst. *Cell* **2021**, *184* (17), 4480-4494.e4415. DOI: 10.1016/j.cell.2021.07.004.
(39) Sánchez-Martínez, C.; Estévez, A. M.; Aragón, J. J. Phosphofructokinase C Isozyme from Ascites Tumor Cells: Cloning, Expression, and Properties. *Biochem. Biophys. Res. Commun.* **2000**, *271* (3), 635-640. DOI: 10.1006/bbrc.2000.2681.
(40) Fu, Q.; Liu, Z.; Bhawal, R.; Anderson, E. T.; Sherwood, R. W.; Yang, Y.; Thannhauser, T.; Schroyen, M.; Tang, X.; Zhang, H.; et al. Comparison of MS2, synchronous precursor selection MS3, and real-time search MS3 methodologies for lung proteomes of hydrogen sulfide treated swine. *Anal. Bioanal. Chem.* **2021**, *413* (2), 419-429. DOI: 10.1007/s00216-020-03009-5.
(41) Song, T.; McNamara, J. W.; Ma, W.; Landim-Vieira, M.; Lee, K. H.; Martin, L. A.; Heiny, J. A.; Lorenz, J. N.; Craig, R.; Pinto, J. R.; et al. Fast skeletal myosin-binding protein-C regulates fast

skeletal muscle contraction. *Proc. Natl. Acad. Sci.* **2021**, *118* (17), e2003596118. DOI: 10.1073/pnas.2003596118.
(42) Ledet, M. M.; Harman, R. M.; Fan, J. C.; Schmitt-Matzen, E.; Diaz-Rubio, M. E.; Zhang, S.; Van de Walle, G. R. Secreted sphingomyelins modulate low mammary cancer incidence observed in certain mammals. *Sci. Rep*. **2020**, *10* (1), 20580. DOI: 10.1038/s41598-020-77639-1.
(43) Montague, B.; Summers, A.; Bhawal, R.; Anderson, E. T.; Kraus-Malett, S.; Zhang, S.; Goggs, R. Identifying potential biomarkers and therapeutic targets for dogs with sepsis using metabolomics and lipidomics analyses. *PLoS One* **2022,** *17* (7), e0271137. DOI: 10.1371/journal.pone.0271137.
(44) Pang, Z.; Chong, J.; Zhou, G.; de Lima Morais, D. A.; Chang, L.; Barrette, M.; et al. MetaboAnalyst 5.0: narrowing the gap between raw spectra and functional insights. *Nucleic Acids Res.* **2021**, *49* (1), 388-96. DOI: 10.1093/nar/gkab382.
(45) Martínez, C. H. R.; Dardonville, C. Rapid Determination of Ionization Constants (pK_a) by UV Spectroscopy Using 96-Well Microtiter Plates. *ACS Med. Chem. Lett.* **2013**, *4* (1), 142-145. DOI: 10.1021/ml300326v.
(46) Tomsho, J. W.; Pal, A.; Hall, D. G.; Benkovic, S. J. Ring Structure and Aromatic Substituent Effects on the pK_a of the Benzoxaborole Pharmacophore. *ACS Med. Chem. Lett.* **2012**, *3* (1), 48-52. DOI: 10.1021/ml200215j.
(47) Metzler, C. M.; Cahill, A.; Metzler, D. E. Equilibriums and absorption spectra of Schiff bases. *J. Am. Chem. Soc.* **1980**, *102* (19), 6075-6082. DOI: 10.1021/ja00539a017.
(48) Heinert, D.; Martell, A. E. Pyridoxine and Pyridoxal Analogs. VI. Electronic Absorption Spectra of Schiff Bases. *J. Am. Chem. Soc.* **1963**, *85* (2), 183-188. DOI: 10.1021/ja00885a017.
(49) Herscovitch, R.; Charette, J. J.; De Hoffmann, E. Physicochemical properties of Schiff Bases. II. Tautomeric equilibrium of substituted N-Salicylidene-2-aminopropanes and p-hydroxy-N-benzylidene-2-aminopropane. *J. Am. Chem. Soc.* **1973**, *95* (16), 5135-5140. DOI: 10.1021/ja00797a007.
(50) Bruyneel, W.; Charette, J. J.; De Hoffmann, E. Kinetics of Hydrolysis of Hydroxy and Methoxy Derivatives of N-Benzylidene-2-aminopropane. *J. Am. Chem. Soc.* **1966**, *88* (16), 3808-3813. DOI: 10.1021/ja00968a024.
(51) Herscovitch, R.; Charette, J. J.; De Hoffmann, E. Physicochemical properties of Schiff bases. III. Substituent effects on the kinetics of hydrolysis of N-salicylidene-2-aminopropane derivatives. *J. Am. Chem. Soc.* **1974**, *96* (15), 4954-4958. DOI: 10.1021/ja00822a037.
(52) Bharate, S. B.; Bhutani, K. K.; Khan, S. I.; Tekwani, B. L.; Jacob, M. R.; Khan, I. A.; Singh, I. P. Biomimetic synthesis, antimicrobial, antileishmanial and antimalarial activities of euglobals and their analogues. *Bioorg. Med. Chem.* **2006**, *14* (6), 1750-1760. DOI: 10.1016/j.bmc.2005.10.027.
(53) Chiba, K.; Arakawa, T.; Tada, M. Synthesis of euglobal-G3 and -G4. *Chem. Commun.* **1996**, *15*, 1763-1764. DOI: 10.1039/CC9960001763.
(54) Dethe, D. H.; B, V. K.; Maiti, R. Biomimetic total syntheses of chromane meroterpenoids, guadials B and C, guapsidial A and psiguajadial D. *Org. Biomol. Chem.* **2018**, *16* (26), 4793-4796. DOI: 10.1039/C8OB01092G.
(55) Tran, D. N.; Cramer, N. Biomimetic Synthesis of (+)-Ledene, (+)-Viridiflorol, (–)-Palustrol, (+)-Spathulenol, and Psiguadial A, C, and D via the Platform Terpene (+)-Bicyclogermacrene. *Chem. Eur. J.* **2014**, *20* (34), 10654-10660. DOI: 10.1002/chem.201403082.
(56) Spence, J. T. J.; George, J. H. Structural Reassignment of Cytosporolides A–C via Biomimetic Synthetic Studies and Reinterpretation of NMR Data. *Org. Lett.* **2011**, *13* (19), 5318-5321. DOI: 10.1021/ol202181g.

(57) Ma, S.-J.; Yu, J.; Yan, D.-W.; Wang, D.-C.; Gao, J.-M.; Zhang, Q. Meroterpene-like compounds derived from β-caryophyllene as potent α-glucosidase inhibitors. *Org. Biomol. Chem.* **2018**, *16* (48), 9454-9460. DOI: 10.1039/C8OB02687D.
(58) Li, C.-J.; Ma, J.; Sun, H.; Zhang, D.; Zhang, D.-M. Guajavadimer A, a Dimeric Caryophyllene-Derived Meroterpenoid with a New Carbon Skeleton from the Leaves of Psidium guajava. *Org. Lett.* **2016**, *18* (2), 168-171. DOI: 10.1021/acs.orglett.5b03117.
(59) Jian, Y.-Q.; Huang, X.-J.; Zhang, D.-M.; Jiang, R.-W.; Chen, M.-F.; Zhao, B.-X.; Wang, Y.; Ye, W.-C. Guapsidial A and Guadials B and C: Three New Meroterpenoids with Unusual Skeletons from the Leaves of Psidium guajava. *Chem. Eur. J.* **2015**, *21* (25), 9022-9027. DOI: 10.1002/chem.201500533.